University of Alberta

Optimal Grade Transition Policies for a High Pressure EVA Polymerization Plant

by

Ian Roger Alleyne

A thesis submitted to the Faculty of Graduate Studies and Research
in partial fulfillment of the requirements for the degree of

Doctor of Philosophy

in

Process Control

Department of Chemical and Materials Engineering

Edmonton, Alberta

Fall 2006

Library and Archives Canada

Published Heritage Branch

395 Wellington Street
Ottawa ON K1A 0N4
Canada

Bibliothèque et Archives Canada

Direction du Patrimoine de l'édition

395, rue Wellington
Ottawa ON K1A 0N4
Canada

Your file Votre référence
ISBN: 978-0-494-22983-5
Our file Notre référence
ISBN: 978-0-494-22983-5

NOTICE:
The author has granted a non-exclusive license allowing Library and Archives Canada to reproduce, publish, archive, preserve, conserve, communicate to the public by telecommunication or on the Internet, loan, distribute and sell theses worldwide, for commercial or non-commercial purposes, in microform, paper, electronic and/or any other formats.

The author retains copyright ownership and moral rights in this thesis. Neither the thesis nor substantial extracts from it may be printed or otherwise reproduced without the author's permission.

AVIS:
L'auteur a accordé une licence non exclusive permettant à la Bibliothèque et Archives Canada de reproduire, publier, archiver, sauvegarder, conserver, transmettre au public par télécommunication ou par l'Internet, prêter, distribuer et vendre des thèses partout dans le monde, à des fins commerciales ou autres, sur support microforme, papier, électronique et/ou autres formats.

L'auteur conserve la propriété du droit d'auteur et des droits moraux qui protège cette thèse. Ni la thèse ni des extraits substantiels de celle-ci ne doivent être imprimés ou autrement reproduits sans son autorisation.

In compliance with the Canadian Privacy Act some supporting forms may have been removed from this thesis.

While these forms may be included in the document page count, their removal does not represent any loss of content from the thesis.

Conformément à la loi canadienne sur la protection de la vie privée, quelques formulaires secondaires ont été enlevés de cette thèse.

Bien que ces formulaires aient inclus dans la pagination, il n'y aura aucun contenu manquant.

Canada

Abstract

This thesis deals with optimal grade transition policies for an EVA polymerization process. The grade transition problem has been studied by many authors. However, very few, if any, of these strategies have been implemented because the solutions overlook some practical problems faced by manufacturing facillities. This research was carried out in several stages, each of which complemented to assist in the final objective of achieving optimal grade transitions. First and foremost, the computing infrastructure at the plant was upgraded to ensure that all pertinent data was archived. This was necessary to make sure that the model developed as part of this research project could be validated with real plant data. The data archiving facility was also needed for the design and development of a data-based soft sensor.

The most significant contributions were made in the development of a first principles model for the high pressure stirred autoclave polymerization plant. The model was built using a commercial software package in close collaboration with plant personnel

to ensure it was practical, usable and sustainable. This model was used to develop optimal grade transition policies which were implemented on the actual plant.

A melt index soft sensor has been developed, implemented and has been in operation at the plant since January 2006. The soft sensor gives an indication of the change in melt index nine (9) minutes before the online instrument. The optimal grade transition strategies have been implemented for two specific grade changes. One of the cases has shown the ability to reduce the off-specification product by over fifty (50) percent in a successful plant trial. An economic analysis of this was done and it was conservatively estimated that implementing grade transition policy for one production line alone would increase the plant's annual revenue by over one hundred and sixty thousand dollars. The plant comprises five production lines and therefore the potential annual savings are enormous.

The developed mechanistic model is widely applicable and can be used for many other simulation and control studies, while the multivariate data based model developed is more applicable for online predictive control and specific optimal grade changes.

Acknowledgements

I would like to think my supervisors, Professor Sirish Shah and Professor Uttandaraman Sundararaj for their constant support, patience, guidance and enlightening advice during my PhD studies at the University of Alberta. Their continuous sacrifice of their time was invaluable in assisting me in making the right decisions at critical points during the course of my studies and research. Their detailed review, insightful suggestions, supportive attitude and interest in my work made it a pleasure to have them as my supervisors. I would also like to thank Mrs. Shah and Mrs. Sundararaj for entertaining me at their respective homes; these times fostered a wonderful social and welcoming atmosphere in the relationship with my supervisors.

During my initial years at the University of Alberta I took and audited many courses. I would like to thank Professors Huang, Mizera, Nandakumar, Meadows, Forbes, Yeung, Zhao Marquez, Sundararaj, Mather, McCaffrey, Hayes, Nelson, Mather, Drs. Yip, Tangirala and Breuer for teaching me the fundamentals which were necessary for my research and equipping me with the tools necessary for a successful career.

I would like to thank Professor Kannan Moudgalya whose advice, assistance and motivation were very inspirational in the early stages of my research.

During the course of this research I was able to interact closely with several industrial partners. I would like to thank Brent West of AT Plastics Inc. for his confidence in

my abilities, guidance and encouragement at the plant. Also I would like to thank Dr. Larry Vande Griend, Dave Rozak, Dr. Carl Watkins, Dirk Hair, Vince Mullen, Dave Gets, Colin Sikora, Yi-Jun Sun, Wei Liu, Emil Erdmann, Mike Payne, Darcy Pacholok of AT Plastics Inc. for their support. I would like to thank Dr. Sundaram Ramanathan and Simon Lingard of Aspen Technology Inc, for their support, advice and constant correspondence during the course of my research, without their assistance the modeling work would not have been possible. Also at Aspen Technology I would like to thank Dean Henley and Noel Phillips. I would like to thank Greg Caskey, Dr. Dave Shook and Dr. Rohit Patwardhan at Matrikon Inc. for their support. I would like to thank Larry Neumeister at Spartan Controls Inc for his advice, support and confidence.

My colleagues in computer process control group at the University of Alberta were always full of advice and motivational comments. I have built friendships there which I will cherish for the rest of my life. I would like to mention Hari, Shoukat, Weihua, Hancong, Edward, Monjour, Wesley, David, Rumana, Fangwei, Ruoyu, Yutong, Sadiq, Salim, Sayed, Vinay, Bushan, Adrian, Enayet, Hailei, Sansal, Gbenga, Mridul, Iqbal, Phanindra, Sankar, Karteek, Saneej, Venkat and Boyi.

I would like to acknowledge the financial support by AT Plastics Inc and NSERC through an Industrial Post Graduate Scholarship and the NSERC-Matrikon-Suncor senior industrial research chair program.

I would most importantly like to thank God for the remarkable things he has done in my life. I would like to thank Lana for her love and support, my parents, my brothers Ron and Okon and my sister Megan for their constant love and understanding.

To:

God and my family, your constant love support and understanding has been my source of strength

Table of Contents

***CHAPTER 1* INTRODUCTION** **1**

1.1 PRESENT STATE OF THE LDPE MARKET 3

1.2 MOTIVATION 5

1.3 PROCESS DESCRIPTION 8

1.4 THESIS OUTLINE 10

***CHAPTER 2* PROCESS DATA ARCHITECTURE AND APPLICATIONS** **12**

2.1 INTRODUCTION 12

2.2 DATA ACCESS AND VISUALIZATION 13

2.2.1 OPC Data Communications *13*

2.2.2 Process Data *14*

2.2.3 Alarm and Event Chronicle *16*

2.2.4 Batch Data Analysis *17*

2.2.5 Data Visualization *17*

2.3 LABORATORY INFORMATION INTEGRATION 19

2.3.1 ODBC Interface *19*

2.3.2 LIMS Views and Data Exchange *19*

2.4 APPLICATION – CONTROLLER PERFORMANCE MONITORING 20

2.4.1 Reactor Loop Performance leading up to Decomposition *21*

2.4.2 Unit Process Stabilization *24*

2.5 APPLICATION – PLANT CALCULATIONS 28

2.5.1 Compressor Mass Flow Model *28*

2.5.2 Zone Mixing Index *30*

2.5.3 Plant Production *32*
2.5.4 Analyzer Corrections *33*
2.5.5 CTA concentration in Reclaimed VA *35*
2.5.6 Initiator Mass Flow Rate *36*
2.6 CHAPTER SUMMARY 37

***CHAPTER 3* FIRST PRINCIPLES MODELING OF EVA POLYMERIZATION 38**

3.1 INTRODUCTION 38
3.2 POLYMER SIMULATION IN COMMERCIAL PACKAGES 40
3.3 INTRODUCTION TO THE MODELING PROCEDURE 42
3.4 MODEL COMPONENTS 43
3.5 THERMODYNAMIC MODEL PROPERTIES 44
3.6 SOAVE-REDLICH-KWONG EQUATION OF STATE 48
3.6.1 SRK Theory *48*
3.6.2 SRK Pure Component Parameters *48*
3.6.3 SRK Binary Interaction *49*
3.7 PERTURBED CHAIN STATISTICAL ASSOCIATING FLUID THEORY EQUATION OF STATE 51
3.7.1 PC-SAFT Theory *51*
3.7.2 PC SAFT Pure Component Parameters *54*
3.7.3 PC SAFT Binary Interaction *55*
3.8 FUNDAMENTALS OF FREE RADICAL POLYMERIZATION MODELING 57
3.8.1 Reaction Kinetics *57*
3.8.2 Summary of Relevant Free Radical Kinetic Parameters from Literature *60*
3.9 POLYMER DISTRIBUTION CALCULATION 66
3.10 INITIATOR DIFFUSION CORRELATIONS 67
3.11 INCORPORATING POOR ZONE MIXING 70
3.11.1 The Floating Zone *70*
3.11.2 Model Modification *71*
3.12 CHAPTER SUMMARY 74

***CHAPTER 4* FIRST PRINCIPLES MODEL REGRESSION 75**

4.1 INTRODUCTION 75
4.2 MODEL VALIDATION VARIABLES 76
4.2.1 Compressor Mass Flow Rate *77*
4.2.2 MI Correlation *78*
4.2.3 Model VA Percentage *81*
4.2.4 Initiator Mass Flow Rate *82*
4.3 MODEL CONFIGURATION 82

4.3.1 Configuration of the Steady State Model 82
4.3.2 Configuration of the Dynamic Model 85
4.4 MODEL REGRESSION 86
4.4.1 Aspen Plus Regression Theory 88
4.4.2 Parameter Sensitivity 90
4.4.3 Iterative Multiple Grade Model Regression Scheme 94
4.4.4 Steady State Model – Regressed Parameters 101
4.5 MODEL VALIDATION 106
4.5.1 Validation of the Steady State Model 106
4.5.2 Dynamic Model – Regressed Parameters 110
4.5.3 Validation of the Dynamic Model 112
4.6 CUSTOM MODELING IN ASPEN DYNAMICS 114
4.6.1 Support for Vapour Phase Polymerization 114
4.6.2 Dynamic Autoclave Modeling Using CSTR's 114
4.6.3 Dynamic Heat Exchangers 115
4.7 CHAPTER SUMMARY 116

***CHAPTER 5* SOFT SENSOR AND DATA BASED MODEL 117**

5.1 INTRODUCTION 117
5.1.1 Soft Sensor Motivation 118
5.1.2 Polymer Soft Sensors 119
5.2 THE EXTRUDER 120
5.3 SOFT SENSOR MODEL STRUCTURE 122
5.3.1 Variable Correlation and Lags 122
5.3.2 Model Disturbances 125
5.3.3 The Basic Model 127
5.3.4 Speed and Temperature Compensated Model 127
5.4 NONLINEAR LEAST SQUARES REGRESSION 129
5.5 BIAS UPDATING OF THE MODEL 131
5.5.1 Online Analyzer Bias 131
5.5.2 Laboratory Bias 132
5.5.3 Unified Bias Update 133
5.6 SOFT SENSOR VALIDATION 137
5.7 THE STATE SPACE MODEL 141
5.7.1 Introduction 141
5.7.2 Overview of Subspace Identification 142
5.7.3 Data Pre-processing 143
5.7.4 The Identified Model 145

5.7.5 Validation of the State Space Model *146*

5.8 CHAPTER SUMMARY 151

***CHAPTER 6* DYNAMIC OPTIMIZATION, RESULTS AND PLANT IMPLEMENTATION .152**

6.1 INTRODUCTION 152

6.2 DYNAMIC OPTIMIZATION 155

6.2.1 Fundamentals *155*

6.2.2 Control Vector Parameterization *156*

6.2.3 Objective Function Formulation *158*

6.3 GENERATION OF OPTIMAL TRAJECTORIES 160

6.3.1 Optimizer Configuration *160*

6.3.2 Optimizer Algorithms *161*

6.3.3 Optimizer Tuning *162*

6.3.4 Grade Transitions Considered *163*

6.4 OPTIMIZER SIMULATION RESULTS 163

6.4.1 Simulated Grade Change - #1 ..... *163*

6.4.2 Simulated Grade Change - #2 ..... *167*

6.4.3 Simulated Grade Change - #3 ..... *169*

6.5 PLANT TRIAL OF OPTIMAL POLICIES 172

6.5.1 Plant Trial - #1 ..... *172*

6.5.2 Plant Trial - #2 ..... *176*

6.6 ANALYSIS OF THE PLANT TRIALS 181

6.6.1 Discussion on Implementation of Optimal Trajectories *181*

6.6.2 Economic Analysis *184*

6.7 CHAPTER SUMMARY 185

***CHAPTER 7* CONCLUDING REMARKS AND FUTURE WORK 186**

7.1 MAJOR CONTRIBUTIONS 186

7.2 GENERALIZATION OF THE OPTIMAL GRADE TRANSITION METHODOLOGY 188

7.3 RECOMMENDATIONS 190

7.3.1 Additions and Modifications to the First Principles Model *190*

7.3.2 Dynamic Modeling Extensions *191*

7.3.3 Data Based Modeling and Control *192*

7.3.4 Extruder Modeling *193*

7.3.5 First Principles Model Based Soft Sensor *193*

7.3.6 Optimizer Modifications *194*

7.3.7 Plant Modifications *194*

7.4 CONCLUDING REMARKS 195

LIST OF REFERENCES **197**

APPENDIX A PARAMETER ESTIMATION DETAILS **204**

A.1 DATA SETS USED 204

A.2 PARAMETER SOURCES 206

List of Tables

Table 1-1 – LDPE End Use Applications (Ek 2002) 3
Table 1-2 – Downgrade descriptions 7
Table 2-1 – Historian Point Configuration 15
Table 2-2 – LIMS and Historian Data Exchange 20
Table 2-3 – ProcessDoctor Report 23
Table 3-1 – Simulation Packages and Features 41
Table 3-2 – Model Component Summary 44
Table 3-3 – Thermodynamic Equation of State Assignment 47
Table 3-4 – SRK Pure Component Parameters 49
Table 3-5 – SRK Binary Interaction Parameters 50
Table 3-6 – PC-SAFT Pure Component Parameters (Tumakaka and Sadowski 2004) 55
Table 3-7 – PC SAFT Binary Interaction Parameters 56
Table 3-8 – Polymerization Kinetics 58
Table 3-9 – Literature Free Radical Kinetics for Ethylene 1 62
Table 3-10 – Literature Free Radical Kinetics for Ethylene 2 63
Table 3-11 – Literature Free Radical Kinetics for Vinyl Acetate 64
Table 3-12 – Literature Free Radical Kinetics for Propylene 65
Table 3-13 – Literature Free Radical Reactivity Ratios 65

Table 3-14 – Regressed Gel Effect Parameters 69
Table 4-1 – Validation Variables 77
Table 4-2 – Melt Index Correlation Data 78
Table 4-3 – Dynamic Equipment 86
Table 4-4 – Estimation Parameter to Variable Pairing (Hendrickson 1997) 90
Table 4-5 – Parameter to Variable Coupling for Regression 93
Table 4-6 – Regressed Free Radical Kinetics 1 102
Table 4-7 – Regressed Free Radical Kinetics 2 103
Table 4-8 – Regressed Free Radical Kinetics 3 104
Table 4-9 – Regressed Free Radical Kinetics 4 105
Table 4-10 – Regressed PC-SAFT Binary Interaction 105
Table 4-11 – Dynamic Model Regression Results 110
Table 4-12 – Manipulated Variables Effect on Model 112
Table 5-1 - Extruder variables correlation and lag with log of rheometer measured melt index 123
Table 5-2 – Identification and Validation Data Set Details 145
Table 5-3 – Control Scheme for the State Space Model 150
Table 6-1 – Grades Considered for Dynamic Optimization 163
Table 6-2 - Implemented Change #1 Plan (values scaled) 173
Table 6-3 – Implemented Change #2 Plan (values scaled) 176
Table 6-4 – Grade Change #2 Implemented Strategy (values scaled) 178
Table 6-5 – Economic Analysis 185

List of Figures

Figure 1-1 – Market growth for LDPE produced in low and high pressure processes (Meyers 2005) 4
Figure 1-2 – Ethylene Prices and Volatility (Source: Platts 2005 and GlobalView Software) 5
Figure 1-3 – AT Plastics Downgrade Distribution – 2005 6
Figure 1-4 – Plant Flowsheet 9
Figure 2-1 – Current Historian and DCS Architecture 14
Figure 2-2 – Revised System Architecture 18
Figure 2-3 – ProcessDoctor Treemap view of 33 regulatory control loops critical to 5R reactor 22
Figure 2-4 – Separation Vessel Schematic 25
Figure 2-5 – Control Before and After Positioner Change 26
Figure 2-6 – Control After Tuning with New Positioner 27
Figure 2-7 – Secondary Compressor Schematic 28
Figure 2-8 – Compressor Flow Model Flow Chart (* -Benzler and Von Koch 1955) 29
Figure 2-9 – Autoclave Segment (poor mixing variables) 30
Figure 2-10 – Reactor Mixing Index 31
Figure 2-11 – Test Hopper Configuration (used for mass flow calculation) 32
Figure 2-12 – VA Measurement Correction 34

Figure 3-1 – First Principles Modeling Steps 43
Figure 3-2 – Aspen Plus Steady State Plant Flow Sheet 46
Figure 3-3 – Depiction of segment-segment interaction in SAFT and PC-SAFT (Aspen Technology 2002) 52
Figure 3-4 – Diagram of Free Radical Reactions 59
Figure 3-5 – Initiator 2 Diffusion Correlation 69
Figure 3-6 – Initiator 3 Diffusion Correlation 70
Figure 3-7 – Floating Zone 71
Figure 3-8 – Modeling Poor Zone Mixing 72
Figure 3-9 – Poor Initiator Mixing Profile 73
Figure 4-1 – Melt Index Correlation with M_n and M_w Plot 79
Figure 4-2 – ln(MI) to M_n Correlation Plot 80
Figure 4-3 – ln(MI) to M_w Correlation Plot 81
Figure 4-4 – Reactor Flow Sheet 83
Figure 4-5 – Reactor Groups for Regression 84
Figure 4-6 – Trust Region Optimization 88
Figure 4-7 – Quality Variable Sensitivity to Plant Conditions 91
Figure 4-8 – M_n Sensitivity to β-Scission 92
Figure 4-9 – Flowchart for Regression 94
Figure 4-10 – Reactor Regression Scheme 97
Figure 4-11 – Full Plant steady State Model Regression Scheme 99
Figure 4-12 – Dynamic Model Regression 100
Figure 4-13 – Floating Zone Temperature Validation 107
Figure 4-14 – Reactor Conversion Validation 107
Figure 4-15 – Percentage VA Validation 108
Figure 4-16 – Melt Index Validation 108
Figure 4-17 – Steady State Full Plant Model Validation 109
Figure 4-18 – Dynamic Model Flow Sheet 111
Figure 4-19 – Dynamic Model Validation 113
Figure 4-20 – Dynamic Heat Exchanger 116
Figure 5-1 – Extruder Schematic 121

Figure 5-2 – Visual Inspection Plot for Time Delay 124
Figure 5-3 – Delay Estimation Algorithm for two Extruder Variables 125
Figure 5-4 – Disturbances effecting Extruder Variables 126
Figure 5-5 – Time Weighting factor for Bias 134
Figure 5-6 – Bias updating flow sheet (30 min. execution period) 136
Figure 5-7 – Soft Sensor during a Cooler Cook Event 137
Figure 5-8 – S and T Compensated Model Dynamic Validation Plot 138
Figure 5-9 - S and T Compensated Model Validation Plot (several grades) 139
Figure 5-10 – Soft Sensor & Bias Update During a Grade Change 140
Figure 5-11 – Block Diagram of State Space Model (Cock and Moor 2003) 142
Figure 5-12 – Data Based Model Identification Steps 143
Figure 5-13 – Schematic of the Plant Model 145
Figure 5-14 – State Space Model Validation (∞ step ahead prediction horizon) 147
Figure 5-15 – State Space Model Validation (5 steps ahead prediction horizon) 147
Figure 5-16– State Space Model Validation (20 steps ahead prediction horizon) 148
Figure 5-17 – Pressure and ln(MI) model correlation 148
Figure 5-18 – Propylene Flow and ln(MI) model correlation 149
Figure 6-1 – Manipulated Variables for Simulated Grade Change - #1 165
Figure 6-2 – Controlled Variable for Simulated Grade Change - #1 166
Figure 6-3 – Manipulated and Controlled Variables for Simulated Grade Change - #2 168
Figure 6-4 – Manipulated Variables for Simulated Grade Change - #3 170
Figure 6-5 – Controlled Variable for Simulated Grade Change - #3 171
Figure 6-6 – Operator Implemented Grade Change 174
Figure 6-7 – The Implemented Optimal Grade Change 175
Figure 6-8 – Optimal Policy for Plant Implementation #2 177
Figure 6-9 – Operator Implemented Grade Change #2 179
Figure 6-10 – The Implemented Optimal Grade Change #2 180
Figure 6-11 – Trial #2 – MI 182
Figure 6-12 – Trial #2 – VA 182

List of Symbols

P	absolute pressure (bar)
E_a	activation energy (J/kmol-K)
ΔV	activation volume (m^3/kmol)
X_{Avg}	average of quantity X over some specified time period
$k_{i\alpha j\beta}$	binary interaction parameter between different polymer segment types α and β of component i
X^i_{SF}	component i segment mole fraction in polymer
M^i_{Wseg}	component i segment molecular weight
Z	compressibility factor
P_C	critical pressure (bar)
T_C	critical temperature (^oC)
β_{Zij}	Flow split fraction from zone i to zone j
k_{ij}	general binary interaction parameter
R	ideal gas constant (J/kmol-K)
ε_{ij}	interaction energy
$\dot{M}_X$	mass flow of component or stream X

x_A mass fraction of component A

X^i_{MP} mass percent of component i in polymer

MI Melt Index

M_N Number average molecular weight

N_{seg} number of segments in polymer

k_o pre-exponential factor (1/sec – first order reactions, m^3/kmol-s – second order reaction)

x scalar

$\|\mathbf{F}(\mathbf{x})\|_2^2$ second norm of $\mathbf{F}(\mathbf{x})$ squared

S speed (RPM)

T temperature (K)

t_E time at which event E occurred

X_{SPOT} value of quantity X acquired the last time a SPOT was entered

X_t^n value of the n^{th} instance of X at time t

$\mathbf{x}$ vector or matrix

v volume (m^3/mol)

M_W Weight average molecular weight

$Zero_{SD}$ Zero mixing index spatial standard deviation (°C)

Za_{Mxl} Zone 'a' mixing index (%)

Za_{SD} Zone 'a' temperature spatial standard deviation (°C)

List of Abbreviations

CFD – Computational Fluid Dynamics

CSTR – Continuously stirred tank reactor

CTA – Chain Transfer to Agent

CVP – Control Vector Parameterization

DCS – Distributed Control System

EOS – Equation of State

EVA – Ethylene Vinyl Acetate

GPC – Gel Permeation Chromatography

GUI – Graphical User Interface

HPS – High Pressure Separator

HPS- Low Pressure Separator

HYSQP – Hybrid SQP

ICI – Imperial Chemical Industries

LCN – Local Control Network

LDPE – Low Density Polyethylene

LIMS – Laboratory Information Management System

LP-CLR – Low Pressure Cooler

MIMO – Multiple inputs, multiple outputs

MPC – Model Predictive Control

MWD – Molecular Weight Distribution

N4SID – Numerical algorithms for subspace system identification

NLP – Nonlinear Programming

ODBC – Open Database Connectivity

OLE – Object Linking and Embedding

OPC – OLE for Process Control

PC-SAFT – Perturbed Chain Statistical Associating Fluid Theory

PV – Process Variable

PVA – Polyvinyl acetate

QP – Quadratic Programming

RGC – Return Gas Cooler

RPI – Relative Performance Index

SAFT – Statistical Associating Fluid Theory

SISO – Single input, single output

SPOT – QC laboratory reading for a quality variable

SQL – Structured Query Language

SQP – Successive Quadratic Programming

SRK – Soave-Redlich-Kwong

TPN – Total Plant Network

VLE – Vapour Liquid Equilibrium

Engineers participate in the activities which make the resources of nature available in a form beneficial to man and provide systems which will perform optimally and economically.

L. M. K. Boelter, 1957

Chapter 1

Introduction

Advanced control techniques have been relatively under-utilized in polymer manufacturing compared to other large scale process industries. This is due to the complex operating characteristics and inherent nonlinearity of the process which makes well developed linear control theory difficult to apply. Polymer materials have been playing an increasingly important role in all aspects of modern life. As a result, efficient production of a polymer with tailored properties has become important to manufacturing plants. Polymer manufacturing processes fall into different classifications, mostly based mostly on the type of reactors, chemical reactions and the properties of the products which can be produced.

Natural polymers have always existed; these include DNA, RNA, proteins and polysaccharides. Properties of polymers have attracted attention as early as the 1820's. One of the earliest documented studies was by Thomas Hancook who

discovered that when high shear forces are applied to natural rubber its viscosity reduces (Young and Lovell 1991).

Low Density Polyethylene (LDPE[1]) was an unexpected discovery in the early 1930s by ICI. Fawcett and Gibson of ICI were granted a patent for its discovery in 1936. At that point there was no specified market for the polymer (Meyers 2005). However, its electrical insulation properties coupled with attractive mechanical properties made it very attractive for cable insulation. The original LDPE reactors were based on a high pressure CSTR (autoclave) design. These rectors have been developed extensively and the main reactors used currently are autoclaves and tubular (plug flow) reactors.

This research is focused on the modeling and control aspects of optimal grade transition strategies for a particular polymerization reactor. The major aspects covered here include the infrastructure required for collection and dissemination of plant data, first principles and data based modeling of a high pressure autoclave polymerization process and the generation of optimal grade transition strategies. The reactor examined is a high pressure polymerization reactor based on an ICI license. These reactors operate in the temperature range of 150 to 300 ^{o}C and pressures ranging from 1200 to 1700 bars. Care is taken not to exceed the 300 ^{o}C boundary because at high temperature combined with high pressure a violent uncontrollable reaction can occur. This results in the breakdown of ethylene molecules to carbon, and is called a reactor decomposition. This reactor has the capability of producing LDPE grades with melt indices ranging from 0.3 to 2000 and copolymer EVA grades ranging from 0 to 28% vinyl acetate content. The grades considered here were only EVA grades ranging from 16 to 28%. At the core of this process is the free radical polymerization of ethylene and vinyl acetate to form EVA. The properties of the final product depend on the plant's operating conditions such as reactor temperatures, reactor pressure and flow rates of components to the reactor. By changing reactor conditions, we can tailor the properties of the polymer.

There has been a significant amount of research into the physical properties and reaction mechanisms of LDPE, and on computer simulations on and efficient control

[1] LDPE will be used as a general term to represent homopolymers and EVA copolymers.

of the LDPE polymerization production process. However, it should be noted that not much of the research has involved actual industrial data or has been actually applied to operating facilities. Another important factor is the use of two main forms of reactors (tubular and autoclave). The majority of the research and advanced modeling has been done on tubular reactors. This research was performed in close collaboration with industry. Thus the solutions developed are well suited for implementation and sustainability at an operating facility.

1.1 Present State of the LDPE Market

LDPE applications have become very widespread. Table 1-1 gives a summary of some of the current main commercial applications of LDPE. Polyethylene is the most common polymer worldwide and has received the most attention by academics in the polymer literature.

Application	Use
Film	65%
Extrusion coating	10%
Other extrusion	8%
Injection moulding	7%
Blow moulding	4%
Others	6%

Table 1-1 – LDPE End Use Applications (Ek 2002)

Figure 1-1 shows the past and predicted LDPE growth. It is clear that the LDPE market has maintained sustained growth and it is predicted to continue doing so.

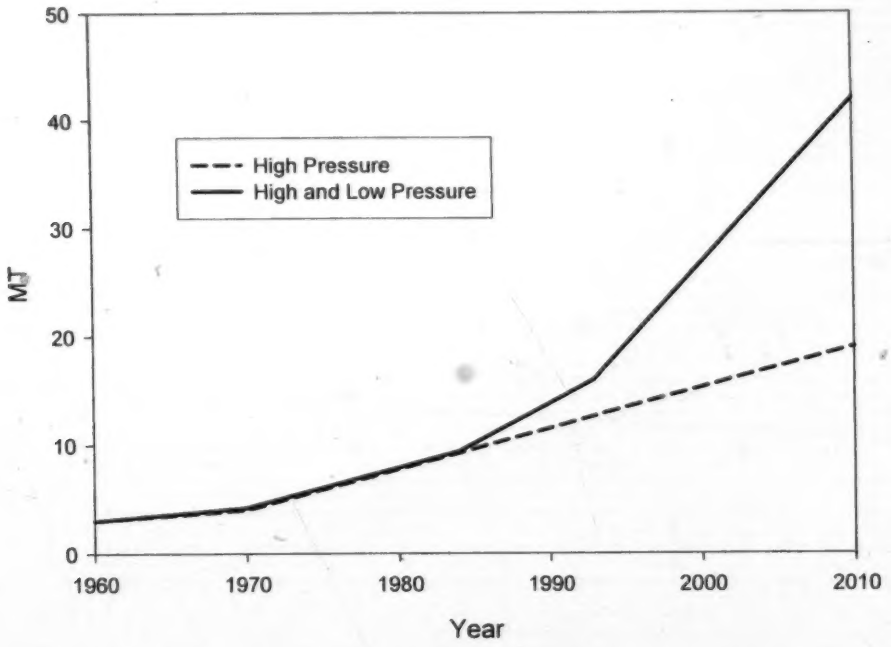

Figure 1-1 – Market growth for LDPE produced in low and high pressure processes (Meyers 2005)

In 1990, polyethylene production was estimated at approximately 25 million tonnes per year: 65% of this was low density made in high pressure reactors and 35% was high density homopolymer and linear-low density polyethylene manufactured in low pressure reactors (Kiparissides et al. 1993).

The main raw material used in the production of LDPE is ethylene. Ethylene prices have been very volatile over the last decade (Figure 1-2). This price has been dependent on many factors which include ethylene supply and demand, polymer supply and demand and the political stability of the regions where certain key producers are located. This volatility makes profit margins very difficult to predict. Therefore, manufactures must to operate at the lowest possible operating cost to guarantee certain profit margins.

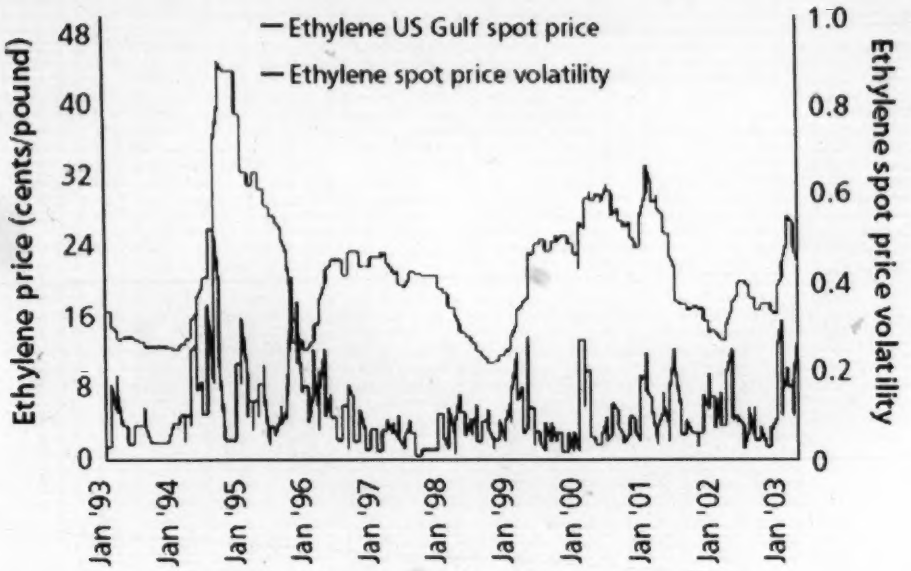

Figure 1-2 – Ethylene Prices and Volatility (Source: Platts 2005 and GlobalView Software)

1.2 Motivation

A polymer manufacturing plant usually includes many elements which are similar to other manufacturing plants such as refineries. However, one characteristic which sets most polymer plants apart is the frequent requirement to produce different products. There are now certain polymers which are classed as commodity polymers; these usually have large production requirements. Another classification is speciality polymers; which usually have small production requirements. Thus, commodity polymers are typically produced in high throughput facilities that are not required to produce products with different quality specifications very regularly. However, the facility considered here like many other polymer plants produces a mix of commodity and specialised polymers based on the customer needs. This requirement forces the plant to run frequently varying production campaigns. The period during the change in product from one grade specification to another is known as the grade change.

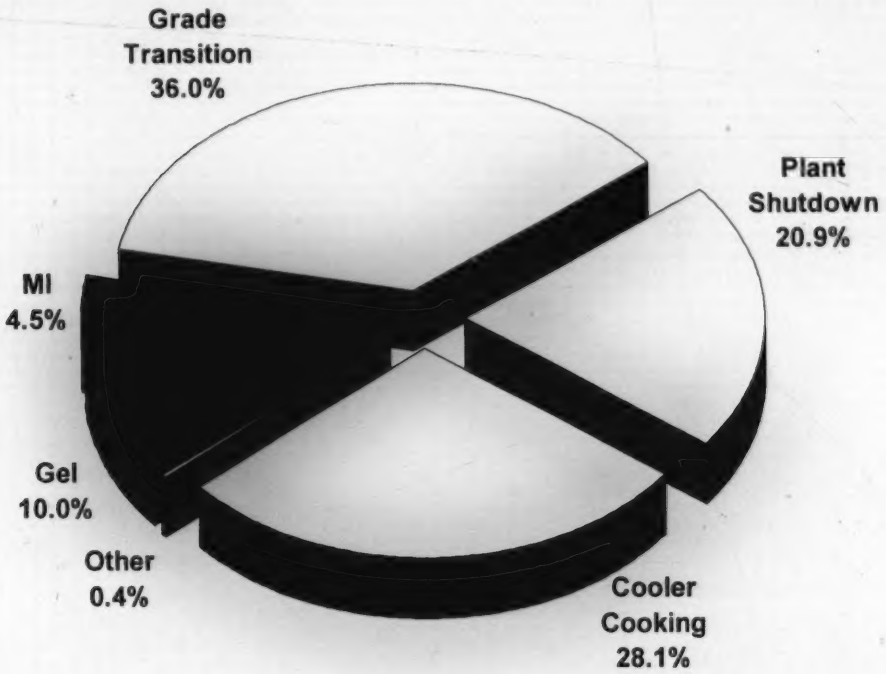

Figure 1-3 – AT Plastics Downgrade Distribution – 2005

The product produced during this period usually cannot be sold at the usual profit margins. Figure 1-3 shows the distribution of the downgrade product at the AT Plastics 5R plant for 2005. The downgrade due to grade changes accounted for 36% of the total downgrade and was the largest contributor. Table 1-2 gives a description of the classifications used for the analysis of the downgrade distribution.

DOWNGRADE REASON	DESCRIPTION
Grade Transition	Off specification product produced due to a grade change (includes plant shutdown downgrade if shutdown was required to make the grade change)
Plant Shutdown	Off specification product produced due to plant shutdown or start-up
Cooler Cooking	Off specification product produced due to heat exchanger de-fouling (does not include gel)
Other	Off specification product produced due to an unclassified reason.
Gel	Off specification product produced due to the product gel count out of specification
MI	Off specification product produced due to melt index out of specification (usually caused by poor controller performance)

Table 1-2 – Downgrade descriptions

Therefore, the financial impact of more efficient (optimal) grade transitions is clear. This research was focused on this problem and methods for creating optimal grade transitions.

This problem has been addressed by many authors using different perspectives. The main method used has involved the use of a detailed first principles model to build a dynamic simulation which was used as the basis for optimization. This has become more feasible as dynamic modeling in commercial packages had matured (Chen 2002).

Other authors have used commercial packages for dynamic simulations; Chatzidoukas et al. 2003 used gPROMS for grade transition optimization in a gas-phase olefin polymerization fluidized bed reactor. Aspen Dynamics was used by Khare et al. 2002 for dynamic simulation and grade transition optimization of slurry

high-density polyethylene (HDPE) process. There have been many authors who have published results on the implementation of optimal control trajectories (Chen and Huang 1981; MacGregor et al. 1984; Kravaris et al. 1989; Ponnuswamy et al. 1987; Kozub and Macgregor 1992; McAuley and Macgregor 1993; Ohshima and Tanigaki 2000; Kiparissides et al. 2002; Chatzidoukas, Perkins et al. 2003). These were all simulation based implementation and they were not specific to the autoclave process.

The paper published by Cervantes et al. 2002 discussed the use of dynamic optimization of a large scale plant model to find the optimal grade transition strategies for a tubular LDPE plant. They created a detailed model of the plant; using mass and energy balance for all significant reacting components. The dynamic optimization problem was solved using simultaneous nonlinear programming. Orthogonal collocation was used to discretize the state variables. This strategy seemed promising; however, there are no published results for application to a LDPE autoclave with peroxide based initiators.

Chatzidoukas, Perkins et al. 2003 considered the optimal grade transition problem for a gas-phase olefin polymerization fluidized bed from the viewpoint of optimizing the traditional objective function to reduce the time required for a grade change. They also looked at the optimal pairing of control variables for every transition. This type of work has not been publicly documented for the LDPE autoclave process. Pladis and Kiparissides 1999 built a dynamic model for the autoclave that showed promise for simulating grade transitions; however, no optimization was performed. None of the documented work has been applied to a production facility.

1.3 Process Description

The work described here was based on a reactor located at AT Plastics Inc. site in Edmonton, Canada. The process is based on the ICI high pressure low density polyethylene autoclave process. A process flow diagram for the process is shown in Figure 1-4. The plant was designed to produce homopolymers and copolymer grades with up to 28% vinyl acetate having melt indices ranging from 0.3 to 2000.

The main monomers used are ethylene and vinyl acetate, and propylene is sometimes

used as a modifier. The fresh ethylene gas passes into the primary stock tank where it mixes with recycled gas from the booster compressor. Liquid propylene, if required for a particular polymer grade may be injected into the primary compressor suction line. The mixture is then compressed by the primary compressor.

Gas delivered from the primary compressor is then mixed with the intermediate pressure recycle gases before being further compressed by the secondary compressor. Gas from the secondary compressor is cooled prior to entering the reaction vessel. To make the EVA copolymers, liquid vinyl-acetate is injected into the secondary compressor suction line at a suitable rate to achieve the required grade.

The reaction vessel is a stirred autoclave. It is split into several mixing zones. The temperature of each of these zones is controlled by the injection of diluted solutions of organic peroxide catalysts into the zone. This initiates exothermic polymerization in the stirred reactor.

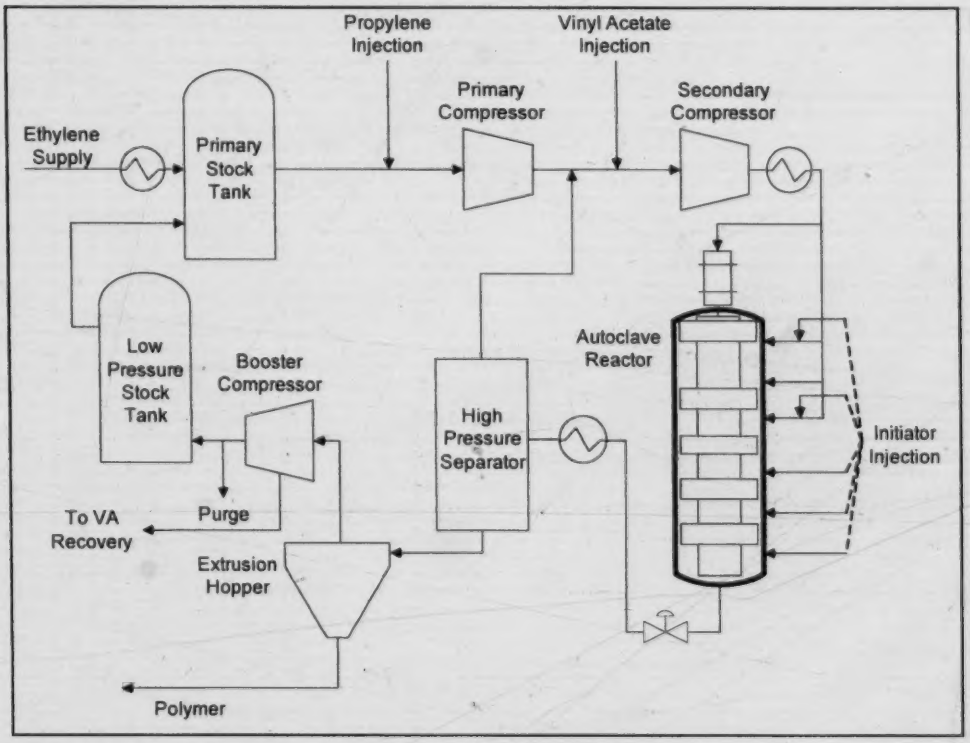

Figure 1-4 – Plant Flowsheet

Approximately 20% of the gas feed is converted to polymer in one pass. The

molecular weight of the polymer produced is controlled by the reactor pressure, temperature, reactor feed gas conditions and the use of vinyl acetate and propylene.
The mixture of gas and polymer leaving the reactor is reduced in pressure through a valve prior to entering the product cooler, where the mixture is cooled. The cooled product enters into a high pressure separator (HPS) where the bulk of the unconverted gas is separated from the polymer. The gas from the HPS is then recycled via the recycle system through the return gas coolers to the suction of the secondary compressor.
Molten polymer from the bottom of the HPS is passed to the extrusion hopper where further separation of gas and polymer takes place. The low pressure (LP) recycle gas returns to the low pressure stock tank which also receives gas from compressor gland leaks.
A purge gas stream is taken from the discharge of the booster compressor just prior to delivery to the primary stock tank. This is done to control the concentration of inerts (mainly ethane, methane carbon dioxide and propylene when necessary) that would otherwise build up in the reactor feed gas. The molten polymer from the extrusion hopper is fed into extruder where low molecular weight components are de-volatilized prior to pelletization.

1.4 Thesis Outline

This research reported in this thesis has transgressed several paths to a common goal. This would be reflected in the organization of the chapters. Chapter 2 gives details on the implementation of the plant historian and its integration with other plant systems. These include the OPC interface to the DCS, ODBC interface the plant LIMS and future plans for integration and data visualization. The purpose of installing this infrastructure was to collect process data for identification, monitoring and validation of process models. The first principles model is described in Chapter 3. Here details of the thermodynamics, reaction kinetics and modeling developments are given. Regression, validation and custom modeling are described in Chapter 4. In Chapter 5 the data based model is described. A soft sensor for the polymer melt index was built;

this was used to build a plant model using multivariable system identification. The application of the first principles model for designing optimal grade transition trajectories and the details on the dynamic optimization are detailed in Chapter 6. The results from the simulations and two plant trials are also shown and discussed. The optimal grade changes were compared with operator based changes, and analyzed. The major contributions of this body of work, future directions and conclusions are given in Chapter 7.

"Everything should be made as simple as possible, but not simpler."

Albert Einstein

Chapter 2

Process Data Architecture and Applications[2]

2.1 Introduction

One of the main objectives of this research project was to evaluate, design and implement optimal grade transitions control policies for a polymer process, with the AT Plastics high pressure polymerization unit as a candidate process. One critical item in path to achieve this objective was the information infrastructure necessary to facilitate the modeling and control activity at the AT Plastics plant.

An important requirement in any modeling exercise, whether the model is a mechanistic or an estimated one, is to be able to validate the model with actual plant data.

---

[2] Some of this chapter was presented at the *Matrikon MVP Conference*, May 2005, Edmonton, Canada by Alleyne et al.

An equally important requirement prior to evaluating and implementing the optimal or sub-optimal grade transition control policies is to make sure that the base regulatory control layer is configured correctly and is in a satisfactory operational state.

Both of these requirements necessitated the installation of an IT infrastructure at AT Plastics for data gathering and archiving. The architecture and systems installed for collection of plant data is described here. An important prerequisite for the model building and validation part of this research is the availability of process data. There were many data repositories at the plant site; these were integrated using different interfaces to give access to all relevant information. Two main applications using the information infrastructure will be described. These include controller performance monitoring and online calculations. The importance of these calculations will be emphasized later on, in the first principles and data based modeling work.

2.2 Data Access and Visualization

The plant uses a Honeywell TDC 3000 distributed control system (DCS). When the project began, we realised that the data collection and dissemination configuration was not adequate for the 'modeling, validation, control and monitoring objectives' of this project.

2.2.1 OPC Data Communications

OPC is an acronym for OLE (Object Linking and Embedding) for Process Control. This is a standard developed by the OPC Foundation for communication of process data between systems. There are many regulatory control vendors and advanced control vendors of systems used in plants. These systems make use of plant data through OPC communication. OPC allows the end user to have the freedom to choose a mix of systems without system interconnectivity issues.

There are many standards published by the OPC Foundation; the three main ones are OPC DA - Real-time Data Access (OPC Foundation 1998,OPC Foundation 1998), OPC AE - Alarm and Event (OPC Foundation 2002) and OPC HDA -Historical Data

Access (OPC Foundation 2001). As the names imply, DA is used for collection of real-time process data, AE for collection of alarms and events and HDA for historical data. Each standard has its application depending on the function required.

2.2.2 Process Data

The plant uses a Honeywell TDC 3000 DCS. OPC DA was used to acquire data from the DCS. A PC with a Honeywell K4LCN card was installed and connected to the Honeywell local control network (LCN). This PC also had Honeywell's App Solution Pack installed which includes the Honeywell TPN (Total Plant Network) server (OPC server).

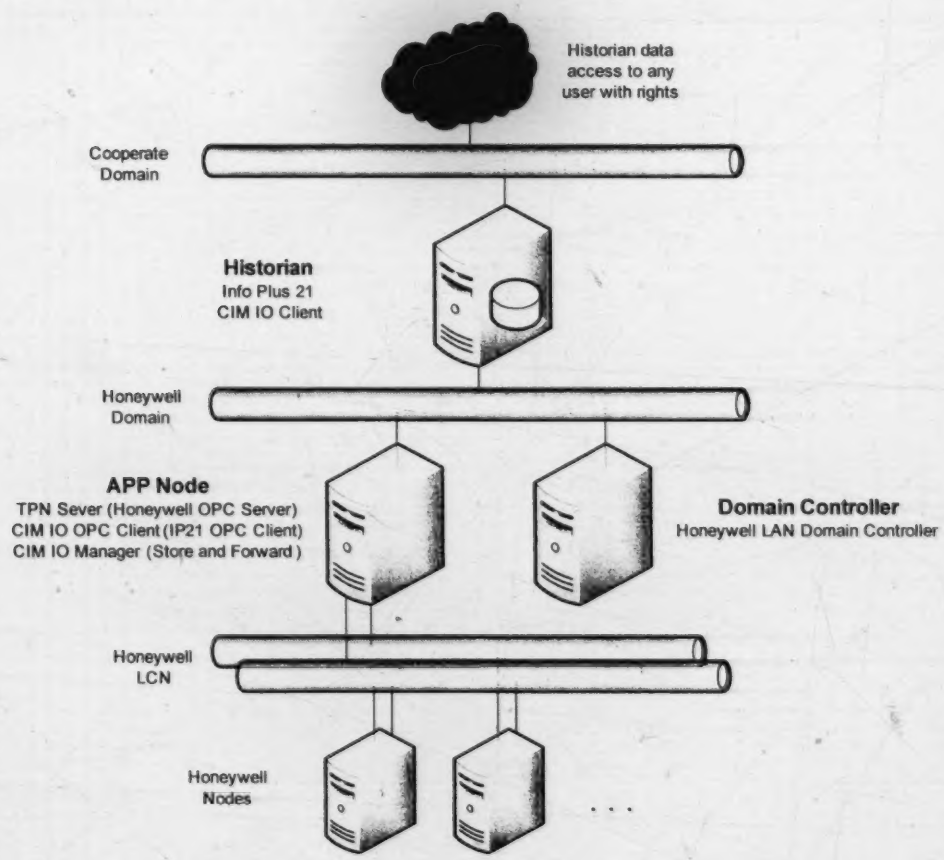

Figure 2-1 – Current Historian and DCS Architecture

Three plant Historians were evaluated: Honeywell's PHD, OSISoft's PI and Aspen Tech's Info Plus 21. Info Plus 21 was chosen mostly because of its reputation in the polymer industry, availability of advanced control solutions and support through a local vendor Matrikon Inc. Info Plus 21 uses CIM-IO to acquire data from any source.

The CIM-IO for OPC client was used to communicate with the Honeywell TPN Server. CIM-IO also supported additional features such as store and forward. This was very useful for this application and was implemented. This allowed a maximum of three days worth of data (based on the size of the store buffer, number of tags and frequency of updates) to be stored on the APP Node in a situation where communication with the Historian cannot be established. This architecture is shown in Figure 2-1.

All critical process data was collected once per second with no compression. This was mainly because it was anticipated there would be need for high time resolution uncompressed data for analysis. This gave an OPC throughput rate averaging around eight hundred (800) real reads per second. Table 2-1 gives a summary of the historian point configuration.

POINT TYPE	SAMPLE RATE (SECONDS)	Compression	Store at least every
Analog Process Data (Real)	1	No	NA
Critical Shutdown Points (Discrete)	1	Yes	30 minutes
Equipment Status (Discrete)	5	Yes	30 minutes
Controller Modes and Set Points	5	Yes	30 minutes

Table 2-1 – Historian Point Configuration

The historian was required to store a significant amount of data on a daily basis therefore as a result of this the server included 670 GB for archiving. This was configured using six hot swappable hard disks in a RAID five array configuration. This was anticipated to give at least two years of online data.

2.2.3 Alarm and Event Chronicle

This feature was not initially installed with the historian. However, after using the historian data for analysis of plant events, it was realised that it would be useful to have the alarm and operator logged data from the DCS stored on the historian as well. The design described below will be included in the next phase of historian improvement.

After evaluating the available solutions, Matrikon's ProcessGuard was chosen. This was based on the OPC link already being heavily loaded (based on Honeywell's recommendation of six hundred points per second). ProcessGuard would collect data directly from the DCS using one of its printer ports. The alarm strings would then be parsed, stored and analyzed by ProcessGuard. The system architecture is shown in Figure 2-2.

This solution would be useful for alarm management as well. This is a key area which can often be overlooked at most process plants until an event occurs. ProcessGuard will assist in management of the number and severity of alarms the operator receives. After collection of alarms for process events over a period of time, the alarm strategies can be modified to reduce nuisance alarms.

It is useful to note that the alarms would not be stored again on the historian; however they will be stored once in ProcessGuard and both systems will be time synchronized. The visualisation package, which is described later, collects data from Info Plus 21 and ProcessGuard to display the alarms and events along with the process trends. The timestamps of all data collected will be based on the DCS times. This is one of the features of OPC which allows the timestamps to be passed from the DCS to the Historian along with the values to be stored.

2.2.4 Batch Data Analysis

The AT Plastics site produces polymers in a semi-batch process. The reaction part of the process is continuous for a particular grade campaign; whereas the packaging is batch. Thus it is useful to store and compare data based on similar campaigns. This becomes more difficult as the number of campaigns increase. Thus a package for tracking and retrieving the data for similar campaigns becomes imperative for analysis. This was another point of difficulty realised once the historian was installed and in use. The batch tracking application will be installed in the next phase of historian improvements, mentioned previously.

Another important use of the batch system is for tracking decomposition events, cooler cooks and plant shutdowns. This can allow comparison of decompositions and the events causing them. This would allow easy data collection and analysis to facilitate the preventative detection and diagnosis of such events. Batch 21 from Aspen Technology Inc. was chosen as the application to be used. This package will also be integrated with the visualization package so that batch, alarm and process data can be available to the user.

Batch 21 uses a SQL server base. The batch start and end times are stored along with characteristics of the batch. This process operating data is only stored on the historian, the batch server uses a SQL based database to store the batch definitions. This ensures there is no duplication of data. The architecture for integrating the batch system with the current historian is shown in Figure 2-2.

2.2.5 Data Visualization

Once the data became available it was clear that a stable and easily maintainable system was required for dissemination of the plant data. Another important factor in deciding on the system was that the plant data should be integrated with other data sources on the site, one of the main systems being the SQL based LIMS (Laboratory Information Management System) system.

It was decided that a secure web-server environment should be used for the dissemination of data. In this architecture the user would only require an internet

browser to access and store the plant data on a local machine. This also reduced the maintenance since only the server needs to be maintained.

The application chosen to do this was Matrikon's ProcessNET. This application allows the visualization of the data on many data sources. There is no duplication of data on the ProcessNET server. This application will be used for viewing, querying, reporting and saving data from Info Plus 21, Batch 21, ProcessGuard, ProcessDoctor (will be described later) and WinLIMS. The architecture for this implementation can be seen in Figure 2-2.

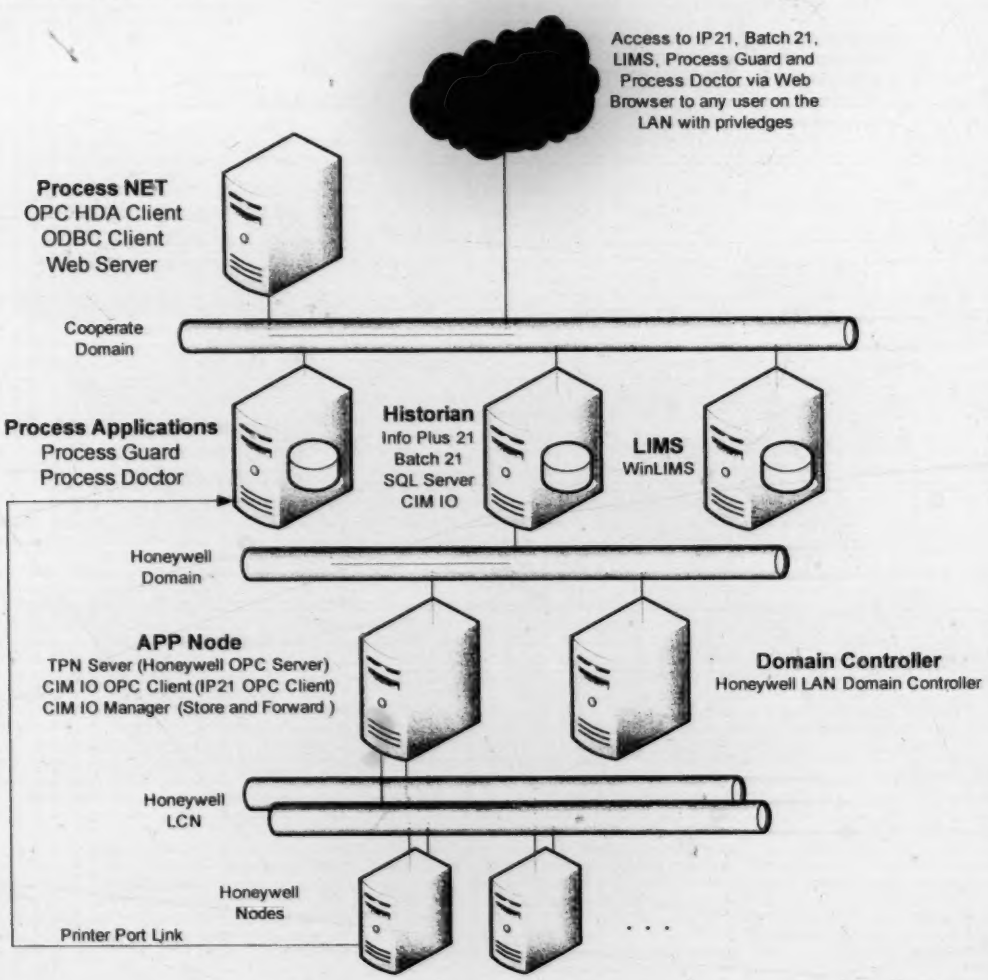

Figure 2-2 – Revised System Architecture

2.3 Laboratory Information Integration

The LIMS was implemented during the course of this project. It contained valuable information which was previously manually entered. This system was tightly integrated with the plant historian.

2.3.1 ODBC Interface

The LIMS system being used on the site is QSI's WinLIMS. This system stores the grade recipes, customer information, QC information and manages the lot and batch numbers. This information would be important for characteristics of each batch as well. Therefore there must be tight integration between the systems. The LIMS uses Microsoft SQL server as its database. This application allows external access using ODBC.

Info Plus 21 includes an application called SQL Plus. This application allows the writing of SQL queries for reading from and writing to the historian. It also supports communication with external ODBC databases and its queries can be scheduled in Info Plus 21. This application was used to create the link between Info Plus 21 and the LIMS.

2.3.2 LIMS Views and Data Exchange

There were several values required to be read from the LIMS into the historian. More efficient SQL queries were created by reading the values from the LIMS as a group rather than individually. Thus, the data had to be grouped on the LIMS. SQL supports a database item called a 'view'. These are virtual tables whose contents are populated by a query when they are accessed. These views can be accessed just as tables can from an external application using ODBC. Table 2-2 shows the configuration of the ODBC data exchange between the LIMS and the historian. The data exchange initiated by the historian is done using SQL Plus and is updated every minute (see the

appendix for the SQL Plus programs). The data exchange initiated by the LIMS is updated every ten minutes.

DATA	INITIATED BY	DATA SOURCE	DATA DESTINATION
Grade	LIMS	LIMS	Historian
Batch #	LIMS	Historian	LIMS
Batch Averages	LIMS	Historian	LIMS
Batch Start and End Time	LIMS	Historian	LIMS
Laboratory quality checks	Historian	LIMS	Historian
Quality limits	Historian	LIMS	Historian

Table 2-2 – LIMS and Historian Data Exchange

The data exchange between these systems is not required to be any faster than a batch change (typically in the range of 30 to 45 minutes). However the faster updates were used on the laboratory quality checks because these were critical for the bias update on the soft sensor (described in Chapter 5).

2.4 Application – Controller Performance Monitoring

With the goal of optimal grade transitions, the architecture of having a model based optimizing controller generate and write set point trajectories during grade transitions was envisioned. This optimizer will create the set point trajectories but not the final control action; this would remain the task of the Honeywell DCS. The DCS contains standard PID algorithms for regulatory control.

The performance of the advanced control depends heavily on the regulatory control performance. This has been well documented by Brisk 2004. This work indicated there have been great advances in control technology; the bottom line benefits on the plant could be increased by two to six percent of the operating cost by implementing this technology. The greatest opportunities were only achieved through good performance of the regulatory control layer.

Before any advanced control was attempted, the regulatory control at the plant was analysed using available commercial packages. The controllers were monitored and repaired to ensure acceptable performance.

At the AT Plastics plant site, it was clear that some loops were not performing as they should. However, without sufficient archived data to be analysed, no action was taken for years. With the installation of the historian, the historical data necessary for controller performance monitoring was now available.

Matrikon's ProcessDoctor was used for controller performance monitoring. This was done in conjunction with another project, whose goal was to find the root cause of a decomposition. An overview of the analysis done on thirty-three (33) control loops leading up to the time of the decomposition will be given. The diagnosis of the causes of decomposition in one case indicated significant interaction between control loops in a particular unit. This interaction was stabilized after repairing the problems diagnosed by an analysis using ProcessDoctor.

2.4.1 Reactor Loop Performance leading up to Decomposition

One of the first steps taken in the analysis of the decomposition was isolating the control loops critical to the reactor. This was done mostly based on process knowledge and meeting with operations and plant personnel. It was found that thirty-three loops were critical to the reactor operation. An analysis of these loops was done using ProcessDoctor. Figure 2-3 shows a tree map view of the thirty control loops critical to the 5R reactor. Here the larger size indicates the more important loops and the color gives an indication of the RPI (relative performance index). The RPI as calculated by ProcessDoctor, is a benchmark which compares the existing control loop performance with a reference control loop benchmark chosen by the user. The RPI is bounded by $0 \leq RPI \leq \infty$ with '<1' indicating deteriorated performance, '1' indicating no change of performance, and '>1' indicating improved performance (W. Mitchell 2004). This tree map view gives a clear indication of the critical control loops which could be the causes of process instability. Once this information is viewed, more detailed analysis can be done using reports.

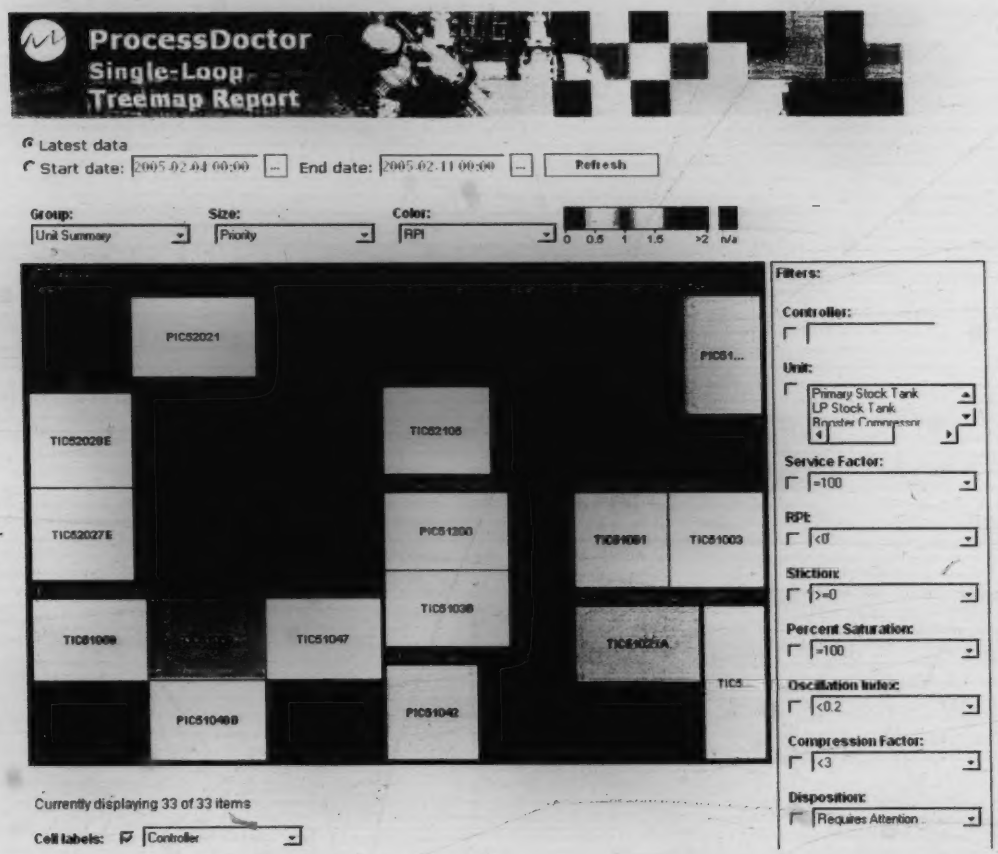

Figure 2-3 – ProcessDoctor Treemap view of 33 regulatory control loops critical to 5R reactor

Reports are flexible and can give a quick summary of important information related to the performance of relevant control loops. However, for the purposes of this discussion only the control loop oscillation period was important. Therefore, Table 2-3 shows the oscillation period found by ProcessDoctor with the associated control loop description and the ProcessDoctor analysis result. These analysis results are very useful as they can give an automated diagnosis of problems associated with the control loop, thus reducing the time required for solving plant problems.

Description	ProcessDoctor Analysis Result	Oscillation Period (min.)
Purge Flow Controller	Large Stiction. Oscillations. Large standard deviation.	2.24
Compressor Oil Cyclone	CV offset. High saturation (67%). Lack of capacity or poor tuning.	NA
3rd Stage Suction Separator	Oscillations. CV offset. High saturation (69%).	1.31
2nd Stage Suction Separator	Oscillations. Small CV offset. High saturation (49%).	17.52
Booster 1st Stage Suction Separator	Oscillations. High saturation (70%).	12.23
HP Separator Level Controller	Reasonable performance	
Primary Discharge Controller	Oscillations. Large settling time.	15.38
Primary Stock Tank Pressure	Oscillations. Large settling time.	30.25
Purge Separator Tank Pressure	Oscillations. Large stiction.	1.74
Reactor Pressure	Oscillations.	14.74
Zone 1A Temperature	Oscillations.	17.15
Zone 1B Temperature	Oscillations.	17.39
Zone 2 Temperature	Oscillations.	17.42
Zone 3 Temperature	Large settling time.	
Zone 4 Temperature	Large settling time.	

Table 2-3 – ProcessDoctor Report

From this report it was noticed that two major oscillation periods are present in the control loops critical to the reactor. One period was in the range of two (2) minutes and another was in the range of seventeen (17) minutes. These oscillation periods in conjunction with process flow information can be very useful in finding the root cause of the oscillations using ProcessDoctor. This is based on the theory that the majority of chemical engineering unit processes behave as low pass filters. Thus by looking at common oscillation periods and analyzing the flow sheet the root cause can be roughly identified.

It was noticed that the oscillations with a period in the range of two minutes were found to be related to the purge separator or a process unit just upstream or downstream of the separator, this was be examined next. The oscillations with a period in the range of seventeen minutes appear as though they may be caused by oscillations on the discharge of the primary compressor.

2.4.2 Unit Process Stabilization

The process to be examined here is a separation vessel at the AT Plastics 5R facility. A schematic of this vessel is shown in Figure 2-4, this particular process separates the liquid and gas in the low pressure recycle which is being purged. The purge flow after the booster compressor in Figure 1-4 is the inlet to this unit process. This process includes three coupled control loops. Standard PI control is used on all of these loops. ProcessDoctor was used to analyze these loops. These loops were known to be a source of difficulty during regular plant operation. There had been many efforts previously to tune these loops, this proved fruitless every time. Many reasons for the poor performance of these loops had been proposed one predominant explanation was that the loops interact excessively and therefore the performance will always be poor. It was found that these loops had sustained oscillation with similar dominant frequencies. This indicated that the oscillations may have been caused by one source (one of the control loops performing poorly or an external disturbance). It was found after further analysis with ProcessDoctor that the flow control loop had significant valve stiction. The diagnosis from ProcessDoctor led to further testing of the flow

loop. In manual mode it was found that movement of the valve in the 5 – 40 % range caused no change in the flowrate; thus indicating the valve was sticking in that range. One method for removing valve stiction is the use of a valve positioner. The positioner on this valve was changed (since one was already installed). Figure 2-5 shows the behaviour of the flow control loop and the process variable (PV) of the level and pressure control loops before and after the positioner change. It was immediately noticed that the performance of the flow control loop was much better.

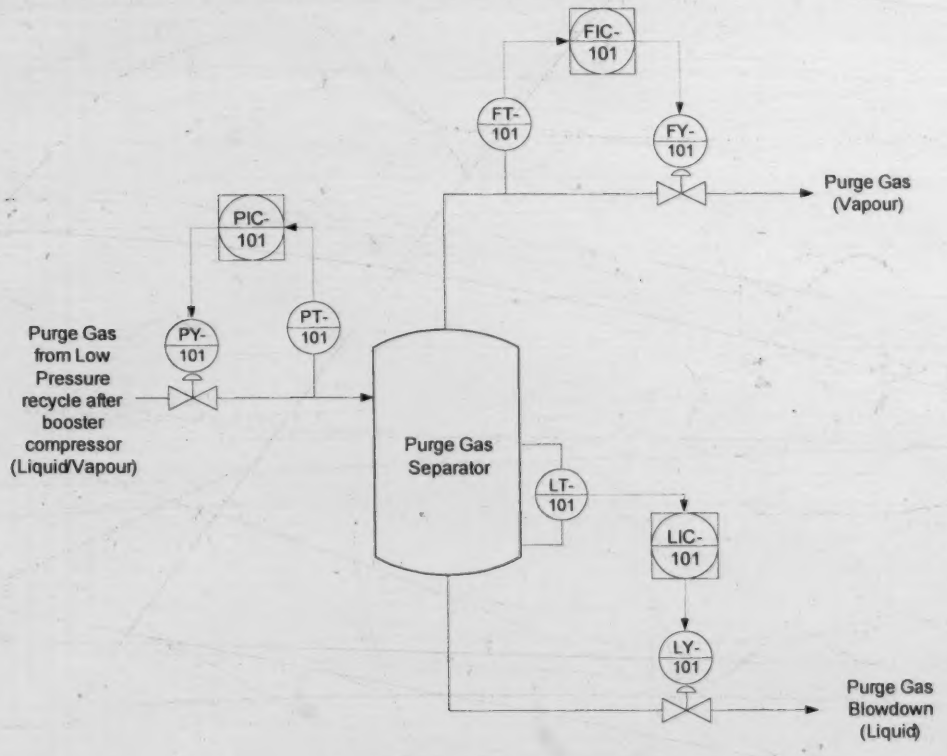

Figure 2-4 – Separation Vessel Schematic

Figure 2-6 shows the PV of the loops with tuning after the positioner was changed. This simple data analysis exercise isolated the root cause of oscillations and proved to remove all oscillations and stabilized all three control loops. There was still interaction between the loops as seen in Figure 2-6, but this interaction behaves as a disturbance and is quickly compensated for by the PI controller. After repairing the final control element, *only* then the performance of the loops could be improved through tuning.

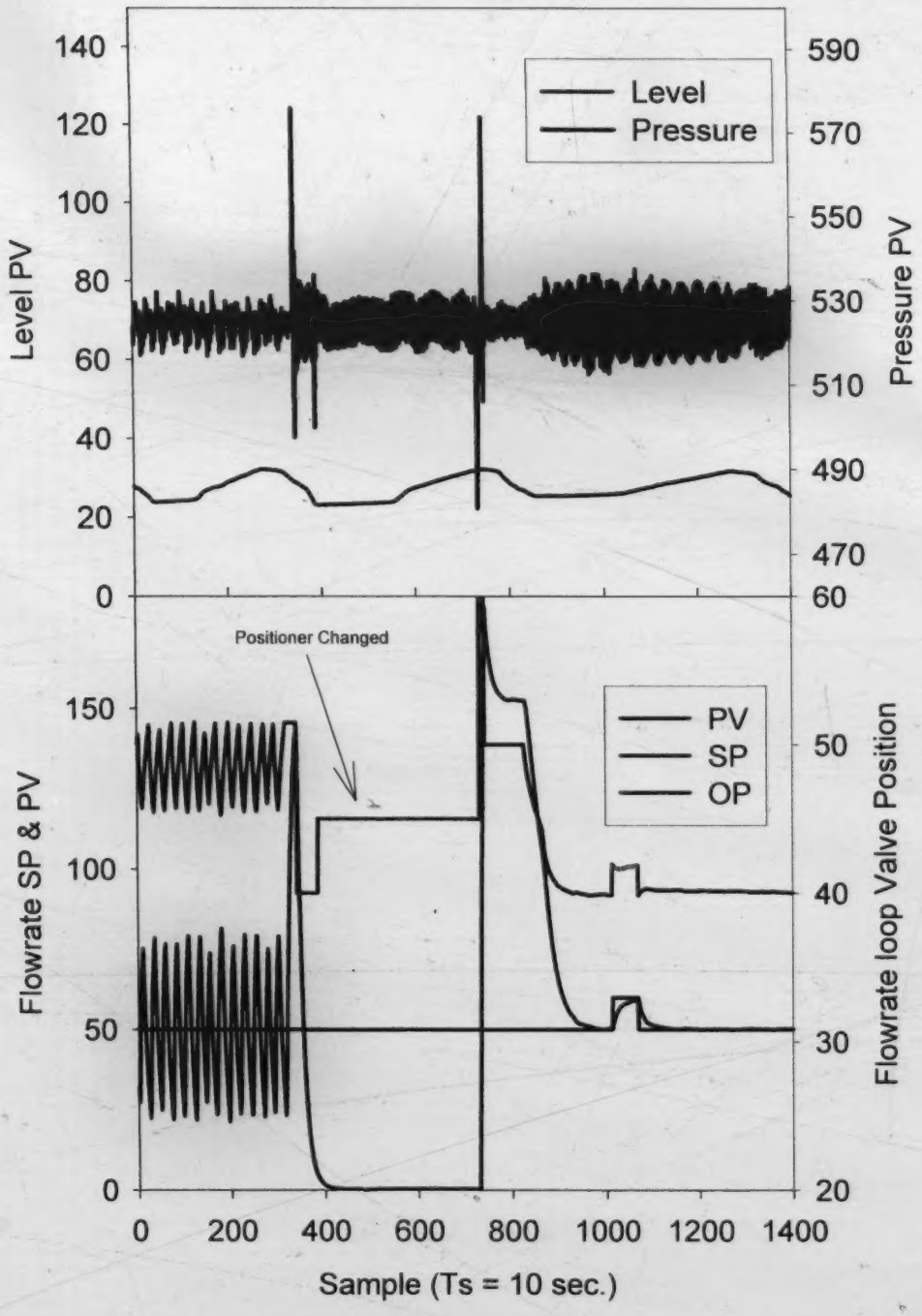

Figure 2-5 – Control Before and After Positioner Change

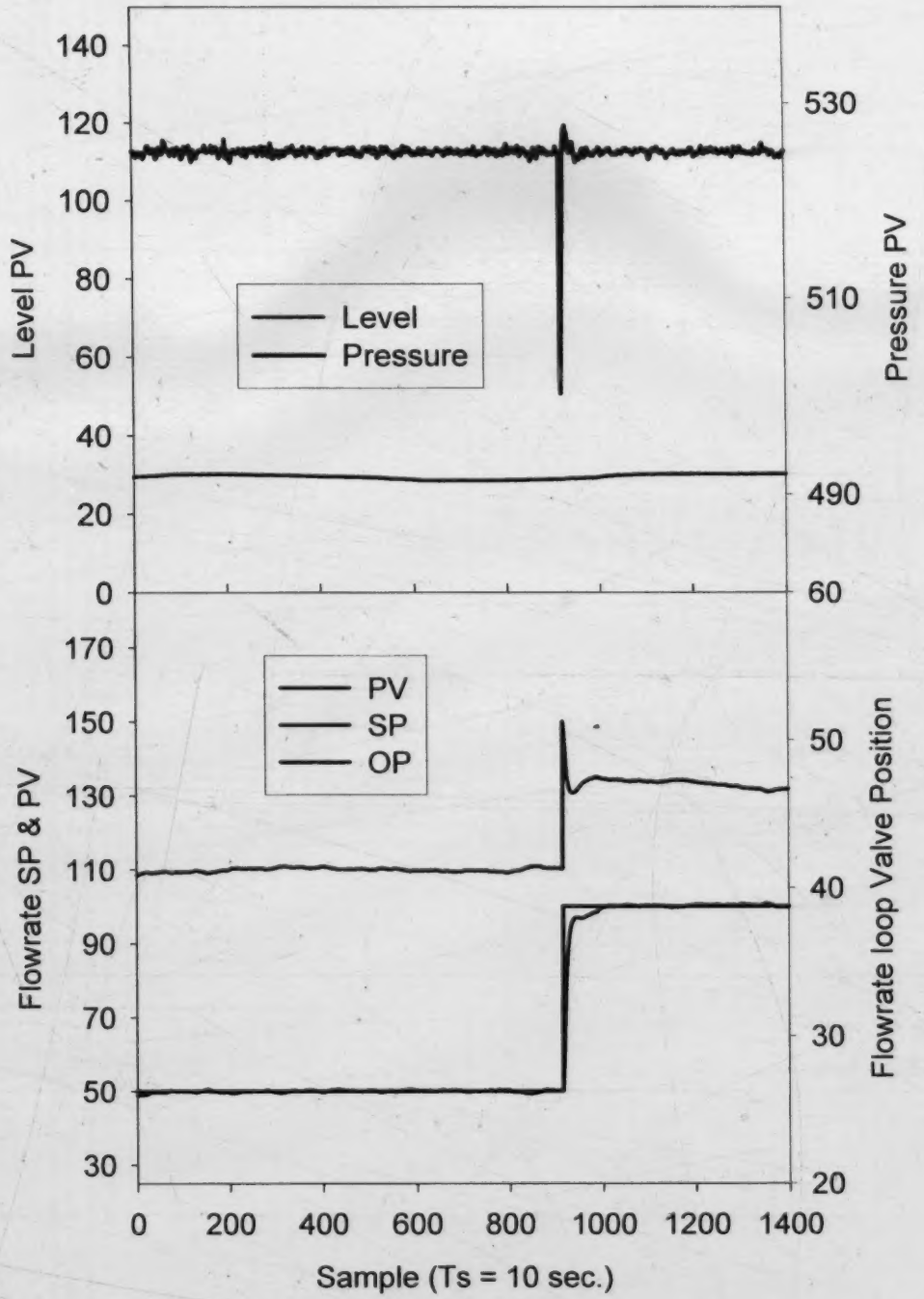

Figure 2-6 – Control After Tuning with New Positioner

2.5 Application – Plant Calculations

There are certain calculated variables which were important for building and validation of the models that will be discussed later on. There were some other calculations which were built and were not used in the model; however they were important for monitoring the process and gave a better understanding of the operation. Here calculations which were implemented online will be detailed. These calculations have been developed from process knowledge, basic mass, energy and component balances and theories which have been developed based on chemical engineering principles.

2.5.1 Compressor Mass Flow Model

A model of the mass throughput for the secondary compressor was implemented online. As seen from Figure 1-4 the reactor is fed by the secondary compressor. A detailed schematic of the compressor is shown in Figure 2-7.

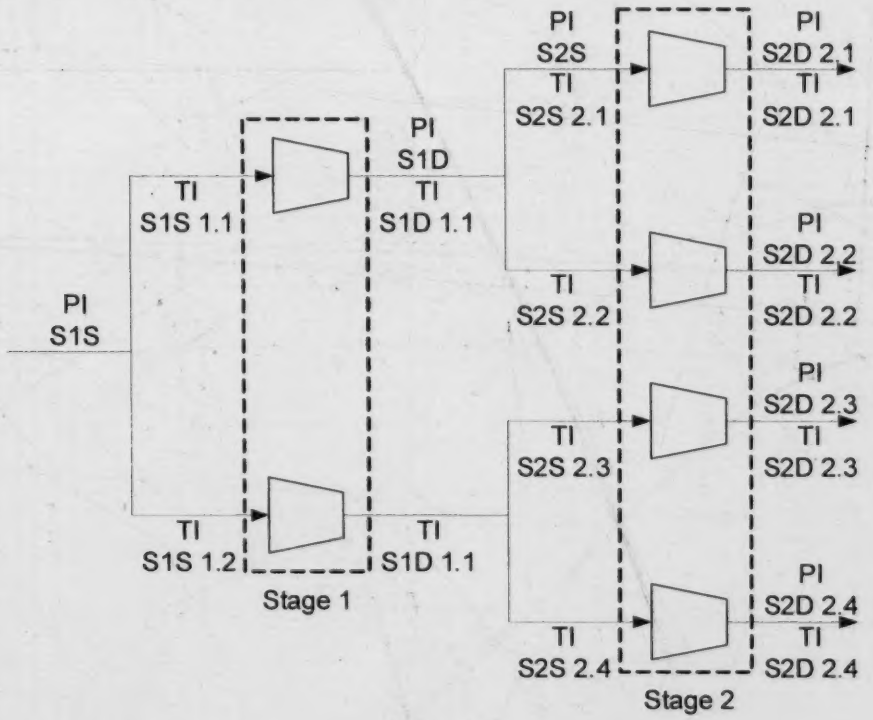

Figure 2-7 – Secondary Compressor Schematic

There was no other available source to find the total gas feed to the compressor. This calculation proved to be very important for regression of the first principles model parameters and validation for the model.

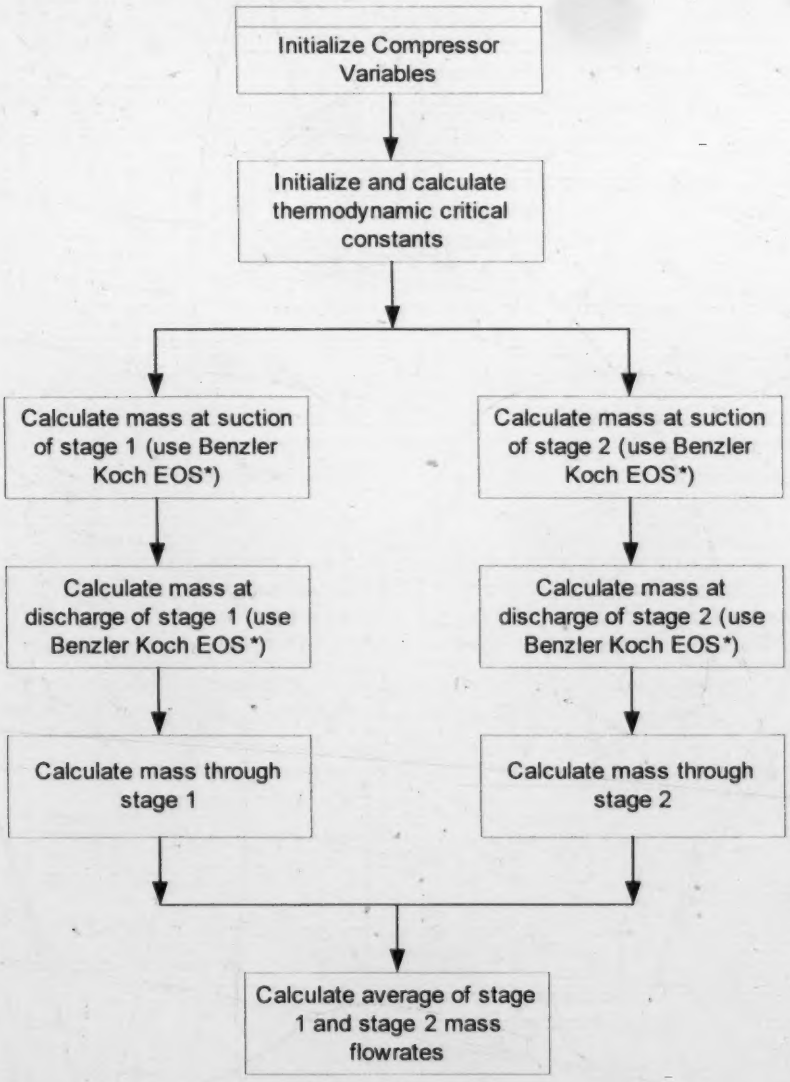
Initialize Compressor Variables
Initialize and calculate thermodynamic critical constants
Calculate mass at suction of stage 1 (use Benzler Koch EOS*)
Calculate mass at suction of stage 2 (use Benzler Koch EOS*)
Calculate mass at discharge of stage 1 (use Benzler Koch EOS*)
Calculate mass at discharge of stage 2 (use Benzler Koch EOS*)
Calculate mass through stage 1
Calculate mass through stage 2
Calculate average of stage 1 and stage 2 mass flowrates

Figure 2-8 – Compressor Flow Model Flow Chart (-Benzler and Von Koch 1955)*

The suction and discharge conditions of the secondary compressor limit the selection of flow meters which can be used, thereby making it a very costly addition to the plant instrumentation. However, the suction and discharge temperature and pressure

of each stage could be used with thermodynamic relationships to find the mass at several monitored points on the compressor. Then these point masses can be used to estimate the mass flow through the compressor. The flow chart followed for this model is shown in Figure 2-8. This model was implemented online and used all variables shown in Figure 2-7. The model was calculated every second. In most cases when there was more than one input value available averages were taken, some logic for removing a bad sensor from the calculation was implemented, because of the availability of duplicate measurements in most cases.

2.5.2 Zone Mixing Index

There has been much research into the mixing regimes which are present within the autoclave reactor. Poor mixing has been found to be the reason the zones in an autoclave may not behave like an ideal CSTR.

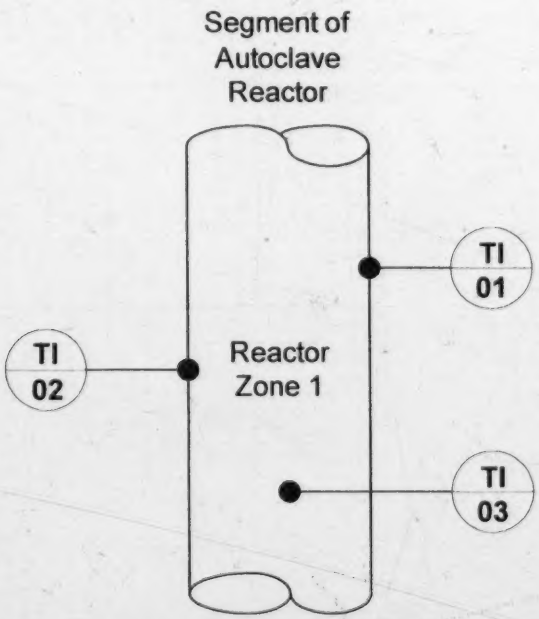

Figure 2-9 – Autoclave Segment (poor mixing variables)

Figure 2-9 shows the typical temperature sensor configuration for a particular zone on an autoclave. The sensors are usually spread as much as possible radically and axially. Any difference in the measurements within one zone gives an indication of

poor mixing. Equation (2.1) shows the relationship used to find the mixing index for each zone.

$$Za_{Mxl} = 100\left(1 - \frac{Za_{SD}}{Zero_{SD}}\right) \tag{2.1}$$

This index has been set so a value of 100% indicates full mixing. This calculation finds the spatial standard deviation of all the temperature measurements in a particular zone. The ratio of this spatial standard deviation to a theoretical zero mixing index standard deviation is found (this is set by analysing historical data and finding the maximum standard deviation during normal operation with no relevant instrumentation faults).

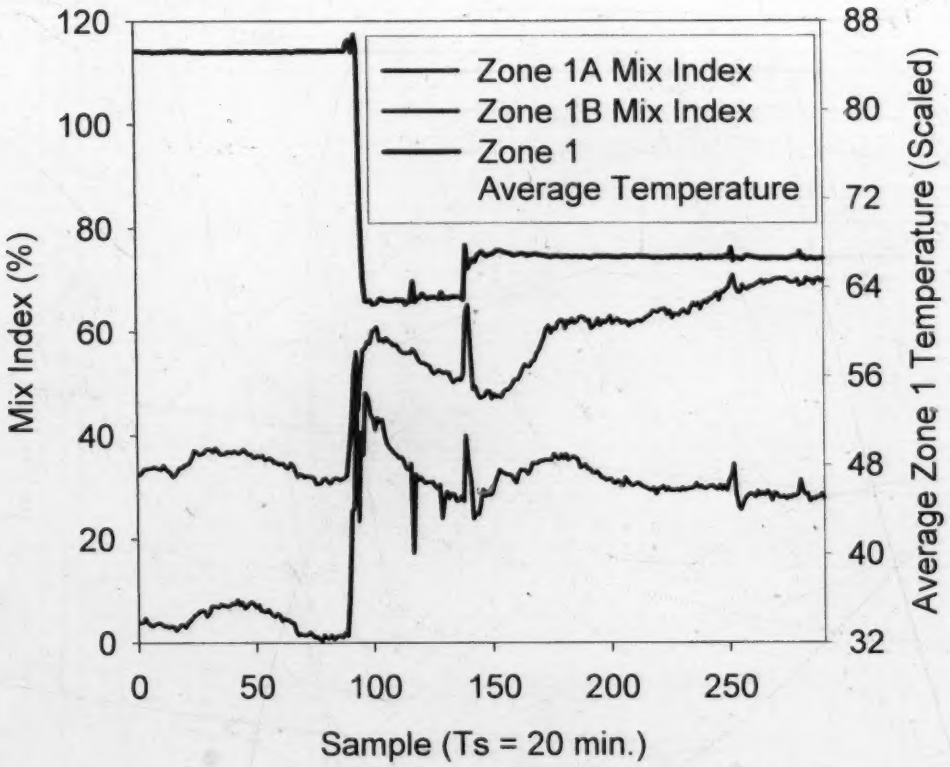

Figure 2-10 – Reactor Mixing Index

This calculation proved to be very robust and reliable. Figure 2-10 shows the Zone 1 mixing index during dynamic and steady state periods. This has vast potential for increasing initiator efficiency (refers to a factor which indicates the mass of initiator would participate in the reactions) since the initiator is less efficient at lower mixing indexes. It was noticed that as the temperature decreased the zone mixing improved.

2.5.3 Plant Production

The quantity of polymer produced by the plant is an important variable which is related directly to the conversion in the reactor. Figure 2-11 shows the test hopper configuration.

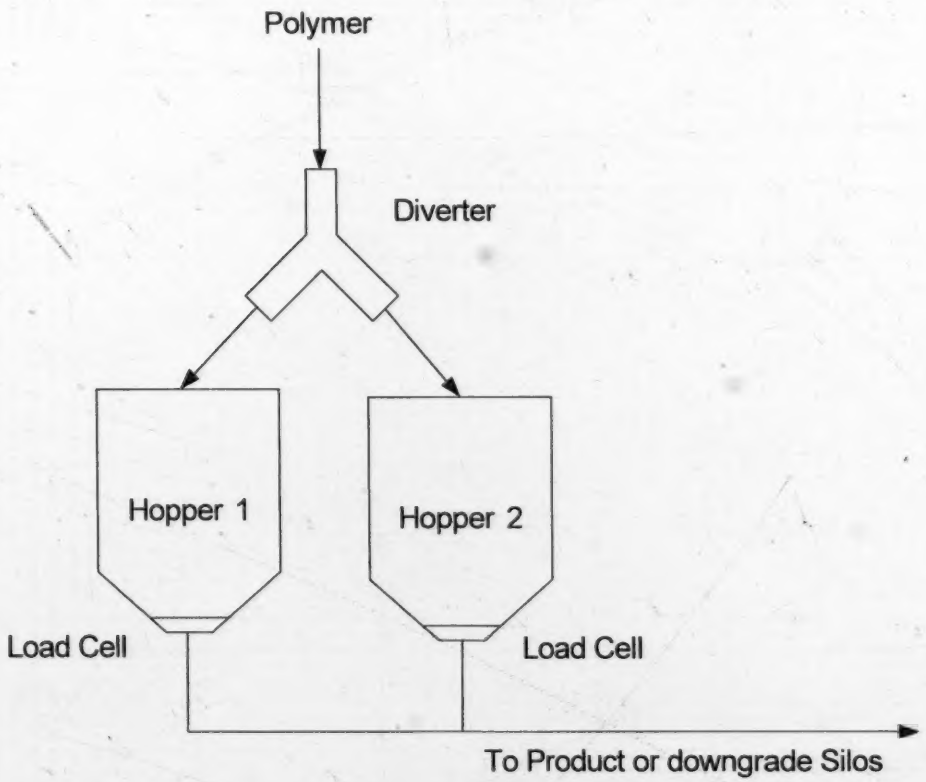

Figure 2-11 – Test Hopper Configuration (used for mass flow calculation)

Each test hopper has a load cell which measures the instantaneous mass in the cell. Only one cell is used at any time. One is usually being filled by new product as the

other is being emptied. The status of the diverter valve is available to the control system. A calculation was built which measured the difference in the load cell reading of the active hopper every 5 seconds. This was then scaled to give a mass flow rate in kg/hr. The average of this calculated value was used as a validation variable for the plant model developed later on.

$$F_m = k\left(Diverter_1 \times \left(LS_0^1 - LS_{-5}^1\right) + Diverter_2 \times \left(LS_0^2 - LS_{-5}^2\right)\right) \qquad (2.2)$$

The relationship used to find the mass flow is shown in equation (2.2). Here LS represents the reading from the respective load cell.

2.5.4 Analyzer Corrections

There are two main analyzers used in this process. These give feedback on the percentage VA in the product and the melt index of the product. These readings are very critical for steady state and dynamic fitting and validation of the model. Both these readings had problems which made the raw plant values unacceptable for model validation.

Percentage VA

This analyzer measures the percent of the mass in the polymer formed using VA molecules. It is based on FTIR spectroscopy. This method of analysis injects an incident infrared light source onto a sample. The reflected spectrum gives an indication of the sample composition. The spectrum is usually very complex; thus the Fourier transform of the spectrum is used to find the major components, giving a numerical value for the composition. These analyzers are mature in industry but have been found to drift and contain offsets. The analyzer considered here was found to be susceptible to an offset. The measurement however did capture the dynamics. Therefore a simple updating scheme was used to effectively compensate for the errors; Figure 2-12 shows an example of the scheme being applied. The SPOT here refers to a laboratory check on the value. This is done using another instrument which is more reliable, but is not online. The final corrected signal and error are stored on the plant historian.

$$e_T = VA\_SPOT_T - VA_T \tag{2.3}$$

$$VA\_Corrected = VA + e_T \tag{2.4}$$

Equation (2.3) and (2.4) show the method used for finding the corrected VA percentage where e, VA_SPOT, VA and $VA\_Corrected$ represent the error, the VA laboratory measurement, the raw online measurement and the corrected measurement respectively. The subscript T is used to represent a particular time. This is important here because the error at one time instant is applied for all time until a new spot is available.

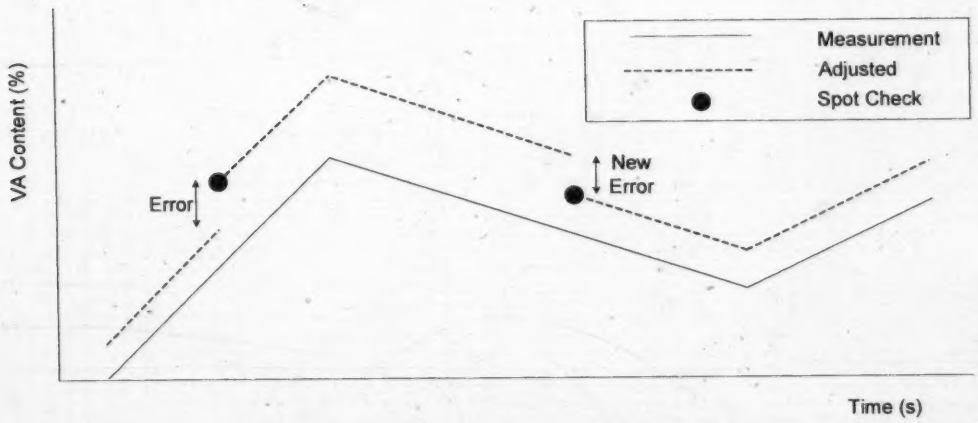

Figure 2-12 – VA Measurement Correction

Melt Index - Online Rheometer

This instrument is an online rheometer; it will be described in more detail in Chapter 5. This instrument measures the melt index of the polymer produced. This instrument is very flexible and can measure a large range of melt indices. Due to this flexibility, the instrument has different output ranges for accuracy. The range is set by a program which includes several parameters for correlating the melt index with the instruments measured pressure and temperature. There is a correlation computation for each grade produced by the plant. All of these programs use either of two ranges, 0 – 100 g/10 min. or 0 – 1000 g/10 min. The problem arises from the fact that there is only one output on the unit and its range is 0 – 100 g/10 min. Thus the measurement works

well once the 0 – 100 gm/min. range is used. However once the 0 – 1000 gm/min. range is used, the actual reading transmitted, displayed on the DCS and historized is divided by 10. This problem seems simple at first but once data analysis is attempted it can cause problems. This problem was rectified by using the soft sensor which is described in Chapter 5. The soft sensor was used to get information on the range of the actual melt index. Equations (2.5) and (2.6) show the method used for finding the corrected melt index where MI^{SS}, MI and $MI\_Corrected$ represent the soft sensor MI, the MI measurement and the corrected MI respectively. This corrected value is stored on the plant historian as well.

$$\begin{aligned} &if\ MI^{SS} < 100 \\ &MI\_Corrected = 10 \times MI \qquad (2.5) \\ &otherwise \\ &MI\_Corrected = MI \qquad (2.6) \end{aligned}$$

2.5.5 CTA concentration in Reclaimed VA

This calculation was used manually to find the content of impurity in the reclaimed VA which behaves as a CTA (chain transfer to agent). This can be viewed as an unmeasured disturbance. This disturbance proved to be significant in the first principles model. This calculation is based on a change in reclaimed VA percent in the total VA feed to the reactor while the VA content in the polymer is kept constant. This calculation uses a pair of simultaneous equations which can be derived from the assumption that the total VA injection flow should be a constant ratio of the ethylene injection flow, these equations are:

$$FVA_{T1} + x_{VA} RVA_{T1} = k \times ETH_{T1} \qquad (2.7)$$

$$FVA_{T2} + x_{VA} RVA_{T2} = k \times ETH_{T2} \qquad (2.8)$$

Only two components are considered important here. These are VA and the CTA components. Equation (2.9) is based on this.

$$x_{VA} = (1 - x_{CTA}) \qquad (2.9)$$

These three relationships can be modified to give the following equation.

$$x_{CTA} = 1 - \left(\frac{-\left(FVA_{T1} ETH_{T2} - FVA_{T2} ETH_{T1}\right)}{RVA_{T1} ETH_{T2} - RVA_{T2} ETH_{T1}} \right) \tag{2.10}$$

The variables are defined below:

FVA Fresh VA

ETH Fresh Ethylene flow

RVA Reclaim VA flow

k Ethylene to VA ratio

From these calculations the mass fraction of CTA was always found to be in the range of 1% to 10%.

2.5.6 Initiator Mass Flow Rate

The mass flow rate of initiator injection into the autoclave reactor is not measured. This is typically the case for the high pressure reactor. An approximate value for the mass flow rate into the reactor was need for model regression (this will be seen later on). Positive displacement pumps are used for the injection of initiator. The flow of initiator into the autoclave is used to control the temperature for the respective zone. Linear correlations between the temperature controller's outputs (pump loadings) and the strokes per minute were found and can be seen in the appendix. Each stroke delivered a constant volume of initiator to the autoclave. Equation (2.11) shows the relationship used to find the mass flow delivered by the initiator pumps.

$$\dot{M}_{Initiator} = k \rho_{mix} \frac{L \pi D^2}{4} S\left(TIC_{OP}\right) \tag{2.11}$$

Where

$\dot{M}_{Initiator}$ represents the initiator mass flow rate (kg/hr)

k represents a scaling factor for units

ρ_{mix} represents the mixture density (approximate value)

L represents the stroke length

D represents the pump cylinder diameter

S represents the number of strokes per minute (function of pump loading)

TIC_{OP} represents the respective temperature controller output

2.6 Chapter Summary

In this chapter, details on the necessary IT infrastructure for the collection and dissemination of data were given. The data obtained was critical for the next stages of the research. Some implemented applications using this infrastructure were detailed. These included:

- Controller performance monitoring – Which was a necessary step before implementing optimal transitions
- Online Calculations – This included several necessary plant calculations which were used for regression and validation of the first principles model.

"An idealist is a person who helps other people to be prosperous."

Henry Ford (1863 – 1947)

Chapter 3

First Principles Modeling of EVA Polymerization[3]

3.1 Introduction

Polymerization plants are constantly seeking to increase their production efficiency. One of the most valuable tools to do this is a process model. Typically in academia first principles models are built in computational packages such as MATLAB and SIMULINK. The use of such packages has several limitations when it comes to long term sustainability at actual plant sites. This is because the code generated in these packages is generally complex. Parameters for tuning of the model are usually buried deep within the code. Such models usually last as long as the person who developed it

[3] Portions of this chapter were presented at the 54th Canadian Chemical Engineering Conference (CSChE), October 2004, Calgary AB, Canada and Aspen Tech's User Group Meeting, October 2005, Houston TX, USA by Alleyne et al.

remains on the project. The model then becomes very cumbersome and difficult to maintain by anyone else. Since this research was undertaken closely with industry, long term use of the model was important at a plant site, where there are not many modeling or simulation experts. Thus it was chosen to build this model using a commercial user-friendly package, using as many standard blocks as possible. This then gives the site access to a group of experts they can call on for support with maintenance and development of the model. It also simplifies long term maintenance because the model parameters for maintenance and model modification are available in a user friendly interface. For many decades, commercial packages have been designed for modeling of hydrocarbon and chemical processes. These tools are usually easy to use and are typically modular in nature with unit processes encapsulated into customizable blocks which can be linked via input and output streams.

With the increasing computing power available today, simulations which once would have taken days to converge are now easily solved within minutes or seconds. In particular, polymerization simulations have been known to be computationally intensive; this is partially due to the relatively complex thermodynamic computations and nonlinear reaction kinetics. Previous simulation packages typically simplified the thermodynamics to simple phase equilibrium equations.

Over the last thirty years there have been many mathematical representations developed to describe the fundamentals of polymerization processes. Modeling studies on free radical polymerization of ethylene have been documented by Chen et al. 1976; Thies 1979; Lee and Marano 1979; Goto et al. 1981; Mavridis and Kiparissides 1985; Feucht et al. 1985; Shirodkar and Tsien 1986; Brandolin et al. 1988; Kiparissides, Verros et al. 1993; Pladis and Kiparissides 1999; Hamielec A. E. 2000.

More and more detailed modeling of polymerization processes is being performed. There has been a significant amount of work done on the prediction of the detailed MWD of the polymer based on the reaction rates and their contribution to the chain length and the amount of chain branching (Wells and Ray 2005). MWD is typically obtained experimentally using GPC (gel permeation chromatography).

Polymer thermodynamics has been receiving increasing attention. It is now accepted that thermodynamic theories which include the chain behavior have been found to give a good representation of polymer and polymer solution behavior. Over the last twenty years, significant efforts have been made in the field of statistical thermodynamics. These theories have developed equations which have eventually become practical for use as equations of state. Some of the developments for the current equations came from models such as the Perturbed-Hard-Chain Theory (Donohue and Prausnitz 1978), the Sanchez-Lacombe Equation of State (Sanchez I. C. 1976), the Generalized Flory-Dimer Theory (Bokis et al. 1994) and the Statistical Associating Fluid Theory (Chapman et al. 1990, Huang and Radosz 1990). These theories have been extended to the Perturbed-Chain Statistical Associating Fluid Theory (PC-SAFT) EOS (Gross and Sadowski 2002; Gross et al. 2003).

3.2 Polymer Simulation in Commercial Packages

There is a limited number of advanced process engineering simulation packages available presently. A summary of them is given in Table 3-1.

All the theories mentioned in the previous section have been implemented to different extents by the various polymer simulation packages. Thus there are a few commercial packages available which are able to predict the steady state and dynamic polymer properties using plant operating conditions. Three of the main packages are Aspen Polymers Plus® by Aspen Technology, Inc., Predici® by Computing in Technology and gPROMS® by Process Systems Enterprise Limited. Only more recently have commercial simulators directly incorporated polymer modeling technology and thermodynamics specific for polymer simulations. This has been primarily handled by academic researchers or modeling "specialists" in centralised engineering organizations (Ko et al. 1992). Early polymer simulations were built by approximating them as heavy hydrocarbons (Chen 2002); thus the polymer properties were not tracked. There was also a lack of integration of these custom simulators with mature process flow sheet modeling. This overly simple method of polymer modeling caused many manufactures to lose confidence in its applicability.

Name	COMPANY	FEATURES
Aspen Plus, Polymers Plus, Aspen Dynamics, Aspen Custom Modeller	Aspen Technology	Steady State and Dynamic Full Plant Simulations, Polymer, Large Thermodynamic and Component Database, Regression, Dynamic Optimization
Predici	Computing in Technology	Steady State and Dynamic Reactor Simulations, Polymer, Small Thermodynamic and Component Database, Regression, Dynamic Optimization
gPROMS	Process Systems Enterprise Limited	Steady State and Dynamic Full Plant Simulations, Large Thermodynamic and Component Database, Regression, Dynamic Optimization
PRO/II	SimSci-Esscor Invensys	Steady State and Dynamic Full Plant Simulations, Polymer, Medium Thermodynamic and Component Database, Regression
LDPE Autoclaves	LPRE	Steady State and Dynamic Full Plant Simulations, Polymer, Very Small Thermodynamic and Component Database, Regression, In Development
PolyEFF	EFFTech Engineering Software	Steady State Reactor Simulations, Polymer, Very Small Thermodynamic and Component Database, Regression, In Development

Table 3-1 – Simulation Packages and Features

However, over the last decade there has been a significant increase in the number of

industrial applications of polymer models. There have been varying levels of successful implementations of these modeling technologies (Ramanathan S. 1992). Some industrial applications of low density polyethylene polymerization (free radical polymerization) have been reported by Ko 1990; Orbey et al. 1998; Bokis et al. 2002. Polymer process steady state models are now routinely used offline to help develop new processes, design new plants, troubleshoot existing plants and optimize plant operations (Chen 2002).

3.3 Introduction to the Modeling Procedure

Building a full model for this plant was not a trivial task. It involved many steps. Generally the model was built with the objective that it should be as simple as possible. In this regard many assumptions were initially made. As the model was being validated, many assumptions had to be revised. This resulted in an iterative model building process where at each step assumptions were checked and modified followed by taking steps backward, modifying assumptions, and then fitting and validating again. Figure 3-1 shows the general path followed. It is useful to note that these steps are general and can be applied to several polymerization processes.

First a significant amount of time was spent learning the process and understanding the main goals for the modeling effort. The properties of different thermodynamic relationships were then examined and ones used in the model were based on process conditions. Then the parameters for the respective thermodynamic relationships were found in the available literature. The same was then done for the reaction kinetic data; however, not all values for the literature based kinetic data were available or fully trusted. Where values were unknown or there was little confidence in them, regression was done, and the limits were set larger than the values we had more confidence in. Once the reactor model was regressed and validated for the required grades, the recycle loops were then built in. The dynamic requirements were then added to the model. The dynamic model was then validated against historical dynamic plant data and additional data fitting was done where necessary. Once the dynamic full plant model was complete the model was ready for applications.

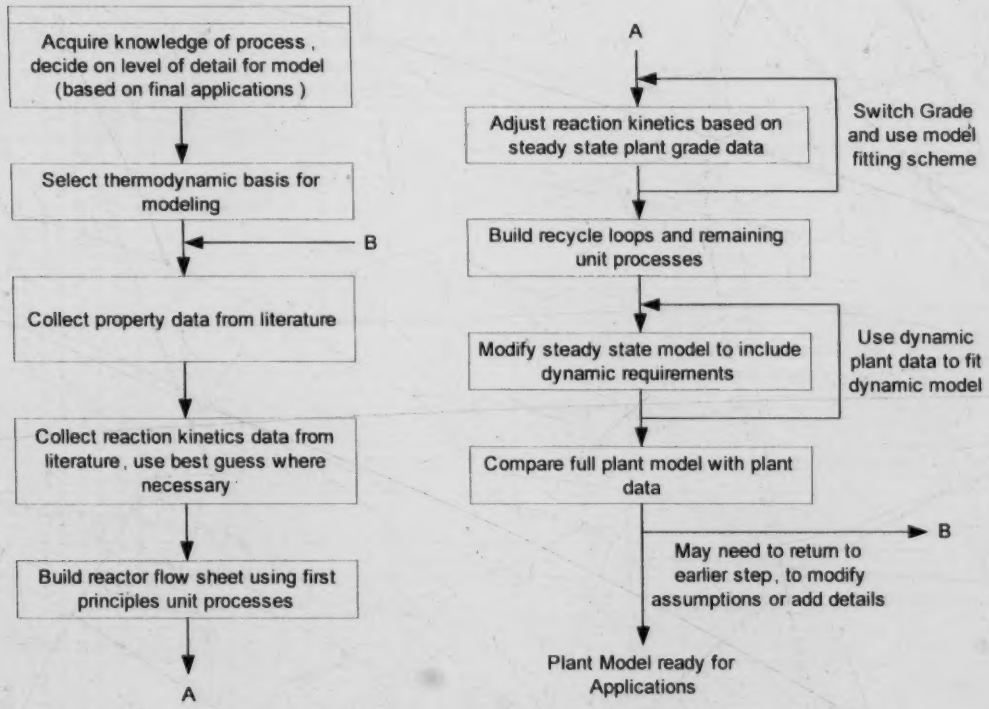
Acquire knowledge of process , decide on level of detail for model (based on final applications)
Select thermodynamic basis for modeling
B
Collect property data from literature
Collect reaction kinetics data from literature, use best guess where necessary
Build reactor flow sheet using first principles unit processes
A
A
Adjust reaction kinetics based on steady state plant grade data
Switch Grade and use model fitting scheme
Build recycle loops and remaining unit processes
Modify steady state model to include dynamic requirements
Use dynamic plant data to fit dynamic model
Compare full plant model with plant data
B
May need to return to earlier step, to modify assumptions or add details
Plant Model ready for Applications

Figure 3-1 – First Principles Modeling Steps

3.4 Model Components

Table 3-2 summarises the main components in the process and their purpose in the process. The source component column represents the Aspen Plus database component whose parameters were used for the respective component's thermo-physical property and VLE calculations. Acetone, solvent and initiators are present in trace amounts; therefore their thermodynamic properties would not have much effect on the final result. These approximations are used to make the simulation less computationally complex. Acetone was used as a general component which represents all CTA components present as impurities. These are generated usually from the decomposition of the initiator and built up in the recycle loops. Some of it is condensed at the booster compressor like VA. A similar case was found for the

solvent. The thermodynamic behaviour of the CTA components and solvent was found to be similar to VA, thus they were approximated by VA.

Component	Purpose	Source Component
Ethylene	Monomer	Ethylene
Vinyl Acetate	Monomer	Vinyl Acetate
Propylene	Monomer	Propylene
Acetone	Lumped initiator by-products	Vinyl Acetate
Solvent	Initiator solvent	Vinyl Acetate
Ethylene Segment	Ethylene in polymer chain	Ethylene Segment
Vinyl Acetate Segment	Vinyl Acetate in polymer chain	Vinyl Acetate Segment
Propylene Segment	Propylene in polymer chain	Propylene Segment
A	Initiator 1	Ethylene
X12	Initiator 2	Ethylene
X29	Initiator 3	Ethylene
Z2	Initiator 4	Ethylene
Ethylene Vinyl Acetate	Polymer	Ethylene Vinyl Acetate

Table 3-2 – Model Component Summary

It was noticed that the use of reclaim VA increased the concentration of CTA components and required the use of less propylene to attain the same melt index. Thus the role of Acetone (impurities) was found to be more important for the reaction kinetics.

3.5 Thermodynamic Model Properties

The plant covers a wide range of operating flow rates, pressures and temperatures. Also the components and region on the phase envelope changes based on the unit process being examined. Thus the appropriate thermodynamic method had to be chosen based on these factors. One advantage of using the Aspen Plus system for the

first principles model was its excellent thermodynamic database. All the model components used were available in the database and no fitting was required (Aspen Technology 2005), there were cases where there were discrepancies with the trusted literature data; here as would be seen later on fitting was done. The Aspen's thermodynamic values were replaced with the literature values in these cases. Equation of state models are appropriate for systems at moderate to high pressures (Khare et al. 2004). Equations of state also tend to be a more seamless solution because they provide smooth and reliable results across the vapour to liquid transition. As mentioned before equations of state for polymer modeling have matured significantly recently (in particular PC-SAFT). However, there have been cubic equations of state models which work very well for simple compounds not operating in the supercritical region (such as SRK). Therefore it was decided to use two equations of state. These were, PC-SAFT (Perturbed Chain Statistical Associating Fluid Theory) for the unit processes involving polymer components and operating in the supercritical phase region and SRK (Soave-Redlich-Kwong) for the remaining unit processes. The Aspen Plus process flow sheet for the full plant is shown in Figure 3-2.

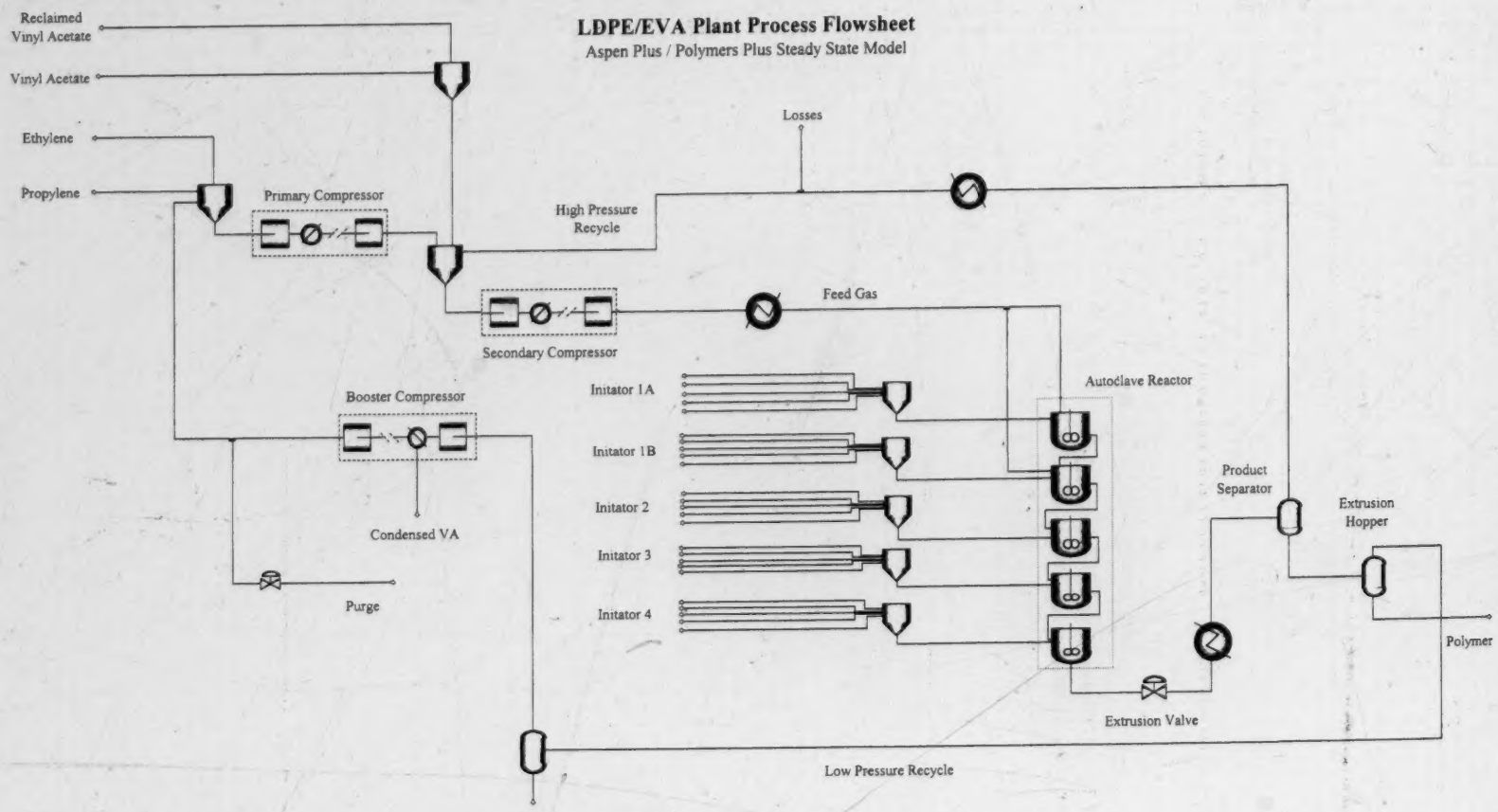

Figure 3-2 – Aspen Plus Steady State Plant Flow Sheet

The assignment of the thermodynamic property set based on unit process is shown in Table 3-3.

Unit Process	Thermodynamics	Phase Constraints
VA Mixer	SRK	Vapour - Liquid
Feed Mixer	SRK	Vapour Only
Initiator Mixer	PC-SAFT	Liquid Only
Primary Compressor	SRK	Vapour Only
Secondary Feed Mixer	SRK	Vapour Only
Secondary Leak Split	SRK	Vapour Only
Secondary Compressor	SRK	Vapour Only
Feed Gas Coolers	PC-SAFT	Vapour Only
Autoclave Reactor Zones	PC-SAFT	Vapour Only
Reactor Outlet Valve	PC-SAFT	Vapour Only
Product Cooler	PC-SAFT	Vapour - Liquid
High Pressure Separator Inlet Valve	PC-SAFT	Vapour - Liquid
High Pressure Separator	PC-SAFT	Vapour - Liquid
High Pressure Recycle Cooler	SRK	Vapour Only
Losses Split	SRK	Vapour Only
Low Pressure Separator Inlet Valve	PC-SAFT	Vapour - Liquid
Low Pressure Separator	PC-SAFT	Vapour - Liquid
Low Pressure Stock Tank Inlet Valve	SRK	Vapour - Liquid
Low Pressure Stock Tank	SRK	Vapour - Liquid
Low Pressure Recycle Cooler	SRK	Vapour Only
Booster Compressor	SRK	Vapour Only
Booster Compressor Coolers	SRK	Vapour - Liquid
Purge Split and Purge Valve	SRK	Vapour Only

Table 3-3 – Thermodynamic Equation of State Assignment

3.6 Soave-Redlich-Kwong Equation of State

The actual equation of state used was called Polymer SRK in the Aspen Plus database. This is an extension of the SRK equation of state. However this equation of state was only used on the recycle portions of the process (this was where the polymer content expected was negligible) and thus more importantly the basic cubic SRK equation of state was used and not the polymer extensions. More over the SRK equation of state has been commonly applied for modeling ethylene systems in low to medium pressures.

3.6.1 SRK Theory

The conventional Soave-Redlich-Kwong equation used for pure component substances follows (Soave 1972):

$$P = \frac{RT}{v-b} - \frac{a(T)}{v(v+b)} \tag{3.1}$$

Where:

$$b = 0.08664\frac{RT_C}{P_C} \tag{3.2}$$

$$a = 0.42748\frac{R^2T_C^2}{P_C}\alpha \tag{3.3}$$

α refers to a temperature dependent function and the Mathias and Coperman form is used (Mathias and Copeman 1983):

$$\alpha = \left[1 + c_1\left(1 - T_r^{0.5}\right) + c_2\left(1 - T_r^{0.5}\right)^2 + c_3\left(1 - T_r^{0.5}\right)^3\right]^2 \tag{3.4}$$

$$T_r = \frac{T}{T_C} \tag{3.5}$$

Where c_1, c_2, c_3 are the Mathias-Copeman constants for the particular component.

3.6.2 SRK Pure Component Parameters

Table 3-4 shows the SRK pure parameters for the important components of the

model.

Component	$T_c(^oC)$	P_c (*bar*)	C_1	C_2	C_3	Z_{RA}[4]
Ethylene	9.19	51.40	0.656	-0.363	0.677	-
Vinyl Acetate	245.98	40.36	0.998	0.136	-0.296	-
Propylene	91.75	46.91	0.738	-0.347	0.675	-

Table 3-4 – SRK Pure Component Parameters

3.6.3 SRK Binary Interaction

For the mixtures, equation (3.1) is modified within Aspen Plus to give:

$$P = \frac{RT}{v+c-b} - \frac{a}{(v+c)(v+c+b)} \tag{3.6}$$

Where:

$$a = a_0 + a_1 \tag{3.7}$$

a_0 is the standard quadratic mixing term:

$$a_0 = \sum_{i=1}^{n}\sum_{j=1}^{n} x_i x_j \sqrt{a_i a_j}\left(1-k_{ij}\right) \tag{3.8}$$

a_1 is an additional, asymmetric (polar) term:

$$a_1 = \sum_{i=1}^{n} x_i \left(\sum_{j=1}^{n} x_j \left(a_i a_j\right)^{1/6} l_{j,i} \right)^3 \tag{3.9}$$

$$b = \sum_i x_i b_i \tag{3.10}$$

$$c = \sum_i x_i c_i \tag{3.11}$$

$$c_i = 0.40768\left(\frac{RT_{Ci}}{P_{Ci}}\right)\left(0.29441 - z_{RAi}\right) \tag{3.12}$$

(Aspen-Technology 2003)

[4] This parameter is only required when the form expressed in equation (3.6) is used.

The binary interaction parameters are implemented in Aspen Properties using the following relationships:

$$k_{ij} = k_{ij}^1 + k_{ij}^2 T + k_{ij}^3 T^2 \qquad (3.13)$$

Where k_{ij}^4 and k_{ij}^5 represent the valid temperature range.

$$l_{ij} = l_{ij}^1 + l_{ij}^2 T + l_{ij}^3 T^2 \qquad (3.14)$$

Where l_{ij}^4 and l_{ij}^5 represent the valid temperature range.

Table 3-5 shows the SRK binary interaction parameters for the important components of the model (the majority of these had very little interaction so no value was required).

Parameter	Ethylene-VINYL ACETATE	ETHYLENE-PROPYLENE	VINYL ACETATE-PROPYLENE
k_{ij}^1	-	-	-
k_{ij}^2	-	-	-
k_{ij}^3	-	-	-
k_{ij}^4	-273.15	-273.15	-273.15
k_{ij}^5	726.85	726.85	726.85
l_{ij}^1	-	-	-
l_{ij}^2	-	-	-
l_{ij}^3	-	-	-
l_{ij}^4	-273.15	-273.15	-273.15
l_{ij}^5	726.85	726.85	726.85

Table 3-5 – SRK Binary Interaction Parameters

3.7 Perturbed Chain Statistical Associating Fluid Theory Equation of State

A review of the application of PC-SAFT for LDPE polymerization was done by Aspen Technology (Aspen Technology 2002). LDPE polymerization occurs at high temperatures and pressures. The thermodynamic properties of the components can be found using activity coefficient models or equation of state models (EOS). The polymerization of ethylene occurs close to or above critical pressures; it is found that EOS models are better at prediction under these conditions.

As mentioned previously, the PC-SAFT equation of state was used for segments of the model where predicting the thermodynamics of the polymer chain was important and where the components were under supercritical conditions. The PC-SAFT binary interaction was very important for predicting the gas/ polymer separation in the high pressure and low pressure separators.

3.7.1 PC-SAFT Theory

Some of the basic ideas of PC-SAFT will be discussed here. The PC-SAFT model is a theoretical equation of state, developed by Gross and Sadowski. It is based on the SAFT equation of state with some modifications to the expressions for the dispersive forces. It has been proposed for the thermodynamic modeling of systems containing long-chain molecules (such as polymers). These molecular chains are assumed to be freely jointed segments which exhibit forces amongst each other. PC-SAFT has been shown to give a more realistic relationship for the thermodynamic behaviour of polymer molecules and is equally applicable to smaller molecules. The predictive abilities of PC-SAFT for the VLE behaviour of polymer solutions and binary interaction of small molecules, has been shown to be superior to SAFT and the Peng-Robinson equation of state.

This EOS is based on the perturbation theory of fluids. This allows us to express the thermodynamic properties of a fluid as the sum of a reference term and a perturbation term.

The perturbation term in SAFT takes into account the attractive (dispersion) interactions between molecules. In PC-SAFT, the perturbation theory concept applies to segments that are connected to chains rather than between disconnected segments (which is the case in SAFT). This is equivalent to considering attractive (dispersion) interactions between the connected segments instead of disconnected ones as shown in Figure 3-3.

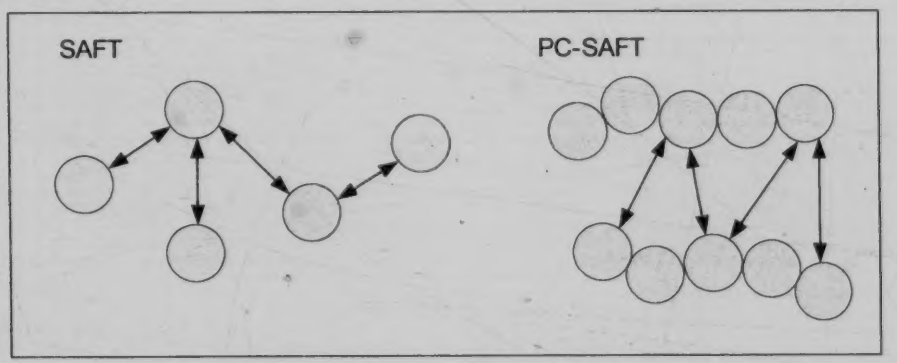

Figure 3-3 – Depiction of segment-segment interaction in SAFT and PC-SAFT (Aspen Technology 2002)

Therefore it is clear that this concept offers a more realistic picture of how chain molecules, such as hydrocarbons, oligomers, and polymers, behave in a solution.
In SAFT, the perturbation (attractive) contribution is a series expansion in terms of reciprocal temperature, and each coefficient depends on density and composition. PC-SAFT expresses the attractive term of the equation as a sum of two terms (first- and second-order perturbation terms):

$$\frac{A^{pert}}{RT} = \frac{A_1}{RT} + \frac{A_2}{RT} \qquad (3.15)$$

Where A denotes the Helmholtz free energy. (The Helmholtz free energy is used frequently in statistical thermodynamics to express equations of state because most properties of interest, such as the system pressure, can be obtained by proper differentiation of A) The helmholtz free energy coefficients A_1 and A_2 have a dependence on density, composition, and molecular size (the terms A_1 and A_2 are

used in the derivation of the theory of PC-SAFT and can be found in Chapman et al 1990).

These parameters are obtained by fitting experimental vapour pressure and liquid molar volume data for pure components. Also, a k_{ij} binary interaction parameter is used to fit phase equilibrium binary data.

Perturbation theory also separates the molecular forces into an attractive and repulsive part. Hard chain expressions have been derived for describing the repulsive part (Chapman, Gubbins et al. 1990). The attractive forces are divided into the contribution due to dispersion and association. From these forces the compressibility factor is calculated as the sum of the ideal gas contribution and these forces:

(Gross and Sadowski 2002)

$$Z = Z^{ig} + Z^{hc} + Z^{disp.} + Z^{assoc.} \quad (3.16)$$

Where:

$$Z = \frac{Pv}{RT} \quad (3.17)$$

$Z^{assoc.}$ can be neglected for non-associating systems, however it needs to be considered for polar systems (vinyl acetate). Z^{ig} is the ideal gas compressibility factor and is equal to one (1). The "segment approach" was applied using PC-SAFT for polar systems by Tumakaka and Sadowski 2004. They showed polar PC-SAFT has good predictive capabilities for systems involving components with polar interactions. The normal PC-SAFT would give an acceptable representation but with a fitted binary interaction parameter.

For the basic PC-SAFT three pure component parameters are required for each component. These are:

m characteristic chain length

σ characteristic diameter

ε segment energy

To include the polar interaction between the molecules, one additional parameter is required for pure components.

x_p fraction of dipolar segments on a molecule

PC-SAFT has an optional binary interaction parameter, k_{ij} (mentioned previously) which is typically not necessary for systems whose molecules do not have much interaction.

There has been some work on extending PC-SAFT to co-polymer systems (Gross, Spuhl et al. 2003) and an internal correction parameter is included here ($k_{i\alpha i\beta}$). This parameter accounts for the cross-dispersive energy between the segments. It is similar to the formulation of the general mixing rule. The fluid mixing rule was adopted in the dispersion term, giving:

$$\varepsilon_{i\alpha i\beta} = \sqrt{\varepsilon_{i\alpha}\varepsilon_{i\beta}}\left(1-k_{i\alpha i\beta}\right) \tag{3.18}$$

$$\sigma_{i\alpha i\beta} = \frac{1}{2}\left(\sigma_{i\alpha}+\sigma_{i\beta}\right) \tag{3.19}$$

The work of Gross and Sadowski 2002 implies the following:

1. PC-SAFT has better predictive capability for the VLE of hydrocarbon systems than SAFT.
2. PC-SAFT has better predictive capability for the VLE of polymer/solvent solutions at low pressures than SAFT.
3. It also can predict the liquid-liquid equilibrium of polymer solutions at high pressures better than SAFT.
4. Although PC-SAFT somewhat over-predicts the critical point of pure substances, the predicted critical point is much closer to the measured value in PC-SAFT than in SAFT.
5. The correlative capability of PC-SAFT is superior, especially for the phase equilibria of polymer solutions at high pressures.

3.7.2 PC SAFT Pure Component Parameters

As mentioned before each species used in the model must have the three PC-SAFT component parameters. A summary of these for the major components in the mode can be seen in Table 3-6. The pure component parameters are given for polymers as well. Mass fraction missing rules are used to find the EVA parameters based on polyethylene and polyvinyl acetate. Table 3-6 incorporates the polar interaction

parameters (μ and x_p). VA is the only polar parameter used which had a significant mass fraction at any point in the model.

Component	M^C (G/MOL)	M/M^C (MOL/G)	Σ (Å)	E/K (K)	μ (D)	X_P
Ethylene	28.05	0.05679	3.4450	176.47	-	-
Vinyl Acetate	86.09	0.03662	3.3879	232.33	1.79	0.2596
Propylene	42.081	0.04657	3.5356	207.19	-	-
Polyethylene	-	0.0263	4.017	249.5	-	-
PVA	-	0.02552	3.5089	214.4	1.79	0.2596

Table 3-6 – PC-SAFT Pure Component Parameters (Tumakaka and Sadowski 2004)

M^C represents the molar mass of each component and m represents the number of segments. The three core PC-SAFT parameters in Table 3-6 were used in the model. The polar interaction was not implemented in the PC-SAFT implementation in Aspen Plus and thus was not used. This however, was not found to be significant for the required application.

3.7.3 PC SAFT Binary Interaction

PC SAFT was used for prediction of the VLE in the high pressure and low pressure separators. The accuracy of the mass in the recycle stream was very important to match the plant production. This depended heavily on the accuracy of the phase separation in these separators. The PC-SAFT binary interaction in Aspen Plus supports three types of binary parameters; these include solvent-solvent, solvent-segment and segment-segment. Assuming the binary parameter between different segments is zero, the cross energy parameter for a solvent-copolymer pair was calculated as:

$$\varepsilon_{ip} = \sum_{A}^{Nseg} X_A \sqrt{\varepsilon_{ii}\varepsilon_{AA}}\left(1-k_{iA}\right) \qquad (3.20)$$

Where:

ε_{ip} - Cross energy parameter for a solvent-copolymer pair

ε_{ii} - ε_i energy parameter for pure solvent *i*

ε_{AA} - ε_A energy parameter for pure segment of homopolymer *A*

k_{iA} - Binary parameter for a solvent-segment pair; it is determined from VLE or LLE data of the solvent *i* - homopolymer *A* solution

The cross energy parameter for a copolymer-copolymer pair in the mixture was calculated as:

$$\varepsilon_{p_1p_2} = \left(1 - k_{p_1p_2}\right)\sqrt{\varepsilon_{p_1}\varepsilon_{p_2}} \qquad (3.21)$$

Where:

$\varepsilon_{p_1p_2}$ - Cross energy parameter for a copolymer-copolymer pair

$k_{p_1p_2}$ - Binary parameter for a copolymer-copolymer pair

ε_{p_1} - Energy parameter of pure copolymer p_1

ε_{p_2} - Energy parameter of pure copolymer p_2

The binary interaction parameter, k_{ij} allows complex temperature dependence:

$$k_{ij} = a_{ij} + b_{ij}/T_r + c_{ij}\ln T_r + d_{ij}T_r + e_{ij}T_r^2 \qquad (3.22)$$

Where:

$$T_r = \frac{T}{T_{ref}} \qquad (3.23)$$

T_{ref} - Reference temperature, default value: 273.15 K

$a_{ij}, b_{ij}, ..., e_{ij}$ - constants (Aspen Technology 2005)

Table 3-7 shows the binary interaction parameters obtained from Tumakaka and Sadowski 2004. These were used as initial values for a_{ij} in equation(3.22).

Co-polymer system	component pair	$k_{i\alpha j\beta}$
EVA/Ethyene	LDPE/ethylene	0.04
	PVA/ethylene	0.03
	Ethylene segment/vinyl acetate segment	0.0287

Table 3-7 – PC SAFT Binary Interaction Parameters

The temperature dependence relationship was needed for the final model. The fitting and final values will be shown later on in the fitting of the full plant model.

3.8 Fundamentals of Free Radical Polymerization Modeling

Free radical polymerization occurs at high pressures. Organic peroxides provide the source of free radicals. A free radical is a short-lived reactive intermediate with an unpaired electron. The reaction is initiated when a free radical reacts with a monomer molecule to form another radical which propagates to other un-reacted monomer. This is a very fast reaction because of the high pressure. The chain eventually terminates, forming long chains (Meyers 2005).

3.8.1 Reaction Kinetics

Here a generalized method for the kinetic mechanism describing the free radical polymerization of ethylene (homopolymer) in high pressure reactors is considered (Ehrlich and Mortimer 1970; Goto, Yamamoto et al. 1981). The elementary reactions which make up the kinetic mechanism are summarized in Table 3-8 and shown in Figure 3-4 (Modified from Aspen Technology 2000).

Reaction	Description	Kinetics[5]
Initiator Decomposition	Primary free radicals are formed by the decomposition of initiator molecules (organic peroxides). These free radicals are unstable molecules with a free electron.	$I \xrightarrow{k_d} 2R^*$
Chain Initiation	Monomer molecules react with the primary free radicals to form polymer radicals with a chain length of one (P_1).	$R^* + M \xrightarrow{k_{ci}} P_1^*$
Propagation	The polymer chain grows as monomer molecules successively add to the polymer radicals. The radical site moves to the last	$P_n^* + M \xrightarrow{k_p} P_{n+1}^*$

[5] * - radical in mid-chain

added monomer.

REACTION	DESCRIPTION	KINETICS
Termination by combination	Two polymer radicals (live polymer) react with each other to form one dead polymer chain.	$P_n^* + P_m^* \xrightarrow{k_{tc}} D_{n+m}$
Termination by dis-proportionation	Two polymer radicals (live polymer) react with each other to form two dead polymer chains.	$P_n^* + P_m^* \xrightarrow{k_{td}} D_n + D_m$
Chain transfer to monomer	Active free radical sites on the polymer chain and a monomer molecule react to form a dead polymer chain and a polymer radical.	$P_n^* + M \xrightarrow{k_{tM}} D_n + P_1^*$
Chain transfer to agent	Active free radical sites on the polymer chain and a chain transfer agent molecule react to form a dead polymer chain and a polymer radical.	$P_n^* + A \xrightarrow{k_{tA}} D_n + P_1^*$
Beta Scission	The free radical breaks away from the live polymer chain to form a dead polymer chain and a new primary free radical.	$P_n^* \xrightarrow{k_{tbs}} D_n + R^*$
Chain transfer to polymer	Intermolecular reactions between a polymer radical and a dead polymer chain causes long chain branches (LCB)	$P_n^* + D_m \xrightarrow{k_{tP}} D_n^* + P_m$
Short-chain branching (back-biting)	The active free radical site at the end of the live polymer chain transfers to the fifth carbon atom from the end and propagates.	$P_n^* \xrightarrow{k_{scb}} P_n^*$

Table 3-8 – Polymerization Kinetics

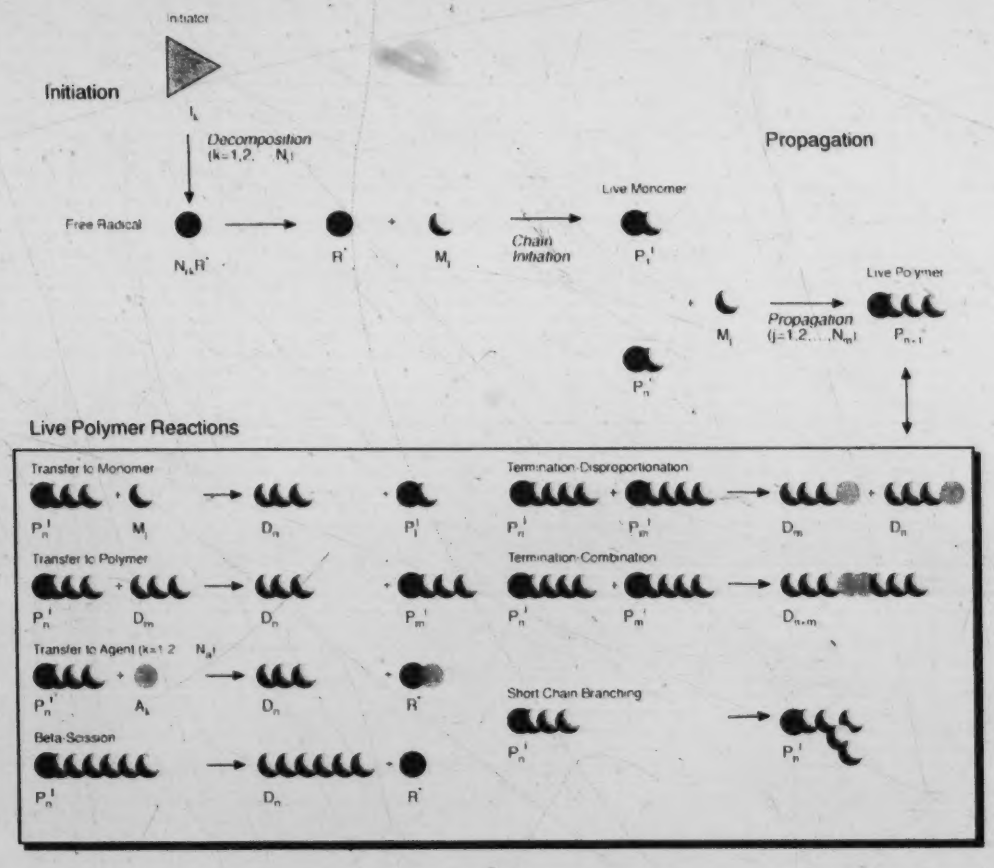

Figure 3-4 – Diagram of Free Radical Reactions

When unsaturated modifiers such as propylene and copolymers such as vinyl acetate are used, these copolymerize with ethylene. This requires an expansion in the reaction kinetics to include additional chain initiation, propagation, chain transfer and termination reactions to cover the co-monomer and active segment.

The reactivity in the copolymerization scheme is assumed to depend on the active segment to which the free radical is attached. Therefore for a two monomer system the propagation reactions are:

$$P_n^1 + M_1 \xrightarrow{k_p^{11}} P_{n+1}^1$$

$$P_n^1 + M_2 \xrightarrow{k_p^{12}} P_{n+1}^2$$

$$P_n^2 + M_1 \xrightarrow{k_p^{21}} P_{n+1}^1$$

$$P_n^2 + M_2 \xrightarrow{k_p^{22}} P_{n+1}^2$$

where P_n^i represents a live polymer radical having n segments with the free radical attached to a segment from monomer i and k_p^{ij} represents the propagation rate constant for the addition of monomer j to a live polymer chain with the free radical attached to a segment from monomer i (Bokis, Ramanathan et al. 2002). This was extended for a three monomer system, which for the propagation reaction as shown above would contain nine terms.

The reaction rate constants are calculated from the Arrhenius expression. The modified expression which is used in Aspen's Polymers Plus is shown in equation (3.24) and (3.25)

$$k_{T_{ref}} = k_o \exp\left(\frac{-E_a}{RT_{ref}}\right) \tag{3.24}$$

$$k = k_{T_{ref}}^{'} \exp\left[-\left(\frac{E_a}{R} + \frac{\Delta VP}{R}\right)\left(\frac{1}{T} - \frac{1}{T_{ref}}\right)\right] \tag{3.25}$$

Where $k_{T_{ref}}$ represents the pre-exponential factor at reference temperature (T_{ref})

3.8.2 Summary of Relevant Free Radical Kinetic Parameters from Literature

It was mentioned before that the majority of the modeling work available on free radical polymerization has been on the tubular process. One advantage of this is that the reaction kinetics published from these sources should be applicable for the autoclave process. Table 3-9 to Table 3-13 give the free radical kinetics available in the literature. It was found that fitting of these parameters were still required. Of these

the kinetics published by Iedema et al. 2003 was used as the starting point for the model regression.

Source	Propagation			Termination by combination			Termination by dis-proportionation		
	k_{po}	E_p	ΔV_p	k_{tco}	E_{tc}	ΔV_{tc}	k_{tdo}	E_{td}	ΔV_{td}
	(m^3/kmol.s)	(J/kmol)	(m3/kmol)	(m^3/kmol.s)	(J/kmol)	(m3/kmol)	(m^3/kmol.s)	(J/kmol)	(m3/kmol)
Agrawal and Han 1975	1.250E+08	3.266E+07	0.0207	2.200E+10	4.187E+06	0.0101			
Chen et al. 1976	2.950E+07	2.969E+07	0.0000	1.600E+09	1.005E+07	0.0000			
Lee and Marano 1979	5.887E+07	2.972E+07	-0.0230	1.075E+09	1.248E+06	-0.0140	3.246E+08	0.000E+00	0.0050
Goto, Yamamoto et al. 1981	1.560E+08	4.405E+07	-0.0185	8.330E+07	1.256E+07	0.0130			
Donati et al. 1982	3.100E+04	2.581E+07	-0.0248	3.100E+04	3.140E+06	0.0000			
Feucht, Tilger et al. 1985	4.800E+07	3.718E+07	0.0000	9.700E+08	3.014E+06	0.0000	9.700E+08	3.014E+06	
Gupta et al. 1985	2.950E+07	2.969E+07	0.0000	1.600E+09	1.005E+07	0.0000			
Shirodkar and Tsien 1986	5.800E+07	3.253E+07	-0.0215	2.800E+08	1.248E+06	0.0010	1.300E+08	0.000E+00	
Brandolin, Capiati et al. 1988	1.000E+06	2.196E+07	0.0000	3.000E+08	1.654E+07	0.0000			
Pladis and Kiparissides 1999	1.250E+08	3.377E+07	-0.0197	1.250E+09	4.184E+06	0.0130			
Iedema, Grcev et al. 2003	1.250E+08	3.377E+07	-0.0197	1.250E+09	4.184E+06	0.0130	1.250E+09	4.184E+06	0.0130
Ham and Rhee 1996	1.000E+06	2.712E+07	-0.0231	3.000E+08	1.654E+07		3.000E+08	1.654E+07	0.0000
Zhou et al. 2001	5.887E+07	2.970E+07	-0.0237	1.075E+09	1.250E+06	-0.0145			
Schmidt et al. 2005	1.880E+07	3.431E+07	-0.0270	8.110E+08	4.598E+06	0.0156			

Table 3-9 – Literature Free Radical Kinetics for Ethylene 1

Source	Chain transfer to polymer			Chain transfer to monomer			β-Scission		
	k_{tpo} (m3/kmol.s)	E_{tp} (J/kmol)	ΔV_{tp} (m3/kmol)	k_{tmo} (m3/kmol.s)	E_{tm} (J/kmol)	ΔV_{tm} (m3/kmol)	k_{bso} (s-1)	E_{bs} (J/kmol)	ΔV_{bs} (m3/kmol)
Agrawal and Han 1975									
Chen, Vermeychuk et al. 1976	9.000E+05	3.768E+07	0.0000				2.720E+11	8.374E+07	0.0000
Lee and Marano 1979	4.116E+05	3.226E+07	-0.0200	5.823E+05	4.626E+07	-0.0200			
Goto, Yamamoto et al. 1981	4.860E+08	5.895E+07	0.0044	1.560E+09	5.455E+07	-0.0235	2.360E+07	6.083E+07	-0.0185
Donati, Marini et al. 1982									
Feucht, Tilger et al. 1985	1.700E+06	1.959E+07	0.0000	4.600E+06	2.303E+07				
Gupta, Kumar et al. 1985	9.000E+05	3.768E+07	0.0000	2.950E+08	3.943E+07		2.950E+08	3.943E+07	0.0000
Shirodkar and Tsien 1986	7.500E+06	3.555E+07	-0.0016	1.300E+09	4.160E+07				
Brandolin, Capiati et al. 1988	4.400E+06	3.977E+07	0.0000				7.300E+06	4.737E+07	0.0000
Pladis and Kiparissides 1999	4.957E+08	5.494E+07	0.0044	1.250E+05	3.377E+07	-0.0197	1.292E+05	4.715E+07	-0.0168
Iedema, Grcev et al. 2003	4.380E+08	5.494E+07	0.0044	4.000E+04	3.377E+07	-0.0197	1.292E+05	4.715E+07	-0.0168
Ham and Rhee 1996	3.000E+04	3.925E+07	0.0198	1.000E+06	4.931E+07	0.0198	2.430E+07	4.068E+07	0.0000
Zhou, Marshall et al. 2001				5.823E+05	4.620E+07	-0.0206			
Schmidt, Busch et al. 2005	1.020E+08	4.915E+07	0.0034	3.420E+07	7.595E+07	-0.0055	1.292E+07	4.715E+07	-0.0168

Table 3-10 – Literature Free Radical Kinetics for Ethylene 2

Source	Propagation			Termination by combination			Termination by dis-proportionation		
	k_{po} (m^3/kmol.s)	E_p (J/kmol)	ΔV_p (m3/kmol)	k_{tco} (m^3/kmol.s)	E_{tc} (J/kmol)	ΔV_{tc} (m3/kmol)	k_{tdo} (m^3/kmol.s)	E_{td} (J/kmol)	ΔV_{td} (m3/kmol)
Beuermann et al. 2001	1.470E+07	2.070E+07	-0.0107						
Zhang and Ray 1997				3.700E+09	1.339E+07	0.0000			
Brandrup et al. 1999		3.520E+07			1.420E+07				

Source	Chain transfer to polymer			Chain transfer to monomer			β-Scission		
	k_{tpo} (m^3/kmol.s)	E_{tp} (J/kmol)	ΔV_{tp} (m3/kmol)	k_{tmo} (m^3/kmol.s)	E_{tm} (J/kmol)	ΔV_{tm} (m3/kmol)	k_{bso} (s^{-1})	E_{bs} (J/kmol)	ΔV_{bs} (m3/kmol)
Beuermann, Buback et al. 2001									
Zhang and Ray 1997	1.088E+04	2.636E+07	0.0000	7.616E+03	2.636E+07	0.0000			
Brandrup, Immergut et al. 1999									

Table 3-11 – Literature Free Radical Kinetics for Vinyl Acetate

Source	Propagation			Termination by combination			Termination by dis-proportionation		
	k_{tpo} (m^3/kmol.s)	E_{tp} (J/kmol)	ΔV_p (m3/kmol)	k_{tpo} (m^3/kmol.s)	E_{tp} (J/kmol)	ΔV_{tc} (m3/kmol)	k_{tpo} (m^3/kmol.s)	E_{tp} (J/kmol)	ΔV_{td} (m3/kmol)
Brandrup, Immergut et al. 1999	3.906E+07								

Source	Chain transfer to polymer			Chain transfer to monomer			β-Scission		
	k_{tpo} (m^3/kmol.s)	E_{tp} (J/kmol)	ΔV_{tp} (m3/kmol)	k_{tpo} (m^3/kmol.s)	E_{tp} (J/kmol)	ΔV_{tm} (m3/kmol)	k_{tpo} (s^{-1})	E_{tp} (J/kmol)	ΔV_{bs} (m3/kmol)
Brandrup, Immergut et al. 1999									

Table 3-12 – Literature Free Radical Kinetics for Propylene

Reactivity Ratio	r	T deg C	P(ATM)	Source
Pee/Pev	1.06	90	1010	Brandrup, Immergut et al. 1999
Pvv/Pve	1.09	90	1010	Brandrup, Immergut et al. 1999
Pee/Pep	3.2			Brandrup, Immergut et al. 1999
Ppp/Ppe	0.62			Brandrup, Immergut et al. 1999

Table 3-13 – Literature Free Radical Reactivity Ratios

3.9 Polymer Distribution Calculation

The component balance of all the species in the flow sheet on a mole basis and the energy balance of the unit process is the foundation of the Aspen Plus application. In finding the polymer distribution, we start with the material balance equations for all species polymer and non-polymer. Then the population balance equations for live and dead polymer are included. These equations for the polymer include the range of chain lengths and the kinetic scheme dictates how much of each length is present. Since the maximum chain length is usually large and it is not always required to obtain the distribution, the statistical averages which characterize the distribution can be used. Therefore we can transform the population balance equations into a set of moment equations. Usually the first second and third moments are all that are required.

These are calculated from:

Live polymer ith moment: $\mu_i = \sum_n n^i [P_n]$ (3.26)

Bulk polymer ith moment: $\lambda_i = \sum_n n^i ([P_n]+[D_n])$ (3.27)

Then the degree of polymerization averages can be calculated:

Number average degree of polymerization: $DP_n = \frac{\lambda_1}{\lambda_0}$ (3.28)

Weight average degree of polymerization: $DP_w = \frac{\lambda_2}{\lambda_1}$ (3.29)

Polydisperty index: $PDI = \frac{DP_w}{DP_n}$ (3.30)

Then the weight averages can be calculated:

Number average molecular weight: $M_n = DP_n \times MW_{seg}$ (3.31)

Weight average molecular weight: $M_w = DP_w \times MW_{seg}$ (3.32)

(MW_{seg} = average weight of each repeat unit) (Bokis, Ramanathan et al. 2002).

The polymer distribution is not actually measured at the plant (this is common for most polymer manufacturing processes). The melt index is used as the main quality

measurement. This gives an idea of the distribution and the plant is controlled by the operator using this. Thus the fit of the simulated distribution to the plant distribution was not the main focus, since it would not be applicable in finding optimal grade transitions.

3.10 Initiator Diffusion Correlations

As described later, one of the main steps in building the autoclave model involved fitting the parameters which had a significant effect on the free zone temperatures. It was found that the important parameters for fitting the free zone temperatures were the initiation and termination kinetics. There were two main initiators used at the plant for the polymer grades which were modeled. These initiators had different mixing characteristics based on the data obtained, thus a correlation was found for each.

As described by Buback et al. 2002, radical-radical termination is in general diffusion controlled. These theories were first developed in the late nineteen forties by Von Ernst Trommsdorff 1948. This gel effect attempts to model the diffusion control on the rate of polymerization and termination. There is a change in the ability of the free radicals as the polymer chain grows. As can be expected as the polymer chain grows and becomes tangled, the ability of the free radicals to diffuse will be retarded. Therefore the gel effect parameter decreases as the reaction mixture viscosity increases. Here the similar concepts from this gel effect were used and extended to form the initiator diffusion correlations. The reaction mixture viscosity is directly proportional to the autoclave zone temperature and conversion. The rate constant at a particular conversion and temperature is therefore modified as shown in equation (3.33) by a gel factor (G_F).

$$k_{eff} = k_o G_F \left(T_Z, X_Z\right) \tag{3.33}$$

Where

k_{eff} is the effective pre-exponential factor

G_F is the gel factor

T_Z is the zone temperature

X_Z is the total conversion at zone

A direct relationship between the initiator rate constant and the termination rate constants were found after sensitivity runs on the model. After attempting to fit several grades which used different initiators or even mixtures of initiators injected at different points along the autoclave, it became clear that applying the gel effect to the termination reaction did not suffice for the calculation. The free radical diffusivity was found to be dependent on the particular initiator mixture used, the temperature profile along the zones and the polymer mass fraction profile along the zones. Thus instead of applying the gel effect to the termination rate constant it was applied to the initiator rate constant. The gel factor was calculated based on the mass fraction of polymer in the particular zone and the temperature in the particular zone.

There are two built in correlations available in Aspen Plus. These are shown in equation (3.34) and (3.35).

$$G_F = \frac{a_1}{1 + a_2 X_{PF}^{a_3}} \tag{3.34}$$

$$G_F = \left(\frac{a_1 + a_2 T}{1 - a_9 X_{PF}} e^{-\left[(a_3 + a_4 T) X_{PF} + (a_5 + a_6 T) X_{PF}^2 + (a_7 + a_8 T) X_{PF}^3\right]} \right)^{a_{10}} \tag{3.35}$$

$a_1, a_2, \ldots, a_{10}$ correlation parameters

X_{PF} weight fraction of polymer

It was found that using equation (3.34) did not capture the variations for all grades. Thus equation (3.35) was used. Two correlations were built since there were two main initiators used for the grades considered.

Table 3-14 shows the regressed gel correlation parameters. Figure 3-5 and Figure 3-6 show the plot of the correlations found. These were incorporated in the final model and were found using the regression procedure which will be described later.

Parameters	a_1	a_2	a_3	a_4	a_5	a_6	a_7	a_8	a_9	a_{10}
Initiator 2	1.724E+00	2.570E-06	2.282E-02	7.232E-03	-1.050E-05	-1.300E-03	2.090E-05	4.073E-03	-5.040E-03	8.118E+00
Initiator 3	1.357E+00	-5.630E-05	7.140E-04	9.071E-03	-1.540E-05	3.030E-05	-1.015E-01	-2.830E-03	9.260E-05	7.480E+00

Table 3-14 – Regressed Gel Effect Parameters

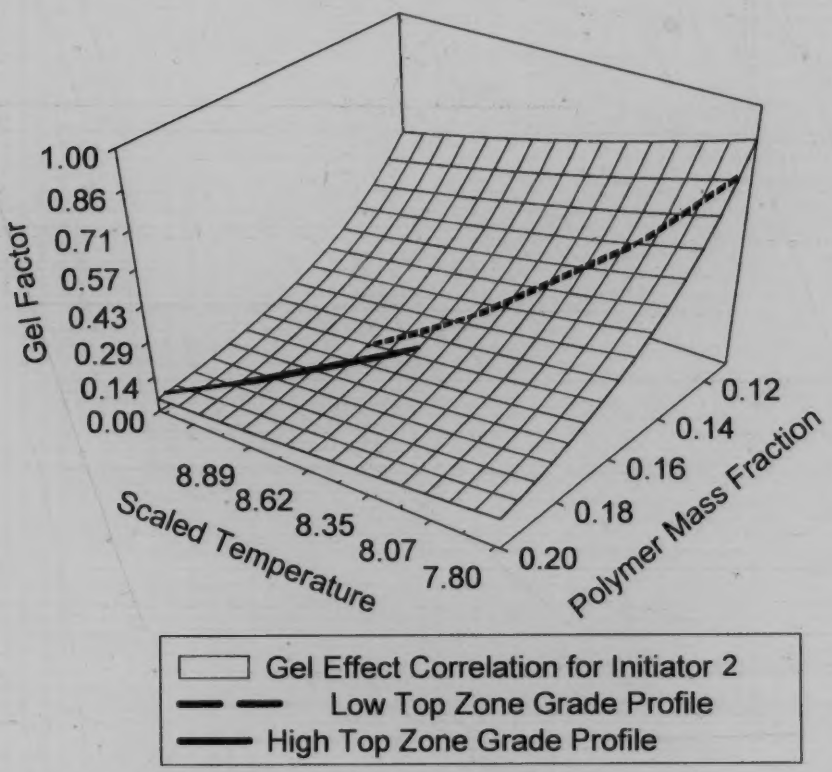

Figure 3-5 – Initiator 2 Diffusion Correlation

It is noticed that a similar effect was observed for both correlations. However, the change in the gel effect for initiator two was more significant in the high top zone temperature region. The use of high top zone and low temperature top zone refers to a distinction made between products running in the high and low temperature range for zone one.

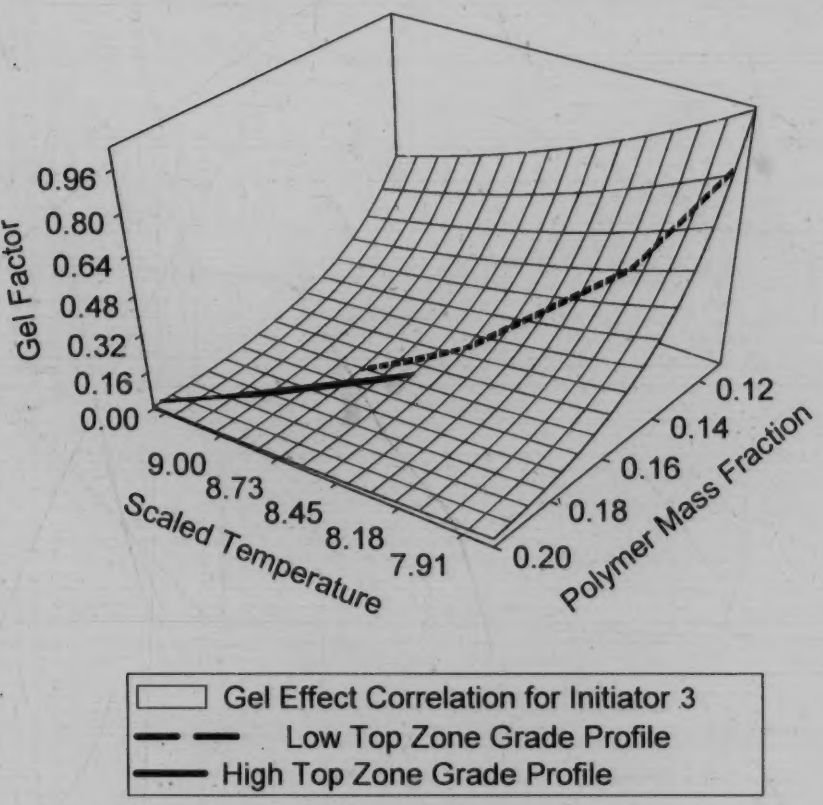

Figure 3-6 – Initiator 3 Diffusion Correlation

3.11 Incorporating Poor Zone Mixing

Luft 1977, Pladis and Kiparissides 1998 documented the importance of the autoclave's zone macromolecular mixing behaviour in modeling of high pressure autoclaves. This effect was initially assumed to be negligible. However, after attempting to fit several grades, difficulty was found in fitting zones where there was no direct initiator flow.

3.11.1 The Floating Zone

Based on the recipe there are some zones which may have no initiator flowing to them. These zones are usually lower in the autoclave. They will show a temperature

increase, indicating that there is still polymerization due to the presence of free radicals and unused initiator. Figure 3-7 shows a segment of an autoclave. Here zone 2 is a floating zone.

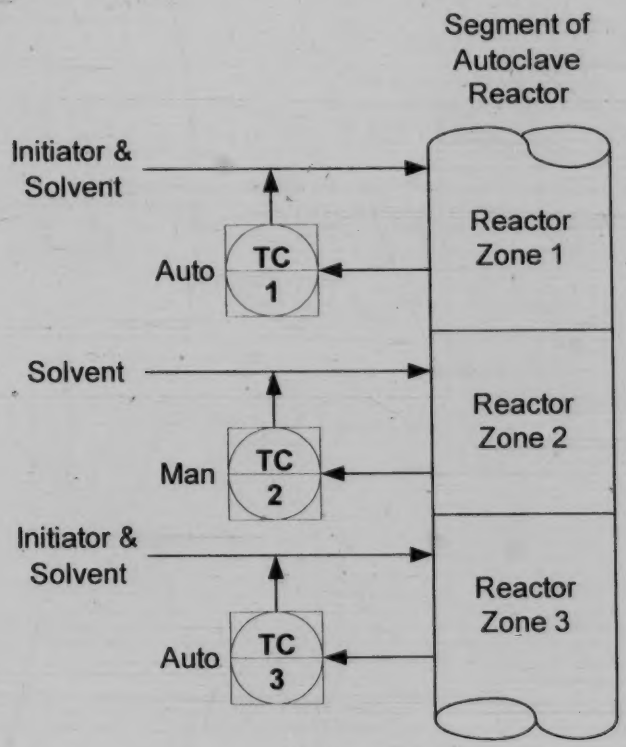

Figure 3-7 – Floating Zone

3.11.2 Model Modification

Poor mixing can cause several effects which do not comply with standard chemical engineering assumptions. Each zone of the autoclave was assumed to be a well mixed CSTR. This is not actually true. Several modeling studies (Kiparissides et al. 1993; Zhang and Ray 1997; Pladis and Kiparissides 1999) and CFD studies (Tosun and Bakker 1997; Kolhapure and Fox 1999; Schmidt, Busch et al. 2005; Wells and Ray 2005) have shown the importance of modeling the imperfect mixing effects.

Here the major problem caused by poor mixing was the unpredected, higher concentration of initiator in the lower zones. This caused the predicted temperatures in the lower zones to be less than the actual plant temperatures. This was due to the poor mixing of initiator. More initiator agglomerated into unmixed regions in the zone. These regions moved into the lower zones where these unmixed regions became better mixed. Thus behaving like another source of initiator. This was modeled by allowing a fraction of the initiator to bypass the zone without participating in the polymerization reactions. This causes higher initiator use and higher floating zone temperatures than with perfect mixing.

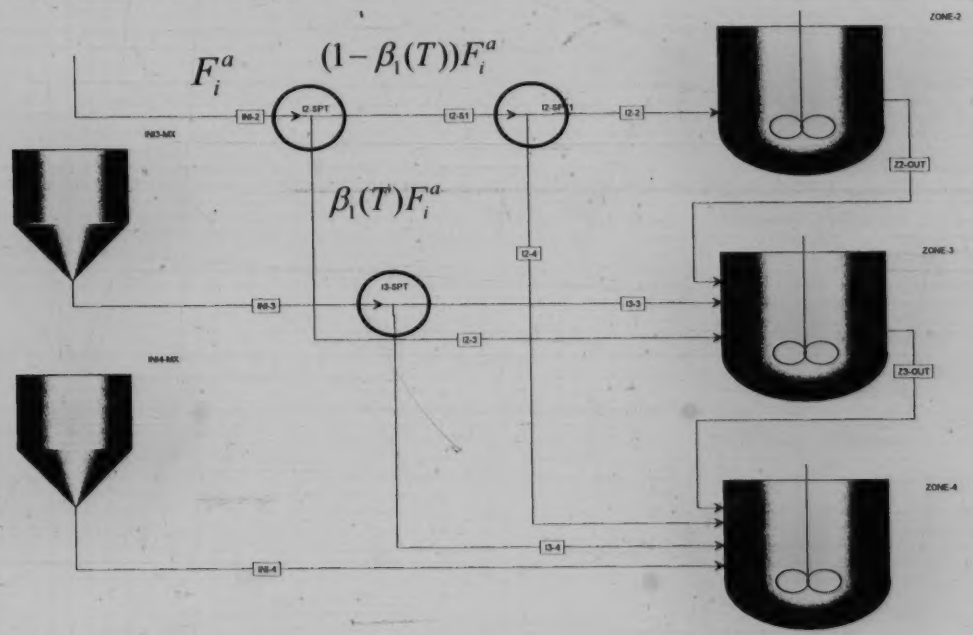

Figure 3-8 – Modeling Poor Zone Mixing

Figure 3-8 shows the method used to implement the poor initiator mixing in the model.

$$\beta_{Zij} = a_1 T_{Zi} + a_2 \qquad (3.36)$$

Where

β_{Zij} represents the flow split fraction from zone i to zone j

T_{Zi} represents the operating temperature of zone i

a_1, a_2 represent regressed constants

The correlation shown in equation (3.36) was used to modify the fraction of initiator flowing into the lower zone based on the zone operating temperature. Thus controlling the initiator mixing based on the zone temperature. a_1 and a_2 were fit using the floating zone temperatures and will be described later on.

The regressed parameters for $\beta_{Z_{24}}$ were:

$a_1 = 0.000301$

$a_2 = -0.05447$

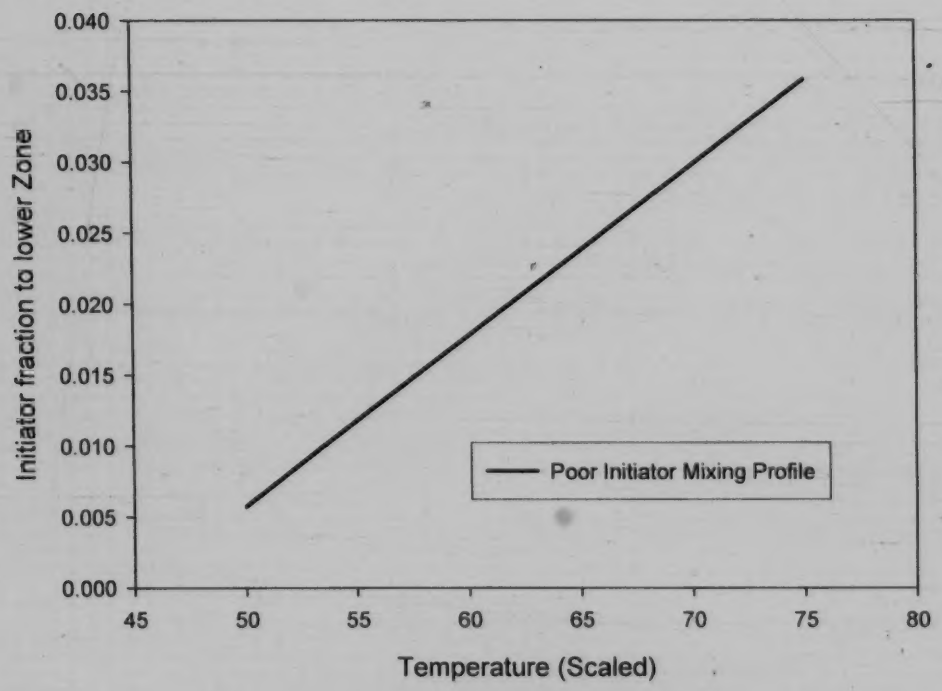

Figure 3-9 – Poor Initiator Mixing Profile

The mixing profile for this zone is shown in Figure 3-9. This shows the mixing in the zone becomes poorer as the zone operating temperature increases. This result agrees with the mixing index and plant data show in section 2.5.2.

3.12 Chapter Summary

The fundamental principles utilized in developing the first principles modeling for the EVA polymerization plant were detailed in this chapter. Details on the two equations of state were given and their applications were described. The reaction kinetics for free radical polymerization was explored. Then the additions made to the modeling theory for high pressure autoclave polymerization were detailed. This included a novel method for application of a unique gel effect to each initiator and modeling of the poor initiator mixing.

Though I am not naturally honest, I am so sometimes by chance.

William Shakespeare (1564 - 1616)

Chapter 4

First Principles Model Regression[6]

4.1 Introduction

Many parameters or coefficients in the mass, energy and component balances are required for the model. These coefficients have to be estimated from plant data using regression techniques. This chapter outlines the regression and other strategies used for parameter estimation. The variables used for regression, the results of the regression and the validation of the steady state and dynamic first principles model are also detailed.

In the published work on the use of first principles models for polymerization processes there is usually a significant amount of fitting required. This can be a very time consuming step and if certain steps are not followed cautiously, the process can take longer than expected and even give erroneous results. For high pressure EVA

[6] Portions of this chapter were presented at the 55th Canadian Chemical Engineering Conference (CSChE), October 2005, Toronto ON, Canada and Chemical Process Control 7 (CPC7), January 2006, Banff AB, Canada, by Alleyne et al.

polymerization there is no available literature on the best method for going about this regression process. Authors such as Ghiass and Hutchinson 2003 have given some details on the development of their EVA model. However, details on the parameter regression process were not stated. There are many optimization algorithms available for regressing large numbers of parameters (Cervantes, Tonelli et al. 2002). The conventional formulation of the problem is using least squares regression. However, just applying these techniques blindly can lead to a large number of parameters to regress using a limited number of plant measurements. This can lead to a badly posed problem and thus can give results which cover a very limited range of plant operation. It was found that regression of the model parameters can give excellent results for certain plant variables; however validation using independent plant data sets gave poor results. This was especially found in the case where the model parameters were fit for a very limited range of operation. The systematic approach developed here allows optimum use of the limited number of the plant variables while fitting the most important components of the model. This is a very practical procedure based mostly on the common measurements available from the plant. This sequential and iterative regression scheme can be extended for application to other types of polymerization processes.

4.2 Model Validation Variables

The model incorporated several EVA grades. There are several variables which were used for validation of the model. These were used to fit the reaction kinetics, thermodynamic parameters and the other correlations mentioned previously. Some of these validation variables were readily available from plant measurements and from the model while some others were required to be calculated from plant measurements and model properties respectively. All of the plant's product grades have specific operating recipes. These recipes have been documented and used as the basis for configuration of the simulation model. The grades vary in the content of VA, propylene and initiator concentration and operating pressure. The grades also vary in operating temperatures and the zones on which temperature control is done. This

variation in temperature control scheme causes some additional complexity for steady state modeling. Thus grade grouping, which is described later, was done. Table 4-1 shows the main variables available from the process which were used for the multiple grade model fitting.

Validation Variable	Plant Comment	Model Comment
Total Conversion *	Calculated from plant mass	Calculated from
Polymer Production	production, gas chromatographs,	monomer flows
Ethylene Conversion	feed flow rates, compressor flow	and polymer flows
Vinyl Acetate Conversion	rates and online product analysis	– directly available
Propylene Conversion	(percentage VA in polymer)	in model
Melt Index *	Online measurement available	Calculated
Vinyl Acetate Percent *	(slow)	Calculated
Floating zone temperature*	Available directly	Available directly
Weight average molecular weight Number average molecular weight	Available from offline GPC analysis of selected polymer grades	Available directly
Reactor heat duty*	The reactor should be operating close to adiabatic.	Available directly

Table 4-1 – Validation Variables

* indicates primary validation variables, others can be used where necessary.

4.2.1 Compressor Mass Flow Rate

The secondary compressor compresses the total monomer feed to the reactor. This calculation was detailed in section 2.5.1. This mass flow is a combination of each fresh component feed, the low pressure and high pressure recycle streams. A simple thermodynamics model based on the suction and discharge pressures and temperatures of each compressor stage was used to calculate the total mass flow being feed to the reactor (offline model used by Kumar et al. 2003). This therefore was an important variable for fitting and validating the model mass flow rate.

4.2.2 MI Correlation

As mentioned before the properties which are calculated by the mechanistic model (Mn, Mw…) are not those used for actual polymer quality control on the plant. One of the most widely used specifications which the polymer must meet is the melt index. This measure is based on the amount of polymer melt at a particular temperature which will flow through an orifice of a particular size for a predetermined time. This value is related to the polymer physical properties such as Mn and Mw, but a theoretically derived mathematical relationship does not exist. Thus a correlation had to be found. The data in Table 4-2 show the melt index data collected from the plant and the weight and number average molecular weight from GPC tests for five grades.

Grade	MI	Mn	Mw
1	1.15	2.21E+04	1.06E+05
2	6.05	1.68E+04	7.40E+04
3	6.79	1.64E+04	6.55E+04
4	25.79	1.35E+04	5.50E+04
5	878.50	5.93E+03	2.14E+04

Table 4-2 – Melt Index Correlation Data

The logarithmic transformation of the melt index is known to have a strong correlation with plant variables. Equation (4.1) was published by Vinodograv and Malkin 1980.

$$MI = \bar{M}_w^{-3.5} \quad (4.1)$$

From this, the correlation shown in equation (4.2) was proposed.

$$MI = e^{(A \times M_n + B \times M_w + C)} \quad (4.2)$$

From Table 4-2, the parameters of the correlation were found to be:

A = -4.20e-4

B = 1.20e-5

C = 9.61

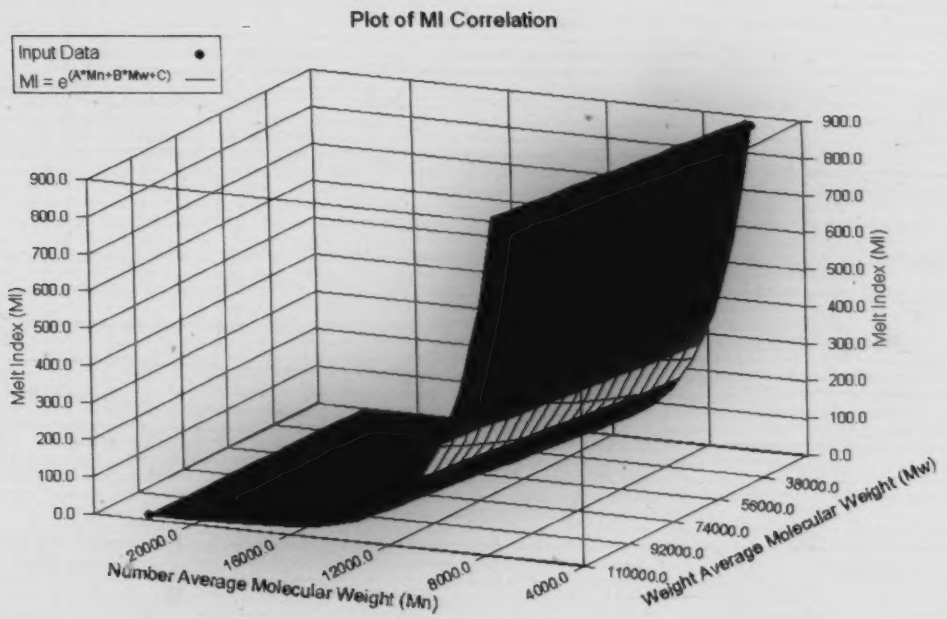

Figure 4-1 – Melt Index Correlation with M_n and M_w Plot

Figure 4-1 shows a plot of the correlation for the range of values used for fitting. This correlation was then simplified to the forms shown in equations (4.3) and (4.4).

$$MI = e^{(m_1 \times M_n + c_1)} \tag{4.3}$$

$$MI = e^{(m_2 \times M_w + c_2)} \tag{4.4}$$

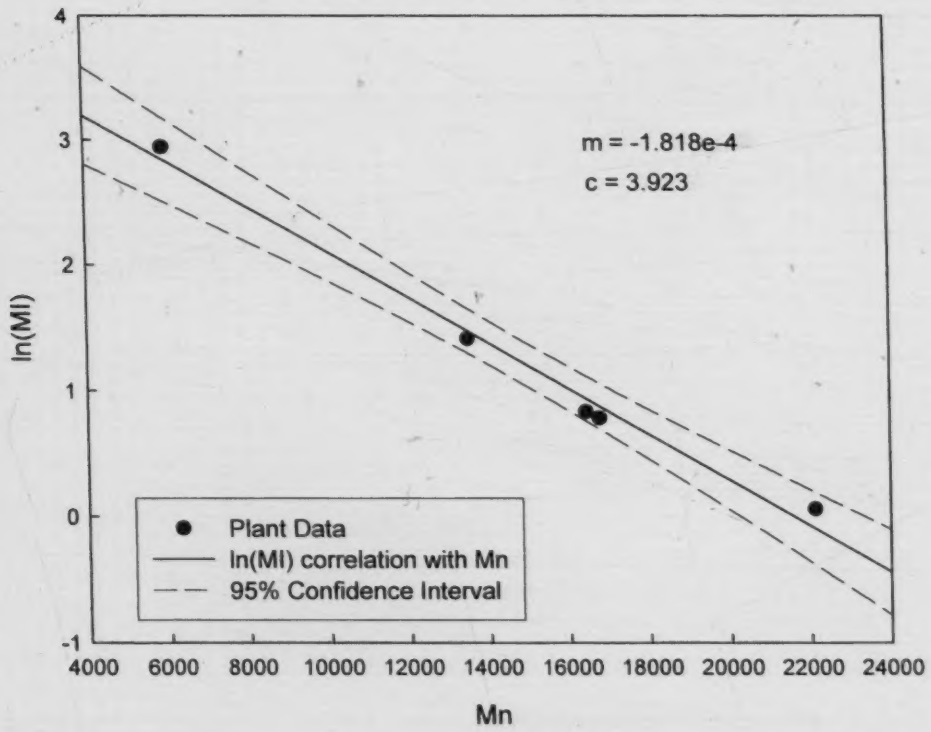

Figure 4-2 – ln(MI) to M_n Correlation Plot

Figure 4-2 shows the linear relationship found between the logarithm of the melt index and the number average molecular weight.

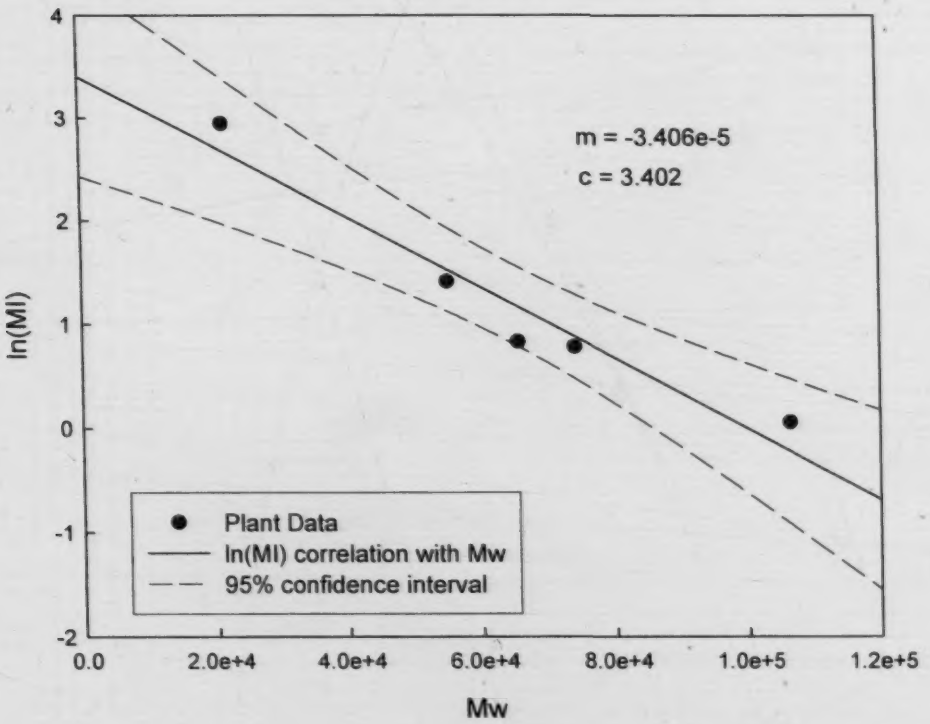

Figure 4-3 – ln(MI) to M_w Correlation Plot

Figure 4-3 shows the same relationship for the weight average molecular weight. The distribution averages were found using GPC lab tests on separate samples, each reading is made up of an average of three samples.

The MI to Mn correlation was used to calculate the MI in the first principles model, since a better fit was found here. This can be seen from the tighter confidence interval and better regression coefficient, as shown in Figure 4-2.

4.2.3 Model VA Percentage

The percentage vinyl acetate monomer in the polymer is another important measure of the polymer quality. The mole fraction of each monomer segment was tracked within the model. The relative reactivity between ethylene and VA dictated the ratio of ethylene to VA segments in the EVA co-polymer chains. The percentage VA was not available directly in the model but was calculated using equation(4.5).

$$X^i_{MP} = \frac{M^i_{Wseg} X^i_{SF}}{\sum_j M^j_{Wseg} X^j_{SF}} \times 100 \qquad (4.5)$$

Where

X^i_{MP} mass percent of component i in polymer

M^i_{Wseg} component i segment molecular weight

X^i_{SF} component i segment mole fraction in polymer

4.2.4 Initiator Mass Flow Rate

This calculated value was used to ensure that the initiator mass flow rates used in the model were comparable with the predicted mass flow rate. This calculation was detailed in section 2.5.6. For the steady state model these were implemented using design specifications within Aspen Plus. In Aspen Dynamics, PID controllers were included to directly mimic the plant operation.

4.3 Model Configuration

Details on the configuration required in Aspen Plus and Aspen Dynamics for the implementation of the model will be given next.

4.3.1 Configuration of the Steady State Model

The first block built was the steady state reactor model. This, as described previously, included detailed thermodynamics and free radical kinetics. Then the reactor model was integrated with the surrounding unit processes to build the steady state plant model. These unit processes also include detailed thermodynamics. The steady state plant model was then extended to the dynamic model by including equipment hold-ups and measurement time delays to mimic the available online plant measurements. The flow sheet used for the reactor model is shown in Figure 4-4. The autoclave reactor comprises several mixing zones. These can be modeled as a complex multi-segment and multi-recycle model as shown by Pladis and Kiparissides 1999. However, the majority of the autoclave behaviour will be shown to be captured here

by a simpler multi-zone model. The autoclave being modeled comprised four zones, with the first zone being split into two mixing regimes.

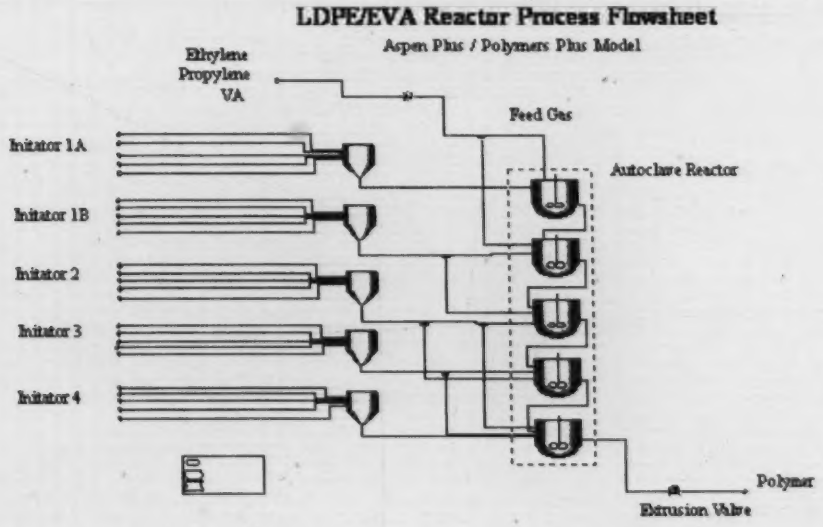

Figure 4-4 – Reactor Flow Sheet

There was also a significant amount of model configuration which was done in FORTRAN. This language was supported by Aspen Plus for custom modeling, such as the correlations described before for the melt index and VA percentage. The following were the custom blocks configured using calculator blocks:

- Grade Database (stores the grade information for all grades and accesses the correct entry based on a model parameter)
- Monomer Conversion
- MI Correlation
- Percentage VA Calculation
- Initiator Flow Correlation
- CSTR pressure equalizer (forces all CSTRS to run at the same pressure)
- Poor Mixing Calculation

The temperature controllers as mentioned before; were configured in the design specification. The following is a list of all the controllers configured in design specifications:

- Zone temperature controllers (initiator flow was the manipulated variable in controlled zones while zone temperature was simulated as a manipulated in free zones)
- Purge flow controller

The different grades produced by this reactor are as result of several different operating conditions and configurations. The modeling package was built to handle changes in the operating conditions of the unit processes. However, changes to the model configuration during the regression process, such as temperature controllers changing modes, were not supported. This required an innovative method to regress the model parameters. Sub-models (Aspen Plus Hierarchies) were used for this. Each sub model was actually a copy of the same model shown in Figure 4-4.

Figure 4-5 shows the configuration used for parameter regression. All of the grades selected for fitting were divided into classifications based on common floating zones. There were three different floating zone configurations. Thus, there were three sub-models each with different floating zones. One common set of reaction kinetics was used for all of the sub models. One flaw of this method of parameter estimation is that the model takes three times as long to converge on every run. However, at the end of the fitting process the parameter estimates were suitable for all grades being considered.

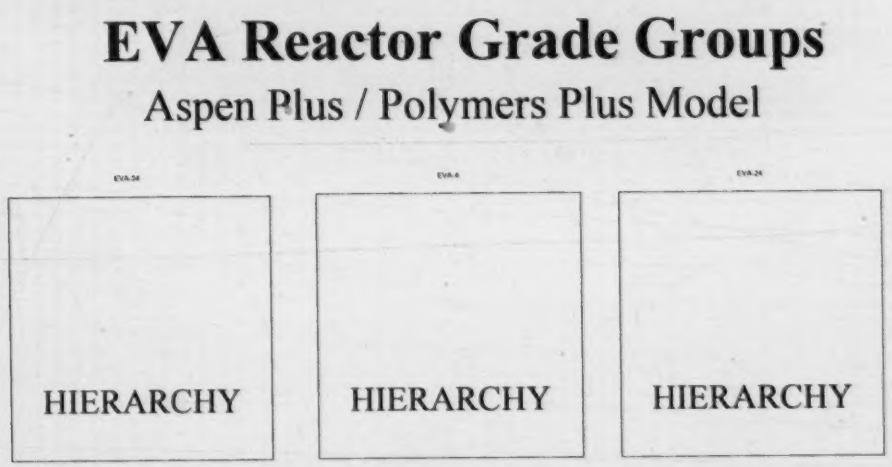

Figure 4-5 – Reactor Groups for Regression

There are impurities within the process. These impurities are present in the feed components or they are generated during the decomposition of the initiator. One major source of impurities is the reclaimed VA stream. The majority of the VA which was recycled in the low pressure loop of the process condenses at the conditions present in the inter-stage coolers of the booster compressor. The majority of the ethylene remains in the stream and is recycled. The condensed VA is sent to a VA recovery plant. This plant attempts to remove all impurities from the condensed VA stream. The product from this plant is called reclaimed VA. This reclaimed VA is mixed with fresh VA at a controlled ratio. There are several impurities which have an effect on the reactions. To simplify the effect of impurities, all components acting as impurities were lumped together as one component. This component was called Acetone. The chain transfer to agent reaction in the free radical kinetics was used to model the effect of impurities (referred to as Acetone in the model). The amount of impurities in the feed to the reactor was unknown, however based on the calculations detailed in section 2.5.5; we can get a rough idea about the amount of CTA in the reclaimed VA feed.

4.3.2 Configuration of the Dynamic Model

The steady state model developed in Aspen Plus was exported for use in Aspen Dynamics. There are two types of dynamic models supported in Aspen Dynamics. These are flow driven and pressure driven. The flow driven model does not strictly enforce pressure-flow relationships in the model and does not require "pressure changers" (valves, pumps, compressors) between every unit processes which contain vapour accumulation. For simplicity the flow driven simulation was used for this model.

The Aspen Dynamics model does not support the FORTRAN calculator blocks and the design specifications which were developed in Aspen Plus (discussed in section 4.3.1). Therefore these had to be converted to Aspen Custom Modeller Language. Aspen Dynamics supports control schemes; this allowed direct implementation of several configurations important for the dynamic model. These included:

- PID controllers
- Ratio Controller for the VA/Reclaimed VA
- Time Delays for MI and Percent VA Measurements

The flow sheet for the dynamic mode is shown in Figure 4-18. The important controllers can be seen here with their respective control connections. There are several dynamic elements of chemical engineering processes which can be modeled. The most important dynamic element was the mass accumulation. Table 4-3 summarizes the unit processes where the mass accumulation was modeled.

Unit Process	Dynamic regression
Feed Gas Coolers	Yes
Primary Compressor Inter-stage Coolers	No
Booster Compressor Inter-stage Coolers	No
Secondary Compressor Inter-stage Coolers	No
Product Cooler	Yes
High Pressure Separator	No
Low Pressure Separator	No
Return Gas Cooler	Yes
Low Pressure Recycle Cooler	Yes

Table 4-3 – Dynamic Equipment

4.4 Model Regression

The model regression was found to be one of the most important exercises in the modeling of this process. The number of parameters available for fitting and the significant interaction between them caused this step to be more complex than was initially anticipated. The steady state regression step included the fitting of reaction kinetics and correlation parameters where necessary.

One unique characteristic of the steady state parameter regression for this particular process is the large number of parameters to be regressed. There is some available literature in this area. The problem to be solved here relates to the identifiably of the

model parameter and the best experimental design for the model to identify these parameters. Typically for these large models, it is difficult to find the sensitivity of the model parameters by changing the different manipulated model variables. When the number of parameters to be fitted is more manageable, sensitivity runs can give an indication of the ability to estimate the model parameters. An example of the application of theoretical methods for analyzing the identifiably of a polymer process was given by Yao et al. 2003. Here a sensitivity matrix was created based on several runs of the model. As is usually the case with plant data, scaling was required to give a useful comparison of the sensitivities. This iterative technique required initial estimates for the parameters. Parameter estimates for ethylene polymerization are available as seen in Table 3-9 and Table 3-10. Information on the other monomers, vinyl acetate and propylene were not as easily available, but reasonable assumptions were made. Once the sensitivity matrix was formed, information on the ability to estimate the parameters was be found. One other important piece of information is the coupling of modeling parameters and process variables. Many times a modeller is not familiar with a particular process. By using the higher magnitude elements within the sensitivity matrix, one can find the best parameter to variable coupling for fitting.

Here, however a different method was followed. Initially a significant amount of time was spent understanding the process. Also because of the close interaction with industry there was a wealth of information available on the parameter to variable couplings. Therefore based on a-priori knowledge, a strategy for fitting the model parameters for this particular process was developed.

The use of carefully selected grades can allow the fitting of specific parameters. For example, grades with low VA and propylene content can be used to fit the ethylene based parameters. Grades with high VA content but low propylene content can be used to fit the VA based parameters; and so on. Hence a multi-grade parameter estimation scheme for the model was developed. This was based on the grades typically produced on the plant and the data available for different grades.

4.4.1 Aspen Plus Regression Theory

Data Fit is a component of the Aspen Plus application. This component was used for regressing the parameters of the model. Data Fit is based on NL2SOL, which is an adaptive non-linear least squares algorithm. The algorithm implemented in Data Fit was described by John E. Dennis et al. 1981, this is a trust region unconstrained optimization method with some modifications. Trusted region optimization approximates the objective function to a simpler function which gives a reasonable local approximation of the objective function behaviour.

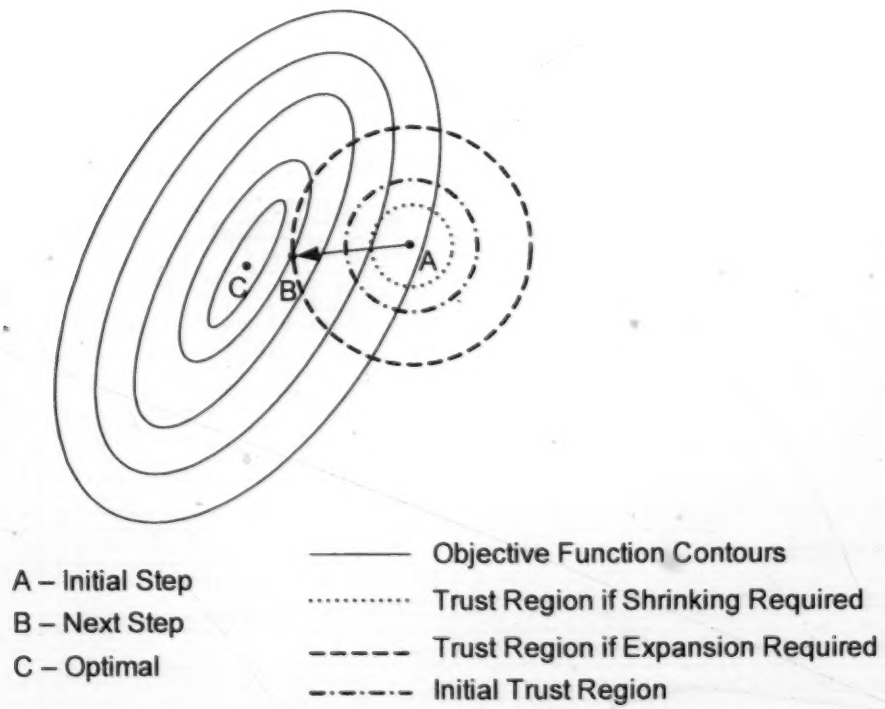

Figure 4-6 – Trust Region Optimization

A trial step is then made on the decision variables by minimizing the approximate function. Then the new value of the objective function is computed. This is usually referred to as the trusted region sub problem. If the value of the objective function is less than the previous value (for minimization) the step is accepted. Typically if this

step does not work the trusted region will be reduced and the sub problem run again. The gradient information is typically stored in the Gauss-Newton Hessian. Figure 4-6 shows a typical step using Trusted Region Optimization.

The algorithm used in Data Fit replaces the Gauss-Newton Hessian with a Hessian which includes an approximation to the difference between it and the quadratic Taylor expansion of the linearized function. Also the algorithm does not only reduce the trusted region but may switch the approximation model.

The objective function created by data fit is shown in equation (4.6).

$$\underset{X_p, X_{ri}}{\text{Min}} \frac{1}{2} \sum_{i=1}^{N_{Sets}} \left(W_i \left(\sum_{j=1}^{N_{exp}i} \left(term_1 + term_2 \right) \right) \right) \tag{4.6}$$

$$term_1 = \sum_{l=1}^{N_{ri}} \left(\frac{\left(X_{mri} - X_{ri} \right)}{\sigma_{X_{mri}}} \right)^2 \tag{4.7}$$

$$term_2 = \sum_{m=1}^{N_{rr}} \left(\frac{\left(X_{mrr} - X_{rr} \right)}{\sigma_{X_{mrr}}} \right)^2 \tag{4.8}$$

Subject to:

$$X_{plb} = X_p = X_{pub} \tag{4.9}$$

$$X_{rilb} = X_{ri} = X_{riub} \tag{4.10}$$

Where:

N_{Sets} represents the number of data sets specified for regression

$N_{exp}i$ represents the number of experiments in data set i

N_{ri} represents the number of reconciled input parameters

N_{rr} represents the number of measured result variables

W_i represents weight for data set i

X_p represents the vector of varied parameters

X_{mri} represents the measured value of the reconciled input variables

X_{mrr} represents the measured values of the result variables

X_{rr} represents the calculated value for the result variables

σ represents the standard deviation for the measured variables

The measured variables were average steady state operating data. The averages were found from at least three distinct steady state operating periods. During the data fitting process there were two parameters which were used to improve the estimates found by the algorithm. These were the initial step size (default = 1) and the relative perturbation size (default = 0.005). The initial step size sets the initial step size of the trust region. This was moved within the range 0.1 to 10 once a solution was found. The relative perturbation size was increased up to 0.5 once a solution was found. This procedure could some times help if the optimizer converged at a local minimum point.

4.4.2 Parameter Sensitivity

Knowledge of the necessary couplings for regression between the validation variables and the estimated parameters requires in depth knowledge of the first principles of the process. As mentioned, this model contains many parameters which require fitting. Thus a systematic scheme for doing this had to be developed.

Reaction Parameters used for Estimation	Estimation and Validation Variable				
	Conversion	MWN	MWW	FLCB	FSCB
Chain Initiation	X				
Chain Propagation	X				
Chain Transfer to Monomer		X			
Chain Transfer to Polymer			X	X	
Chain Transfer to Agent		X			
Chain Transfer to Solvent		X			
Beta-Scission		X			
Termination by Disprop.	X				
Termination by Combination	X				
Short Chain Branching					X

Table 4-4 – Estimation Parameter to Variable Pairing (Hendrickson 1997)

A fundamental part of this is having a clear understanding of the correct parameter to variable combinations for regression. Hendrickson 1997 attempted modeling of a similar type of process. Table 4-4 shows his pairings. Quickly after inspection of this table one realizes that there is not a one to one pairing for the parameters to variables. Figure 4-7 from Meyers 2005 shows the sensitivity of several common polymer quality variables to reactor temperature and pressure (applicable for tubular and autoclave reactors).

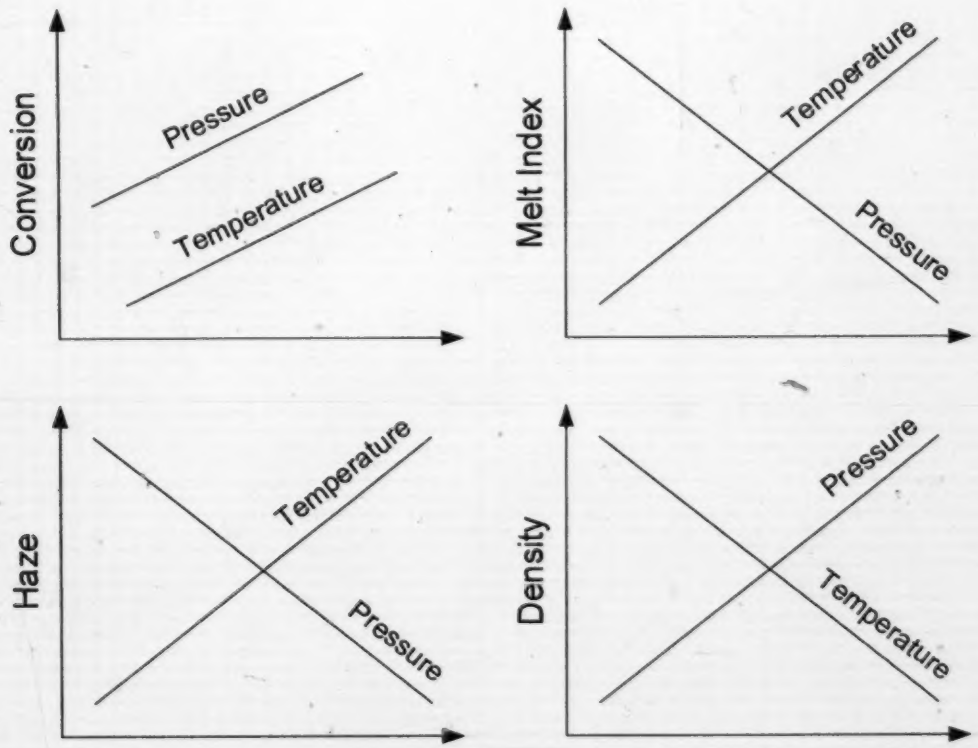

Figure 4-7 – Quality Variable Sensitivity to Plant Conditions

From these several couplings can be implied. Sensitivity runs on the steady state model with literature values were available or assumed values were used to find couplings that were not easily discernable. An example of this can be seen in Figure 4-8.

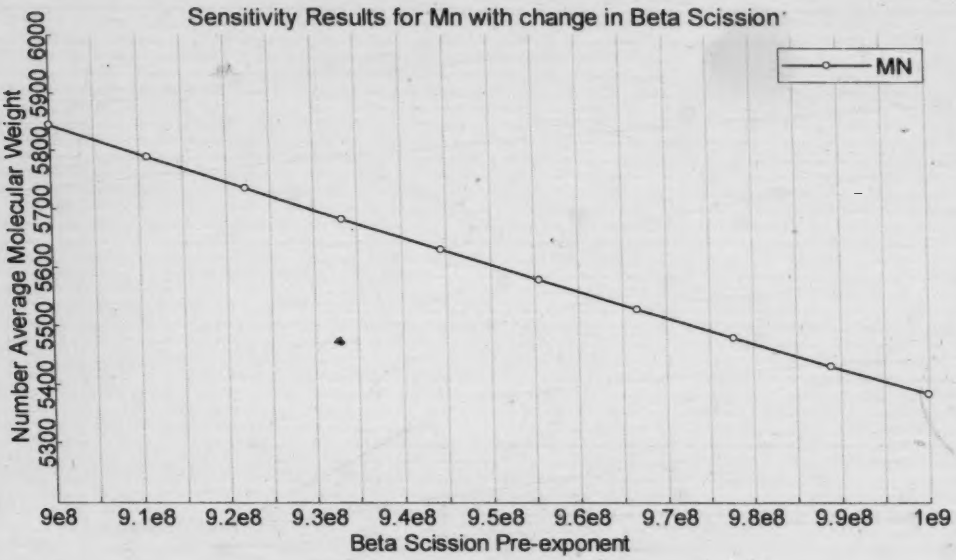
Sensitivity Results for Mn with change in Beta Scission
MN
Number Average Molecular Weight
5300 5400 5500 5600 5700 5800 5900 6000
9e8 9.1e8 9.2e8 9.3e8 9.4e8 9.5e8 9.6e8 9.7e8 9.8e8 9.9e8 1e9
Beta Scission Pre-exponent

Figure 4-8 – M_n Sensitivity to β -Scission

These relationships were built to separate the parameter regression process into discrete elements. Each of these regression elements would comprise of some parameter for estimation and plant readings which were tightly coupled with the parameter. However, it was found that there was significant interaction between many of the parameters. Therefore the concept of discrete fitting elements was not possible for all elements. A sequential and iterative regression scheme had to be developed. This will be discussed and shown next.

Table 4-5 shows the parameter to variable couplings used as the basis for the regression scheme which was developed. This was based on prior plant knowledge, information available in the literature and sensitivity runs on an approximate model. Minor couplings are not indicated. These may case problems while regressing parameters but the effects of these should be compensated for by the iterative technique.

Parameters to Estimate	Measurement used for Estimation and Validation (Variables)							
	Conversion[1]	T_{FLOAT}[2]	Duty	MI[2]	% VA[2]	MWW[3]	PDI[3]	Flow[1]
Initiator Efficiency & Activation Volume		X	X					Initiator
Chain Initiation	X		X					
Chain Propagation	X		X	X	X		X	
Chain Transfer to Monomer				X				
Chain Transfer to Polymer				X		X		
Chain Transfer to Agent				X				
Beta-Scission				X				
Termination	X		X					
Gel Effect Correlation		X	X					
Zone Poor Mixing Correlation		X						
PC-SAFT Binary Interaction (F)								Total to reactor
Equipment mass hold up (D)				X	X			
Measurement dead time (D)				X	X			

Table 4-5 – Parameter to Variable Coupling for Regression

F – requires full plant model for estimation D – requires dynamic model and data for estimation

Duty – the autoclave should be adiabatic, therefore the duty should be ideally 0, a small value of -5000 W is used in the simulation.

[1] – Calculated [2] – Average from historian [3] – from GPC analysis of polymer samples

4.4.3 Iterative Multiple Grade Model Regression Scheme

There has not been much research focused on finding the best method to actually regress the model parameters once the couplings discussed earlier have been found. It is intuitive that finding the parameter to variable pairings is important, but once this is done the steps which follow are typically ad-hoc and subjective.

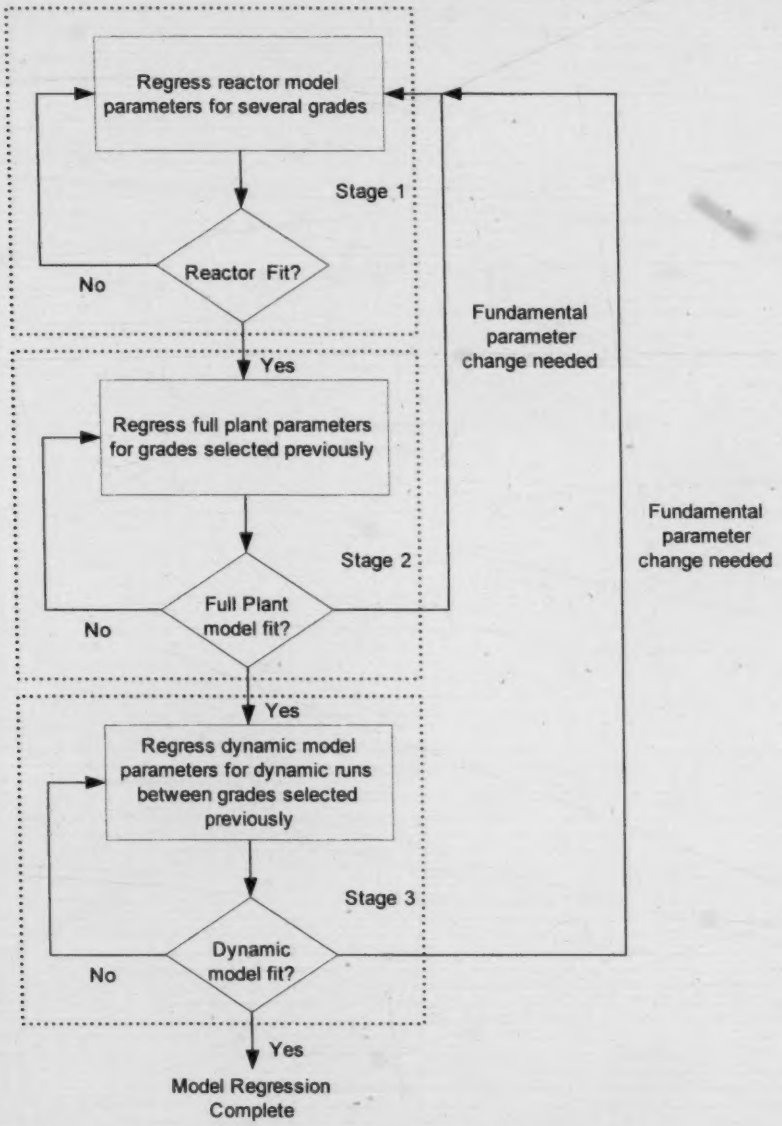

Figure 4-9 – Flowchart for Regression

A systematic method for parameter regression for this complex model has been developed. The steps defined here were developed based on the requirement of the modeling applications, to configure the steady state model followed by the dynamic model, the sensitivity and interaction of the model parameters and the variables available for validation. Figure 4-9 shows the high level regression steps. This has been broken into three stages.

At stage 1 the reactor parameters only are regressed. These parameters include any thermodynamics, reaction kinetics and reactor specific correlations. The data used for regression and validation are averages of plant variables during steady state conditions. One advantage of attempting the 'reactor-only-fit' first is that there were no recycle loops at this point. This allows faster convergence of the model with the "sequential modular" Aspen Plus solver (explained in 4.6.2).

Stage 2 extends the reactor model to include the other unit processes which comprise the plant. This is necessary based on the objective of the model which was optimal grade transition trajectories. The manipulated variable trajectories had to be the actual manipulated variables which the operators use. Therefore modeling of the full plant was necessary. At this point steady state plant data was used to regress thermodynamic parameters which affect certain key sections of the plant flow sheet. The parameters which affect the VLE in the separators were the main area of focus. The system losses were also taken into consideration at this point. There is the possibility of having to return to Stage 1. This occurs in the case where the VLE parameters have exceeded the acceptable limits or the solution is unattainable. The unattainable situation was encountered, on further inspection it was noticed that the conversion of one of the monomers was causing the problem. This required moving back to stage 1 and fitting the conversion for that particular monomer then moving to step 2 again. After acceptable results were obtained from stages 1 and 2, stage 3 could be started.

Stage 3 was carried out by exporting the model to Aspen Dynamics, modified and converging successfully on steady state simulations. This required some modifications to the model which will be described later. The main focus of step 3 was to capture the critical dynamic aspects of the model. Since the dynamic model

would be validated against measurements directly from the plant it was important that the model captured the time delays and time constants for each measurement. On a typical plant the time delays are caused by transport lags and measurement lags. The significant part of the time constant for this process was due to the mass of gas accumulated in the system. The majority of the gas in the system was always ethylene. However VA and propylene do have a significant effect on the reactions. The mass accumulation of ethylene causes the concentration of the other components to change slowly. This can be thought of as a large amount of ethylene flowing into a vessel with a small amount of propylene. If the propylene feed increases, the concentration leaving the tank does not increase immediately. The concentration builds over time; the larger the volume of the vessel, the longer the time. Estimates for the vessel accumulation were taken from the plant design data and estimates for the measurement time delays were found from dialogues with the senior plant operators. At this point it was confirmed that the dynamic model, while running at steady state fit the plant well. Then the dynamic estimation was done focusing on the critical vessels and process measurement delays (the transport lags were lumped into the measurement delays).

Model Regression – Stage 1

Here details on the steps involved in completing stage 1 of the regression scheme are given. The availability of plant data was critical for this type of modeling. In addition to the variables (regressed variables) which were collected from the plant historian (mentioned in Table 4-5), other plant operating variables (regression inputs) were needed to ensure the model mimicked the plant as closely as possible. For stage 1 these additional variables included:

- Propylene content in feed (average GC reading used)
- Reactor pressure
- Temperature of controlled zones
- Feed gas coolers discharge temperature (used to set the reactor feed gas temperature)

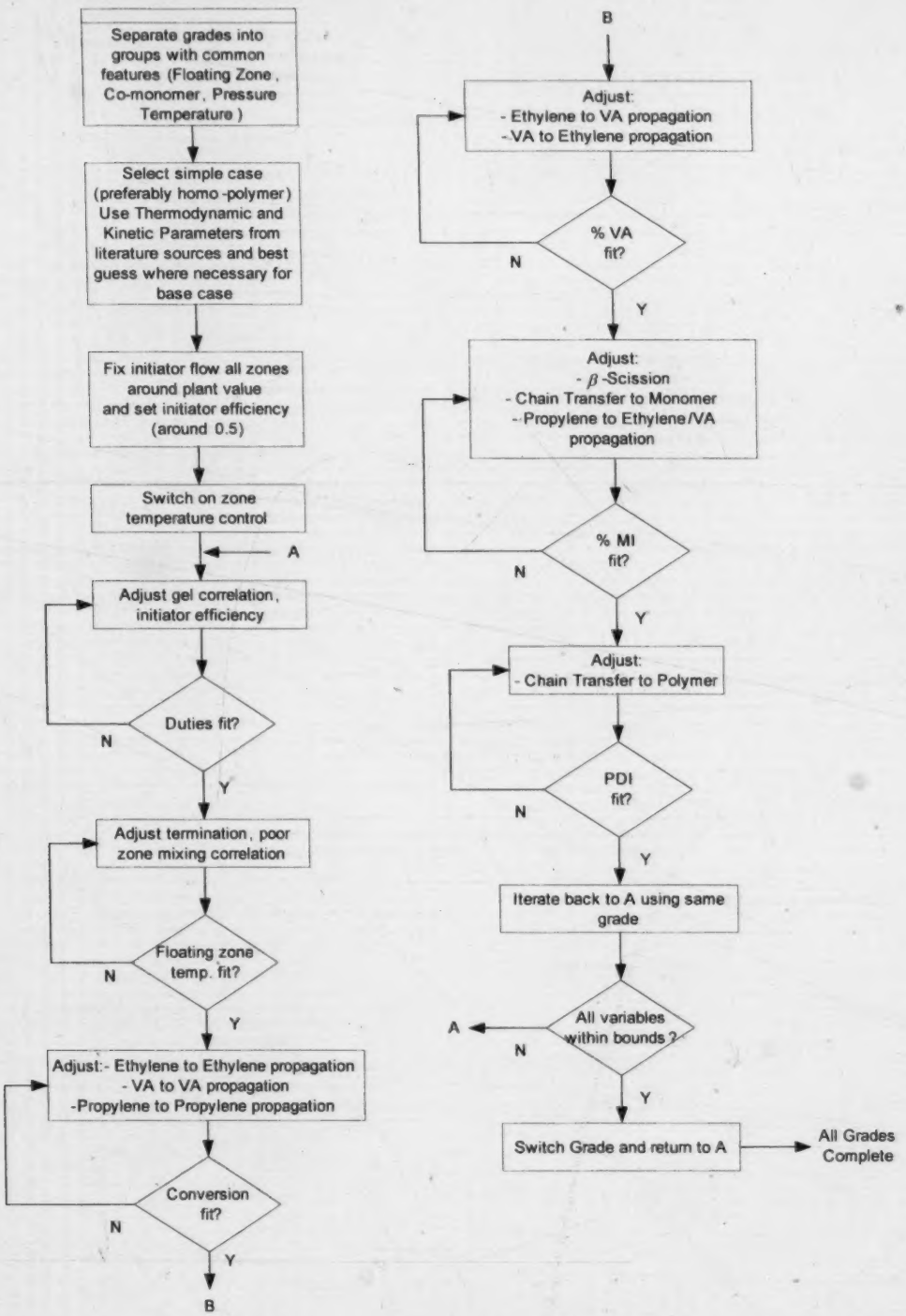

Figure 4-10 – Reactor Regression Scheme

Figure 4-10 shows the flow chart for the reactor regression scheme. The choice of grades here was very important. Here it was more important to group the grades based on similar reactor pressure, controlled zone temperatures and reactor feed composition. This was because of the three distinct parameters which were required to be regressed in each Arrhenius equation (equation (3.25)).

The paring used for these during the fitting process were:

- k_o relates to changes in composition
- E_a relates to changes in temperature
- ΔV relates to changes in pressure

Thus the regression parameters during a regression run would be limited to the specific parameters in the Arrhenius equation which have been changed for the particular grade being run. That is if there was a pressure change in moving from one grade to another, the first grade could be used to fit k_o and the second grade could be used to fit ΔV. This iterative procedure was used to regress the reactor parameters for eight strategically chosen grades which covered the plant's full range of operation.

Model Regression – Stage 2

During the previous stage the feed to the reactor was one simple stream which contained the components expected at that point in the process (see Figure 4-4). Here the other unit processes, recycle and feed streams were added to complete the steady state plant flow sheet (see Figure 1-4). Upon making these modifications and having the flow sheet converge, it was noticed the properties of the product leaving the reactor were different. This was because the reactor feed composition had changed. The challenge was now to regress parameters of the full plant so that the feed composition to the reactor returned to the expected values.

Similar to stage 1, the average of several plant process variables were used as fixed inputs to the model during the regression process. In addition to the variables mentioned in stage1, the following variables were included:

- Ethylene Mass Flow
- Total Vinyl Acetate Mass Flow

- Percentage reclaimed VA in total VA
- Propylene Mass Flow
- Propylene Concentration in Feed
- Purge Mass Flow
- LPS Pressure and Temperature
- HPS Temperature and Pressure

Figure 4-11 shows the steps involved in regressing the parameters for the full plant steady state model. The parameters which were regressed were $a_{ij}, b_{ij}, ..., e_{ij}$ in equation (3.22) and k_{ij}^1, k_{ij}^2 and k_{ij}^3 in equation (3.13).

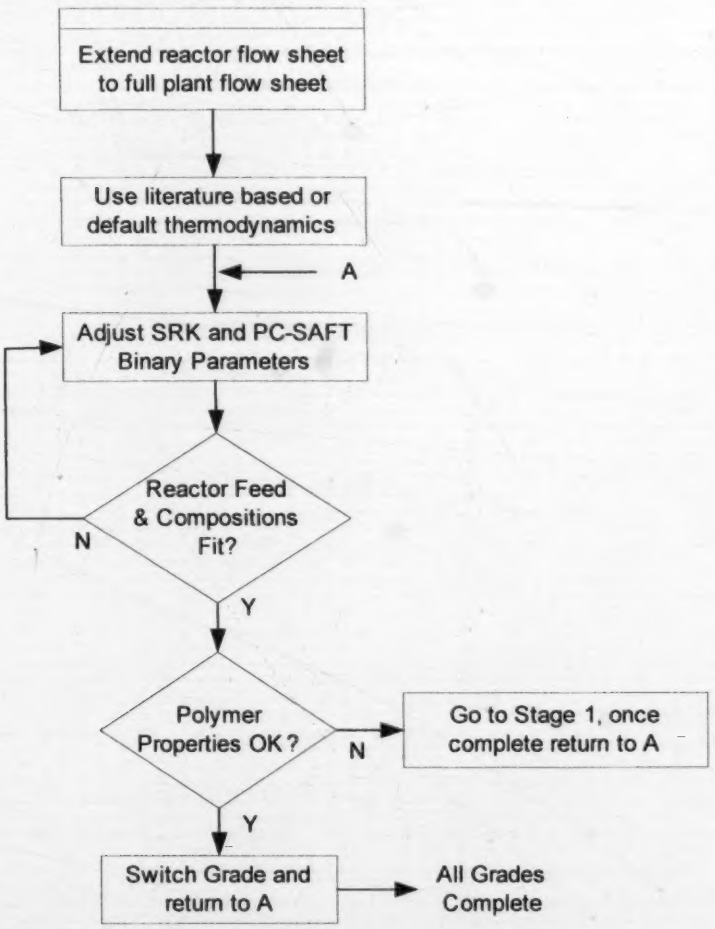
Extend reactor flow sheet to full plant flow sheet
Use literature based or default thermodynamics
A
Adjust SRK and PC-SAFT Binary Parameters
Reactor Feed & Compositions Fit?
N
Y
Polymer Properties OK?
N
Go to Stage 1, once complete return to A
Y
Switch Grade and return to A
All Grades Complete

Figure 4-11 – Full Plant steady State Model Regression Scheme

Model Regression – Stage 3

After stage 2 the steady state model was exported and modified for Aspen Dynamics.

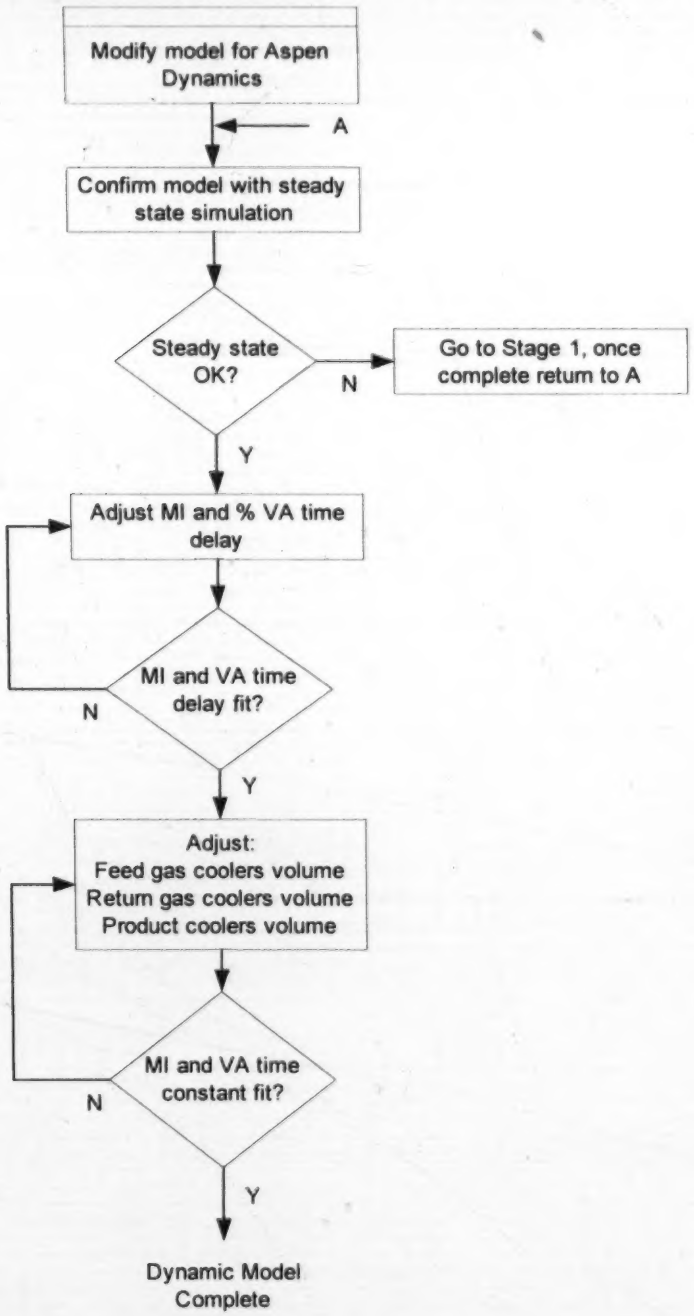

Figure 4-12 – Dynamic Model Regression

The modification required some work is would be described later in section 4.3.2. The steps for fitting the dynamic model are detailed in Figure 4-12.

It was necessary to confirm, if the dynamic model converged to the correct steady state values, and if not stage 1 would be run again. The steady state run of the dynamic model was done using validation data sets for the same grades regressed in step 2. Once these were confirmed, dynamic plant data was used for regressing the dynamic parameters of the model. It is worthwhile to mention here that only a certain number and not all dynamic parameters were regressed. As can be seen in Figure 4-12, the measurement delays were regressed by adjusting the delays of time delay blocks and the time constants were regressed using the volume of three main heat exchangers:

- Feed gas coolers
- Return gas coolers
- Product coolers

This is where the majority of mass hold up occurred.

4.4.4 Steady State Model – Regressed Parameters

The final regressed parameters from stages 1 and 2 are given here. Table 4-6, to Table 4-9 show the regressed parameters for the reaction kinetics. Table 4-10 shows the regressed parameters for the PC-SAFT binary interaction. Table 3-14 showed the regressed gel correlation parameters. Section 3.11.2 gave the regressed coefficients for simulating the poor initiator mixing.

Reaction	Comp 1	Comp 2	Pre-Exp (s^{-1})	Act-Energy (J/kmol)	Act-Volume (m^3/kmol)	Ref. Temp. (°C)	Eff.
INIT-DEC	*Initiator 1*		3.200E+15	1.535E+08	0.021	1.00E+35	0.3
INIT-DEC	*Initiator 2*		1.540E+14	1.249E+08	0.01242	1.00E+35	0.4235
INIT-DEC	*Initiator 3*		3.420E+15	1.236E+08	0.025	1.00E+35	0.3634
INIT-DEC	*Initiator 4*		2.490E+16	1.502E+08	0.02141626	1.00E+35	0.5
CHAIN-INI	*Ethylene*		2.540E+08	3.530E+07	0.08	1.00E+35	
CHAIN-INI	*Vinyl Acetate*		2.540E+08	3.530E+07	0.08	1.00E+35	
CHAIN-INI	*Propylene*		2.540E+08	3.530E+07	0.08	1.00E+35	
PROPAGATION	*Ethylene*	*Ethylene*	1.490E+08	2.852E+07	-0.0007072	1.00E+35	
PROPAGATION	*Ethylene*	*Vinyl Acetate*	1.554E+08	3.011E+07	-0.0149104	1.00E+35	
PROPAGATION	*Ethylene*	*Propylene*	1.794E+08	3.043E+07	-0.0150547	1.00E+35	
PROPAGATION	*Vinyl Acetate*	*Ethylene*	1.224E+08	3.011E+07	-0.5742968	1.00E+35	
PROPAGATION	*Vinyl Acetate*	*Vinyl Acetate*	1.490E+08	3.011E+07	-0.00001552	1.00E+35	
PROPAGATION	*Vinyl Acetate*	*Propylene*	2.610E+08	4.250E+07	-0.0247567	1.00E+35	
PROPAGATION	*Propylene*	*Ethylene*	1.436E+08	3.059E+07	-0.0426918	1.00E+35	
PROPAGATION	*Propylene*	*Vinyl Acetate*	2.610E+08	4.250E+07	-0.0247567	1.00E+35	
PROPAGATION	*Propylene*	*Propylene*	3.500E+08	4.240E+07	-0.02027	1.00E+35	
CHAT-MON	*Ethylene*	*Ethylene*	7.944E+05	4.250E+07	-0.0347	1.00E+35	
CHAT-MON	*Ethylene*	*Vinyl Acetate*	4.791E+07	3.758E+07	0.0073569	1.00E+35	
CHAT-MON	*Ethylene*	*Propylene*	9.094E+03	4.621E+07	-0.000019634	1.00E+35	
CHAT-MON	*Vinyl Acetate*	*Ethylene*	1.035E+04	1.754E+07	0.026419	1.00E+35	

Table 4-6 – Regressed Free Radical Kinetics 1

Reaction	Comp 1	Comp 2	Pre-Exp (s^{-1})	Act-Energy (J/kmol)	Act-Volume (m^3/kmol)	Ref. Temp. (°C)	Eff.
CHAT-MON	*Vinyl Acetate*	*Vinyl Acetate*	4.032E+05	4.630E+07	-0.01458	1.00E+35	
CHAT-MON	*Vinyl Acetate*	*Propylene*	2.820E+05	4.630E+07	-0.0002491	1.00E+35	
CHAT-MON	*Propylene*	*Ethylene*	4.254E+05	4.630E+07	-0.0002491	1.00E+35	
CHAT-MON	*Propylene*	*Vinyl Acetate*	2.800E+05	4.630E+07	-0.0002491	1.00E+35	
CHAT-MON	*Propylene*	*Propylene*	2.820E+05	4.630E+07	0.000241	1.00E+35	
CHAT-AGENT	*Ethylene*	*Acetone*	6.562E+05	5.354E+07	-0.27115	1.00E+35	
CHAT-AGENT	*Vinyl Acetate*	*Acetone*	2.079E+05	5.498E+07	0.000001371	1.00E+35	
CHAT-AGENT	*Propylene*	*Acetone*	4.511E+04	5.498E+07	0.9862	1.00E+35	
CHAT-POL	*Ethylene*	*Ethylene*	4.451E+07	1.243E+08	0.0060594	1.00E+35	
CHAT-POL	*Ethylene*	*Vinyl Acetate*	3.452E+08	8.372E+07	0.021927	1.00E+35	
CHAT-POL	*Ethylene*	*Propylene*	1.450E+08	2.889E+07	0.001641	1.00E+35	
CHAT-POL	*Vinyl Acetate*	*Ethylene*	6.826E+04	1.311E+08	0.0040987	1.00E+35	
CHAT-POL	*Vinyl Acetate*	*Vinyl Acetate*	7.465E+07	5.040E+07	0.005139	1.00E+35	
CHAT-POL	*Vinyl Acetate*	*Propylene*	1.617E+08	5.040E+07	0.0044	1.00E+35	
CHAT-POL	*Propylene*	*Ethylene*	2.058E+07	5.040E+07	0.002205	1.00E+35	
CHAT-POL	*Propylene*	*Vinyl Acetate*	8.730E+07	5.040E+07	0.0044	1.00E+35	
CHAT-POL	*Propylene*	*Propylene*	8.411E+07	5.040E+07	0.0044	1.00E+35	
B-SCISSION	*Ethylene*		6.521E+07	1.143E+08	0.15305	1.00E+35	
B-SCISSION	*Vinyl Acetate*		3.073E+06	1.737E+08	2.2698E-06	1.00E+35	
B-SCISSION	*Propylene*		1.436E+11	4.891E+07	0.002061	1.00E+35	

Table 4-7 – Regressed Free Radical Kinetics 2

Reaction	Comp 1	Comp 2	Pre-Exp (s^{-1})	Act-Energy (J/kmol)	Act-Volume (m^3/kmol)	Ref. Temp. (°C)	Eff.
TERM-DIS	*Ethylene*	*Ethylene*	3.610E+09	4.211E+06	0.01623	1.00E+35	
TERM-DIS	*Ethylene*	*Vinyl Acetate*	3.610E+09	4.211E+06	0.01623	1.00E+35	
TERM-DIS	*Ethylene*	*Propylene*	3.610E+09	4.211E+06	0.01925	1.00E+35	
TERM-DIS	*Vinyl Acetate*	*Ethylene*	3.610E+09	4.211E+06	0.01623	1.00E+35	
TERM-DIS	*Vinyl Acetate*	*Vinyl Acetate*	3.610E+09	4.211E+06	0.01623	1.00E+35	
TERM-DIS	*Vinyl Acetate*	*Propylene*	3.610E+09	4.211E+06	0.01623	1.00E+35	
TERM-DIS	*Propylene*	*Ethylene*	3.610E+09	4.211E+06	0.01623	1.00E+35	
TERM-DIS	*Propylene*	*Vinyl Acetate*	3.610E+09	4.211E+06	0.01623	1.00E+35	
TERM-DIS	*Propylene*	*Propylene*	3.610E+09	4.211E+06	0.01623	1.00E+35	
TERM-COMB	*Ethylene*	*Ethylene*	3.610E+09	4.211E+06	0.01623	1.00E+35	
TERM-COMB	*Ethylene*	*Vinyl Acetate*	3.610E+09	4.211E+06	0.01623	1.00E+35	
TERM-COMB	*Ethylene*	*Propylene*	3.610E+09	4.211E+06	0.02146	1.00E+35	
TERM-COMB	*Vinyl Acetate*	*Ethylene*	3.610E+09	4.211E+06	0.01623	1.00E+35	
TERM-COMB	*Vinyl Acetate*	*Vinyl Acetate*	3.610E+09	4.211E+06	0.01623	1.00E+35	
TERM-COMB	*Vinyl Acetate*	*Propylene*	3.610E+09	4.211E+06	0.01623	1.00E+35	
TERM-COMB	*Propylene*	*Ethylene*	3.610E+09	4.211E+06	0.01623	1.00E+35	
TERM-COMB	*Propylene*	*Vinyl Acetate*	3.610E+09	4.211E+06	0.01623	1.00E+35	
TERM-COMB	*Propylene*	*Propylene*	3.610E+09	4.211E+06	0.01341	1.00E+35	
SC-BRANCH	*Ethylene*	*Ethylene*	3.360E+09	4.580E+07	-0.0235	1.00E+35	
SC-BRANCH	*Ethylene*	*Vinyl Acetate*	3.360E+09	4.580E+07	-0.0235	1.00E+35	

Table 4-8 – Regressed Free Radical Kinetics 3

Reaction	Comp 1	Comp 2	Pre-Exp (s^{-1})	Act-Energy (J/kmol)	Act-Volume (m^3/kmol)	Ref. Temp. (°C)	Eff.
SC-BRANCH	*Ethylene*	*Propylene*	2.550E+09	3.380E+07	-0.0235	1.00E+35	
SC-BRANCH	*Vinyl Acetate*	*Ethylene*	3.360E+09	4.580E+07	-0.0235	1.00E+35	
SC-BRANCH	*Vinyl Acetate*	*Vinyl Acetate*	3.360E+09	4.580E+07	-0.0235	1.00E+35	
SC-BRANCH	*Vinyl Acetate*	*Propylene*	2.550E+09	4.580E+07	-0.0235	1.00E+35	
SC-BRANCH	*Propylene*	*Ethylene*	2.550E+09	3.380E+07	-0.0235	1.00E+35	
SC-BRANCH	*Propylene*	*Vinyl Acetate*	2.550E+09	4.580E+07	-0.0235	1.00E+35	
SC-BRANCH	*Propylene*	*Propylene*	6.930E+08	4.580E+07	-0.0235	1.00E+35	

Table 4-9 – Regressed Free Radical Kinetics 4

Component i	EVA	EVA	EVA	E2-SEG	VA-SEG	E2-SEG	E2	EVA	EVA	VA	E2
Component j	PROP	SOLVENT	ACETONE	E2	E2	VA-SEG	PROP	E2	VA	PROP	VA
a_{ij}	0.55055	-0.0186816	0.06355211	0.04	0.3	0.0287	-8.92E-02	-0.2571	9.42E-02	0.1	0.4485
b_{ij}	0.62756	0	0	0	0	0	-0.15766	8.78E-06	6.12E-06	0	-2.09E-06
c_{ij}	-0.79079	0	0	0	0	0	-5.889	1.85E-05	6.06E-07	0	1.41E-05
d_{ij}	0	0	0	0	0	0	0	0	0	0	0
e_{ij}	0	0	0	0	0	0	0	0	0	0	0

Table 4-10 – Regressed PC-SAFT Binary Interaction

E2 – Ethylene PROP – Propylene SEG – Segment

Refer to Table 3-14 and section 3.11.2 for the other steady state regressed parameters.

4.5 Model Validation

Here the validation results for the reactor model, steady state full plant model and the dynamic model will be detailed.

4.5.1 Validation of the Steady State Model

Here the validation data for the steady state models will be detailed. As mentioned before the data for the steady state regression was obtained from averages of steady state operating periods. The same was done for the validation data sets. The operating periods for the regression and validation data sets were different. Since the final application of the model was for optimal grade transitions, the most critical variables required to be regressed were the melt index and percentage VA. Thus more emphasis was placed on these in the regression.

Figure 4-13 and Figure 4-14 show the validation results for the zone 4 temperatures and conversion for the eight grades regressed. The zone 4 temperature was floating for all grades. The zone 4 temperatures showed a better fit than the reactor conversion. This was because at this point thermodynamic VLE parameters were not regressed. Thus the gas to polymer separation was not accurate. The polymer stream leaving the model was used to calculate the reactor conversion for the model. Therefore the errors in this stream would have propagated to the conversion.

Figure 4-15 and Figure 4-16 show the validation results for the percentage VA and the melt index. The model showed excellent predictive ability for these two critical variables.

Figure 4-17 shows the validation results for all the critical variables for the full plant model. Note these are only the grades which were planned to be used in the dynamic model.

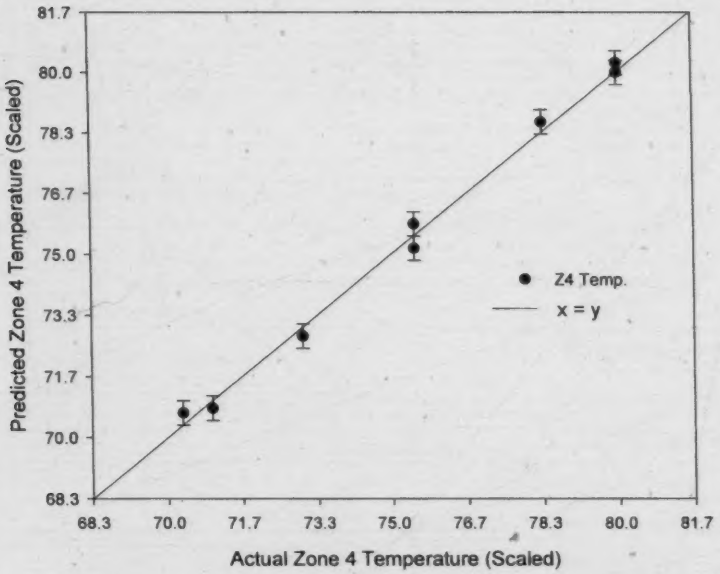

Figure 4-13 – Floating Zone Temperature Validation

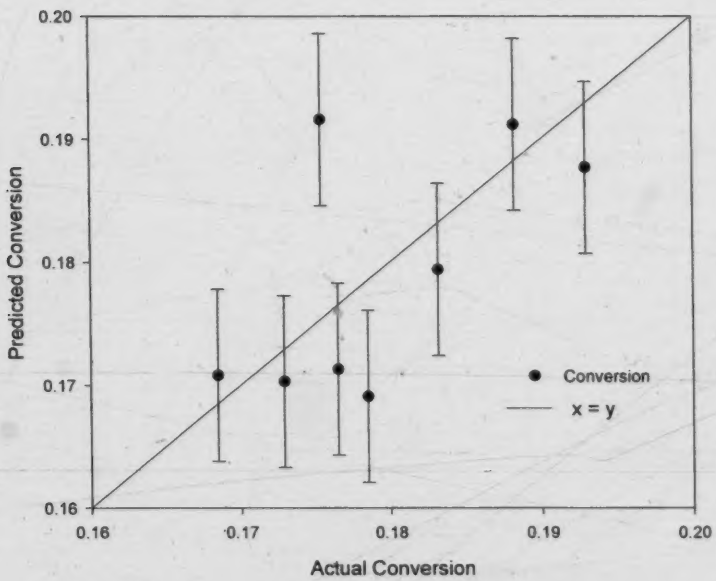

Figure 4-14 – Reactor Conversion Validation

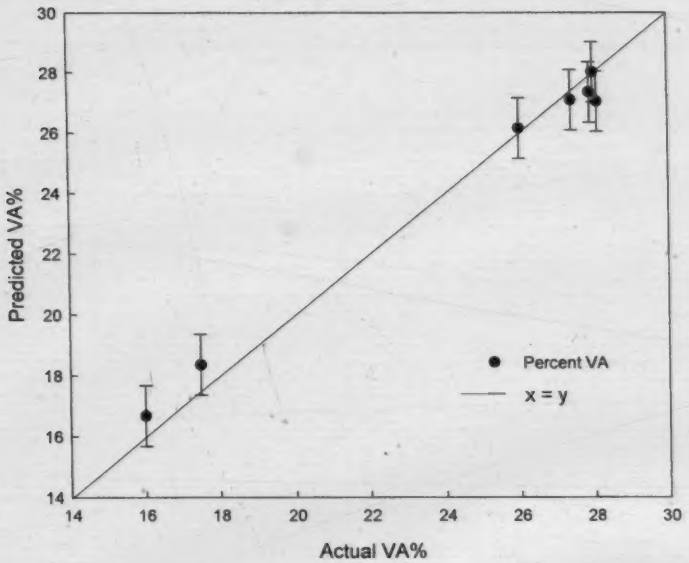

Figure 4-15 – Percentage VA Validation

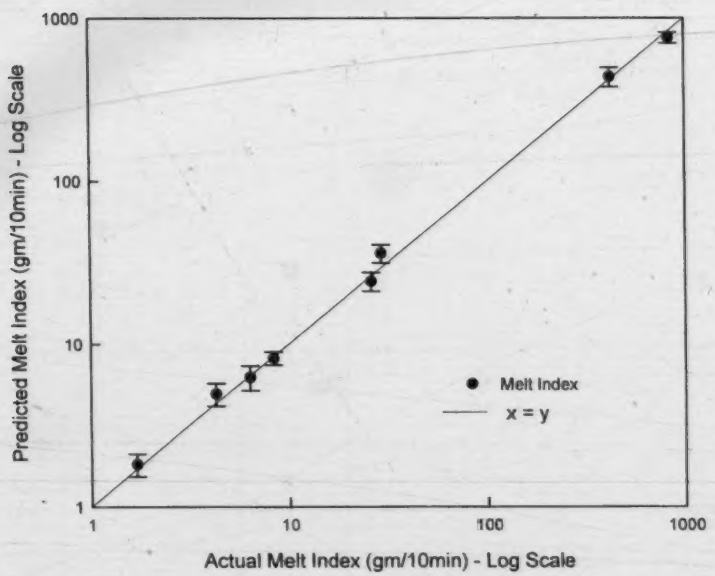

Figure 4-16 – Melt Index Validation

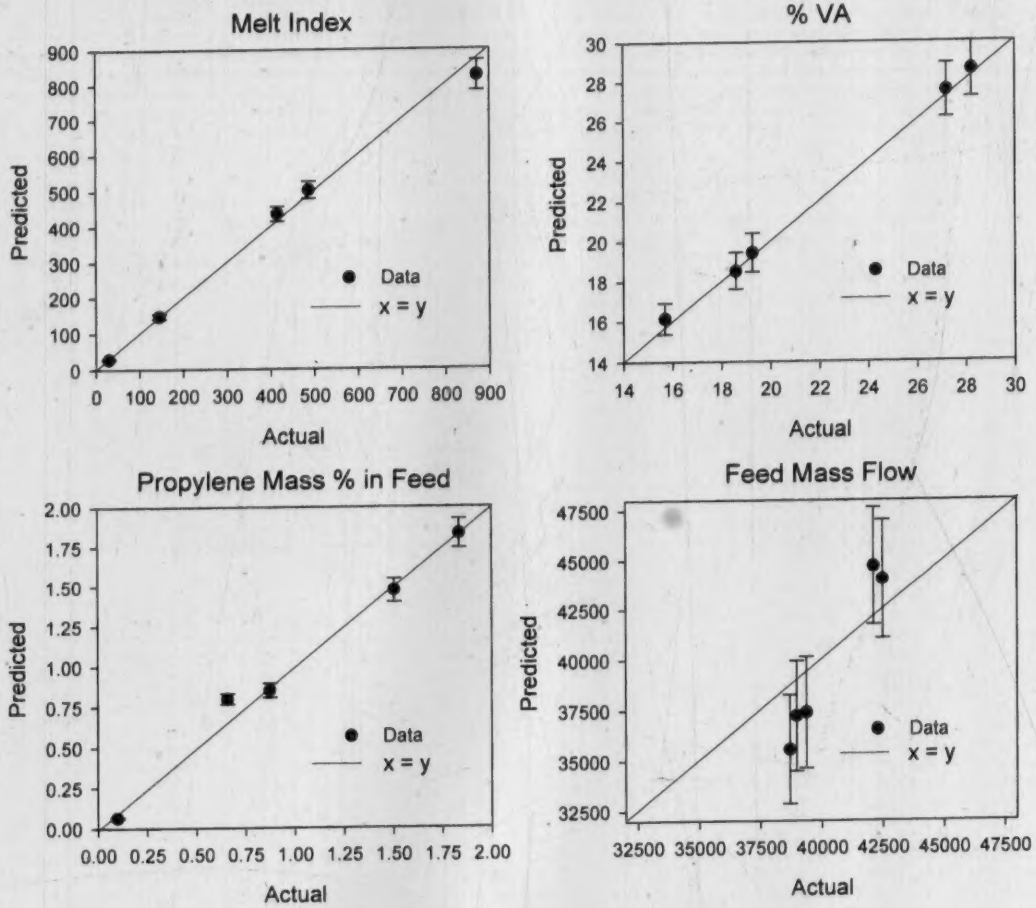

Figure 4-17 – Steady State Full Plant Model Validation

4.5.2 Dynamic Model – Regressed Parameters

The procedure described in Figure 4-12 was used to regress the parameters of the dynamic model. The regressed parameters are summarized in Table 4-11.

regressed parameter	regression result
Feed Gas Coolers (m^3)	4.34
Product Cooler (m^3)	2.78
Return Gas Cooler (m^3)	9.44
Low Pressure Recycle Cooler (m^3)	5.06
Melt Index Measurement Time Delay (min.)	25
Percentage VA Measurement Time Delay (min.)	29.333

Table 4-11 – Dynamic Model Regression Results

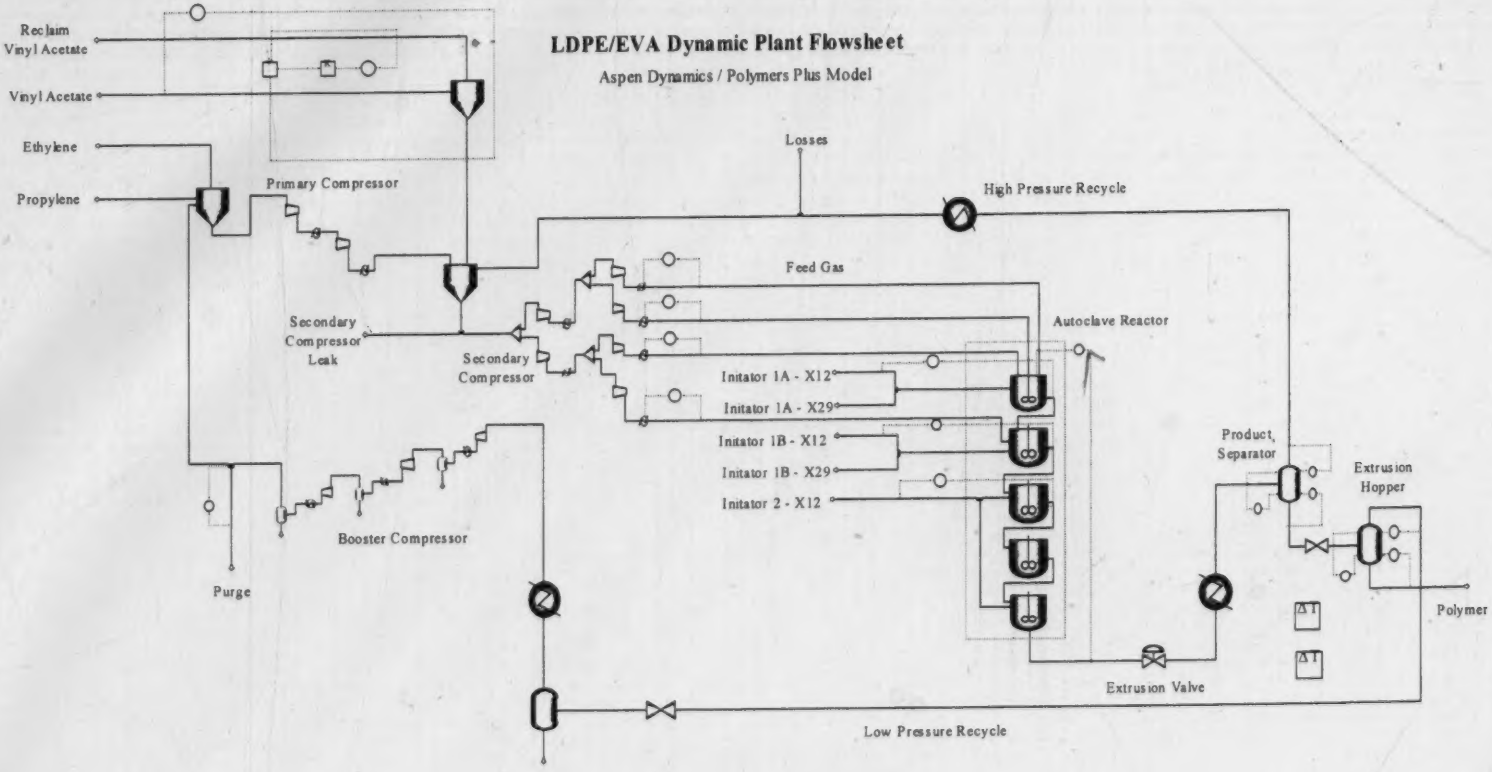

Figure 4-18 – Dynamic Model Flow Sheet

4.5.3 Validation of the Dynamic Model

The dynamic model was validated using two methods. First, the general effects of the typical manipulated variables were documented (from conversations with the plant operators). It was then confirmed that the model gave a similar response. These are show in Table 4-12.

variable	effect on mi
Reactor Pressure	Reverse
Propylene Flow	Direct
VA Flow	Direct
Reclaim VA Flow	Direct
Purge Flow	Reverse
Zone 1 Temperature	Direct
Zone 4 Temperature	Direct

Table 4-12 – Manipulated Variables Effect on Model

Then the data from a typical grade transition was used for validation. The dynamic validation comparison is shown in Figure 4-19. The regressed dynamic model showed an excellent fit to the actual plant data. The online MI measurement went offline at the end of the run so this was not shown. However, from the steady state validation showed previously, the steady state validation was excellent.

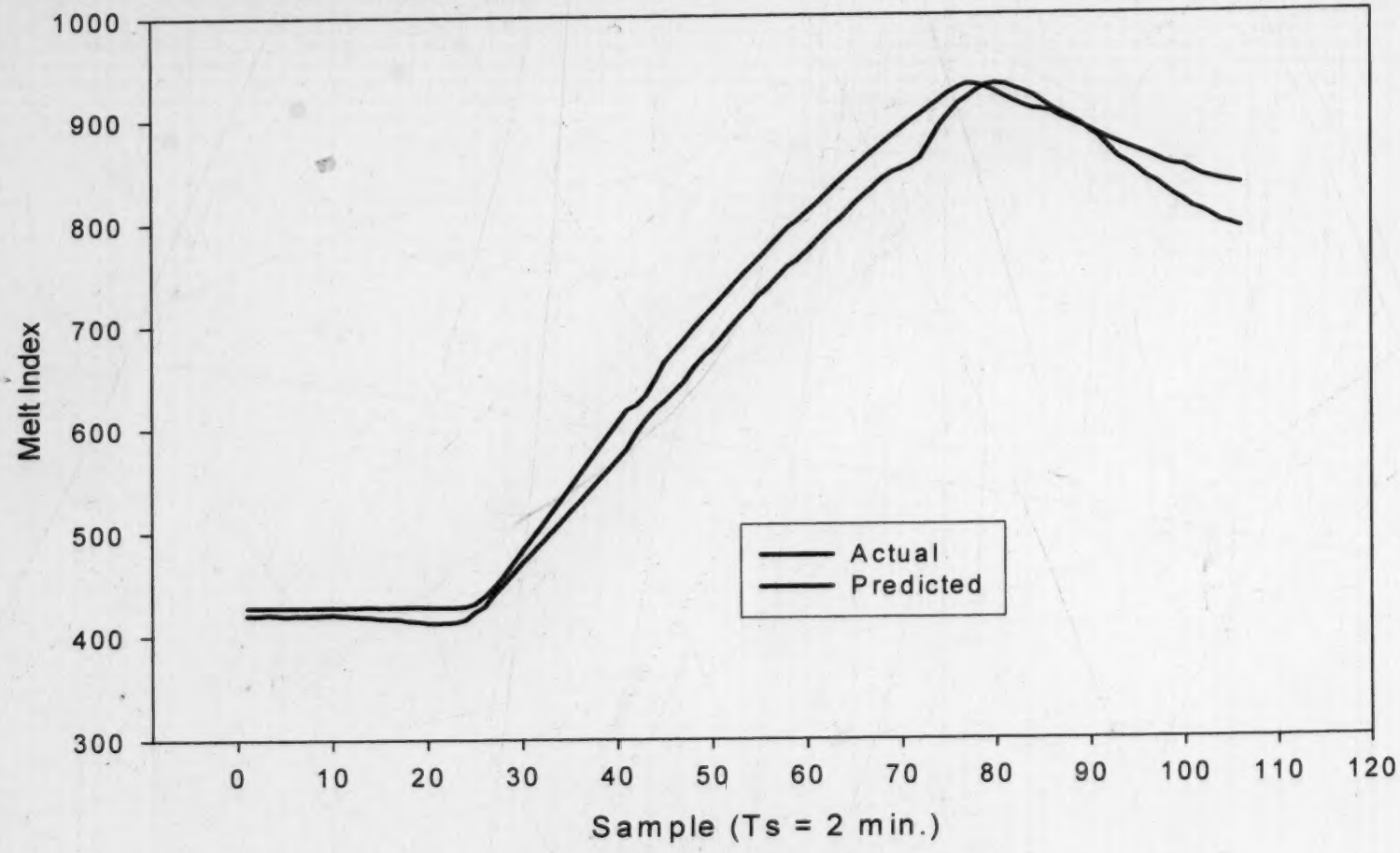

Figure 4-19 – Dynamic Model Validation

4.6 Custom Modeling in Aspen Dynamics

There were some modifications required to be made to the standard modeling components available in Aspen Dynamics to allow simulation of the model. These modifications were implemented closely with Aspen Technology Inc.

4.6.1 Support for Vapour Phase Polymerization

The default CSTR in Aspen Plus was used. Then free radical kinetics was assigned to each CSTR. The phase for the reaction was specified as vapour, since the reactor contents are under supercritical conditions. When this work was started this feature however was not supported in Aspen Dynamics. This required modifying the core Polymers Plus thermodynamic relationships for Aspen Dynamics. Once this was done the free radical reactions could be executed in the vapour phase within Aspen Dynamics.

4.6.2 Dynamic Autoclave Modeling Using CSTR's

The two main methods for solving a flow sheet are sequential modular or equation oriented. A sequential modular solver solves the flow sheet by sequentially solving each equation at a time. If required values are unknown, an initial guess is used. The solver iterates to eventually find a solution. It is a robust method, but can be time consuming, especially when there are recycle loops. The equation oriented method, solves the problem by simultaneously solving all of the flow sheet equations together. This method is faster and is well suited for dynamic modeling, because speed is required, as all the flow sheet equations must be solved at every time instant. However this method requires a square problem, i.e. number of equations should be equal to the number of variables, that way a unique solution can always be found.

Five CSTR's in series were used to model the autoclave. The default configuration in Aspen Dynamic required that every CSTR operating in the vapour phase has its own pressure controller (which is useful for the standard CSTR). Of course, this was not actually the case for the autoclave. Each CSTR was used to simulate a different mixing region within the autoclave, but they should always operate at the same

pressure. Thus the pressure controllers had to be removed. Because the Aspen Dynamics solver is "equation oriented", the flow sheet was no longer square. Thus the governing equations for the mass flow leaving each for the CSTR's which were no longer under pressure control were now required. Thus a relationship was built which forced a very small pressure drop between each CSTR. This governing equation is shown

$$M_{Z_x}^{Out} = k\left(P_{Z_x} - P_{Z_{x+1}}\right) \tag{4.11}$$

Where

$M_{Z_x}^{Out}$ represents the mass flow out of zone x

k represents a constant

P_{Z_x} represents the pressure of zone x

Four of these equations were added and one pressure controller was used for the remaining CSTR. This required configuration the first time it was run. k for all equations was set to be free (set by the simulation solver). Then the pressures were set to fixed values (set by the user) and the pressure of each CSTR was set to less than the previous pressure by 0.01 kg/cm^2 manually. The simulation was then initialized. This initialized the value of k (usually a very large value, $\cong 1e6$) based on the mass flows leaving each CSTR in the steady state model. Then k for each equation was set to be fixed and the mass flow leaving all the CSTR's except the last were set to be free. The flow leaving the last CSTR was set by the autoclave pressure controller. This forced a pressure to mass flow relationship for all the CSTRs. Thus all of them were running at approximately the same pressure and the flow leaving the last CSTR affects the flow leaving all CSTR's and thus controls the pressure in each CSTR.

4.6.3 Dynamic Heat Exchangers

The standard heat exchanger model used did not include the dynamic mass accumulation. A more complex heat exchanger model is required for this. This would then require defining a cooling component stream, the heat capacity for both

materials and the heat exchanger efficiency. The mass accumulation model from the complex model was modified for use within the simple heater exchanger model.

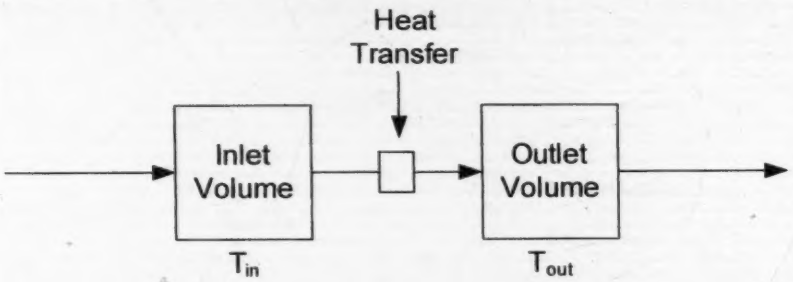

Figure 4-20 – Dynamic Heat Exchanger

Figure 4-20 shows the basic model of the heat exchanger. The model contains two theoretical volumes, which operate like two tanks. Each of these tanks has a theoretical level controller which keeps the tanks from overflowing. The outlet flow of each of the volumes is controlled by the level controller. This gives a good basic approximation to the dynamic heat exchanger and was used for every dynamic heat exchanger in the model.

4.7 Chapter Summary

This chapter detailed the model regression procedure. This task was not trivial, since the model contained a vast number of parameters which required regression. The results of the regression were given. These kinetic parameters were critical for the modeling of free radical polymerization. These can be transferred for use by other facilities interested in modeling free radical polymerization with similar monomers. The validation results were given for the steady state reactor, the steady state full plant model and the dynamic full plant model. The model showed an excellent fit with the plant data. The custom modeling required within Aspen Dynamics for modeling this process was also explained.

A weak man has doubts before a decision, a strong man has them afterwards.

Karl Kraus (1874 - 1936)

Chapter 5

Soft Sensor and Data Based Model[7]

5.1 Introduction

The control of polymer quality has become increasingly important as the production of polymer grades has increased in quantity and diversity. An important quality variable of interest for a multi-grade production facility, such as AT Plastics, is the polymer melt index. On a typical polymerization plant there is an extruder downstream of the reactor. This chapter first outlines details on the use of the operating variables of such an extruder as an empirical sensor for the melt flow index. The results of this sensor will be used with several regularly sampled plant variables to build a multivariable model for the process. This model has several applications,

[7] Portions of this chapter were presented at IFAC's ADCHEM Symposium, April 2006, Gramado, Brazil, by Alleyne et al.

including development of optimal grade transition strategies via implementation of online multivariable predictive control.

An empirical model was built in several stages. First a simple model was built which related the polymer's melt index with the extruder pressure. After several modifications a model which also included the extruder's speed and temperature as compensation variables plus a bias updating procedure were developed. The final bias updated model has been installed at the plant for over six (6) months and detects a change in the melt index nine (9) minutes before the online instrument.

This chapter is organized as follows. First the background on the soft sensor will be explained, followed by the details on the design of the soft sensor. This soft sensor was then used to identify a linear multivariable plant model for a particular grade change. Before the system identification could be done data pre-processing was required.. Subspace system identification was used to successfully identify the multivariable plant model. The procedure followed in the identification of the state space system model will be discussed. The chapter concludes with validation results of the state space model to check for the adequacy of the model.

5.1.1 Soft Sensor Motivation

The increased reliance on polymers with specifically tailored properties for different applications has been documented extensively (Alperowicz 2005). Previously the specifications for polymer grades and products were very relaxed. However, with the advent of much larger capacity plants; many smaller plants are moving from commodity to speciality polymers with the prospect of higher profit margins. These products however have tighter specifications. Thus variability which was acceptable before is no longer tolerable. This implies online properties of polymers need to be controlled more tightly. The more diverse, lower volume product requirements needed by certain customers forces the product specification required from the plant to change regularly. Therefore reliable online polymer quality measurements are critical for making these product changes efficiently.

The online measurement for the melt index was determined by an online rheometer. This instrument gave an update every six (6) minutes and was subject to transport lags. These two problems were not significant as there are system identification algorithms which can compensate for these issues. However, a more significant issue, because of the large range of melt index measurement required, was that the rheometer used several models and die sizes. Each die has a manufacturer's recommended pressure range for which the readings are accurate. However, once the instrument gets close to any of the limits, i.e. the polymer is too hard or soft for the particular die and measurement temperature, the readings become unreliable. This is acceptable if the plant is running a grade campaign which does not have a significant change in melt index. Therefore, the goal of modelling the grade transitions was severely hampered because the rheometer data during the grade transitions were plagued with issues such as the unit having to be switched off or becoming unreliable, as it needed die changes or gave inaccurate results because it was at the end of its calibrated range. It was clear that some new measurement device or sensor was required to give online polymer melt index values.

5.1.2 Polymer Soft Sensors

The measurement of polymer quality through the use of indirect variables (soft sensors) has been the subject of much research. McAuley and MacGregor 1991 developed a soft sensor for the UNIPOL polymerization process; this was based on a simplified first principles model and the available plant measurements such as reactor feeds and compositions. This soft sensor used a recursive estimation technique to update model parameters. Ohshima and Tanigaki 2000 gave a comprehensive review of property estimation methods published for different polymerization processes. The typical design of these soft sensors involves building relationships between the process control variables, such as the reactor, pressure and temperature and the polymer property to be controlled. The method of building this relationship typically involves methods such as linear observers (Lines et al. 1993), extended Kalman Filters (Scali et al. 1997), nonlinear parameter estimation (Kiparissides et al. 1996),

neural networks (Chan and Nascimento 1994) and partial least squares (Han et al. 2005). Here a unique approach is taken; the product from the polymerization reactor is extruded by an online extruder, where many process variables are monitored.

Watari et al. 2004 and Nagata et al. 2000 independently used measurements from an extruder to estimate the properties of molten polyethylene. However, their methods required the installation of a fibre optic sensor at the end of the extruder to obtain NIR (near infra-red) readings. The method proposed here uses raw data which is commonly measured and monitored on extruders to give an indication of the melt index of the polymer produced in the reactor.

5.2 The Extruder

A schematic of the extruder is shown in Figure 5-1. The extruder is made up of a screw in a barrel. The extruder applies a controlled temperature gradient and pressure to molten polymer which is forced through its annulus using the screw then finally through a die. This energy transfer to the polymer causes a change in the properties of the polymer. The extruder's screw is driven by a motor. The motor's frequency is modulated (thus screw speed) to maintain a constant level in the extruder feed hopper. Side streams are usually added to the extruder where additives can be mixed with the molten polymer in the extruder. Several pressures and temperatures were monitored along the extruder barrel. There is a mesh screen pack between the last two pressure sensors on the extruder. This mesh is very fine and becomes clogged with solids and gel particles over time. This causes the extruder variables, predominantly the upstream pressure, to change even if the flow rate and other conditions are constant. All the pressures monitored on the extruder drift due to annulus and die fouling; while the pressures just before the screen pack have an even more significant drift because the screen pack becomes clogged as mentioned before. The screen pack is changed once it becomes excessively clogged and different screen pack mesh sizes are sometimes used, based on the product being produced.

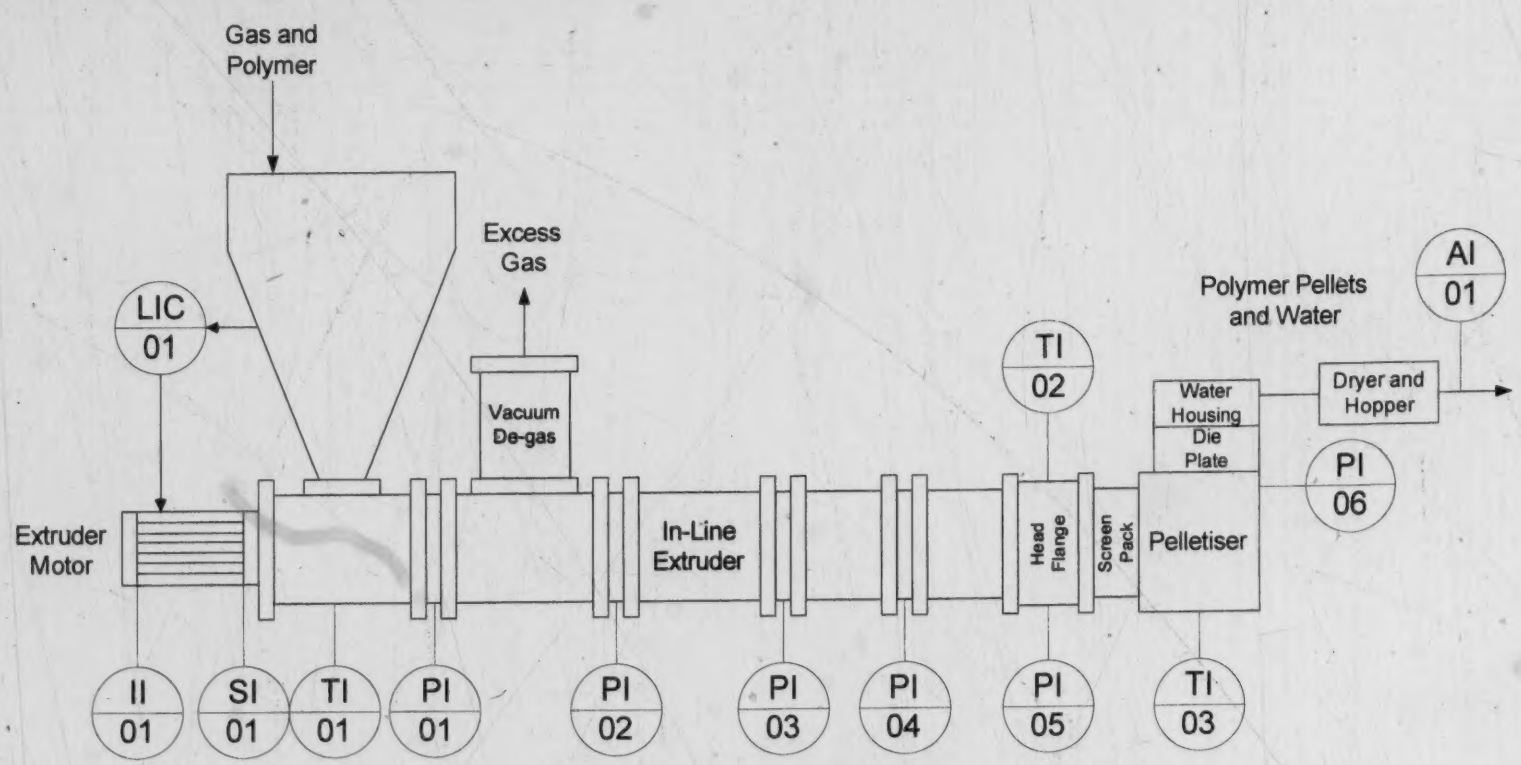

Figure 5-1 – Extruder Schematic

After the extruder there is a pelletizer. The polymer pellets are dried, and then pass through a hopper before a side stream is used to measure the melt index with the online rheometer.

The extruder is down stream of the reactor thus changes in the melt index of the polymer would occur first at the reactor and its effect mirrored at the extruder. Clearly, the online rheometer being down stream of the extruder detects changes in the melt index much later than the monitored variables at the extruder would. This was due to the transport delays and the sample processing time of the online instrument.

5.3 Soft Sensor Model Structure

The steps in building the soft sensor for the melt index are detailed here. It was observed that the plant operators relied on the extruder pressure to give them an indication of the melt index of the polymer whenever the online reading was offline.

5.3.1 Variable Correlation and Lags

All of the variables monitored on the extruder were correlated with the polymer's melt index. It has been shown (McAuley and MacGregor 1991) that the melt index has significant log-linear relationship with the plant process variables such as temperature and pressure. The same relationship was noticed in the data reported here and therefore log-transformed variables were used in the analysis. Table 5-1 shows a summary of the correlation of the extruder variables with the log of the melt index.

The variable used for fitting and validation of the soft sensor was the online rheometer. It was expected that the online analyzer providing these readings would be delayed (explained in 5.2).

Thus a delay estimation algorithm and cross-validation via visual inspection were used to estimate the time delays between all independent variables and the online reading. The lags between the extruder variables and the online rheometer are also shown in Table 5-1. The cross correlation between the variables was found using standard correlation analysis. The data set used to calculate the correlation comprised

16340 one minute samples form fifteen (15) different grades with melt indices ranging from 1.7 to 870 gm/min.

variable	correlation	lag (MIN.)
PI-01	-0.742	13.92
PI-02	-0.799	13.50
PI-03	-0.881	12.08
PI-04	-0.712	10.08
PI-05	-0.917	10.00
PI-06	-0.981	9.92
TI-01	-0.887	7.83
TI-02	-0.705	5.33
TI-03	-0.947	4.91
SI-01	0.922	10.25
II-01	-0.863	10.33

Table 5-1 - Extruder variables correlation and lag with log of rheometer measured melt index

Figure 5-2 shows one of the plots used to determine the time delay between the signals based on visual inspection. The most significant deviations in the data (large peaks) were used to visually confirm the time delay.

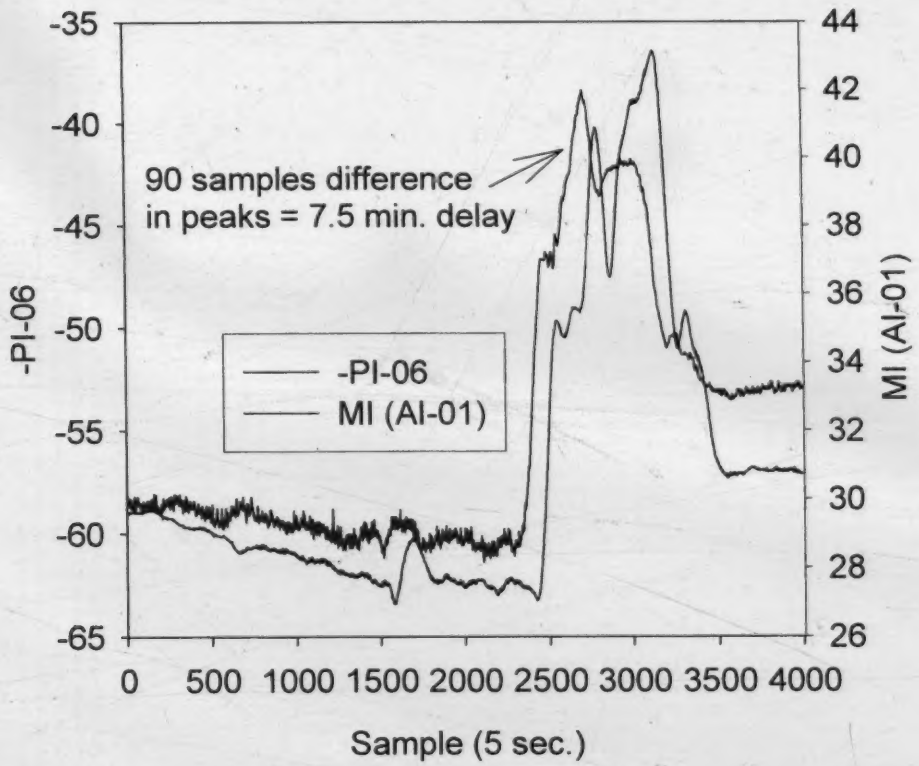

Figure 5-2 – Visual Inspection Plot for Time Delay

The delay estimation algorithm used was defined by (Moddemeijer 1988). It is a relatively old algorithm, it is available online and it was simple to use. The algorithm requires no a priori information about the signals; however, it assumes the signals to be stochastic and stationary. These assumptions are not fully true for the signals being considered here. As mentioned before, the extruder variables drift with time. However, over relatively short times, they can be considered stationary. This method involves splitting the two signals into a past and future vector. Then the capture of information between the concatenated past and future vectors is calculated. A function which continuously splits the data series into the past and future vectors is used to find which split gives the maximum common information. The capture of information is stored in a variable pair called the criterion. The maximum value of the

criterion gives the number of sample times which correspond to the estimated time delay between the two signals.

Figure 5-3 shows the criterion plotted against sample intervals for two of the extruder variables (sample time = 5 seconds).

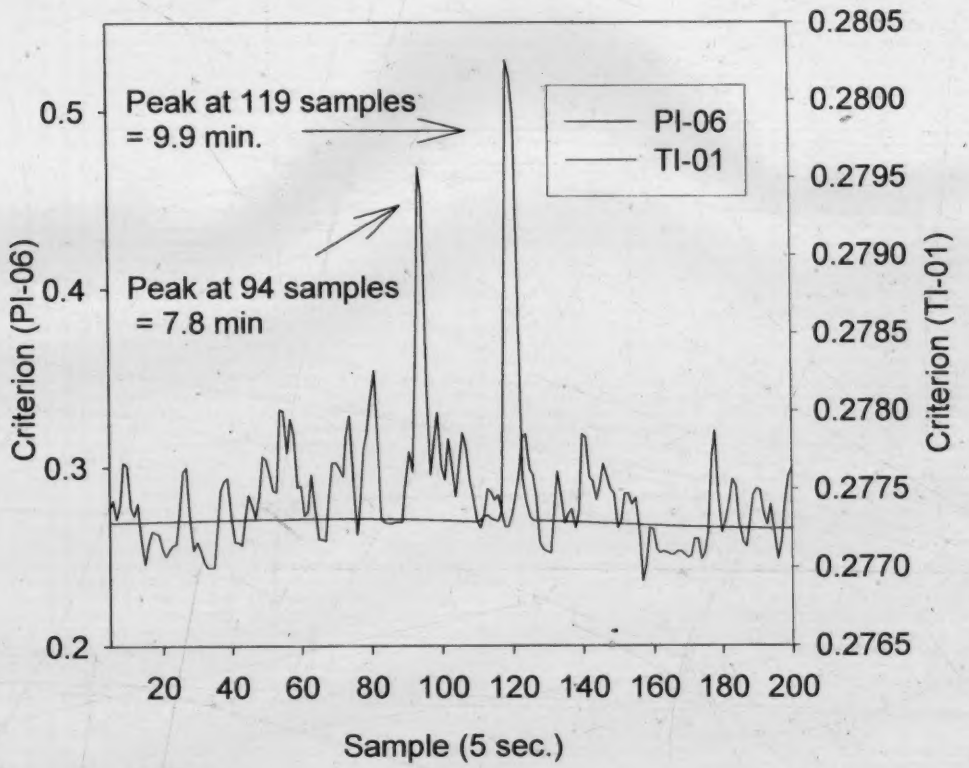

Figure 5-3 – Delay Estimation Algorithm for two Extruder Variables

5.3.2 Model Disturbances

The main disturbances affecting the extruder variables are the screen pack fouling and cooler fouling. The typical disturbances caused by these are shown in Figure 5-4. This figure clearly shows that a screen pack change causes a significant change in the operating pressure for PI-05. A cooler cook event causes a change in the pressure and melt index. However the steady state melt index after the event is the same while the corresponding steady state pressures are not. Hence all the extruder pressures drift due to fouling and only the pressure upstream of the screen pack is affected by screen

pack fouling. The screen pack mesh size can sometimes be changed based on the grade being run. This causes inconsistencies in the correlation.

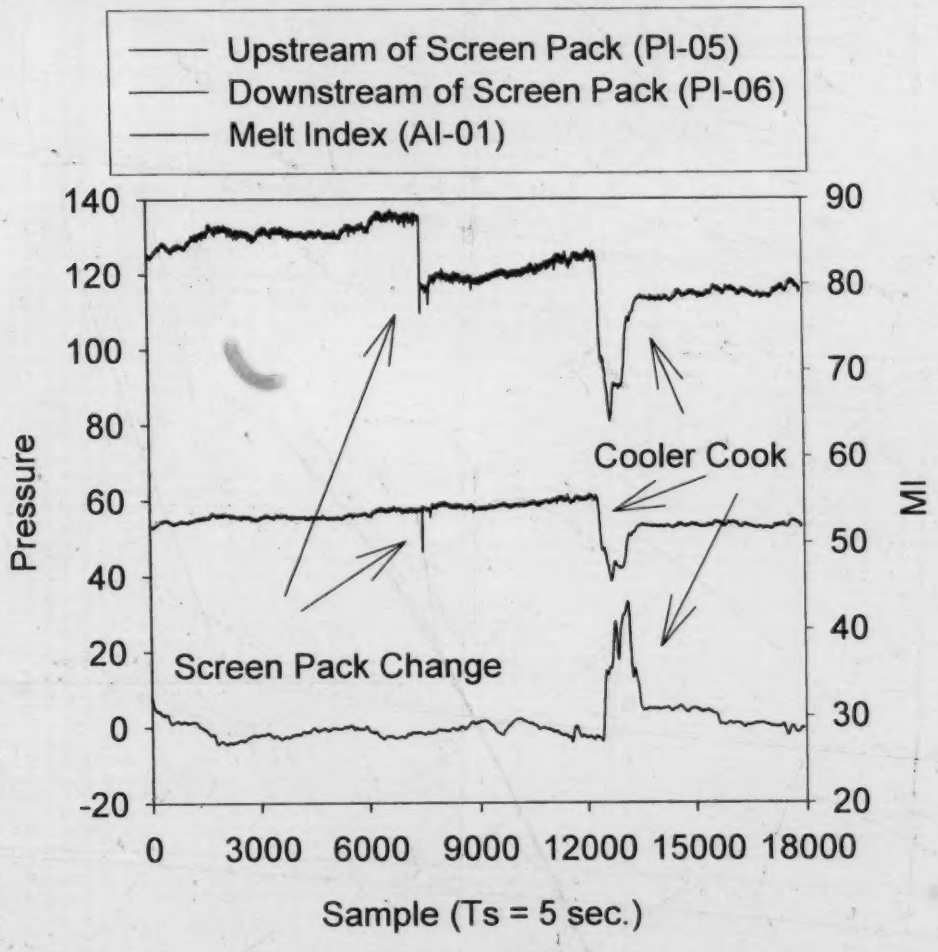

Figure 5-4 – Disturbances effecting Extruder Variables

The most important variables were chosen based on the physics and rheology of the extruder and the correlation. As described, the melt index range for products produced by this facility is very large. Initially, one simple model was developed which covered the entire product range. However, during events such as cooler cooks and grade changes, the melt index for each grade showed an exaggerated change. Thus, a speed and temperature modified model was developed.

5.3.3 The Basic Model

The selection of plant variables which comprise the soft sensor was based on the correlation with the melt index, time delays and lack of disturbances. The model was based on Equation (5.1).

$$MI = f(P) \quad (5.1)$$

where

P is the pressure at PI-06 (the variable with the highest correlation).

MI is the melt index and the form of MI is

$$MI = \exp\left(a + b\left(P^{\alpha}\right)\right) \quad (5.2)$$

a, b and α were constants found using regression. These values provided information about the relative behaviour of the melt index (increasing or decreasing and rate of change). However, the absolute value was found to contain errors; due to the speed of the extruder being controlled by the hopper level controller, the extruder barrel temperature being changed based on the grade and the fouling of the coolers and screen pack.

5.3.4 Speed and Temperature Compensated Model.

This model was based on equation (5.1) but includes some more information about the physics of the extruder. Equation (5.3) shows the basis of the model.

$$MI_{T_r,S_r} = f\left(P_{T_r,S_r}\right) \quad (5.3)$$

where

MI_{T_r,S_r} is the melt index at a reference temperature, T_r and reference speed S_r.

P_{T_r,S_r} is the pressure at a reference temperature, T_r and reference speed S_r.

In this application the extruder can be viewed as a pseudo melt indexer. Within a typical melt index instrument, the melt index is measured by applying a fixed pressure to the polymer at a fixed temperature and the polymer is forced through a die. The mass of polymer which flows through the die in a fixed time interval is the

melt index. With the extruder, the pressure applied to the polymer depends on the extruder speed and temperature. This gives the relationship shown in Equation (5.4).

$$MI_{T,S} = f\left(P_{T,S}\right) \tag{5.4}$$

where

$MI_{T,S}$ is the melt index at a operating temperature, T and operating speed S.

$P_{T,S}$ is the pressure at a operating temperature, T and operating speed S.

This equation can be modified to give Equation (5.5); which compensates for the change in temperature and speed.

$$MI_{T_r,S_r} = f\left(P_{T,S}\right) + f\left(T - T_r\right) + f\left(S - S_r\right) \tag{5.5}$$

Equation (5.5) reports a melt index similar to that measured by the rheometer.

The relationships internal to these functions are not exactly known, but based on the high correlations observed. A linear compensation for the speed was added. The relationship which included the speed compensation was of the form shown in Equation (5.6).

$$MI_{T,S_r} = \exp\left(a + b\left(P^{\alpha}\right)\right)\left(c + d\left(S\right)\right) \tag{5.6}$$

This was expressed in the form shown in equation (5.7).

$$MI_{T,S_r} = \exp\left(a + b\left(S\right) + c\left(SP^{\beta}\right) + d\left(P^{\alpha}\right)\right) \tag{5.7}$$

The relationship shown in equation (5.8) was found after the initial regression.

$$\beta = -\alpha \tag{5.8}$$

Thus equation (5.9).

$$MI_{T,S_r} = \exp\left(a + b\left(S\right) + c\left(\frac{S}{P^{\alpha}}\right) + d\left(P^{\alpha}\right)\right) \tag{5.9}$$

Where a, b, c, d and α are constants fit using least squares regression.

A relationship between the melt index and temperature (TI-03) was found by manipulation of the variables and observing the relationships which gave the highest correlation. The relationship found is shown in equation (5.10).

$$MI \propto \frac{1}{T^2} \tag{5.10}$$

Thus equation (5.9) was extended to equation (5.11) which included both speed and temperature compensation.

$$MI_{T_r,S_r} = \frac{\exp\left(a + b(S) + c\left(\frac{S}{P^{\alpha}}\right) + d\left(P^{\alpha}\right)\right)}{T^2} \qquad (5.11)$$

5.4 Nonlinear Least Squares Regression

The model described by equation (5.11) was nonlinear. Therefore non-linear regression was used to regress the parameters of the soft sensor. Given that we have a model structure and data available for a large number of different products, the model's parameters were regressed using the non linear least squares solver in Matlab's optimization tool box. The solver required the function to be defined as the difference between the measured values and calculated values from the model. The function defined can be seen in equation (5.12).

$$f_i(S,P,T) = MI_i - \frac{\exp\left(a + b(S_i) + c\left(\frac{S}{P_i^{\alpha}}\right) + d\left(P_i^{\alpha}\right)\right)}{T_i^2} \qquad (5.12)$$

Where i represents the sample index and MI_i represents each sample of the measured melt index.

This can be expressed as:

$$\mathbf{F}(\mathbf{x}) = \begin{bmatrix} f_1(\mathbf{x}) \\ f_2(\mathbf{x}) \\ f_3(\mathbf{x}) \\ \mathrm{M} \\ f_m(\mathbf{x}) \end{bmatrix} \qquad (5.13)$$

The objective function was formulated as shown in equation (5.14).

$$\min_x \frac{1}{2}\left\|\mathbf{F}(\mathbf{x})\right\|_2^2 = \frac{1}{2}\sum_i f_i(\mathbf{x})^2 \qquad (5.14)$$

This algorithm uses trust region optimization which was briefly described in section 4.4.1. Having a suitable initial guess was very important for the convergence of this problem. The regressed parameters for the smaller models such as equation (5.2) were used as initial guesses in the final model. For the unknown parameters a best guess was used.

During the regression process, the regressed parameters were found to favour the larger dependent variable values (the model fit well for large MI and not as well for small MI). Thus equation (5.14) was modified to the weighted least squares regression form. Three main regression schemes were considered.

- Relative Weighting – Here the difference is weighted by the dependent variable, this is shown in equation (5.15).

$$f_i(\mathbf{x}) = \frac{y_i - y_{Model}}{y_i} \tag{5.15}$$

  Where

  y_i represents the dependent variable

  y_{Model} represents the model calculated dependent variable

- Weighting by the dependent variable – Here the difference is weighted by the square root of the dependent variable, this is shown in equation (5.16).

$$f_i(\mathbf{x}) = \frac{y_i - y_{Model}}{\sqrt{y_i}} \tag{5.16}$$

- Weighting by the variance – Here the difference is weighted by the standard deviation, this is shown in equation (5.17).

$$f_i(\mathbf{x}) = \frac{y_i - y_{Model}}{\sigma} \tag{5.17}$$

The variance of the measurements increased as the value of the measurement increased. Estimating the variance would mean splitting the data set into different regions and finding the variance for each. This could lead to additional complications. The use of 'normalized' variables as shown in equation (5.15) and (5.16) proved to be suitable and required no additional estimation. The weighting scheme defined in

equation (5.15) was eventually used. Thus equation (5.12) was modified to give equation (5.18).

$$f_i(S,P,T) = \frac{MI_i - \dfrac{\exp\left(a + b(S_i) + c\left(\dfrac{S}{P_i^{\alpha}}\right) + d\left(P_i^{\alpha}\right)\right)}{T_i^2}}{MI_i} \qquad (5.18)$$

5.5 Bias Updating of the Model

The compensated model which was described previously was found to operate well for a certain period of time and at certain grades, then drifting occurred. This was attributed to the significant changes in the extruder operating conditions due to fouling. In order to compensate for this characteristic of the process a bias updating scheme for the model was implemented. Here a unique situation was encountered, because there were two variables which were available for potentially calculating the bias. These were the laboratory values which were available every two to three hours and the online instrument. Each one of these possessed inherent problems which required the development of a logical procedure to make an intelligent selection about the bias which should be applied.

5.5.1 Online Analyzer Bias

The online bias was calculated every half hour based on average values over the last half hour. Equation (5.19) shows the method used for calculating the new a_{Calc}.

$$a_{Calc} = \ln\left(MI_{Avg} \times T_{Avg}^2\right) - b\left(S_{Avg}\right) - c\left(\frac{S_{Avg}}{P_{Avg}^{\alpha}}\right) - d\left(P_{Avg}^{\alpha}\right) \qquad (5.19)$$

Where

MI_{Avg} represents the average of the online melt index over the last half hour

T_{Avg} represents the average of the extruder die plate temperature over the last half hour

S_{Avg} represents the average of the extruder screw speed over the last half hour

P_{Avg} represents the average of the extruder die plate pressure over the last half hour

The bias which was calculated in equation (5.20) was stored in the historian.

$$bias_{Online} = a_{Calc} - a \tag{5.20}$$

The bias calculated in equation (5.20) is checked to ensure that it lies within reasonable bounds, as shown below.

$$-1.5 \le bias_{Online} \le 1.5 \tag{5.21}$$

It is important to note that the bias is only applied to one of the parameters in the soft sensor model. This is because the bias is only attempting to compensate for offset errors caused by fouling.

5.5.2 Laboratory Bias

The laboratory bias was calculated when a new laboratory value was available. The ODBC connection to the LIMS (see section 2.3) was used to store the test results from the laboratory in the historian. Each of these laboratory samples is called a SPOT at the plant. This term will be used here as well to refer to the laboratory results. Equation (5.22) shows the method used for calculating the new a_{SPOT}.

$$a_{SPOT} = \ln\left(MI_{SPOT} \times T_{SPOT}^2\right) - b\left(S_{SPOT}\right) - c\left(\frac{S_{SPOT}}{P_{SPOT}^a}\right) - d\left(P_{SPOT}^a\right) \tag{5.22}$$

Where

MI_{SPOT} represents the value of the online melt index at the lat SPOT time

T_{SPOT} represents the value of the extruder die plate temperature at the lat SPOT time

S_{SPOT} represents the value of the extruder screw speed at the lat SPOT time

P_{SPOT} represents the value of the extruder die plate pressure at the lat SPOT time

The bias which was calculated in equation (5.23) was stored in the historian.

$$bias_{SPOT} = a_{SPOT} - a \tag{5.23}$$

The condition in equation (5.24) was used to reject clearly erroneous SPOTs from causing an incorrect update.

$$abs\left(a_{SPOT} - \bar{a}\right) > 1.5 \times \sigma_a \tag{5.24}$$

Where

$\bar{a}$ represents the average $\bar{a}$ over the last four hours

σ_a represents the standard deviation of a over the last four hours

5.5.3 Unified Bias Update

The online bias and the laboratory bias both have situations where each is more applicable. The laboratory melt index reading is considered to be accurate and the online instrument is usually calibrated to meet it. Therefore when a new value is available from the laboratory it would be ideal to use it to update the model. However, the laboratory values are available infrequently, generally every two hours or longer. The online reading is always available (unless there is some fault or change in the instrument's operating conditions). This value can give valuable information on the bias when there has not been a SPOT for a significant period of time. Because both the online and SPOT bias contain valuable information, a scheme to combine them into a unified bias update was designed. This scheme was based on the integrity of the both pieces of data. When a SPOT has just been received from the laboratory, its integrity is considered to be high, significantly higher than the online reading. However, as time goes on, the SPOT's integrity decreases and eventually the online reading would have higher integrity, particularly if the new spot has not been received for a significant period of time. There was also the need to make adjustments to the bias only when needed; this would allow the soft sensor to be less susceptible to discontinuities (unnecessary changes in bias).

A weighted averaging scheme based on time was used for combining the two bias values mentioned before. The time since the last SPOT was calculated as shown in equation (5.25)

$$t_{\Delta} = t_{Now} - t_{SPOT} \tag{5.25}$$

Where

t_{Δ} represents the time since the last SPOT

t_{Now} represents the current time

t_{SPOT} represents the time of the last SPOT

The time since the last SPOT was used in equation (5.26) to find the time weighting factor β.

$$\beta = \frac{\left(1 - \tanh\left(t_{\Delta} - 4\right)\right)}{2} \tag{5.26}$$

Where β represents the time weighting factor. Figure 5-5 shows β's behavior as the SPOT gets older.

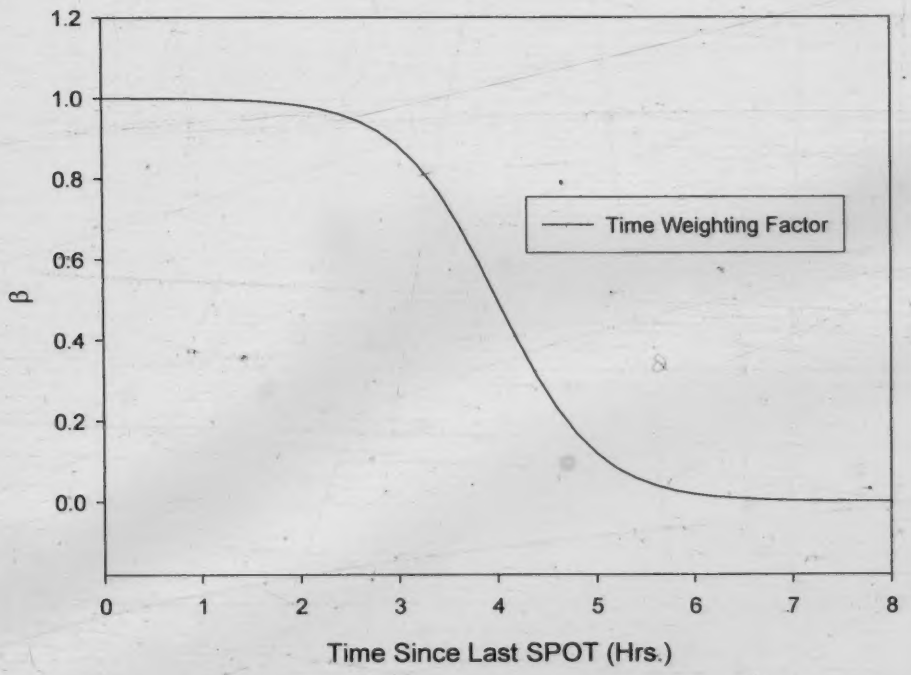

Figure 5-5 – Time Weighting factor for Bias

The unified bias is calculated by using β to find the time weighted average of the bias values as shown in equation (5.27).

$$bias = \left(1 - \beta\right) bias_{Online} + \beta bias_{SPOT} \tag{5.27}$$

It can be seen that once the SPOT is less than two hours old the value of the bias was approximately the value calculated from the SPOT. As the SPOT gets older than two

hours the value begins tending towards the bias calculated from the online measurement.

After implementation it was noticed that the bias did not change significantly during steady state operation. Therefore a simple mean change detection algorithm was used to detect a sustained change in the mean of the SPOT. Only when this change was detected would the bias be updated. A bias update was done only if the condition in equation (5.28) is met.

$$abs\left(\overline{bias_{New}} - \overline{bias_{Old}}\right) > k_T \times \sigma_{Bias} \tag{5.28}$$

Where

$\overline{bias_{New}}$ represents the average bias over the last four hours

$\overline{bias_{Old}}$ represents the average bias between eight and four hours ago

σ_{Bias} represents the standard deviation of the bias over the last four hours

k_T represents a tuning factor which was set to, 2.1, for acceptable updates

Once the bias update was accepted, the bias calculated in equation (5.27) was used to calculate the parameter a in the model based on

$$a_{Calc} = a - bias \tag{5.29}$$

Equation (5.30) shows how a_{Calc} was used to calculate the new melt index.

$$MI_{Bias} = \frac{\exp\left(a_{Calc} + b(S) + c\left(\frac{S}{P^{\alpha}}\right) + d\left(P^{\alpha}\right)\right)}{T^2} \tag{5.30}$$

Figure 5-6 shows the flow sheet of the procedure developed for implementing the unified bias updating scheme.

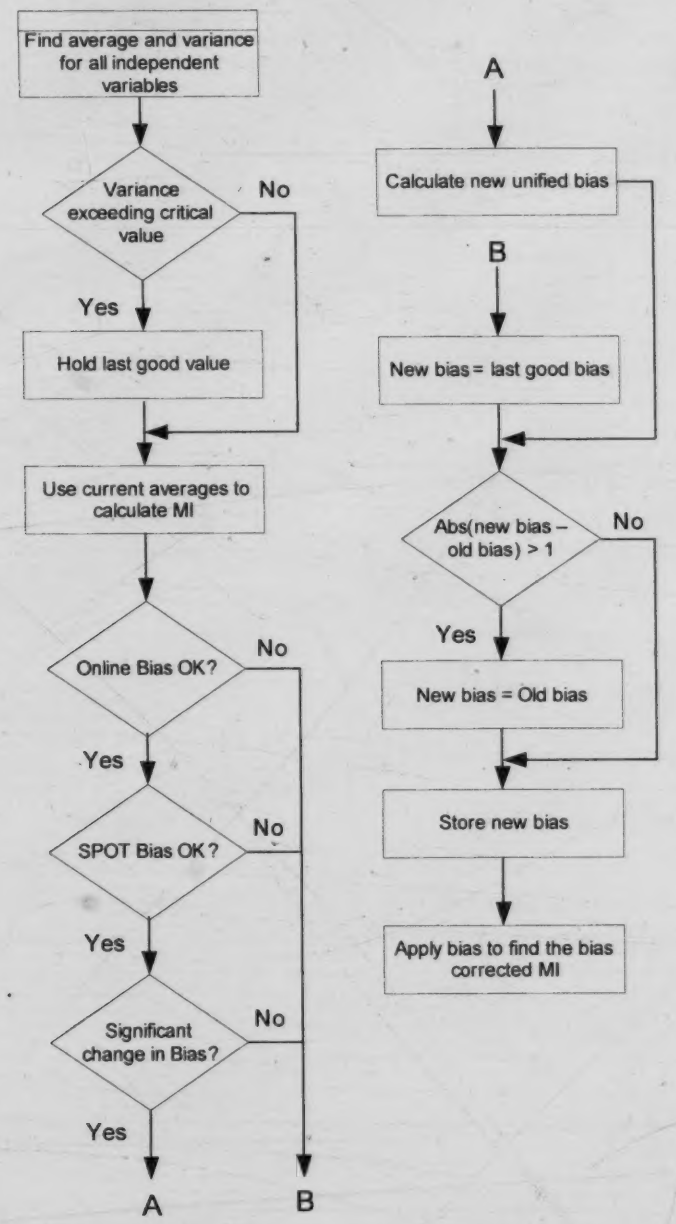

Figure 5-6 – Bias updating flow sheet (30 min. execution period)

5.6 Soft Sensor Validation

The model with and without the temperature compensation are shown in Figure 5-7. It was noticed that without the temperature compensation there was a significant overshoot during the dynamic periods (such as cooler cook events and grade transitions) and the model was more susceptible to fouling errors. The temperature compensation alleviated the majority of the overshoot and some of the offset due to fouling; this is as shown during a typical cooler cook in Figure 5-7.

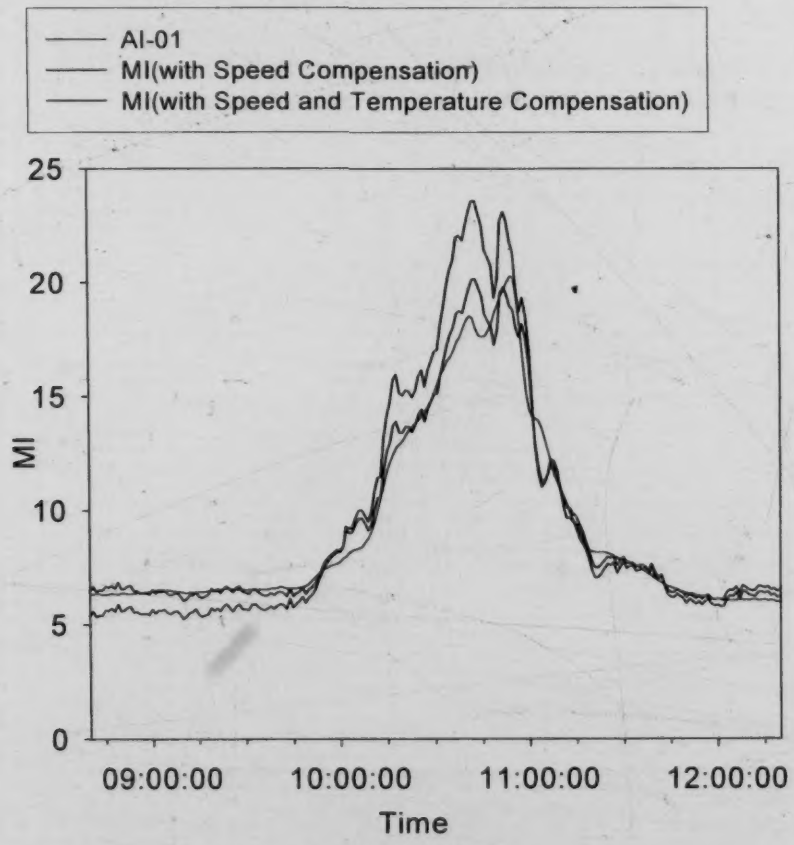

Figure 5-7 – Soft Sensor during a Cooler Cook Event

The model was modified during the fitting process. This included lagging the independent variables to take advantage of the time delay information found previously in Table 5-1. Lagging of the independent variables improved the fit during

the non-liner least squares regression. However, upon implementation, it was found that using the lagged independent variables did not give any significant advantage and actually the predictive ability of the model was lost. Because the model was for the extruder which was upstream of the online instrument, lagging the variables so the regression with the online instrument was improved meant we were inserting additional time delay into the model. The implemented model used the most current data available from all independent variables and gave a value for the melt index nine (9) minutes ahead of the online rheometer.

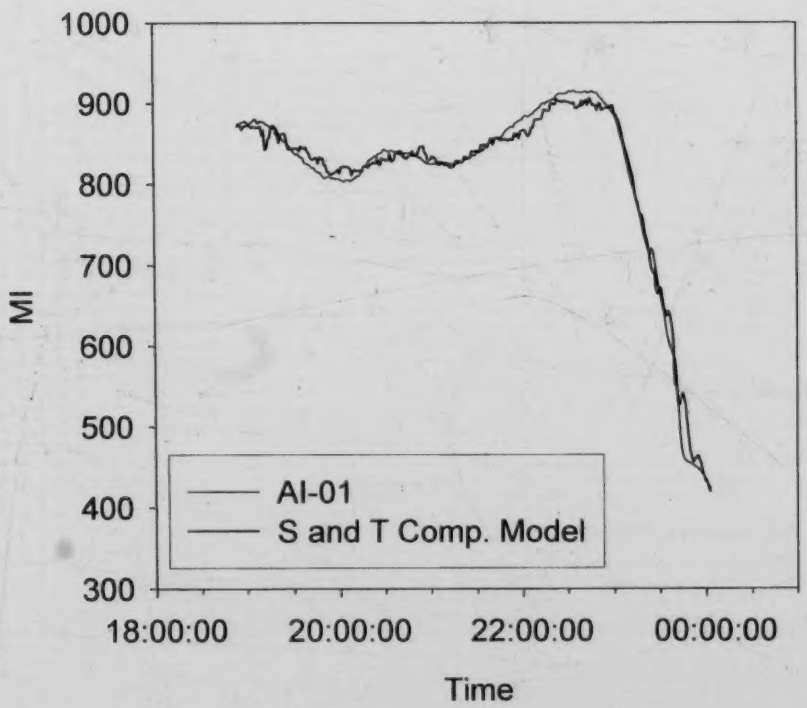

Figure 5-8 – S and T Compensated Model Dynamic Validation Plot

Figure 5-8 shows the validation data for a dynamic run. It can be seen the model captured the dynamics of the melt index change well.

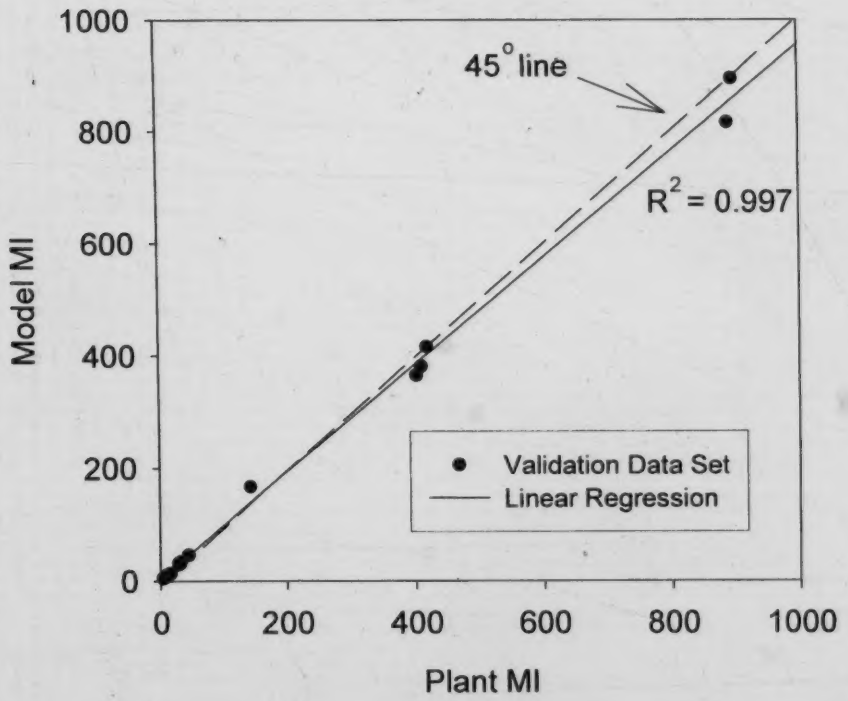

Figure 5-9 - S and T Compensated Model Validation Plot (several grades)

Figure 5-9 shows the validation data for the model. It can be seen the model showed an excellent fit for the full range of grades produced by the plant (these products were produced over a four month period).

Figure 5-10 shows a snapshot of the implemented soft sensor over one (1) day, which included a grade change. It can be seen that the soft sensor with the bias update gave an accurate representation of the MI of the product produced by the reactor. The bias from the online instrument and those calculated from the SPOTs are also shown. These typically follow similar trends, once the online instrument is operating correctly.

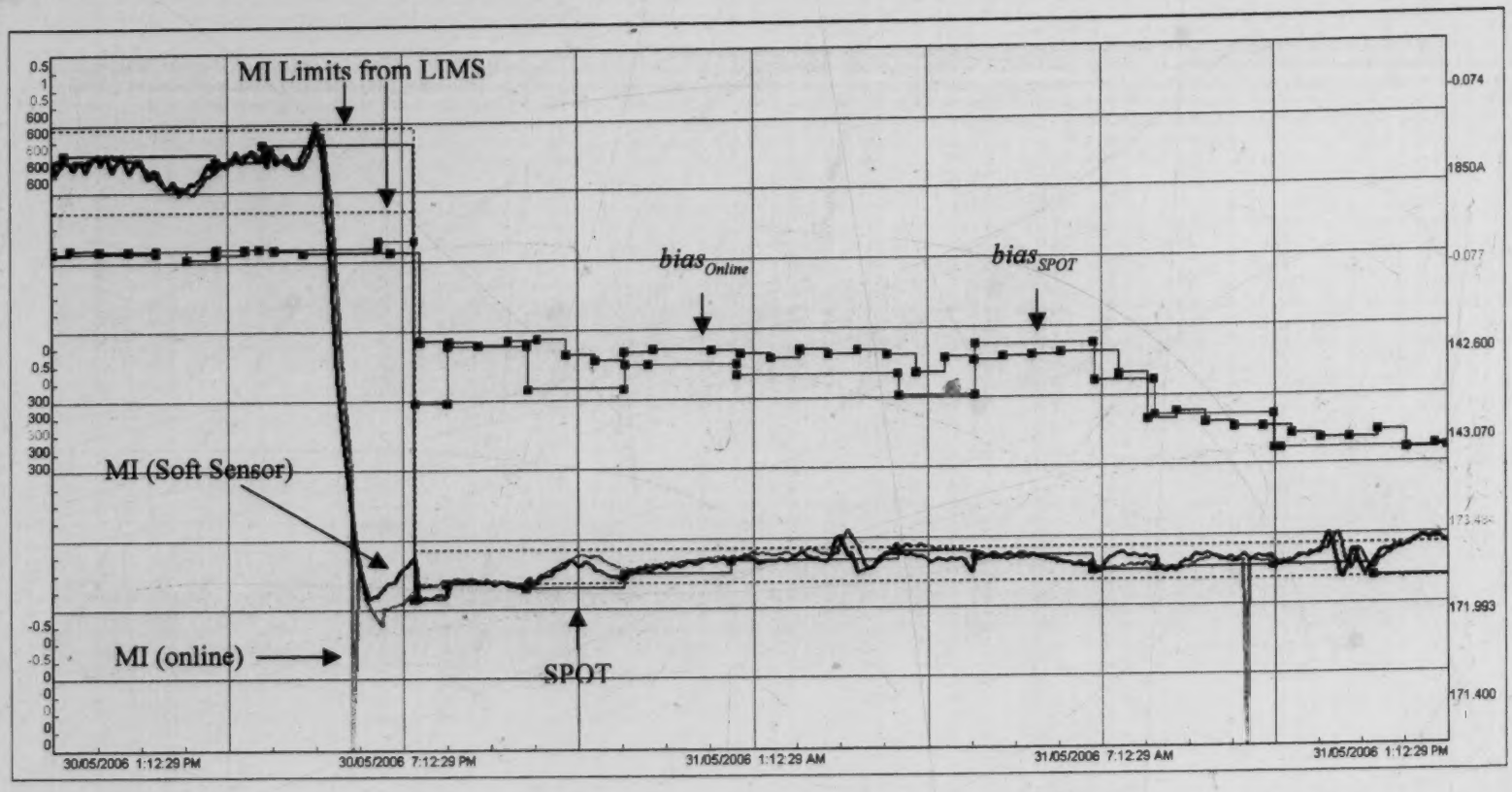

Figure 5-10 – Soft Sensor & Bias Update During a Grade Change

5.7 The State Space Model

5.7.1 Introduction

Chapter 3 and 4 contained the details of a physio-chemical model. This was found to be a time consuming process. A soft sensor for the main quality variable was developed and implemented. A useful application for this soft sensor was its use in the subsequent identification of a lumped, discrete time, linear, time invariant, state space model of the process. This type of model could be used for implementing predictive control using several commercial packages. From the first principles work done before, the actual plant model is known to be non-linear. However, linear models may be able to capture the process dynamics, while running at a particular grade or between specific grade transitions. Before an identification exercise is undertaken, one should ensure that the data set contains persistently exciting inputs (Ljung 1987; Soderstrom and Stoica 1989). Here we were mostly interested in modeling the grade transition periods. These happened frequently and also required significant changes in the plant's operation. Thus there was a large amount of naturally persistently exciting data available for identification. However, as was evident from the first principles modeling, this system contained many non linear components. Also the changes made by the operators are usually performed simultaneously. Thus, the already correlated manipulated variables of the process were being excited simultaneously. This presents a problem for most typical SISO and some MIMO identification algorithms. Thus an identification algorithm capable of identifying a multivariate model, with multiple simultaneous excitation signals was required. The subspace method has proven to be an excellent algorithm for handling such problems (Favoreel et al. 2000; Juricek et al. 2001; Juricek et al. 2005). Therefore this algorithm was used for identification of the model. The general state space model is comprised of a set of difference equations, of the form,

$$\mathbf{x}_{k+1} = \mathbf{A}\mathbf{x}_k + \mathbf{B}\mathbf{u}_k + \mathbf{w}_k \tag{5.31}$$

$$\mathbf{y}_k = \mathbf{C}\mathbf{x}_k + \mathbf{D}\mathbf{u}_k + \mathbf{v}_k \tag{5.32}$$

Where $\mathbf{x}$ is the $(n_x \times 1)$ vector of state variables, $\mathbf{u}$ is the $(n_u \times 1)$ vector of measured inputs, $\mathbf{y}$ is the $(n_y \times 1)$ vector of measured outputs, $\mathbf{w}$ is the $(n_x \times 1)$ vector of process noise and $\mathbf{v}$ is the $(n_y \times 1)$ vector of measurement noise.

Figure 5-11 shows the block diagram for the state space model which was identified using a subspace identification algorithm.

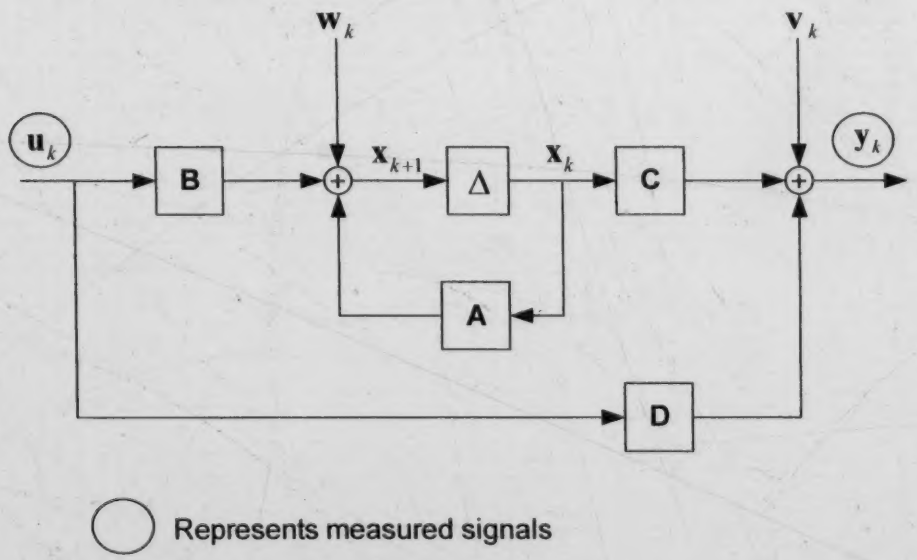

Figure 5-11 – Block Diagram of State Space Model (Cock and Moor 2003)

5.7.2 Overview of Subspace Identification

This is a relatively new method of system identification. There are several implementations of this algorithm. Here the N4SID implementation in MATLAB was used. This was developed by Van Overschee and De Moor 1994 and has its foundations in linear systems theory.

For subspace identification the state vector is defined as a liner combination of past inputs and outputs, by equation (5.33)

$$\mathbf{x}_k = \mathbf{J}\mathbf{p}_k \quad (5.33)$$

Where,

$$\mathbf{p}_k = \left[\mathbf{u}_{k-1}, \mathrm{L}\ , \mathbf{u}_{k-N}, \mathbf{y}_{k-1}, \mathrm{L}\ , \mathbf{y}_{k-N}\right]^T \tag{5.34}$$

The dimension of $\mathbf{p}_k$ is the number of lags, N.

The state vector, $\mathbf{x}_k$ is not specified a-priori and is computed from the input-output data. The calculation of $\mathbf{J}$ for N4SID distinguishes this algorithm from other implementations. Here $\mathbf{J}$ is calculated from a series of linear algebraic arguments which can be derived using successive back substitutions of the original state space equations. Once $\mathbf{J}$ is determined the state space matrices can be estimated using linear least squares regression. The details of the mathematical derivations of subspace methods will not be derived here since this is not the focus of this research. This information can be found in several publications and books.

The implementation of the subspace identification algorithm is also very attractive. It is conceptually straight forward and thus leads to user friendly software implementations (Cock and Moor 2003). For the N4SID implementation the data pre-processing must be done by the user. Once this is done the user is not required to modify any highly technical or theoretical parameters. The parameters which were required to be set were the system order and delay (if desired).

5.7.3 Data Pre-processing

Several similar grade transitions were used to build the state space model. The steps outlined in Figure 5-12 were followed.

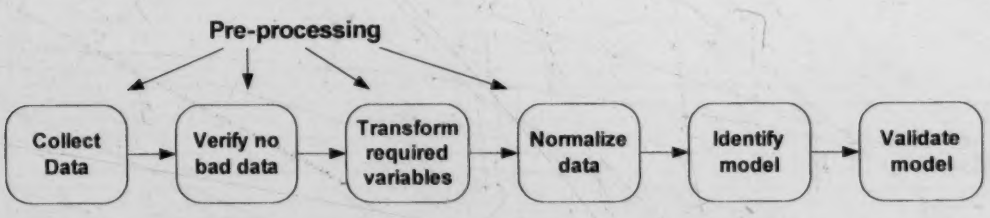

Figure 5-12 – Data Based Model Identification Steps

- The collection of data involved the acquisition of uncompressed process variables from the historian.

- To verify that the data sets contained no bad data, plots for the data sets were inspected to ensure there was no missing or inconsistent data. The data was split into two portions one was an identification data set (75%) and the other a validation data set (25%).
- From the soft sensor work described previously it was known that logarithmic transformation on the melt index gave a linear relationship with plant variables. Therefore the melt index variable in the data set (one of the output variables – this was the soft sensor reading) was transformed with a logarithmic transformation.
- Each of the process variables was stored with the engineering units scale used on the plant. Initially this data was used directly to identify the model. This was a very challenging process and the models generated did not capture the dynamics of the plant well. It was found that once the variables were normalized the identification process gave much better results. Each of the variables were scaled to zero mean and unit variance as shown in equation (5.35).

$$x_{Scaled} = \frac{x - \bar{x}}{\sigma} \qquad (5.35)$$

Where,

x_{Scaled} represents the normalized variable which was used for identification

x represents the raw plant variable

$\bar{x}$ represents the mean of the variable calculated from the full data set

σ represents the standard deviation of the variable calculated from the full data set

The mean and standard deviation were calculated using both the training and validation data.

5.7.4 The Identified Model

The schematic of the model which was identified is shown in Figure 5-13. This model contained thirteen (13) inputs and two outputs. Three grade transition data sets were used to identify and one to validate the model.

These grade transitions were similar, the specifications were:

Start MI Target: 400 gm/10min. **Start VA Target:** 28 %

End MI Target: 878.5 gm/10min. **End VA Target:** 28 %

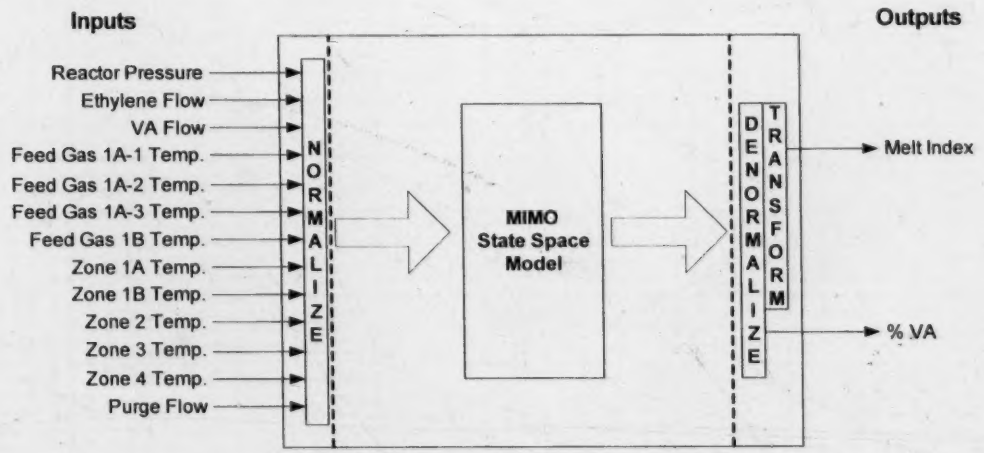

Figure 5-13 – Schematic of the Plant Model

Some details on the data sets used for identification and validation are given in Table 5-2

Data SET	Number of samples	sample interval (sec.)
ID-DATA1	330	60
ID-DATA2	494	60
ID-DATA3	469	60
VAL-DATA	233	60

Table 5-2 – Identification and Validation Data Set Details

Modeling Time Delay

Significant time delays can cause erroneous identification of the subspace model (Overschee and Moor 1996). The time delays for this model were mostly due to instrument measurement delay and were insignificant compared to the time constant of the loops. Thus the dime delay was assumed to be zero.

Model Order

It was known from the first principles modeling that the model contains over one hundred (100) states and its order is actually very high. However, here we were looking for a reduced order approximation, which will not cover the full plant operation, but possesses predictive ability for the particular grade change being considered. The model order was selected based on trial and error. Several orders from two (2) to ten (10) were all identified. It was noticed that there was no longer a significant decrease in the prediction error after a model order of four (4). And actually for higher orders such as six (6) and higher, noise in the data was actually being identified as part of the process model. This caused the validation results to be very erratic and the prediction errors increased. A model order of four (4) was used for the final model.

5.7.5 Validation of the State Space Model

The soft sensor was used as the measured variable for identification and validation of the melt index. There was little excitation of the percentage VA components of the model, since the start and target grades specifications were the same. Figure 5-14, Figure 5-15 and Figure 5-16 show the plots of the validation data for different prediction horizons. While, Figure 5-17 and Figure 5-17 show the auto-correlation for the melt index and the cross-correlation of the melt index with pressure and propylene flow.

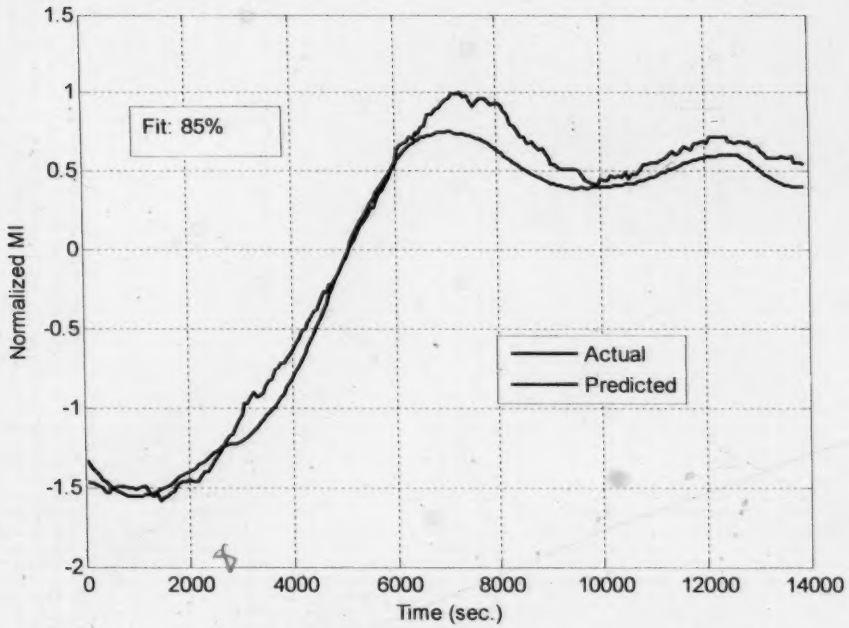

Figure 5-14 – State Space Model Validation (∞ step ahead prediction horizon)

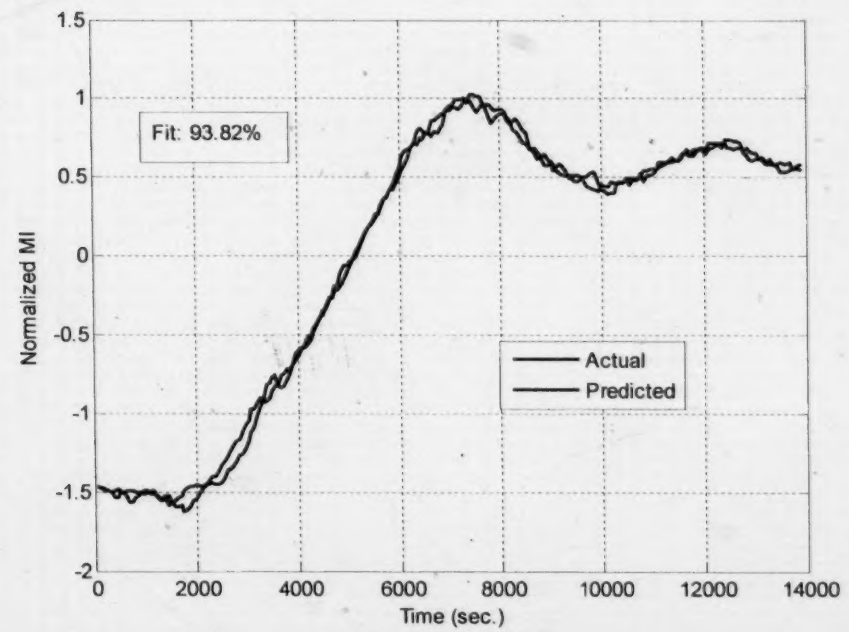

Figure 5-15 – State Space Model Validation (5 steps ahead prediction horizon)

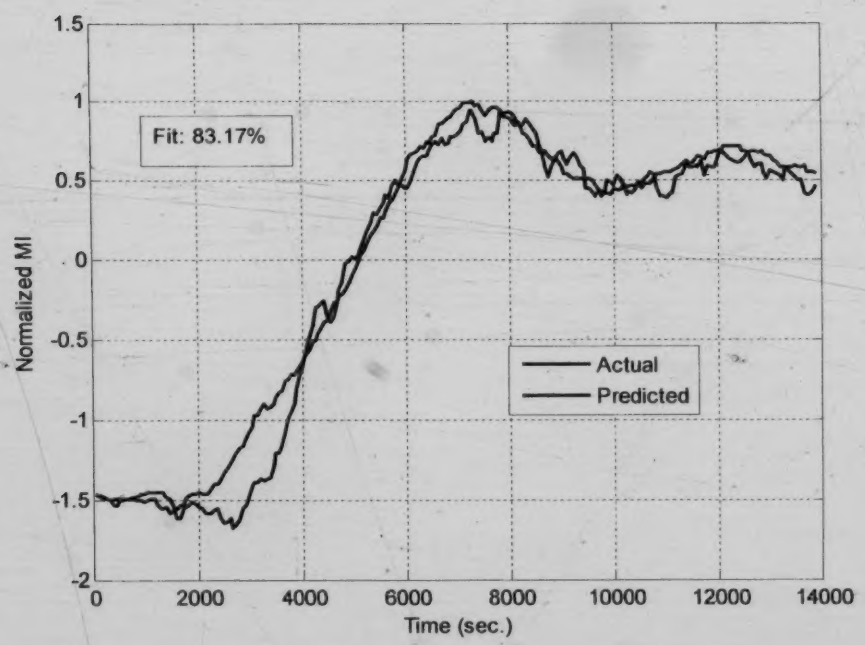

Figure 5-16– State Space Model Validation (20 steps ahead prediction horizon)

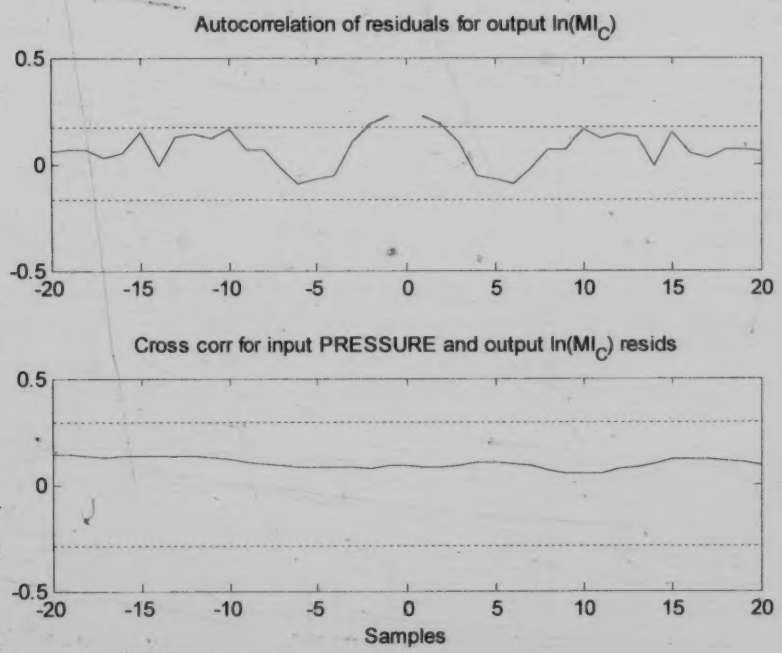

Figure 5-17 – Pressure and ln(MI) model correlation

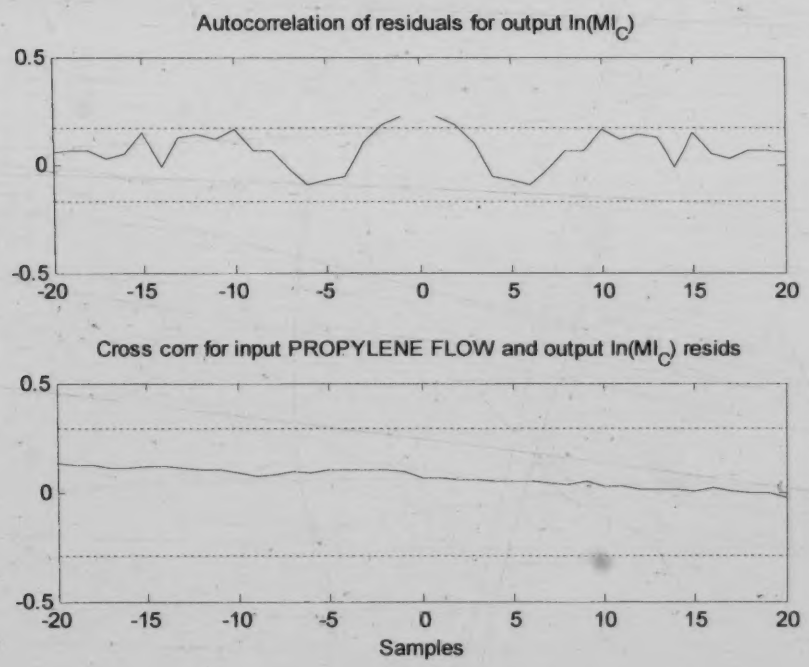

Figure 5-18 – Propylene Flow and ln(MI) model correlation

It can be seen that the model possessed excellent predictive ability. The cross correlation and auto correlation plots lie within the bounds for the critical variables. This indicates overall the model captures the majority of the dynamics of the process for the product change analysed. If this model were implemented using a multivariable predictive controller Table 5-3 shows the suggested controller configuration.

Variable	control assignment
Reactor Pressure	Manipulated
Ethylene Flow	Measured Disturbance
VA Flow	Manipulated
Feed Gas 1A-1 Temperature	Measured Disturbance
Feed Gas 1A-2 Temperature	Measured Disturbance
Feed Gas 1A-3 Temperature	Measured Disturbance
Feed Gas 1B Temperature	Measured Disturbance
Zone 1A Temperature	Manipulated
Zone 1B Temperature	Manipulated
Zone 2 Temperature	Manipulated
Zone 3 Temperature	Measured Disturbance
Zone 4 Temperature	Measured Disturbance
Purge Flow	Manipulated
MI	Controlled
VA	Controlled

Table 5-3 – Control Scheme for the State Space Model

5.8 Chapter Summary

This chapter covered the work done on the development of an extruder based soft sensor, its implementation and an application. The process variables monitored on the plant's online extruder were used to build a model to predict the melt index. A unified bias updating scheme was developed which used laboratory information and an online reading to do corrections of the soft sensor. The soft sensor has been installed at the plant for over six months and indicates a change in melt index nine (9) minutes before the online instrument (see the appendix for a seven (7) day plot of the soft sensor). The soft sensor reading was applied to build a data based state space model which showed excellent validation results. This developed model can be used for several control and monitoring applications.

Mediocrity knows nothing higher than itself, but talent instantly recognizes genius.

Sir Arthur Conan Doyle (1859 – 1930)

Chapter 6

Dynamic Optimization, Results and Plant Implementation

6.1 Introduction

Optimal grade transition strategies for polymerization manufacturing are of crucial importance to polymer manufacturing plants. This is because of the wide variety of polymer products with tailored properties required to be produced by polymerization facilities (see Chapter 1). The majority of the product produced by the polymerization plant can be sold; this is unless the properties are totally unacceptable. However, the product which falls within the tightest specification bands set by the client are usually sold for premium prices. The difference in price between prime product and non

prime for the process considered here is in the range of 14 cents per kilogram. This is a significant amount for a plant which produces 160 tonnes per day. This can lead to the realization of a significant amount of profit if more of the man product is within the prime specifications. One major reason for the product not being within the prime specification is off grade material produced during the grade transition (product change) period. As plants seek to maximize the profit from every kilogram of manufactured product the amount of 'on-spec' product must be increased. At the AT Plastics plant and most other commercial facilities the main method used for grade transition is to follow a set 'recipe' based on past 'trial and error 'operating experience. These transitions involve little process model information and therefore are sub-optimal at best. Experienced operators are allowed to push the limits of what they consider to be safe operation to find and establish new plant standards for common grade transitions. This can cause significant non prime product and even un-sellable product if the properties of the product produced are completely out of sellable specifications. More importantly this can lead to potentially unsafe operating conditions on the plant. The properties of the polymer produced by the plant are a combination of the instantaneous properties produced. Thus manufacturing product during the product change period which is very far out of the specifications to accommodate a fast grade change can cause the full batch of product to fall out of sellable specifications. Thus the optimal grade transition problem becomes more complex. The best grade transitions typically would be comprised of a compromise between safety, the amount of off-grade product manufactured and the constraints on how far the product specifications can be violated to allow the product change to take place quickly.

This problem is common to polymer industries world wide. Therefore as global competitiveness increases, polymer plants are seeking more detailed and proven methods for reducing the off grade product manufactured during product change periods. As such, there are many literature sources devoted to this issue. There have been many authors who have published results on the implementation of optimal control trajectories (Chen & Huang, 1981; MacGregor et al., 1984; Kravaris et al., 1989; Ponnuswamy, Shah, & Kiparissides, 1987; Ramanathan and Ray 1991; Kozub

& MacGregor, 1992; McAuley & MacGregor, 1993; Debling et al. 1994; Ohshima & Tanigaki, 2000; Kiparissides et al., 2002; Chatzidoukas et al., 2003).

Ramanathan and Ray 1991 and Debling, Han et al. 1994 showed the use of a trial and error method for developing grade transition strategies for several polymerization processes. Here the models were developed in the POLYRED simulation package. This work was extended by Takeda and Ray 1999 which included the use of a SQP optimizer in MATLAB for performing control vector optimization on the first principles model. However no actual plant trials have been reported. The implementation also seemed a bit convoluted since the model was implemented in POLYRED and the optimization computation was done in MATLAB.

Dynamic optimization was used by McAuley and MacGregor 1992 to determine the optimal grade transition trajectories for a gas phase polymerization process. While Ohshima et al. 1994 applied dynamic optimization for a gas phase polypropylene reactor. Both these methods applied dynamic optimization to simple models. These models were correlation based approximations of the first principles model and did not capture the detailed operation considered here. The work by McAuley and MacGregor was extended in McAuley and Macgregor 1993, where the previously developed optimal trajectories were incorporated into a non linear MPC formulation. Here the optimal trajectories were used as the reference trajectories for the controller. One drawback of this solution was that the constraints were not explicitly included in the controller design. This study showed the application of the controller to a complex non linear simulation and did not show any plant applications of the controller.

The paper published by Cervantes et al., 2002 discusses the use of dynamic optimization of a large scale plant model to find the optimal grade transition strategies for a tubular LDPE plant. They created a detailed model of the plant; using mass and energy balance for all significant reacting components. Orthogonal collocation was used to discretize the state variables and the dynamic optimization problem was solved using simultaneous nonlinear programming. This strategy seemed promising; however, there are no published results for application to a LDPE autoclave with peroxide initiators.

Chatzidoukas et al., 2003 considered the optimal grade transition problem for a gas-phase olefin polymerization fluidized bed from the view point of optimizing the traditional objective function to reduce the time required for a grade change. They also looked at the optimal pairing of control variables for every transition. This type of work has not been publicly documented for the LDPE autoclave process. Pladis & Kiparissides, 1999 built a dynamic model for the autoclave that showed promise for simulating grade transitions; however, no optimization was applied nor any applications reported.

Of all of the published work reviewed, there was no method which showed the application of dynamic optimization for producing optimal grade transitions for a high pressure EVA reactor. To the best knowledge of this author there are no published articles showing results of implementation of the optimal product change trajectories on an actual production facility.

6.2 Dynamic Optimization

6.2.1 Fundamentals

Here dynamic optimization was used to find the optimal grade transition trajectories for the complex first principles model detailed previously in Chapter 3 and 4. The dynamic optimization implementation in Aspen Dynamics was used for solving the problem. The general formulation of the objective function and constraints for the grade transition optimization problem was described by Takeda and Ray 1999. In Aspen Dynamics a similar formulation was used and is described next.

$$\min_{\mathbf{u}(t)} F\left(\mathbf{u}(t),\mathbf{x}(t)\right) \text{ where } t \in (t_s,t_e) \tag{6.1}$$

subject to:

$$\frac{d\mathbf{x}}{dt} = \mathbf{f}\left(\mathbf{u}(t),\mathbf{x}(t)\right) \tag{6.2}$$

$$\mathbf{y}(t) = \mathbf{g}\left(\mathbf{x}(t),\mathbf{u}(t)\right) \tag{6.3}$$

$$\mathbf{y}_{min} \le \mathbf{y}(t) \le \mathbf{y}_{max} \tag{6.4}$$

$$\mathbf{u}_{min} \leq \mathbf{u}(t) \leq \mathbf{u}_{max} \tag{6.5}$$

$$\Delta\mathbf{u}_{min} \leq \Delta\mathbf{u}(t) \leq \Delta\mathbf{u}_{max} \tag{6.6}$$

Where $\mathbf{u}(t)$, $\mathbf{x}(t)$ and $\mathbf{y}(t)$ are the input, state and output variables. The process model is represented by equations (6.2) and (6.3). This includes the polymer properties, reaction kinetics and plant conditions which control the final polymer properties. Equations (6.4), (6.5) and (6.6) represents the bounds on the outputs, inputs and movement in inputs respectively.

This type of problem is classified as trajectory optimization. The problem is typically difficult to solve directly because of the presence of the time in the objective function and derivatives within the constraints. There are several methods which can be used to solve this class of problem. These include control vector iteration procedures, direct substitution, dynamic programming and control vector parameterization (Takeda and Ray 1999). Here the control vector parameterization method was used, because it was already implemented in Aspen Dynamics and it has been successfully been used to solve other dynamic optimization problems.

6.2.2 Control Vector Parameterization

This was the method used to discretize the input profiles for optimization. Because the profiles were planned to be implemented by the plant operator as controller set point changes, the input profiles were designed to be piecewise constant. The control vector parameterization approximates the input profile with a linear combination of a series of *trial* functions as shown in equation (6.7).

$$u_i(t) = \sum_{j=1}^{k} a_{i,j}\phi_{i,j}(t) \tag{6.7}$$

Where

$u_i(t)$ represents the i^{th} element of the input vector $\mathbf{u}(t)$

$\phi_{i,j}(t)$ represents the trial function

$a_{i,j}$ represents the parameters which are optimized in the control vector

parameterization method

The trial functions must be initially defined. This approach removes the time parameter from the objective function and converts the optimization problem defined in equations (6.1) to (6.6) into a parameter estimation problem which is defined next.

$$\min_{a_{ij}} F\left(a_{ij}\right) \quad (6.8)$$

Subject to:

$$g\left(a_{ij}\right) \leq 0 \quad (6.9)$$

$$h\left(a_{ij}\right) = 0 \quad (6.10)$$

The trial functions used here were a series of step changes. The objective function F, inequality constraint function g and equality constraint function h are all functions of the parameters a_{ij}. This objective function follows the standard NLP formulation and standard constrained optimization algorithms for solving NLP problems can be applied.

There are several well developed methods for solving NLP problems. Here three main methods were used two of them were gradient based (SQP) and one was a direct search method based on comparison of the objective function at different solution points. The gradient based methods require the values of the functions F, g, and h also their gradients ∇F, ∇g, and ∇h with respect to a_{ij} at every step. In SQP these values are required during the solution of the QP sub-problem. These values are obtained from the simulation of the dynamic model using finite difference approximations on the non linear plant at every discretization interval. This requires multiple steady state runs of the dynamic models along the path of the input vectors $\mathbf{u}_i$.

The number and size of the discretization intervals were selected a priori. This along with the very simple trial functions chosen can produce a sub-optimal solution. However, the solutions obtained were significantly better than those used by the plant presently and removing these constraints can make the operator implementable solution impossible.

6.2.3 Objective Function Formulation

The general form of the dynamic optimization solution was shown in section 6.2.1. However, the specific behavior of the controlled quality variables depends on the specific objective function minimized. The specific objective functions were required to be programmed into Aspen Dynamics. There are several schemes for selecting the objective function. These can be based on:

- High sales, therefore reduce product change time
- Off-specification product is being sold for a lot less than on specification product, therefore minimize off specification product
- Off-specification product is being sold for almost the same as on specification product and the demand is high, therefore maximize production

There are several of these which are applicable at different times. However, here we applied a typical time weighted least squares objective as defined by Ogunnaike and Ray 1994.

The objective function for the optimizer was defined in Aspen Dynamics as:

$$F = T_1 + T_2 + T_3 \tag{6.11}$$

where

$$\text{if } MI_{Hi} < MI < MI_{Lo} \text{ and } VA_{Hi} < VA < VA_{Lo}$$

$$T_1 = w_1 \int_{t=t_s}^{t=t_e} \dot{m}_{Polymer}\, dt$$

else

$$T_1 = w_2 \int_{t=t_s}^{t=t_e} \dot{m}_{Polymer}\, dt \tag{6.12}$$

$$\text{if } MI_{Hi} < MI < MI_{Lo}$$

$$T_2 = w_3 \int_{t=t_s}^{t=t_e} t \times \left(MI - MI_{Target}\right)^2 dt$$

else

$$T_1 = w_4 \int_{t=t_s}^{t=t_e} t \times \left(MI - MI_{Target}\right)^2 dt \tag{6.13}$$

$$\text{if } VA_{Hi} < VA < VA_{Lo}$$

$$T_1 = w_5 \int_{t=t_s}^{t=t_e} t \times \left(VA - VA_{Target}\right)^2 dt \tag{6.14}$$

else

$$T_1 = w_6 \int_{t=t_s}^{t=t_e} t \times \left(VA - VA_{Target}\right)^2 dt$$

Where

F represents the function to be minimized

T_1 represents the mass of product produced which are out of the specifications of the start and end product.

T_2 represents the sum of the difference in melt index of the product currently being produced and the target melt index..

T_3 represents the sum of the difference in percentage VA of the product currently being produced and the target percentage VA..

$\dot{m}_{Polymer}$ represents the flow rate of the polymer produced.

t_s represents the time the grade change was started.

t_e represents the time the controlled variables entered the ending grade specifications.

MI_{Target} represents the target melt index for the ending grade

VA_{Target} represents the target percentage VA for the ending grade

MI_{Lo}, MI_{Hi} are the specifications for the melt index

VA_{Lo}, VA_{Hi} are the specifications for the melt index

$w_1, w_2, \text{L}\ , w_6$ are weighting factors

The weighting factors w_2, w_4 and w_6 were set to zero for the optimization since once the properties enter the specifications we considered the grade change complete, all other weights were equally applied and set to unity. However there may be other objective function schemes where they can be used. There were tighter bounds set on the final value constraints of the controlled quality variables; this was used to force them to be very close to the target value.

A derivative constraint was defined in equation was also used to force the quality variables to be within stable at the end of the grade change.

$$-2 < \frac{dy_{i,t_f}}{dt} < 2 \ \forall i \tag{6.15}$$

Where i represents the index of the controlled variable

6.3 Generation of Optimal Trajectories

As mentioned earlier, the built-in dynamic optimization functionality of Aspen Dynamics was used for development of the optimal trajectories.

6.3.1 Optimizer Configuration

Dynamic optimization like any other nonlinear optimization scheme requires a good initial guess for efficient convergence to an optimal solution. The two main controlled variables used in the optimization were the polymer's melt index (MI) and percentage VA (VA). There were several manipulated variables. These were selected based on the manipulated variables used by the operator during the grade change being considered. To keep the optimization problem simple and manageable only the manipulated variables which were usually changed by the operator during a specific change were considered. The product changes implemented by the plant operators were analyzed to find those which possessed the best performance. The performance was based on minimal off-specification product and plant stability. These were used as the initial guess for the dynamic optimization.

The optimizer configuration required upper and lower bounds to be specified at each limit of the discretization interval. Interior point limits could also be defined, but these were not used.

As mentioned before the trial function and number of discretization intervals were required to be defined a prior to the optimization. The trial function selected was piecewise constant (series of steps). The number of disctetization intervals was selected based on the typical length of the product change and the regularity at which changes were made by the operator. The final time was selected initially equal to the

base grade change performed by the operator. Iteratively, as the optimization was run successfully, the final time was reduced. It was found that making around twenty steps gave acceptable results for most product changes. Therefore the sample interval was selected based on having around twenty intervals and an acceptable final time.
This objective function was minimized by the optimizer by moving the selected manipulated variables. For each time instant upper and lower bounds on the manipulated variables were set. Also a maximum move parameter was used for each variable to ensure that steps in the manipulated variables did not exceed acceptable bounds.

6.3.2 Optimizer Algorithms

There were three main algorithms available for dynamic optimization. These were:

- FEASOPT – This is a feasible path, successive path, successive quadratic programming (SQP) optimizer. The optimum of the objective function is found by moving the selected manipulated variables to reduce the value of the objective function. This is a gradient based optimizer. Thus at every time step the gradient information is calculated and the most optimal steps implemented. Because of this each iteration is relatively slow; however it converges within a few iterations. This optimizer can allow the manipulated variables to violate the bounds.
- HYSQP – This optimizer's algorithm is similar to that implemented by FEASOPT; however the bounds on the variables are always respected.
- NELDER MEAD – This is a direct search solver based on the simplex algorithm. It is more robust than the previous two algorithms. It is not a gradient based method. Therefore the sensitivities of the measured variables with respect to the manipulated variables are not calculated. The algorithm is an unconstrained optimization method. However, a penalty function is used to limit the solution to within the bounds. Because this method is a direct search method, it perturbs each of the manipulated variables, to find the best

trajectory for the grade change. Thus, this method usually takes a large number of iterations.

The HYSQP solver was used to generate results for the majority of the grade transitions considered. This solver gave very practical results because the bounds on all of the variables were respected.

6.3.3 Optimizer Tuning

There are several parameters used to assist in the speed of convergence and reliability of the solution. These included:

Optimizer tolerance – this tolerance defined the point at which the optimizer would converge to the optimum. The difference between the values of the objective function at successive iterations of the optimizer is found and compared with the tolerance. If the tolerance is larger, the optimizer stops and returns the solution. The default value was found to be too small and thus was causing several unnecessary iterations of the optimizer.

Step size – This parameter defined the magnitude of the change in each manipulated variable made by the optimizer.

Number of line searches – this parameter defines the number of sub-steps the optimizer takes to try to find the moves which make the largest change in the value of the objective function.

6.3.4 Grade Transitions Considered

The grades modeled in the dynamic model are shown in Table 6-1.

	MI			VA		
	Low	**High**	**Target**	**Low**	**High**	**Target**
Grade #1	24.7	31	27.35	15	17	16
Grade #2	136	170	153	17	19	18
Grade #3	455	450	502.5	17	19	18
Grade #4	136	170	153	27	29	28
Grade #5	336	440	400	27	29	28
Grade #6	778	979	878.5	27	29	28

Table 6-1 – Grades Considered for Dynamic Optimization

Grade transitions were simulated initially between all of the grades using the operator based strategies. Then dynamic optimization was used to find the optimal trajectories.

6.4 Optimizer Simulation Results

We next show the simulation results for some of the grade transitions. A descritization interval of ten (10) minutes was found to be sufficient for most of the policies.

6.4.1 Simulated Grade Change - #1

The results generated for a grade change from grade #5 to grade #2 are shown here. A change in the melt index and the percentage VA content was required. This change was usually more difficult than other changes for the operator because the variables which control both properties are tightly coupled. It is intuitive that the VA flow rate controls the VA content and the propylene (modifier) controls the melt index. It is also known that VA behaves like a modifier; however the effect changes with pressure and temperature. Therefore the difficulty in predicting the best trajectory for

the manipulated variables is evident. For this change typically five (5) plant variables are usually manipulated. These were:

- Total VA feed flow rate
- Propylene feed flow rate
- Reactor Pressure
- Reactor, Zone 2 Temperature
- Purge flow rate

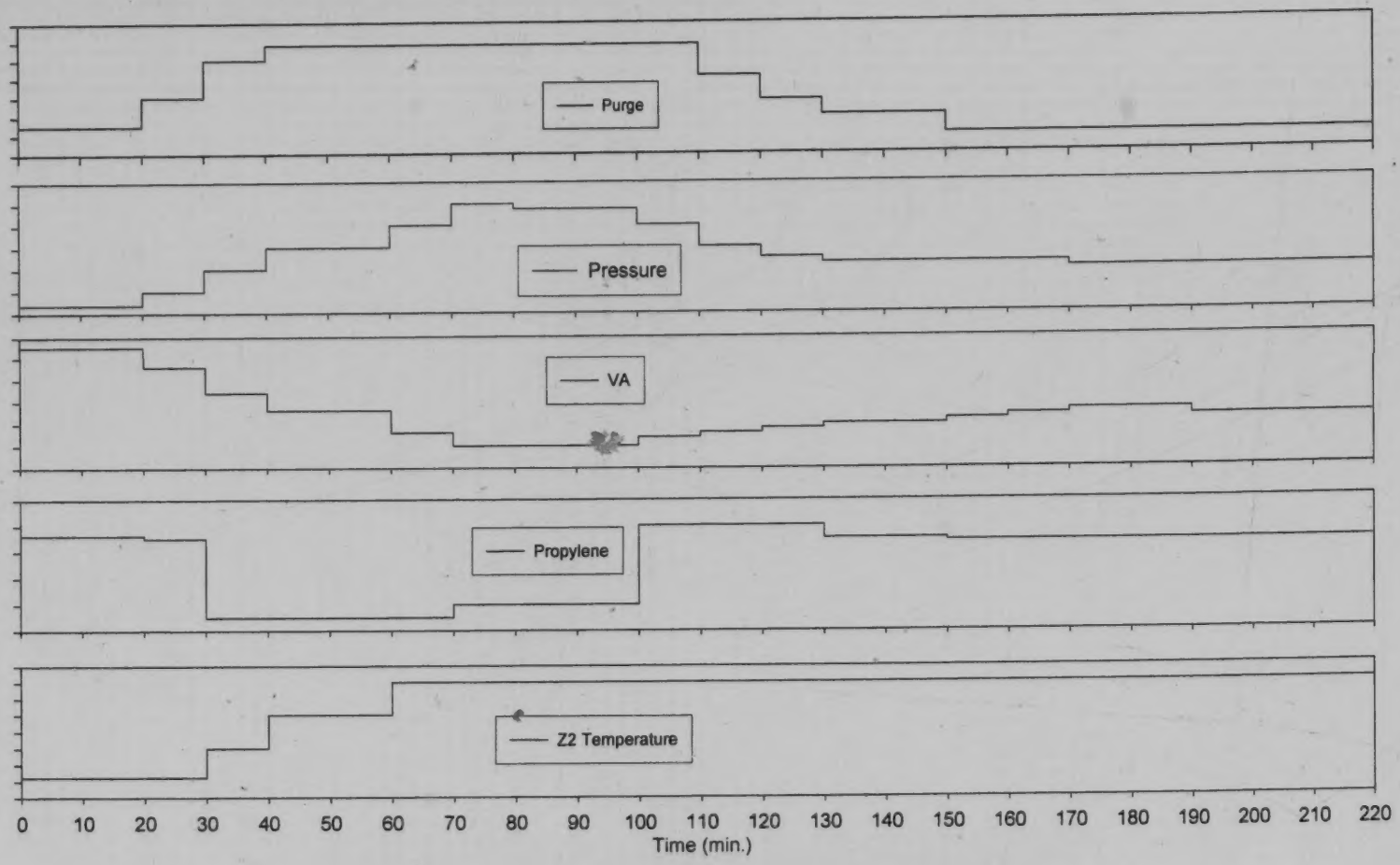

Figure 6-1 – Manipulated Variables for Simulated Grade Change - #1

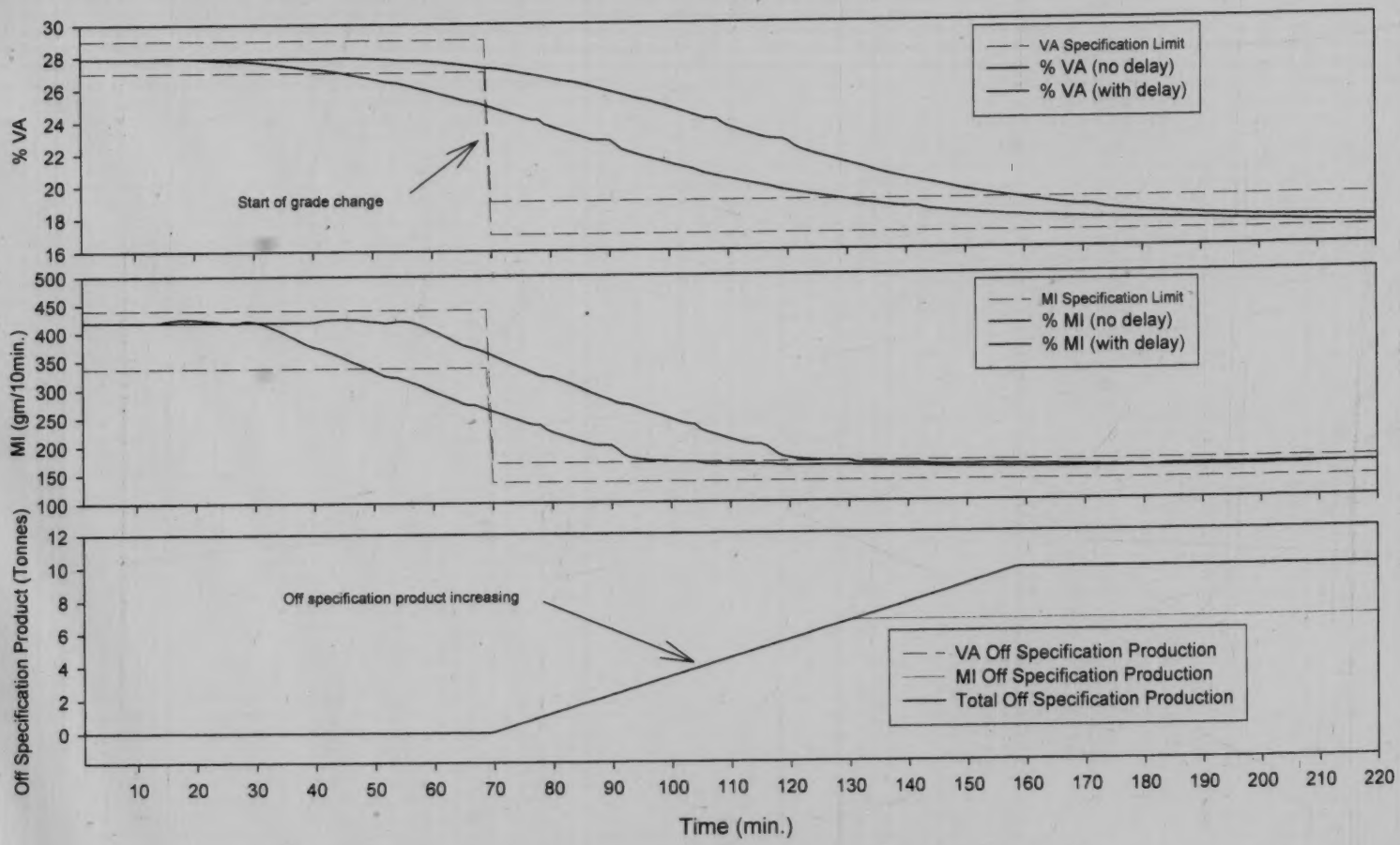

Figure 6-2 – Controlled Variable for Simulated Grade Change - #1

The optimal trajectories found for the manipulated variables are shown in Figure 6-1. The simulated results for this optimal change are shown in Figure 6-2. The two top plots show the MI and %VA with and without the delay. The signal without the delay gives an indication of one very useful application of the dynamic model. This is as a first principles soft sensor. The plant readings for the manipulated variables can be used as inputs to the model. Then the calculated melt index from the model can be used to give an indication of the corresponding change in melt index approximately twenty five (25) minutes before the plant measurement. This grade change has not been attempted at the plant over the last three (3) years. Therefore, there was no recorded information on the actual off specification product manufactured for comparison with the optimal policy.

6.4.2 Simulated Grade Change - #2

The results generated for a grade change from grade #5 to grade #6 are shown next. A change in the melt index only was required. This change is unique in that it goes to one of the extremes of the polymer MI produced by the plant. The final product is the softest polymer produced by the plant and a large overshoot can lead to inability by the extruder to process the polymer. Therefore, the plant operators are usually very conservative during this change. For this change typically five (5) plant variables are usually manipulated. These are:

- Total VA feed flow rate
- Propylene feed flow rate
- Reactor Pressure
- Reactor, Zone 2 Temperature
- Purge flow rate

891

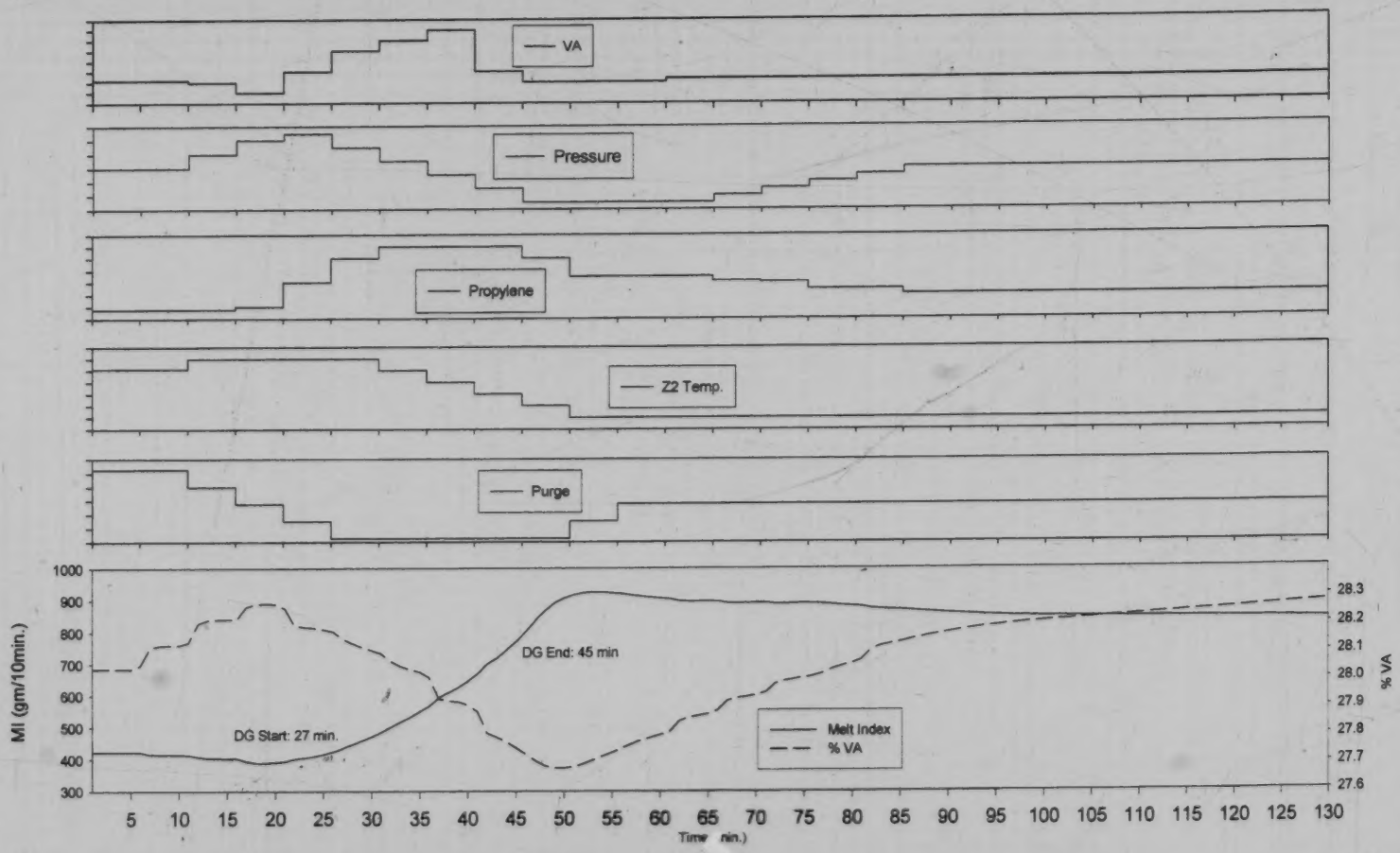

Figure 6-3 – Manipulated and Controlled Variables for Simulated Grade Change - #2

The optimal trajectories found for the manipulated variables and the simulated results are shown in Figure 6-3. Here a descritization interval of five (5) minutes was chosen. This was because the grade change period was short. Therefore, using optimal steps every five (5) minutes did improve the objective function. The total time downgrade product was produced according to the simulation was eighteen minutes. This corresponds to about two and a half (2.5) tonnes of off specification polymer. From the last year of plant history, the average off specification polymer on this change during operator changes was twenty one (21) tonnes and the minimum was eight (8) tonnes.

6.4.3 Simulated Grade Change - #3

The results generated for a grade change from grade #1 to grade #4 are shown here. A change in the melt index and the percentage VA content was required again. For this change typically five (5) plant variables are usually manipulated. These are:

- Total VA feed flow rate
- Propylene feed flow rate
- Reactor Pressure
- Reactor, Zone 2 Temperature
- Purge flow rate

The optimal changes found for the manipulated variables are shown in Figure 6-4. The simulated results for this optimal change are shown in Figure 6-5. This figure also shows the three components which comprise the objective function as described in equation (6.12). The optimizer tries to minimize the value of all components and each is weighted equally. This grade change has not been attempted at the plant over the last three (3) years. Therefore, there was no recorded information on the actual off specification product produced for comparison with the optimal policy.

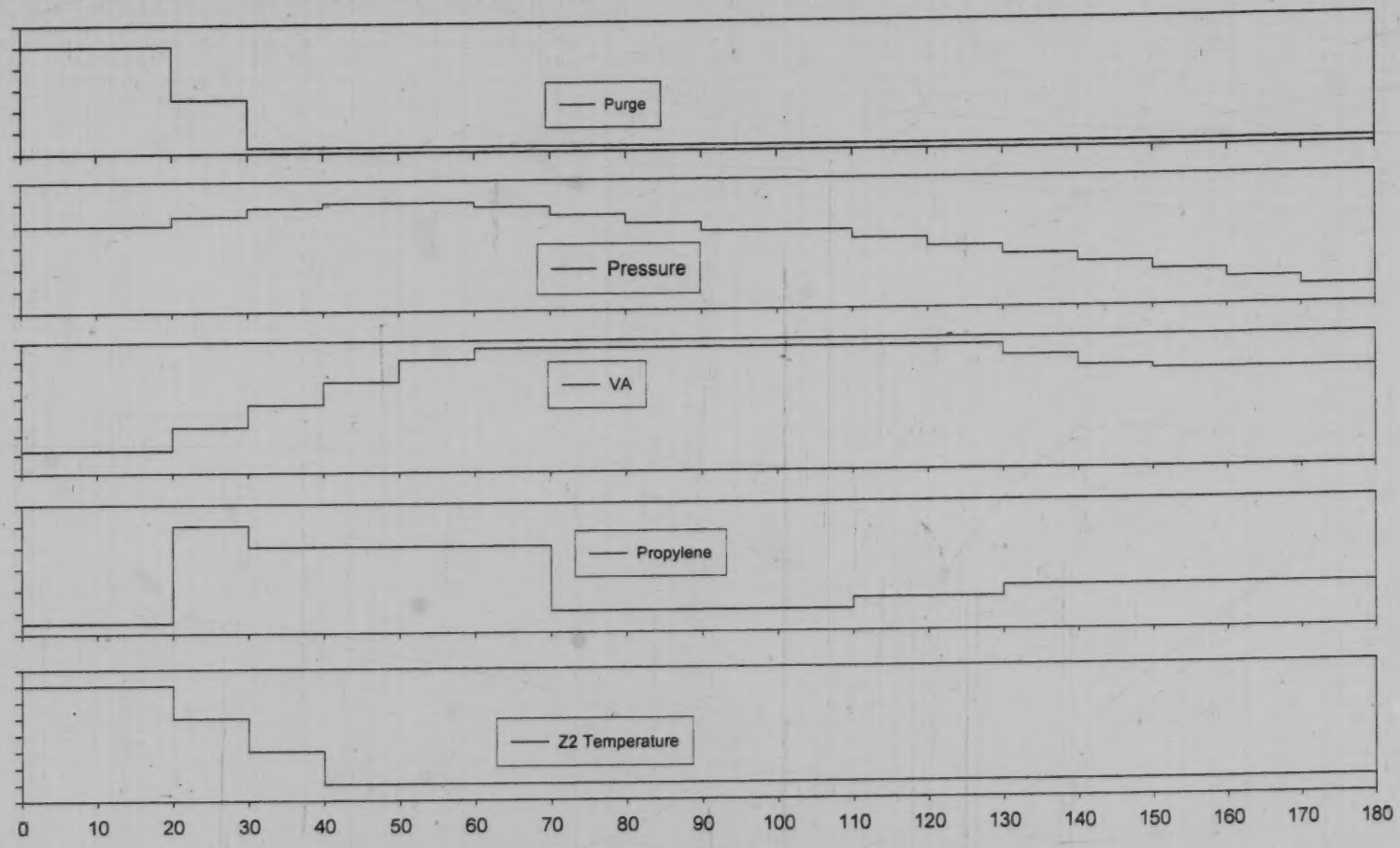

Figure 6-4 – Manipulated Variables for Simulated Grade Change - #3

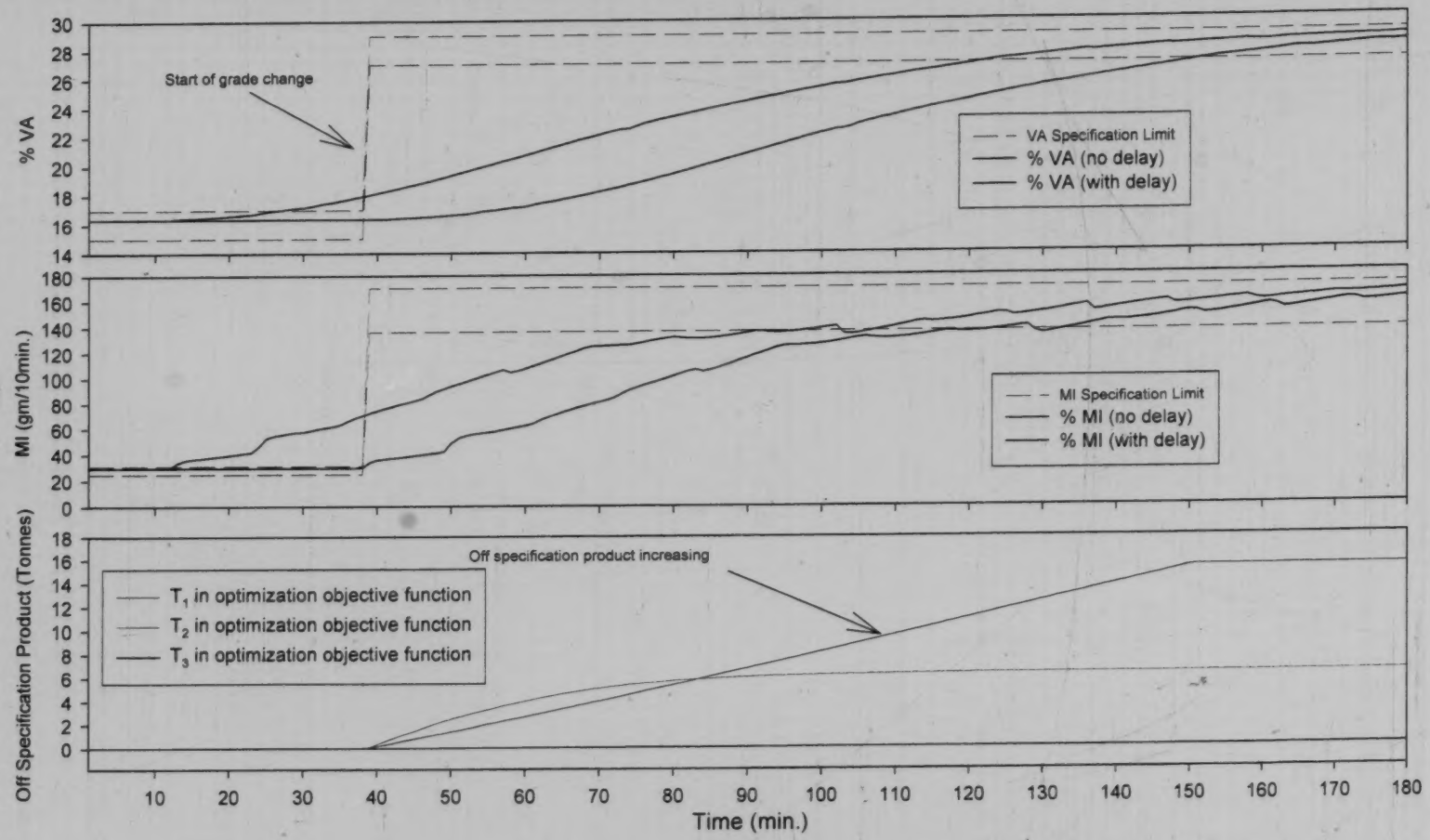

Figure 6-5 – Controlled Variable for Simulated Grade Change - #3

6.5 Plant Trial of Optimal Policies

Two trials of the optimal policies were done at the plant site. One of the trials was a grade transition from Grade #4 to Grade #5. The other was a grade transition from Grade #3 to Grade #2. These were selected based on the plant's production schedule for the available time period.

6.5.1 Plant Trial - #1

The optimal trajectory for the manipulated variables was found. The results of the optimization are shown in Table 6-2. The discretization interval was chosen as five (5) minutes. This was the same change simulated in section 6.4.2. Therefore the simulation plots will not be repeated.

Figure 6-6 shows one of the best implementations of this grade transition performed by an operator. There was one (1) off specification period. The time from start of off specification to steady operation was 50 min. This time corresponds to approximately seven (7) tonnes of off specification polymer.

Figure 6-7 shows the optimal trajectory based grade transition. It can be seen that the time from start of off specification product to steady operation was 9 min. This time corresponds to approximately one and a half (1.5) tonnes of off specification polymer. However it was noticed that the percentage VA was higher than expected from the simulation. After the grade change, the plant's inline extruder began having problems processing the polymer. The operator commented that the polymer became very tacky and sticky. This is one of the properties which VA gives to LDPE. It seemed as though there was more VA in the polymer than expected and the extruder began having problems because of this. The extruder had to be stopped and cleared, before the plant could continue running normally.

Time	Purge	VA Flow	Pressure	Propylene	Zone 2 Temp.	Time
0	25	665	240	17.6	46.4	0
5	20	660.8	244	17.6	46.6	5
10	15	639.4	248	20	46.6	10
15	10	682	250	40	46.6	15
20	5	724.6	246	60	46.6	20
25	5	746	242	70	46.4	25
30	5	767.4	238	70	46.2	30
35	5	682	234	70	46	35
40	5	660.8	230	60	45.8	40
45	10	660.8	230	45	45.6	45
50	15	660.8	230	45	45.6	50
55	15	667.2	230	45	45.6	55
60	15	667.2	232	41	45.6	60
65	15	667.2	234	40	45.6	65
70	15	667.2	236	34	45.6	70
75	15	667.2	238	34	45.6	75
80	15	667.2	240	30	45.6	80
85	15	667.2	240	30	45.6	85
90	15	667.2	240	30	45.6	90
95	15	667.2	240	30	45.6	95
100	15	667.2	240	30	45.6	100
105	15	667.2	240	30	45.6	105
110	15	667.2	240	30	45.6	110
115	15	667.2	240	30	45.6	115
120	15	667.2	240	30	45.6	120
125	15	667.2	240	30	45.6	125

Table 6-2 - Implemented Change #1 Plan (values scaled)

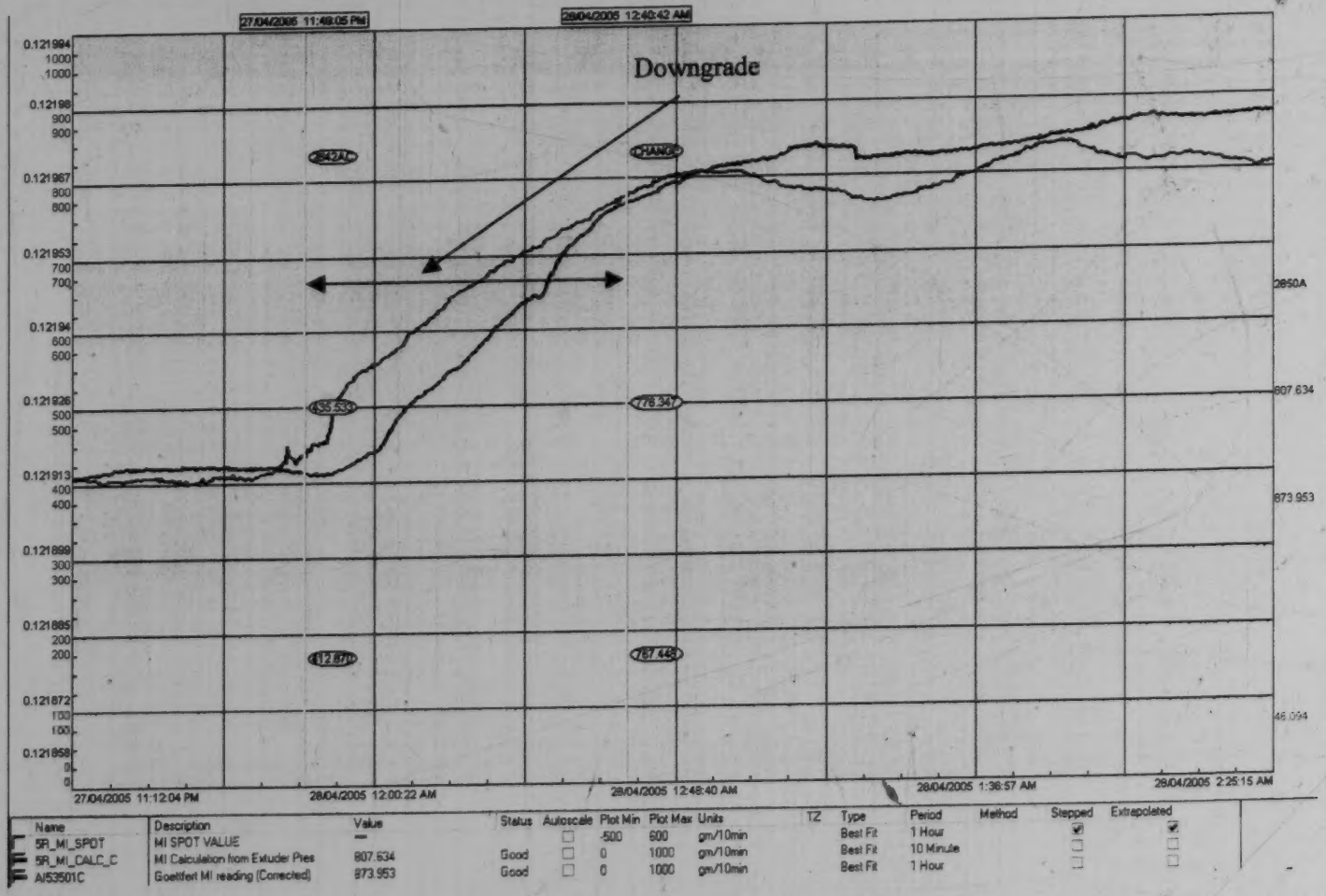

Figure 6-6 – Operator Implemented Grade Change

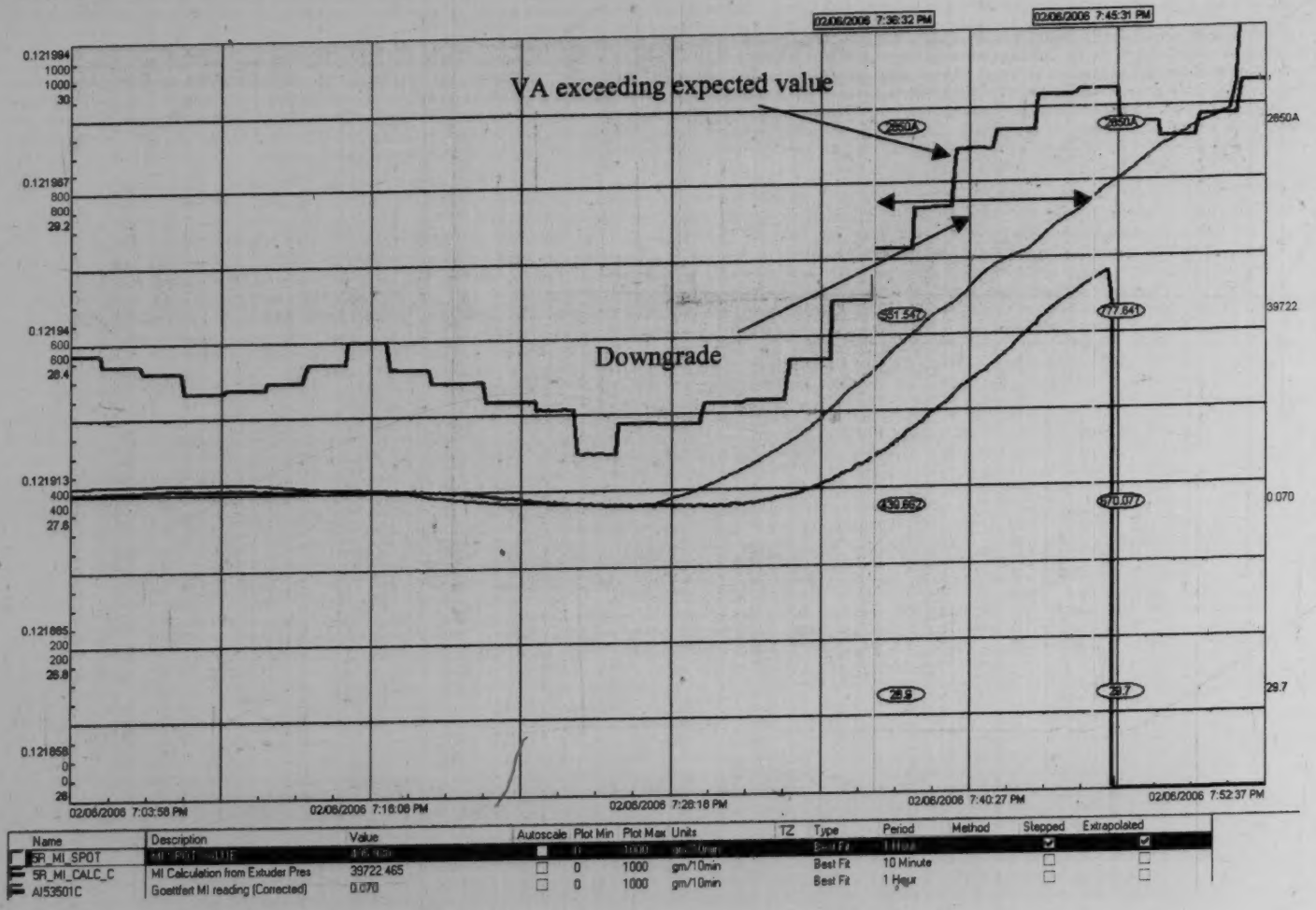
VA exceeding expected value
Downgrade
02/06/2006 7:36:32 PM
02/06/2006 7:45:31 PM
02/06/2006 7:03:58 PM
02/06/2006 7:16:08 PM
02/06/2006 7:28:18 PM
02/06/2006 7:40:27 PM
02/06/2006 7:52:37 PM
2650A
39722
0.070
29.7
Name | Description | Value | Autoscale | Plot Min | Plot Max | Units | TZ | Type | Period | Method | Stepped | Extrapolated
SR_MI_SPOT | | | | | | | | | | | |
SR_MI_CALC_C | MI Calculation from Extruder Pres | 39722.465 | | 0 | 1000 | gm/10min | | Best Fit | 10 Minute | | |
AI53501C | Goettfert MI reading (Corrected) | 0.070 | | 0 | 1000 | gm/10min | | Best Fit | 1 Hour | | |

Figure 6-7 – The Implemented Optimal Grade Change

6.5.2 Plant Trial - #2

The optimal trajectory for the manipulated variables was found. The discretization interval was chosen as ten (10) minutes. The results of the optimization are shown in Table 6-3.

Time	Purge	VA Flow	Pressure	Propylene	Time
0	30	540	382.5	43.2	0
10	60	570	385.5	21.3	10
20	90	465	388.2	3.3	20
30	102	360	391.2	3.3	30
40	102	303	394.2	3.3	40
50	102	303	388.8	3.9	50
60	102	390	381	3.9	60
70	102	435	376.5	3.9	70
80	76.5	495	370.8	3.9	80
90	57	495	367.8	6.6	90
100	45	495	366.3	8.1	100
110	30	495	366.3	11.1	110
120	30	495	366.3	11.4	120
130	30	495	364.8	12.3	130
140	30	495	364.8	12.6	140
150	30	495.3	364.8	12.6	150
160	30	495	364.8	11.7	160

Table 6-3 – Implemented Change #2 Plan (values scaled)

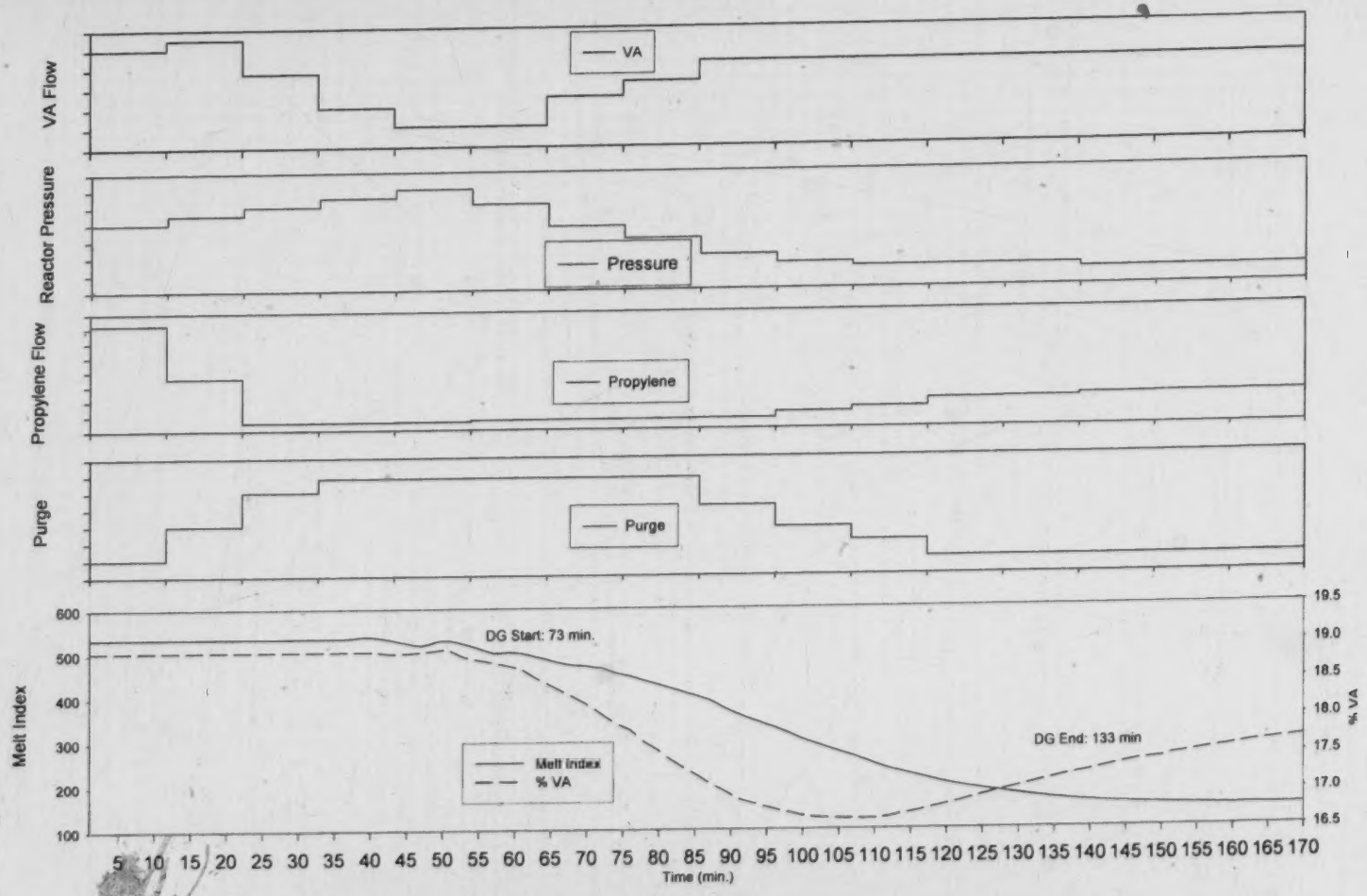

Figure 6-8 – Optimal Policy for Plant Implementation #2

The results and predicted trajectories for the control variables are shown in Figure 6-8.

Table 6-4 shows the actually strategy which was implemented. Changes were required because the feed gas temperatures were higher than those in the model and the return gas coolers were fouled, thus there was less mass accumulation in the system. This caused the MI and VA to undershoot more than expected; this affected the percentage VA more significantly.

Time	Purge	VA Flow	Pressure	Propylene	Time
0	30	528	382.5	43.2	0
10	60	558	385.5	21.3	10
20	90	465	388.2	3.3	20
30	102	360	391.2	3.3	30
40	102	303	394.2	3.3	40
50	102	303	388.8	3.9	50
60	102	390	381	3.9	60
70	102	435	376.5	3.9	70
75	**60**	**495**	**370.8**	**6.6**	**75**
80	60	495	370.8	6.6	80
90	**45**	**525**	367.8	**11.1**	90
100	45	**525**	**360**	11.1	100
110	30	**547.5**	**360**	11.1	110
120	30	**547.5**	**360**	11.4	120
130	30	**555**	**360**	**13.5**	130
140	30	**555**	**360**	**15**	140
150	30	**562.5**	**360**	**15**	150
160	30	**562.5**	**360**	**15**	160

Table 6-4 – Grade Change #2 Implemented Strategy (values scaled)

The values with dark shading were modified from the optimizer's results during implementation.

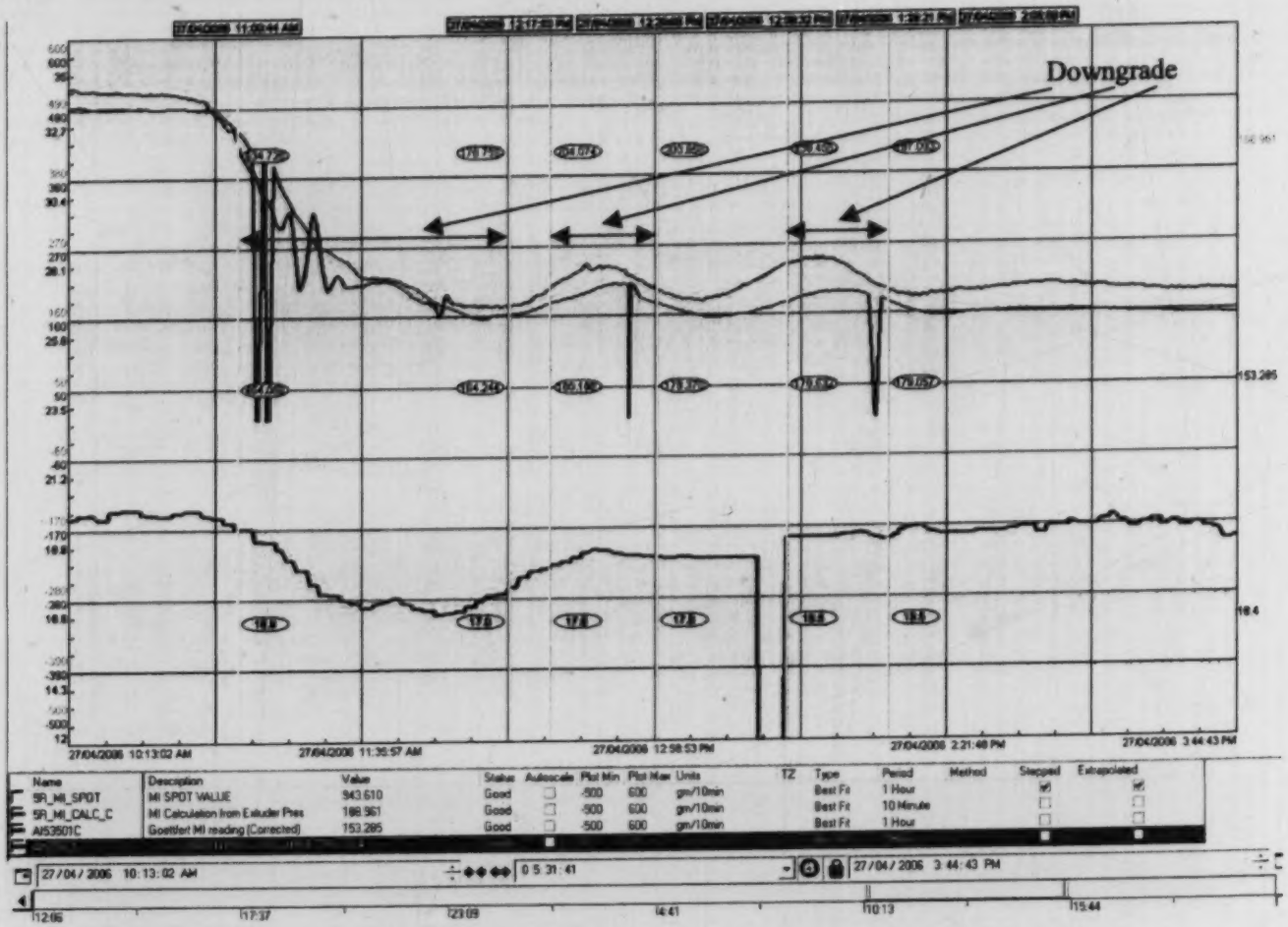

Figure 6-9 – Operator Implemented Grade Change #2

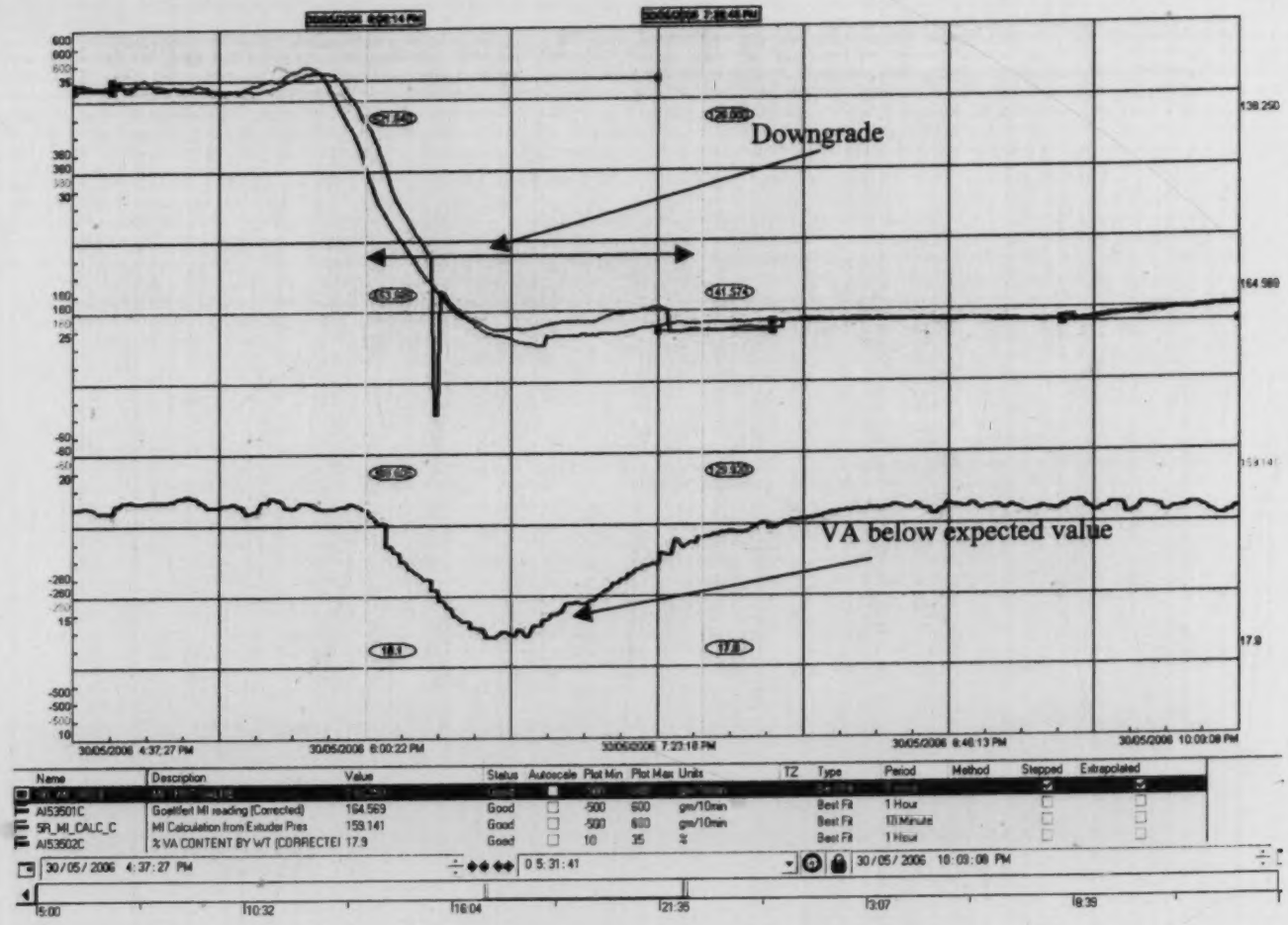

Figure 6-10 – The Implemented Optimal Grade Change #2

Figure 6-9 shows the last time this grade transition was implemented by an operator. There were three (3) off specification periods. The time from start of off specification to steady operation was 3 hr. 5 min. This time corresponds to approximately twenty four (24) tonnes of off specification polymer.

Figure 6-10 shows the optimal trajectory based grade transition. The time from start of off specification product to steady operation was 1 hr. 35 min. This time corresponds to approximately twelve (12) tonnes of off specification polymer. It was noticed that the drop in the percentage VA was larger than what was predicted from the model.

6.6 Analysis of the Plant Trials

One of the plant trials was successful and was able to show that optimal trajectories do give less off-specification product. The other showed the optimal grade transition policy would give reduced off specification product, but certain physical and model limitations should be taken into account.

6.6.1 Discussion on Implementation of Optimal Trajectories

The implementation of the optimal policies at the plant gave very useful results. The trial which was discussed in 6.5.1 clearly showed that the grade changes made on the plant presently by the operators are very conservative. The optimal trajectory indicated a change which was usually done in 45 minutes or more could be done in 18 minutes. The actual test got to the new specification in 9 minutes. This would have been excellent, however the product produced after this period could not be processed by the extruder. There was excessive overshoot in the VA percentage in the polymer. The sudden large change in the VA content in the polymer was thought to be the main reason for the inability to process the polymer. This required some more detailed analysis. Trial #1 showed an overshoot in the VA, while trial #2 showed and undershoot in the VA. On simulation of the model using the manipulated variable trajectories the problem was clearly found. The model was simulated for the second plant trial since there were no interruptions in the process variables on that run.

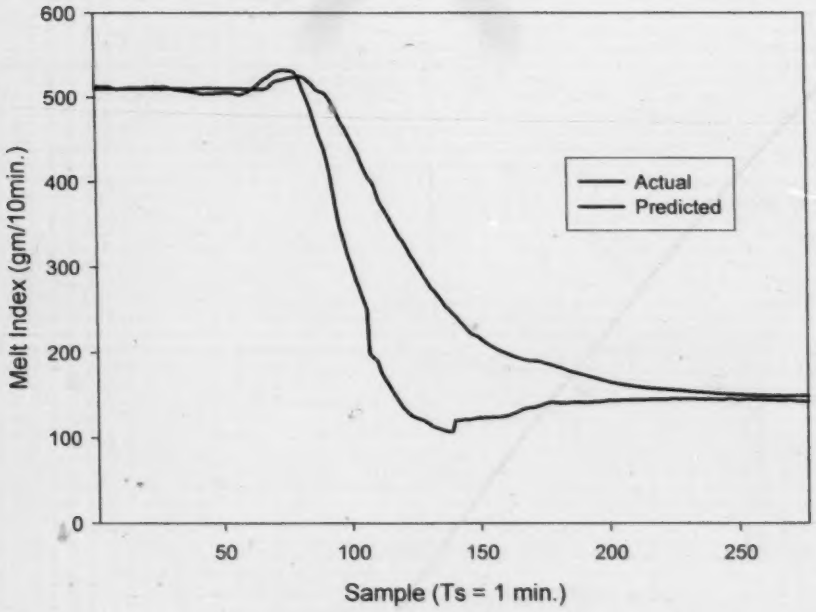

Figure 6-11 – Trial #2 – MI

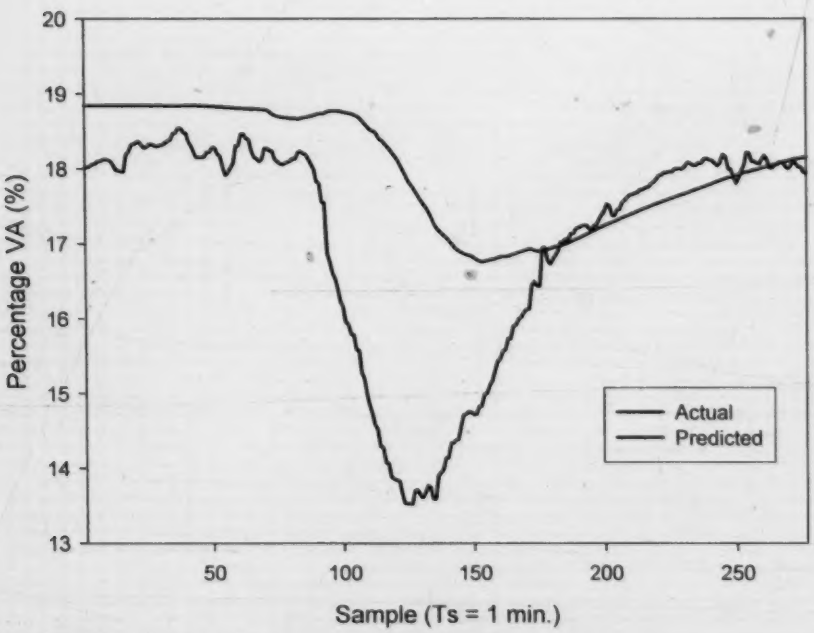

Figure 6-12 – Trial #2 – VA

The simulation results and the actual trajectories for the two main controlled variables are shown in Figure 6-11 and Figure 6-12. These results show that the steady state values for both variables were captured relatively well. One point to note is that during the fitting process the MI was weighted heavier than the VA, since the MI is the plant's main controlled variable. Therefore the steady state values for the MI are expected to be closer to the plant values.

It was seen in the validation plot Figure 4-19 that the dynamics of the MI were fit well. In this validation the VA remained relatively constant. However, when the VA was changed the dynamic validation was not as good. This implied there was a problem with the VA modeling and it was affecting the MI. Two important plant variables which were not available during the model regression process were the concentration of VA in the intermediate pressure stream (gas recycle on the HPS) and the VA concentration in the low pressure stream (gas recycle on LPS). The PC-SAFT VLE parameters dictate the amount of VA which would split into either of these streams. There was too little VA in the intermediate pressure stream and too much in the low pressure stream. This problem becomes more significant during dynamic periods because the accumulation rates in these two streams would be erroneous. This caused the VA to overshoot in trial #1 because the model predicted it would accumulate too slowly in the RGC. This also caused the VA to undershoot in trial #2 because the model predicted it would accumulate too quickly in the LP-CLR. Solving this problem requires getting samples of the VA content in these two streams so the PC-SAFT parameters can be regressed correctly.

Plant trial #2 showed that the model based optimal policies can deliver significant value in decreasing the off specification product produced during the grade transitions. The use of the first principles model base gave the operator a lot more information about a particular grade transition change before it was actually done. The operator has the ability to look at and compare the response of several plant variables before the grade change is implemented.

The optimal trajectories were found to make large changes early in the transition and smaller changes closer to the end. This gives more stable product transitions. This was very important because instability in this high pressure polymerization process

can lead to "decompositions". As can be seen from Figure 6-9 and Figure 6-10, the optimal grade change is a lot more stable and settles in a shorter period of time.

The operator usually has to make predictions about the flow rate of different components required for the measured quality variables to become steady. The system has significant dead time (caused by transport lags and measurement delays) and a very long time constant (caused by the system mass accumulation). Therefore the operator's predictions are usually erroneous and this can cause the oscillations seen in Figure 6-6. Using the optimal policies generated by the first principles model requires significantly less operator prediction and therefore less possibility of an error.

The expected implementation of these optimal strategies would include the operator. The operator would implement each step, and monitor the process. Then as the transition is nearing the end, the operator would make small adjustments to compensate for disturbances and plant-to-model mismatch. In this scheme the operator would be behaving as the feedback element.

6.6.2 Economic Analysis

The long term implementation of the policies developed here and the extension of the model to cover the full range of operation is dependent on the potential financial benefits. Data from AT Plastics for 2005 estimated the total downtime for the 5R production facility only, to be seven thousand, two hundred and thirty three tonnes (7233). Based on this and an estimated reduction in downgrade of forty five percent (a conservative number based mostly on the results shown in trial #2) the following economic justification was proposed:

Description	Value
Total downtime (Tonnes/year):	7233
% of total downtime attributed to grade transitions (%):	36
% of total grade transition time that can be saved (%):	45
Difference in selling price between prime and off specification product ($/tonne)	$0.14
Total yearly revenue:	**$159,448.52**

Table 6-5 – Economic Analysis

The plant trial showed that the optimal policies can reduce the off specification product by more than fifty (50) percent. A more conservative number of forty five (45) percent was used for the analysis. For implementing these optimal policies on only one of their reactors this facility can increase the annual revenue by approximately one hundred and sixty thousand dollars.

6.7 Chapter Summary

In this chapter we explored some of the published work in the area of optimal grade transitions for polymerization reactors. To the best knowledge of this author there were no studies that could be directly applied to this particular process. Then an overview of the fundamentals of dynamic optimization was described. The implementation and configuration required in Aspen Dynamics were then given. Simulation results for three different product changes were detailed. Here the model's applicability as a soft sensor also stood out. The results of the plant trials for two product changes were then given. One of the results showed some limitations of the model and processing constraints of the extruder. The other result showed that the use of optimal policies can potentially reduce the off specification product produced by over 50%. A brief economic analysis of the potential annual revenue showed that the implementation of these optimal policies for one of the facilities production lines can yield revenues in the range of one hundred and sixty thousand dollars.

The big secret in life is that there is no big secret. Whatever your goal, you can get there if you're willing to work.

Oprah Winfrey (1954 -)

Chapter 7

Concluding Remarks and Future Work

7.1 Major Contributions

The research in this thesis was a collaborative effort between the University of Alberta and AT-Plastics Inc. The main contributions of this collaborative project are:

Design and implementation of a plant historian – The data collection and dissemination architecture for first principles and data based modeling were detailed. This information can guide a process engineer on IT issues which are typically seen as being out of his domain. There tends to be no lack of data at most process plants but lack of knowledge on strategies for integration of the correct data on a real time basis. This section will assist with these issues

Plant Calculations – The building of the first principles model required fitting and validation. Plant data available for this was not always in the same form as that

available in the modeling package. However, often the plant variables could be used to generate the required variable. Generally control engineers would collect vast amounts of operating data, and then do the calculations offline. In this work calculations were detailed which were implemented online. These calculations can be extended for use by any facility interested in doing similar modeling of their process.

First Principles Modeling of LDPE and EVA Polymerization in a Stirred Autoclave – A detailed framework for modeling the autoclave in a commercial modeling package was developed. This involved a detailed first principles model, which included unit process based equation of state thermodynamics and full free radical kinetics for all reacting components. Theoretical additions made by other researchers such as the initiator based correlations were added. Some additional theoretical and practical extensions were made to the modeling package to incorporate the poor zone mixing effects.

Development of a Detailed Model Regression Framework – A framework was developed for the regression of the first principles model with every critical operating parameter available on a typical polymerization plant. This framework was designed for regressing large amounts of categorized model parameters to allow a single model to be applicable for several grades. The two main categories of model parameters regressed were thermodynamics, reaction kinetics and dynamic parameters. The procedure developed was used successfully for regressing the parameters of first principles model. The final model covered the full operating range of the plant.

Dynamic Autoclave Modeling – There were several modifications required to extend the steady state model to the dynamic model case. Several of these were non-standard developments which were required. These included:

Addition of support for vapor phase polymerization

Modification of the default CSTR based zone pressure control constraints

Dynamic modeling of the heat exchangers

Development and Implementation of a MI Soft Sensor – A soft sensor for the polymer melt index was developed. A theoretical model was developed, followed by non linear least squares regression regress the model parameters. The model was based on the variables monitored at the inline extruder. Once the extruder was

operating normally, this soft sensor gave a reliable indication of a change in the melt index nine (9) minutes before the online analyzer. This soft sensor has been implemented at the plant for over six (6) months and is currently used by the plant operators.

Unified Bias Updating – Bias updating scheme based on a combination of the QC laboratory readings and online melt index (once deemed to be usable) was developed and implemented.

Optimal Product Change Policies – A suitable objective function for applying dynamic optimization was developed. This was used for developing optimal grade transition policies. The optimal grade transition moves were provided to the plant operator and the policy was then experimentally evaluated on the real process with success.

Academic Contributions – *This work contributes significantly to the body of academic work already available in this area by giving a foundation for industrial implementation of several novel ideas in polymerization modeling, control and optimization.* There were several ideas discussed and developed which can potentially result in profitable applications. These include the use of the dynamic first principles model for advanced control, process and sensor monitoring, economic optimization, creation of optimal grade transitions, process engineering studies and plant constraint analysis. The databased model can be used primarily for localized advanced process control and process and sensor monitoring. The soft sensor developed can be used as a quality estimator of the polymer produced during periods where the online measurement is faulty and can be incorperated in to several feedback control stratigies for control of the polymer quality.

7.2 Generalization of the Optimal Grade Transition Methodology

This work involved the development of a methodology for generation of optimal trajectories for a specific polymerization plant. However, the ideas developed can be extended to other operating facilities operating different processes but with similar

problems.

There were a few important steps which should be executed by an organization undertaking a similar task. Some of these steps are not technical but are necessary for success. These include:

Personnel – For implementing optimal grade transitions, there should be at least one person at the plant site who is familiar with the principles advanced process control and optimization. There should be someone available or the same person referred to before who is familiar with the first principles of the process. This person should be in contact with several parties on the plant including operations, laboratories, sales, production planning, engineering and maintenance.

Time – Undertaking this type of project takes significant time to achieve returns. However, because it requires significant first principles modeling; this brings an excellent understanding of all aspects of the plant and its constraints. Also the rewards of these projects are usually large even though they may take a long time to reach fruition.

Suitable Foundation – The control and data acquisition systems are necessary. The plant information is critical in the model building and validation process. The implementation of online calculations and a system for storing or retrieving specific batches of data as early as possible can make the data fitting and validation process relatively painless. The plants regulatory control loops should be performing well. Without this, the optimum can be found in the model, but can never be implemented.

Model Based – The generation of the optimal strategies for the grade transitions were based on a first principles model. For an operating facility the best practice here would be using an established commercial package for development of the model. A successful previous implementation of the plants specific process in the application is not needed. However, some metrics for choosing an application are:

The support relationship the plant has with the company

The available thermodynamic modeling options

Application supports dynamic simulation

Application supports dynamic optimization

Implementation – The implementation of the optimal trajectories should be

relatively painless. If there are complexities, they should be hidden behind a simple GUI for operator implementation. Implementing an optimal transition on the plant should be similar to changing several set points on the plant. The system should be robust and allow operator intervention at any point.

These steps outlined above are general guidelines. The more specific steps are usually application dependent. However, many of the regression techniques, modeling additions, regressed parameters and other theories detailed in the thesis can be used as a foundation for any application.

7.3 Recommendations

During this research project there were several areas identified which would require additional work. These are categorized, listed and described here.

7.3.1 Additions and Modifications to the First Principles Model

The model developed for the process showed the ability to predict several important plant variables, including the polymer melt index and certain plant flows and concentrations. These are the parts of the model which were found to generate the most interest. However, the implementation of the optimal grade change trajectories revealed an important deficiency of the model. This was the poor dynamic predictive ability of the percentage VA content in the polymer produced. Thus one important improvement of the model would be regressing relevant parameters to improve the prediction. As explained in the discussion of the plant implementations in 6.6.1., this would require additional data which was not available during the project. The most important was laboratory assays for molar compositions of components in the intermediate and low pressure recycle streams.

The first principles model was developed using data for EVA grades. This was because during the time considered, the particular line considered only produced EVA polymers. However, more recently the production line has been used for producing LDPE polymers. A significant amount of research in the modeling of LDPE polymerization has stated the necessity to model the presence of the phase

boundary in the reactor for LDPE polymerization. This implies modeling of the reaction kinetics for the gas and liquid phases. While, for EVA polymerization it is not necessary to consider this phase boundary because the phase boundary moves with the VA composition in the reactor. At the operating conditions in the reactor this boundary is not encountered for EVA polymerization. If this was included in the model, this could allow the extension of the EVA model produced here to cover both LDPE and EVA polymerization.

The primary and booster compressor operate on a common driver. This compressor contains several recycle loops which control the mass throughput of the plant. This was not modeled in much detail in the first principles model. However, adding this would add robustness and accuracy to the model.

7.3.2 Dynamic Modeling Extensions

The optimal trajectories based on the first principles dynamic model were built with the main emphasis on reducing the off-specification product manufactured during grade transitions. However, there are several other plant events which cause downtime or off specification product. These include cooler cooks, initiator type and pump changes, plant shutdown and start-up events. The extension of the dynamic model to include these events could mean optimal operation during these events to also reduce the off specification product.

The modeling of cooler cooks holds a lot of potential for reducing downgrade product. This event occurs very regularly and almost every time it occurs downgrade product is produced. Some initial work was done in this area. Here the calculated compressor mass flow mentioned in section 2.5.1 was used. It was known that the mass flow through the secondary compressor reduces during cooler cooks, because of higher operating temperatures and therefore the density decreases. This was seen in the calculated mass flow rate. The off-specification product manufactured during the cooler cooks occurred because the propylene and VA should have been injected into the system at a constant ratio to the compressor mass flow. Therefore when the compressor mass flow drops, the propylene and VA flow should drop as well. This

compressor mass flow signal can be used for ratio control to allow the needed change in propylene and VA injection.

. Coolers become fouled with polymer during the regular plant operation. The removal of this polymer lining is done by an uncontrolled raise in the temperature of the cooler contents. This causes a large disruption in the plant's operation. If the cooler and the fouling were more accurately modeled, the optimal cooler cook could be found to give minimal disruption in the plant's operation, and thus reduce the off specification product manufactured.

As mentioned in Chapter 4 the Aspen Dynamics model supports two forms of dynamic modeling. These models are either pressure driven or flow driven. Here a flow driven model was used. The pressure driven model has some advantages over the flow driven model. This was clear while the dynamic model was being configured. There are certain effects which needed be added to the model and these could only be added with a pressure driven model. One of these effects includes the reactor's pressure control. This pressure controller's manipulated variable in the model is a flow rate leaving the reactor. However, on the actual plant this controller's manipulated variable was a valve's position. The valve's position possesses a position to pressure drop and flow rate relationship (the valve characteristic). The plant experiences oscillations in the pressure control during certain events. This has been attributed to poor sizing of this control valve. If a more detailed pressure driven model were used then these events could be modeled and solutions to these problems could be developed offline with the dynamic model.

7.3.3 Data Based Modeling and Control

A state space model was estimated using subspace identification methods. This model was based on routine plant data. This model has several applications. These include:

Model Predictive Control – Here multiple linear models can be used for implementing control while running on grade.

Optimal Product Change Strategies – again multiple linear models can be used to model and optimize specific grade changes. The model could also be used as a model predictive controller, which operates in two modes:

- as a controller while a steady grade is running
- an optimal grade transition optimizer. Here the model for one specific grade change was built and showed excellent validation

Model Based Monitoring – The state space model developed using subspace methods can be used for process monitoring. This has several applications in fault detection and isolation. One event which is avoided as much as possible is the reactor decomposition. The state space model can be extended for monitoring the onset of these events. However, this application would require development of a reliable method for using multiple linear models for process monitoring.

7.3.4 Extruder Modeling

A soft sensor based on the process variables monitored on the extruder was developed. This soft sensor suffered from a bias update because of fouling of the extruder, the screen pack and die. This fouling increases the frictional losses and thus the die pressure which is the most critical variable in the soft sensor. More detailed modeling of the extruder and the fouling process can give a more detailed soft sensor which can use the monitored process variables to calculate the melt index while the extruder, the screen pack and die are folded and when they are not.

7.3.5 First Principles Model Based Soft Sensor

The first principles model developed here shows excellent predictive ability. The plant operators have expressed the need for a soft sensor which gives them faster predictions on the melt index. The Extruder based melt index gives them some help but it is still significantly delayed. The dynamic model can be used as an online soft sensor. The model would read certain key plant variables on a regular basis and return the quality variables to the operator without the delay. This knowledge could assist the operator in remaining on specification during any major plant event.

7.3.6 Optimizer Modifications

The optimizer built into Aspen Dynamics was useful for doing some Dynamic Optimization. However, many limitations were found. This occurred as more and more detailed optimization was done. Without scaling any of the manipulated variables and with fixed time instants the optimizer ran and converged. As scaling was added the bounds on the change in the manipulated variable were no longer respected. Allowing the optimizer to change the optimal sampling instant did not return the expected results. It was expected that the optimizer would change the optimal time instants at which the manipulated variable changes should be made. However, optimal changes at the specified discretization instants only were returned. It was also noticed from conversations with the plant operators that simultaneously changing every variable which has an effect on a product change may not be most advisable. A useful option would be to have the ability to set a constraint within the optimizer specifying that only one manipulated variable can be changed at a time and a minimum time before the next manipulated variable move. This allows the optimizer to produce optimal trajectories more like what the operators would usually implement. The changing of multiple variables at one time instant can result in plant instability. Therefore the ability to add this staged change in manipulated variables can produce more stable grade changes. Because of these limitations, it may be more useful to use another optimizer or to program an external optimizer which can transfer real time model operating data and the gradient of the variable in the model for optimization.

7.3.7 Plant Modifications

There are certain physical modifications on the plant which do not allow rapid product changes. Some of these include the limitation on the mass flow of the purge stream. This purge stream was sized relatively small compared to the total flow rate in the low pressure recycle loop during the plant design. This is the main method by which the modifier is removed from the system when the MI is required to be decreased. Thus if the purge flow valve was resized to allow larger flow rates, this

can allow faster product transitions when moving from a high MI to a lower one. Another area which causes significant delays during certain product changes is the lack of automation for the initiator mixing system. The initiators are mixed with the solvent in a very low concentration by the operators. When a grade change using a new initiator or a different concentration of initiator is required; the operator mixes another batch. The operator must then coordinate the batch change and pump change (if necessary) at some point during the product change. These can be automated so that it is done before the actual product change is taking place and a batching system can mix the concentrations exactly based on the product recipe.

7.4 Concluding Remarks

The optimal grade transition problem for an EVA polymerization facility (AT Plastics Inc, Edmonton, Canada) has been analyzed. We have seen, as many other authors have indicated, that the use of a first principles dynamic model for optimization is an excellent method of handling the problem. However, we encountered the difficulty with respect to the lack of generality of other published work in this area. A frame work for development of the first principles model was developed using a combination of novel ideas and established theory. These were combined into a commercial package for long term sustainability in an operating facility. The first principles model regression scheme proved itself by resulting in one universal first principles dynamic model for all production variations. This model was used to successfully develop optimal trajectories for product changes. These optimal changes were tested and proved the ability to reduce the downgrade product by over 50%.

A soft sensor to monitor the melt index of EVA copolymer produced has also been developed and is based on the novel idea of using process variables monitored on the extruder. This soft sensor has been implemented at AT Plastics Inc. and has been in use for the past six (6) months.

These two implementations have received very successful reviews from the AT Plastics Inc. personnel. The soft sensor gives the operator an indication of a change in

melt index nine (9) minutes before the plant's online instrument. While the economic analysis for the optimal grade transitions on one of their polymer manufacturing lines shows they can give a potential increase in revenue of one hundred and sixty thousand dollars per annum. This can increase the plant's revenue by close to one million dollars per annum by implementation on the plants five manufacturing lines.

List of References

Agrawal, S. and C. D. Han (1975). "Analysis of the high pressure polyethylene tubular reactor with axial mixing." AIChE Journal **21**(3): 449-465.

Alperowicz, N. (2005). "A changing lineup." Chemical Week **167**(27): 26-31.

Aspen-Technology (2003) "Soave-redlich-kwong property methods summary." Aspen Technology Online Support **Volume**, DOI:

Aspen Technology, I. (2000). "Aspen polymers plus 10.2 users guide." 2006.

Aspen Technology , I. (2002). Application of pc-saft eos in ldpe process. Boston, USA.

Aspen Technology, I. (2005). "Aspen polymers plus 2004 users guide 1." 2005.

Benzler, H. and A. Von Koch (1955). "Phase diagram for ethylene up to 10,000 atm absolute pressure." Chemie-Ingenieur-Technik **27**(2): 71-75.

Beuermann, S., M. Buback and D. Nelke (2001). "Pressure dependence of the propagation rate coefficient for vinyl acetate polymerizations in bulk and in solution of fluid co2." Macromolecules **34**(19): 6637-6640.

Bokis, C. P., M. D. Donohue and C. K. Hall (1994). "Second virial coefficients for chain molecules." Industrial & Engineering Chemistry Research **33**(1): 146-150.

Bokis, C. P., S. Ramanathan, J. Franjione, A. Buchelli, M. L. Call and A. L. Brown (2002). "Physical properties, reactor modeling, and polymerization kinetics in the low-density polyethylene tubular reactor process." Industrial and Engineering Chemistry Research **41**(5): 1017-1030.

Brandolin, A., N. J. Capiati, J. N. Farber and E. M. Valles (1988). "Mathematical model for high-pressure tubular reactor for ethylene polymerization." Industrial & Engineering Chemistry Research **27**(5): 784-790.

Brandrup, J., E. H. Immergut, E. A. Grulke, A. Abe and D. R. Bloch (1999). Polymer handbook (4th edition), John Wiley & Sons.

Brisk, M. (2004). Process control: Potential benefits and wasted opportunities. The 5th Asian Control Conference, Melbourne, Australia.

Buback, M., M. Egorov, R. G. Gilbert, V. Kaminsky, O. F. Olaj, G. T. Russell, P. Vana and G. Zifferer (2002). "Critically evaluated termination rate coefficients for free-radical polymerization, 1: The current situation." Macromolecular Chemistry and Physics **203**(18): 2570.

Cervantes, A. M., S. Tonelli, A. Brandolin, J. A. Bandoni and L. T. Biegler (2002). "Large-scale dynamic optimization for grade transitions in a low density polyethylene plant." Computers and Chemical Engineering **26**(2): 227-237.

Chan, W.-M. and C. A. O. Nascimento (1994). "Use of neural networks for modeling of olefin polymerization in high pressure tubular reactors." Journal of Applied Polymer Science **53**(10): 1277-1289.

Chapman, W. G., K. E. Gubbins, G. Jackson and M. Radosz (1990). "New reference equation of state for associating liquids." Industrial & Engineering Chemistry Research **29**(8): 1709-1721.

Chatzidoukas, C., J. D. Perkins, E. N. Pistikopoulos and C. Kiparissides (2003). "Optimal grade transition and selection of closed-loop controllers in a gas-phase olefin polymerization fluidized bed reactor." Chemical Engineering Science **58**(16): 3643-3658.

Chen, C. C. (2002). An industry perspective on polymer process modeling. CAST Communications Newsletter. P. Rony, AIChE - CAST Communications.

Chen, C. H., J. G. Vermeychuk, J. A. Howell and P. Ehrlich (1976). "Computer model for tubular high-pressure polyethylene reactors." AIChE Journal **22**(3): 463-469.

Chen, C. H., J. G. Vermeychuk, J. A. Howell and P. Ehrlich (1976). "Computer model for tubular high-pressure polyethylene reactors." **22**(3): 463-469.

Chen, S. A. and N. W. Huang (1981). "Minimum end time policies for batchwise radical chain polymerization - 3. The initiator addition policies." **36**(8): 1295-1305.

Cock, K. D. and B. D. Moor (2003). Contribution to section 5.5, "control systems robotics and automation" of eolss, unesco. Encyclopedia of life support systems. H. D. Unbehauen, Eolss Publishers Co., Ltd. (Oxford, UK). **1:** 933-979.

Debling, J. A., G. C. Han, F. Kuijpers, J. VerBurg, J. Zacca and W. H. Ray (1994). "Dynamic modeling of product grade transitions for olefin polymerization processes." AIChE Journal **40**(3): 506-620.

Donati, G., L. Marini, G. Marziano, C. Mazzaferri, M. Spampinato and E. Langianni (1982). Mathematical model of low density polyethylene tubular reactor, Boston, Mass, USA, ACS, Washington, DC, USA.

Donohue, M. D. and J. M. Prausnitz (1978). "Perturbed hard chain theory for fluid mixtures: Thermodynamic properties for mixtures in natural gas and petroleum technology." **24**(5): 849-860.

Ehrlich, P. and G. A. Mortimer (1970). "Fundamentals of the free- radical polymerization of ethylene." **7**(3): 386-448.

Ek, A. v. (2002). "The sun never sets on ldpe." Hydrocarbon Engineering **7**(7).

Favoreel, W., B. De Moor and P. Van Overschee (2000). "Subspace state space system identification for industrial processes." Journal of Process Control **10**(2): 149-155.

Feucht, P., B. Tilger and G. Luft (1985). "Prediction of molar mass distribution, number and weight average degree of polymerization and branching of low density polyethylene." Chemical Engineering Science **40**(10): 1935-1942.

Ghiass, M. and R. A. Hutchinson (2003). "Simulation of free radical high-pressure copolymerization in a multizone autoclave: Model development and application." Polymer Reaction Engineering **11**(4 SPEC ISS): 989-1015.

Goto, S., K. Yamamoto, S. Furui and M. Sugimoto (1981). Computer model for commercial high-pressure polyethylene reactor based on elementary reaction rates obtained experimentally. Commodity and Engineering Plastics. Symposium held during the 181st National Meeting of the American Chemical Society., Atlanta, Ga, USA, John Wiley & Sons, New York, NY, USA.

Gross, J. and G. Sadowski (2002). "Modeling polymer systems using the perturbed-chain statistical associating fluid theory equation of state." Industrial and Engineering Chemistry Research **41**(5): 1084-1093.

Gross, J., O. Spuhl, F. Tumakaka and G. Sadowski (2003). "Modeling copolymer systems using the perturbed-chain saft equation of state." Industrial and Engineering Chemistry Research **42**(6): 1266-1274.

Gupta, S. K., A. Kumar and M. V. G. Krishnamurthy (1985). "Simulation of tubular low-density polyethylene." Polymer Engineering and Science **25**(1): 37-47.

Ham, J. Y. and H.-K. Rhee (1996). "Modeling and control of an ldpe autoclave reactor." Journal of Process Control **6**(4): 241-246.

Hamielec A. E., O. M., Ramanathan S., Sirohi A., Chen C.-C. (2000). Polymer property distribution functions methodology and simulators. US Patent #6,093,211.

Han, I.-S., C. Han and C.-B. Chung (2005). "Melt index modeling with support vector machines, partial least squares, and artificial neural networks." Journal of Applied Polymer Science **95**(4): 967-974.

Hendrickson, G. (1997). Simulation of a ldpe autoclave reactor with polymers plus. Aspen World, Aspen Technology.

Huang, S. H. and M. Radosz (1990). "Equation of state for small, large, polydisperse, and associating molecules." Industrial & Engineering Chemistry Research **29**(11): 2284-2294.

Iedema, P. D., S. Grcev and H. C. J. Hoefsloot (2003). "Molecular weight distribution modeling of radical polymerization in a cstr with long chain branching through transfer to polymer and terminal double bond (tdb) propagation." Macromolecules **36**(2): 458-476.

John E. Dennis, J., D. M. Gay and R. E. Walsh (1981). "An adaptive nonlinear least-squares algorithm " ACM Trans. Math. Softw. **7**(3): 348-368

Juricek, B. C., D. E. Seborg and W. E. Larimore (2001). "Identification of the tennessee eastman challenge process with subspace methods." Control Engineering Practice **9**(12): 1337-1351.

Juricek, B. C., D. E. Seborg and W. E. Larimore (2005). Process control applications of subspace and regression-based identification and monitoring methods, Portland, OR, United States, Institute of Electrical and Electronics Engineers Inc., Piscataway, NJ 08855-1331, United States.

Khare, N. P., B. Lucas, K. C. Seavey, Y. A. Liu, A. Sirohi, S. Ramanathan, S. Lingard, Y. Song and C.-C. Chen (2004). "Steady-state and dynamic modeling of gas-phase polypropylene processes using stirred-bed reactors." Industrial and Engineering Chemistry Research **43**(4): 884-900.

Khare, N. P., K. C. Seavey, S. Ramanathan, S. Lingard, C.-C. Chen and Y. A. Liu (2002). "Steady-state and dynamic modeling of commercial slurry high-density polyethylene (hdpe) processes." Industrial and Engineering Chemistry Research **41**(23): 5601-5618.

Kiparissides, C., P. Seferlis, G. Mourikas and A. J. Morris (2002). "Online optimizing control of molecular weight properties in batch free-radical polymerization reactors." Industrial and Engineering Chemistry Research **41**(24): 6120-6131.

Kiparissides, C., G. Verros, G. Kalfas, M. Koutoudi and C. Kantzia (1993). "Comprehensive mathematical model for a multizone tubular high pressure ldpe reactor." Chemical Engineering Communications **121**: 193-217.

Kiparissides, C., G. Verros and J. F. MacGregor (1993). "Mathematical modeling, optimization, and quality control of high-pressure ethylene polymerization reactors." Journal of Macromolecular Science - Reviews in Macromolecular Chemistry and Physics **C33**(4): 437-527.

Kiparissides, C., G. Verros, A. Pertsinidis and I. Goossens (1996). "On-line parameter estimation in a high-pressure low-density polyethylene tubular reactor." AIChE Journal **42**(2): 440-454.

Ko, G. H., M. M. Osias, D. A. Tremblay, M. D. Barrera and C.-C. Chen (1992). "Process simulation in polymer manufacturing." Computers & Chemical Engineering, European Symposium on Computer Aided Process Engineering -ESCAPE-1, May 24-28 1992 **16**(suppl): 481-490.

Ko, G. H., S. Anavi, C.-C. Chen (1990). Application of aspen plus in simulation of tubular low-density polyethylene process. AIChE Spring National Meeting, Orlando, FL.

Kolhapure, N. H. and R. O. Fox (1999). "Cfd analysis of micromixing effects on polymerization in tubular low-density polyethylene reactors." Chemical Engineering Science **54**(15-16): 3233-3242.

Kozub, D. and J. F. Macgregor (1992). "Feedback control of polymer quality in semi-batch copolymerization reactors." Chemical Engineering Science **47**(4): 929-942.

Kravaris, C., R. A. Wright and J. F. Carrier (1989). "Nonlinear controllers for trajectory tracking in batch processes." Computers & Chemical Engineering **13**(1-2): 73-82.

Kumar, V., U. Sundararaj, S. L. Shah, D. Hair and L. J. Vande Griend (2003). "Multivariate statistical monitoring of a high-pressure polymerization process." Polymer Reaction Engineering **11**(4 SPEC ISS): 1017.

Lee, K. H. and J. P. J. Marano (1979). "Free-radical polymerization: Sensitivity of conversion and molecular weights to reactor conditions." Polym React and Processes, Based on a Symp at Univ of Akron, Oct 5-6 1978(10): 221-251.

Lines, B., D. Hartlen, F. D. Paquin, S. Treiber, M. d. Tremblay and M. Bell (1993). "Polyethylene reactor modeling and control design." Hydrocarbon Processing **72**(6): 4.

Ljung, L. (1987). System identification : Theory for the user. Englewood Cliffs, NJ, Prentice-Hall.

Luft, G. (1977). "Homopolymerization and copolymerization at high pressures." High Temperatures - High Pressures **9**(5): 501-504.

MacGregor, J. F., A. Penlidis and A. E. Hamielec (1984). "Control of polymerization reactors: A review." Polymer Process Engineering **2**(2-3): 179-206.

Mathias, P. M. and T. W. Copeman (1983). "Extension of the peng-robinson equation of state to complex mixtures: Evaluation of the various forms of the local composition concept." **13**: 91.

Mavridis, H. and C. Kiparissides (1985). "Optimization of a high-pressure polyethylene tubular reactor." Polymer Process Engineering **3**(3): 263-290.

McAuley, K. B. and J. F. MacGregor (1991). "On-line inference of polymer properties in an industrial polyethylene reactor." AIChE Journal **37**(6): 825-835.

McAuley, K. B. and J. F. MacGregor (1992). "Optimal grade transitions in a gas plahse polyethylene reactor." AIChE Journal **38**(10): 1564.

McAuley, K. B. and J. F. Macgregor (1993). Nonlinear multivariable control of product properties in an industrial gas phase polyethylene reactor. Proceedings of the 3rd IFAC Symposium on Dynamics and Control of Chemical Reactors, Distillation Columns and Batch Processes (DYCORD+'92), Apr 26-29 1992, College Park, MD, USA, Publ by Pergamon Press Inc, Tarrytown, NY, USA.

Meyers, R. A. (2005). Handbook of petrochemicals production processes. New York, McGraw-Hill.

Mitchell, W., D. Shook and S. L. Shah (2004). A picture worth a thousand control loops: An innovative way of visualizing controller performance data.

Moddemeijer, R. (1988). An information theoretical delay estimator. Ninth Symposium. on Information Theory in the Benelux, Mierlo, The Netherlands, Enschede.

Nagata, T., M. Ohshima and M. Tanigaki (2000). "In-line monitoring of polyethylene density using near infrared (nir) spectroscopy." Polymer Engineering and Science **40**(5): 1107-1113.

Ogunnaike, B. A. and W. H. Ray (1994). Process dynamics, modeling, and control. New York, Oxford University Press.

Ohshima, M., I. Hashimoto, T. Yoneyama, M. Takeda and F. Gotoh (1994). Grade transition control for an impact copolymerization reactor. IFAC Symposium on Advanced Control of Chemical Processes (ADCHEM'94), Kyoto, Japan.

Ohshima, M. and M. Tanigaki (2000). "Quality control of polymer production processes." Journal of Process Control, The 5th IFAC Symposium on the

Dynamics and Control of Process Systems (DYCOPS-5), Jun 8-Jun 10 1998 **10**(2): 135-148.

OPC Foundation, A. T. F. (2002). Opc ae specification version 1.10. Scottsdale, AZ, USA, OPC Foundation.

OPC Foundation, D. T. F. (1998). Opc da specification version 1.0a, 2.0 and 3.0. Scottsdale, AZ, USA, OPC Foundation.

OPC Foundation, D. T. F. (1998). Opc overview. Scottsdale, AZ, USA, OPC Foundation: 16.

OPC Foundation, H. T. F. (2001). Opc hda specification version 1.0. Scottsdale, AZ, USA, OPC Foundation.

Orbey, H., C. P. Bokis and C.-C. Chen (1998). "Equation of state modeling of phase equilibrium in the low-density polyethylene process: The sanchez-lacombe, statistical associating fluid theory, and polymer-soave-redlich-kwong equations of state." Industrial & Engineering Chemistry Research **37**(11): 4481-4491.

Overschee, P. v. and B. L. R. d. Moor (1996). Subspace identification for linear systems : Theory, implementation, applications. Boston, Kluwer Academic Publishers.

Pladis, P. and C. Kiparissides (1998). "Comprehensive model for the calculation of molecular weight-long-chain branching distribution in free-radical polymerizations." Chemical Engineering Science **53**(18): 3315-3333.

Pladis, P. and C. Kiparissides (1999). "Dynamic modeling of multizone, multifeed high-pressure ldpe autoclaves." Journal of Applied Polymer Science **73**(12): 2327-2348.

Platts (2005). Ethylene spot price volatility. Petrochemical Report.

Ponnuswamy, S. R., S. L. Shah and C. A. Kiparissides (1987). "Computer optimal control of batch polymerization reactors." Industrial & Engineering Chemistry Research **26**(11): 2229-2236.

Ramanathan, S. and W. H. Ray (1991). The dynamic behaviour of polymerization process flowsheets. Engineering Foundation Conference on Polymer Reaction Engineering, Santa Barbara, CA.

Ramanathan S., B. M., Osias M., Ko G., and Chen C.-C. (1992). "Dynamic flowsheet simulation of polymer manufacturing plants." DECHEMA Monographs **127**: 123-132.

Sanchez I. C. , L. R. H. (1976). "An elementry molecular theory of classical fluids. Pure fluids." Journal of Physics and Chemistry **80**(21): 2352-2362.

Scali, C., M. Morretta and D. Semino (1997). "Control of the quality of polymer products in continuous reactors: Comparison of performance of state estimators with and without updating of parameters." Journal of Process Control **7**(5): 357-369.

Schmidt, C.-U., M. Busch, D. Lilge and M. Wulkow (2005). "Detailed molecular structure modeling - a path forward to designing application properties of ldpe." Macromolecular Materials and Engineering **290**(4): 404-414.

Shirodkar, P. P. and G. O. Tsien (1986). "Mathematical model for the production of low density polyethylene in a tubular reactor." Chemical Engineering Science,

ISCRE 9, Ninth Int Symp on Chem React Eng, Vol 1 - Contrib Pap, May 18-21 1986 **41**(4): 1031-1038.

Soave, G. (1972). "Equilibrium constants from a modified redlich-kwong equation of state." Chemical Engineering Science **27**(6): 1197.

Soderstrom, T. and P. G. Stoica (1989). System identification. Englewood Cliffs, NJ, Prentice-Hall International.

Takeda, M. and W. H. Ray (1999). "Optimal-grade transition strategies for multistage polyolefin reactors." AIChE Journal **45**(8): 1776-1793.

Thies, J. (1979). Strategy for modeling high pressure polyethylene reactors. 86th National AIChE Meeting, Houston.

Tosun, G. and A. Bakker (1997). "Study of macrosegregation in low-density polyethylene autoclave reactors by computational fluid dynamic modeling." Industrial & Engineering Chemistry Research **36**(2): 296-305.

Tumakaka, F. and G. Sadowski (2004). "Application of the perturbed-chain saft equation of state to polar systems." Fluid Phase Equilibria **217**(2): 233.

Van Overschee, P. and B. De Moor (1994). "N4sid: Subspace algorithms for the identification of combined deterministic-stochastic systems." Automatica **30**(1): 75-93.

Vinodograv, G. V. and A. Y. Malkin (1980). Rheology of polymers - viscoelasticity and flow of polymers. Moscow, Mir Publishers.

Von Ernst Trommsdorff, H. K. P. L. (1948). "The polymerization of methacrylate." Die Makromolekulare Chemie **1**(3): 169-198.

W. Mitchell, D. S., S. L. Shah (2004). A picture worth a thousand control loops: An innovative way of visualizing controller performance data.

Watari, M., H. Higashiyama, N. Mitsui, M. Tomo and Y. Ozaki (2004). "On-line monitoring of the density of linear low-density polyethylene in a real plant by near-infrared spectroscopy and chemometrics." Applied Spectroscopy **58**(2): 248-255.

Wells, G. J. and H. W. Ray (2005). "Prediction of polymer properties in ldpe reactors." Macromolecular Materials and Engineering **290**(4): 319-346.

Wells, G. J. and W. H. Ray (2005). "Methodology for modeling detailed imperfect mixing effects in complex reactors." AIChE Journal **51**(5): 1508-1520.

Yao, K. Z., B. M. Shaw, B. Kou, K. B. McAuley and D. W. Bacon (2003). "Modeling ethylene/butene copolymerization with multi-site catalysts: Parameter estimability and experimental design." Polymer Reaction Engineering **11**(3): 563-588.

Young, R. J. and P. A. Lovell (1991). Introduction to polymers. New York, Chapman and Hall.

Zhang, S. X. and W. H. Ray (1997). "Modeling of imperfect mixing and its effects on polymer properties." AIChE Journal **43**(5): 1265-1277.

Zhou, W., E. Marshall and L. Oshinowo (2001). "Modeling ldpe tubular and autoclave reactors." Industrial and Engineering Chemistry Research **40**(23): 5533-5542.

Appendix A

Parameter Estimation Details

A.1 Data Sets Used

The majority of the regression of the plant parameters were done using the steady state model, thus steady state operating data was used for this. The details of the data used for regression and validation are detailed here:

- Data for six different grades produced regularly on the plant were used.
- For each data point used for regression and validation, three different steady state periods were averaged.
- Each steady state period consisted of one (1) hour of steady operating data.

Table A - 1 shows a segment of the table used for collection of the plant data. Note: the manipulated variable data was left out due to privacy commitments.

Start Time	22/06/2005 19:25	24/06/2005 1:08	28/04/2005 18:05
End Time	22/06/2005 21:46	24/06/2005 4:21	28/04/2005 21:19
Grade			
Purge			
Reac_Press			
Eth_Flow			
VA_Flow			
Prop_Flow			
RVA/VA %			
Feed_Temp 1			
Feed_Temp 2			
Feed_Temp 3			
Feed_Temp 4			
Z1A_T_SP			
Z1B_T_SP			
Z2_T_SP			
Z3_T_SP			
Z4_T_SP			
HPS Pressure			
HPS Temp			
LPS Pressure			
LPS Temp			
MI	419.162	414.732	872.0921454
% VA	27.4	27.2	28.2308624
Prop. Frac in feed	1.103	0.874	1.505636548
Poly_Production	8165.299	8112.998	8061.83835
Prop Conversion	20.84	20.2	20.49209374
Sec. Comp Flow	42.224	42.504	42.13565704
CONV	19.33805182	19.08761058	19.1330548
VA FLOW	3350.128	3350.022	3222.358445
PCONV	20.83178022	20.18978103	20.49197897
E CONV	19.5	20.3	19.8
P CONV	18.5	18.5	18.2

Table A'- 1 – Segment of Steady State Data Collection

A.2 Parameter Sources

Here the parameters regressed and their initial values are summarized.

The following gives a guid for the tables which follow:

- Bold Italics – Initiator Manufacturer Data Sheet
- Italics – These parameters were from the literature base case used (Iedema, Grcev et al. 2003)
- Regular – a best guess was used for these parameters. These were based on the literature values for similar parameters.

Appendix A - Parameter Estimation Details

Reaction	Comp 1	Comp 2	Pre-Exp (s^{-1})	Act-Energy (J/kmol)	Act-Volume (m^3/kmol)	Ref. Temp. (°C)	Eff.
INIT-DEC	*Initiator 1*		***3.20E+15***	***153460000***	0.021	1.00E+35	0.3
INIT-DEC	*Initiator 2*		***1.54E+14***	***124900000***	0.01242	1.00E+35	0.4235
INIT-DEC	*Initiator 3*		***3.42E+15***	***123620000***	0.025	1.00E+35	0.3634
INIT-DEC	*Initiator 4*		***2.49E+16***	***150150000***	0.02141626	1.00E+35	0.5
CHAIN-INI	*Ethylene*		254000000	35300000	0.08	1.00E+35	
CHAIN-INI	*Vinyl Acetate*		254000000	35300000	0.08	1.00E+35	
CHAIN-INI	*Propylene*		254000000	35300000	0.08	1.00E+35	
PROPAGATION	*Ethylene*	*Ethylene*	*1.250E+8*	*3.377E+7*	*-0.0197*	1.00E+35	
PROPAGATION	*Ethylene*	*Vinyl Acetate*	1.250E+8	3.377E+7	-0.0197	1.00E+35	
PROPAGATION	*Ethylene*	*Propylene*	1.250E+8	3.377E+7	-0.0197	1.00E+35	
PROPAGATION	*Vinyl Acetate*	*Ethylene*	1.250E+8	3.377E+7	-0.0197	1.00E+35	
PROPAGATION	*Vinyl Acetate*	*Vinyl Acetate*	1.250E+8	3.377E+7	-0.0197	1.00E+35	
PROPAGATION	*Vinyl Acetate*	*Propylene*	1.250E+8	3.377E+7	-0.0197	1.00E+35	
PROPAGATION	*Propylene*	*Ethylene*	1.250E+8	3.377E+7	-0.0197	1.00E+35	
PROPAGATION	*Propylene*	*Vinyl Acetate*	1.250E+8	3.377E+7	-0.0197	1.00E+35	
PROPAGATION	*Propylene*	*Propylene*	1.250E+8	3.377E+7	-0.0197	1.00E+35	
CHAT-MON	*Ethylene*	*Ethylene*	*4.000E+4*	*3.377E+7*	*-0.0197*	1.00E+35	
CHAT-MON	*Ethylene*	*Vinyl Acetate*	4.000E+4	3.377E+7	-0.0197	1.00E+35	
CHAT-MON	*Ethylene*	*Propylene*	4.000E+4	3.377E+7	-0.0197	1.00E+35	
CHAT-MON	*Vinyl Acetate*	*Ethylene*	4.000E+4	3.377E+7	-0.0197	1.00E+35	

Table A - 2 – Initial Values Used in Regression 1

Reaction	Comp 1	Comp 2	Pre-Exp (s^{-1})	Act-Energy (J/kmol)	Act-Volume (m^3/kmol)	Ref. Temp. (^oC)	Eff.
CHAT-MON	*Vinyl Acetate*	*Vinyl Acetate*	4.000E+4	3.377E+7	-0.0197	1.00E+35	
CHAT-MON	*Vinyl Acetate*	*Propylene*	4.000E+4	3.377E+7	-0.0197	1.00E+35	
CHAT-MON	*Propylene*	*Ethylene*	4.000E+4	3.377E+7	-0.0197	1.00E+35	
CHAT-MON	*Propylene*	*Vinyl Acetate*	4.000E+4	3.377E+7	-0.0197	1.00E+35	
CHAT-MON	*Propylene*	*Propylene*	4.000E+4	3.377E+7	-0.0197	1.00E+35	
CHAT-AGENT	*Ethylene*	*Acetone*	4.000E+4	3.377E+7	-0.0197	1.00E+35	
CHAT-AGENT	*Vinyl Acetate*	*Acetone*	4.000E+4	3.377E+7	-0.0197	1.00E+35	
CHAT-AGENT	*Propylene*	*Acetone*	4.000E+4	3.377E+7	-0.0197	1.00E+35	
CHAT-POL	*Ethylene*	*Ethylene*	*4.380E+8*	*5.494E+7*	*0.0044*	1.00E+35	
CHAT-POL	*Ethylene*	*Vinyl Acetate*	4.380E+8	5.494E+7	0.0044	1.00E+35	
CHAT-POL	*Ethylene*	*Propylene*	4.380E+8	5.494E+7	0.0044	1.00E+35	
CHAT-POL	*Vinyl Acetate*	*Ethylene*	4.380E+8	5.494E+7	0.0044	1.00E+35	
CHAT-POL	*Vinyl Acetate*	*Vinyl Acetate*	4.380E+8	5.494E+7	0.0044	1.00E+35	
CHAT-POL	*Vinyl Acetate*	*Propylene*	4.380E+8	5.494E+7	0.0044	1.00E+35	
CHAT-POL	*Propylene*	*Ethylene*	4.380E+8	5.494E+7	0.0044	1.00E+35	
CHAT-POL	*Propylene*	*Vinyl Acetate*	4.380E+8	5.494E+7	0.0044	1.00E+35	
CHAT-POL	*Propylene*	*Propylene*	4.380E+8	5.494E+7	0.0044	1.00E+35	
B-SCISSION	*Ethylene*		*1.292E+5*	*4.715E+7*	*-0.0168*	1.00E+35	
B-SCISSION	*Vinyl Acetate*		1.292E+5	4.715E+7	-0.0168	1.00E+35	
B-SCISSION	*Propylene*		1.292E+5	4.715E+7	-0.0168	1.00E+35	

Table A - 3 – Initial Values Used in Regression 2

Reaction	Comp 1	Comp 2	Pre-Exp (s^{-1})	Act-Energy (J/kmol)	Act-Volume (m^3/kmol)	Ref. Temp. (^{0}C)	Eff.
TERM-DIS	*Ethylene*	*Ethylene*	*1.250E+9*	*4.184E+6*	*0.0130*	1.00E+35	
TERM-DIS	*Ethylene*	*Vinyl Acetate*	1.250E+9	4.184E+6	0.0130	1.00E+35	
TERM-DIS	*Ethylene*	*Propylene*	1.250E+9	4.184E+6	0.0130	1.00E+35	
TERM-DIS	*Vinyl Acetate*	*Ethylene*	1.250E+9	4.184E+6	0.0130	1.00E+35	
TERM-DIS	*Vinyl Acetate*	*Vinyl Acetate*	1.250E+9	4.184E+6	0.0130	1.00E+35	
TERM-DIS	*Vinyl Acetate*	*Propylene*	1.250E+9	4.184E+6	0.0130	1.00E+35	
TERM-DIS	*Propylene*	*Ethylene*	1.250E+9	4.184E+6	0.0130	1.00E+35	
TERM-DIS	*Propylene*	*Vinyl Acetate*	1.250E+9	4.184E+6	0.0130	1.00E+35	
TERM-DIS	*Propylene*	*Propylene*	1.250E+9	4.184E+6	0.0130	1.00E+35	
TERM-COMB	*Ethylene*	*Ethylene*	*1.250E+9*	*4.184E+6*	*0.0130*	1.00E+35	
TERM-COMB	*Ethylene*	*Vinyl Acetate*	1.250E+9	4.184E+6	0.0130	1.00E+35	
TERM-COMB	*Ethylene*	*Propylene*	1.250E+9	4.184E+6	0.0130	1.00E+35	
TERM-COMB	*Vinyl Acetate*	*Ethylene*	1.250E+9	4.184E+6	0.0130	1.00E+35	
TERM-COMB	*Vinyl Acetate*	*Vinyl Acetate*	1.250E+9	4.184E+6	0.0130	1.00E+35	
TERM-COMB	*Vinyl Acetate*	*Propylene*	1.250E+9	4.184E+6	0.0130	1.00E+35	
TERM-COMB	*Propylene*	*Ethylene*	1.250E+9	4.184E+6	0.0130	1.00E+35	
TERM-COMB	*Propylene*	*Vinyl Acetate*	1.250E+9	4.184E+6	0.0130	1.00E+35	
TERM-COMB	*Propylene*	*Propylene*	1.250E+9	4.184E+6	0.0130	1.00E+35	
SC-BRANCH	*Ethylene*	*Ethylene*	3.36E+09	45800000	-0.0235	1.00E+35	
SC-BRANCH	*Ethylene*	*Vinyl Acetate*	3.36E+09	45800000	-0.0235	1.00E+35	

Table A - 4 – Initial Values Used in Regression 3

Appendix A - Parameter Estimation Details

Reaction	Comp 1	Comp 2	Pre-Exp (s^{-1})	Act-Energy (J/kmol)	Act-Volume (m^3/kmol)	Ref. Temp. (^oC)	Eff.
SC-BRANCH	*Ethylene*	*Propylene*	2.55E+09	33800000	-0.0235	1.00E+35	
SC-BRANCH	*Vinyl Acetate*	*Ethylene*	3.36E+09	45800000	-0.0235	1.00E+35	
SC-BRANCH	*Vinyl Acetate*	*Vinyl Acetate*	3.36E+09	45800000	-0.0235	1.00E+35	
SC-BRANCH	*Vinyl Acetate*	*Propylene*	2.55E+09	45800000	-0.0235	1.00E+35	
SC-BRANCH	*Propylene*	*Ethylene*	2.55E+09	33800000	-0.0235	1.00E+35	
SC-BRANCH	*Propylene*	*Vinyl Acetate*	2.55E+09	45800000	-0.0235	1.00E+35	
SC-BRANCH	*Propylene*	*Propylene*	6.93E+08	45800000	-0.0235	1.00E+35	

Table A - 5 – Initial Values Used in Regression 4

Component i	EVA	EVA	EVA	E2-SEG	VA-SEG	E2-SEG	E2	EVA	EVA	VA	E2
Component j	PROP	SOLVENT	ACETONE	E2	E2	VA-SEG	PROP	E2	VA	PROP	VA
a_{ij}	0	0	0	0	0	0	0	0	0	0	0
b_{ij}	0	0	0	0	0	0	0	0	0	0	0
c_{ij}	0	0	0	0	0	0	0	0	0	0	0
d_{ij}	0	0	0	0	0	0	0	0	0	0	0
e_{ij}	0	0	0	0	0	0	0	0	0	0	0

Table A - 6 – Initial Values Used in Regression 5

E2 – Ethylene PROP – Propylene SEG – Segment